5-18-2012

# Understanding The Structure-Function Relationships In The Mechanosensitive Channel Of Small Conductance (MscS) And Bacterial Cyclic Nucleotide Gated (bCNG) Ion Channels

Hannah Renee Malcolm
*Washington University in St. Louis*

WASHINGTON UNIVERSITY IN ST. LOUIS

Department of Chemistry

Dissertation Examination Committee:

Joshua A. Maurer (Chair)
Robert E. Blankenship
Jianmin Cui
Elizabeth S. Haswell
Jacob Schaefer
John-Stephen A. Taylor

# Understanding The Structure-Function Relationships In The Mechanosensitive Channel Of Small Conductance (MscS) And Bacterial Cyclic Nucleotide Gated (bCNG) Ion Channels

By
Hannah Renee Malcolm

A dissertation presented to the
Graduate School of Arts and Sciences
of Washington University in
partial fulfillment of the
requirements for the degree
of Doctor of Philosophy

August 2012

Saint Louis, Missouri

# Abstract

In this dissertation, we discuss the relationship between structure and function within the mechanosensitive channel of small conductance (MscS) superfamily. Specifically, we explore the function of the bacterial cyclic nucleotide gated (bCNG) ion channels and the lipid interactions of MscS in the closed and open state. Our main goal was to identify similarities between MscS and bCNG channels and to understand the differences between the two channel families.

The bCNG channel family is a unique subset of the MscS superfamily. These channels are structurally composed of a channel domain homologous to MscS, a non-conserved linker domain, and a cyclic adenosine monophosphate (cAMP) binding domain. Several bCNG channels gate in response to cAMP alone, indicating that these channels function as ligand gated ion channels. bCNG channels are highly homologous to the pore lining helix and the upper vestibule domain of MscS suggesting that these channels should gate in response to mechanical tension. The majority of bCNG channels are unable to gate in response to mechanical tension however, upon the removal of the cAMP binding domain limited mechanosensation is restored to bCNG channels.

Some bacterial genomes are predicted to encode for multiple bCNG homologues. RT-PCR analysis of several different bacterial strains shows that the mRNA for these bCNG homologues is detected at similar levels. When two bCNG channels are heterologously

expressed in *E. coli*, they form heteromultimeric channels. These results suggest that bCNG channels are likely to form heteromultimers *in vivo*.

*E. coli* MscS is a well studied mechanosensitive channel. Previous research has identified critical residues for channel function; these residues are located throughout the channel but are not predicted to interact with the lipid tails. As a mechanosensitive channel, we would expect that the amino acids in the transmembrane domains interact with the hydrophobic lipid tails to allow for gating in response to mechanical tension. To identify these residues, an all atom molecular dynamics simulation was conducted on a closed state model of MscS. The combination of this simulation and phenotypic data identified seven residues in the closed state that interact with the lipids and are essential for channel function. The identification of lipid interacting residues in the closed state of MscS suggests that similar interactions would be important for the open state. However, no lipid interacting residues were identified in the open state of MscS. The lack of lipid interactions suggests that the open state of MscS does not have essential lipid interactions. This has lead us to propose a new gating paradigm for MscS, the Jack-In-The-Box gating model.

This study of the relationship between structure and function within the MscS superfamily has given us a greater understanding of the molecular interactions needed for channel function. We have learned that lipid interactions are essential for gating in response to mechanical tension and that the appendage of the C-terminal cAMP binding domain inhibits mechanical gating of bCNG channels.

# Acknowledgements

First, I would like to thank my parents for all of their love and support over the last six years. Mom, your unending support for my dream of being a scientist has meant more to me than you will ever know, thank you. Dad, your quiet way of putting yet another failed experiment into perspective has kept me sane over the years. I know that these words are not enough but your encouragement may have been the only thing pushing me to finish at times. I will never be able to thank you enough; I am forever in your debt. In many ways, this book is as much yours as it is mine, they say it takes a village to raise a child; apparently it takes a village to write a dissertation too.

To the rest of my family, your support for this quest of science has been wonderful. Thank you for rejoicing in the paper acceptances, although the magnitude of the event may have been lost on you, you did celebrate with gusto. Thank you for looking for the right amount of sorrow when I yet again had another failed experiment to tell you about. I look forward to being able to attend more family functions with all of you now that I am going to be closer. To my grandmothers who could not be here, this is for you. Thank you for supporting my dream even when it meant that I moved further away and missed so much, I love you.

To Josh, I think the best thing to start with is thank you, although that is woefully inadequate. Your constant support has allowed me to become a scientist that I hope you will be proud of. Thank you for the moments when I wanted to quit and came up with some ridiculous plan for my life and you would just look at me and say ‘I don’t think you

would be happy.' I think the best thing to say is that I would do this all again knowing how hard this was going to be. Moreover, thank you for always believing that I could make it even when I didn't think it was possible.

To the rest of the fab five, Matt Hynes, Natalie LaFranzo, Matt Strulson, and Dawn Johnson, our journey towards this has been wonderful. I enjoyed the moments where we could just be friends and not co-workers: those weekends spent in the lab were less painful knowing that we were all going to be in there together. All of you brought something special to our group and I know I will never work with a group as wonderful as you. To the other members of the Maurer group past and present, thank you for all of your help.

I would like to thank Professor Donald Elmore for all of his help of the years putting this thesis together. A special thanks goes to Yoonie, for all of her assistance and keeping our conference calls lively.

Barrie, thank you for the moments when we could talk about how much we just want to be a lady-who-lunches and knowing that it would never work out. I can't wait to see what you do with science; it is going to be worth every sucky moment I promise.

To the other scientists in my life: thank you for sharing this adventure with me. It has been fun to share a beer over the highs and lows of grad school. I look forward to more beer and less grad school talk.

To the non-science friends, watch out fun-Hannah is coming back to Texas. Thank you for listening when I needed a friend and reminding me that there was life after grad school. Stacee, your phone calls always seemed to come at the moment when I needed them and if there wasn't a call I could always listen to the most recent random message. I can't wait to live near you and drink a beer and watch some aggie football. Mimi, your quiet perseverance through law school showed me this could be done, thank you for showing me there was always a little hope. Kleck, you bring something special to my life, your random thoughts always keep me grounded.

To my dog Lily, while this is very unorthodox, thank you. I promise that I will come home on time and that there will be more walks in your future. You have been patient and I am looking forward to taking Dallas by storm with you.

I would like to thank Robert Blankenship, Jianmin Cui, and Jacob Schaefer for being on my committee. Your helpful comments have pushed me to work hard and figure out the answers. Thank you to John-Stephen Taylor and Elizabeth Haswell for taking time to be on my defense committee.

Thank you from the bottom of my heart,

Hannah

# Table of Contents

# List of Figures

**Chapter One**



**Chapter Two**



**Chapter Three**

**Chapter Four**



**Chapter Five**



**Chapter Six**

**Chapter Seven**



**Chapter Eight**

# List of Tables

**Chapter Six**



**Chapter Seven**

# List of Abbreviations

| | |
|---|---|
| bCNG | Bacterial cyclic nucleotide gated |
| cAMP | Cyclic adenosine monophosphate |
| CFU | Colony forming unit |
| CNG | Cyclic nucleotide gated |
| cNMP | Cyclic nucleotide monophosphate |
| *E. coli* (Ec) | *Escherichia coli* |
| Ec | *Escherichia coli* |
| GOF | Gain of function |
| HA | Human influenza hemagglutinin |
| HPLC | High pressure liquid chromatography |
| IPTG | Isopropyl β-D-1-thiogalactopyranoside |
| LB | Luria Bertani Broth |
| LGIC | Ligand gated ion channel |
| LIC | Ligation independent cloning |
| LOF | Loss of function |
| MscS | Mechanosensitive channel of small conductance |
| MD | Molecular Dynamics |
| NCBI | National Center for the Biotechnology Information |
| OD | Optical Density |
| PAGE | Poly-acrylamide gel electrophoresis |
| PCR | Polymerase chain reaction |

| | |
|---|---|
| POPE | Palmitoyl oleoyl phosphatidylethanolamine |
| RT-PCR | Reverse Transcriptase-polymerase chain reaction |
| SDS | Sodium dodecyl sulfate |
| TB | Terrific Broth |
| TM | Transmembrane domain |
| WT | Wildtype |

# Chapter One

# 1.1 Ion Channels

---

### *1.1.1 Ion Channels*

Ion channels have been identified in all phylogenetic kingdoms and in all different cell types within each kingdom (Hille 2001). These channels are involved in maintaining the membrane potential in cells and regulating the internal osmolyte concentrations. Transmembrane pores are found in different sizes ranging from very small, 21 amino acids per subunit in alamethacin, to very large and complex, over 400 amino acids per subunit (Unwin 1993; Leitgeb et al. 2007). The variations in number of amino acids is not the only difference between channels, some channels are homomultimers, composed of several of the same subunit, and some are heteromultimers, composed of different subunits.

In general, ion channels can be classified into one of three classes: ligand gated, voltage gated, or mechanogated (Figure 1.1.1). Ligand gated ion channels gate in response to a ligand binding event. The most common examples of ligand gated ion channels are found

in neurons in the brain and gate in response to small molecules, such as acetylcholine. Voltage gated ion channels gate in response to changes in the membrane potential. These channels are essential, since depolarization of the cell membrane leads to cell death. The third class of ion channels, the mechanogated channels, which gate in response to changes mechanical tension. In bacteria mechanogated channels rescue the cells from imminent cell death due to an increase in internal tension and in mammalian cells mechanogated channels are involved in touch sensation.

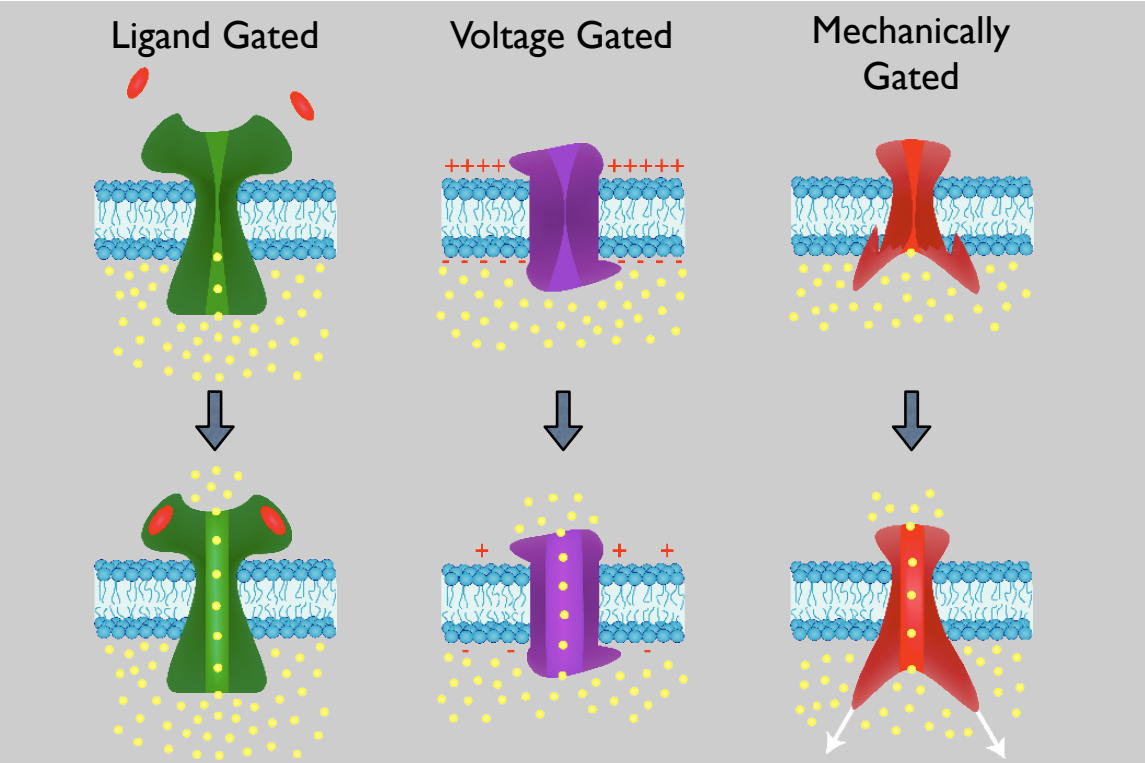


**Figure 1.1.1:** Schematic of the three classes of ion channels: Ligand gated, voltage gated, and mechanosensitive.

Mechanogated, or mechanosensitive, channels have been identified in both mammalian cells and bacterial cells. In mammalian cells, some mechanosensitive ion channels can be anchored to the cytoskeleton and thus gate in response to cytoskeletal changes (Milac et al. 2011). However, as bacteria do not have a cytoskeleton, bacterial mechanosensitive ion channels gate in response to changes in the membrane tension. The change in membrane tension changes the curvature of the cell membrane and causing the channel to open in response to tension (Figure 1.1.2).

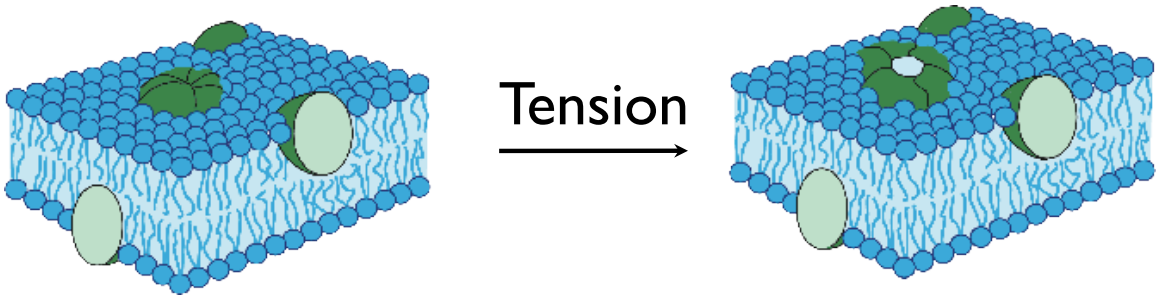


**Figure 1.1.2:** A schematic of mechanosensitive channels embedded within a bacterial membrane showing that upon the application of tension the channels opens allowing ions to pass.

In *Escherichia coli* (*E. coli*) there are seven known mechanosensitive channels: MscL, MscS, MscK, YnaI, YbdG, YpeJ, and YbiO (Berrier et al. 1992; Schumann et al. 2010; Sukharev et al. 1997). The mechanosensitive channel of large conductance (MscL) and the mechanosensitive channel of small conductance (MscS) are the best studied bacterial mechanosensitive channels. MscL and MscS gate in response to mechanical tension in the cell membrane induced by osmotic shock.

A crystal structure of the *Mycobacterium tuberculosis* (Tb) MscL homologue has been solved (Chang et al. 1998; Steinbacher et al. 2007). MscL homologues have been identified in many different bacterial genomes with the best studied homologue being from *E. coli* (Ec) (Iscla et al. 2011; Anishkin and Sukharev 2009; Maurer and Dougherty 2003; Maurer et al. 2008; Sukharev et al. 1994). Using the Tb-MscL crystal structure as a starting point a structural model of the Ec-MscL channel has been created (Elmore and Dougherty 2003; Maurer et al. 2000). Many different groups have studied regions of Ec-MscL and determined their function during channel gating.

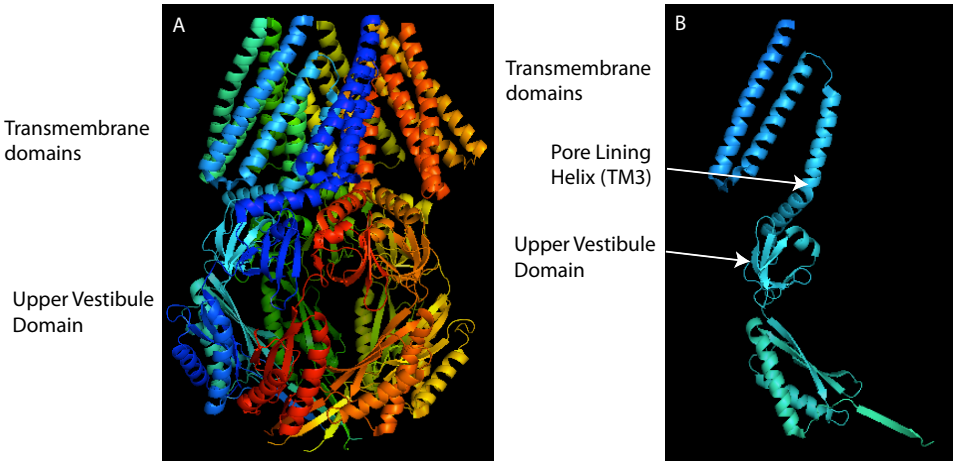


**Figure 1.1.3**: Regions of interest in Ec-MscS show on the full desensitized crystal structure (A) and a single monomer (B).

Ec-MscS is a homo-heptamer, a channel containing seven identical but separate subunits (Bass et al. 2002) (Figure 1.1.3). In a single subunit, there are three transmembrane domains are found within the lipid bilayer and an intracellular vestibule domain. The third transmembrane domain is the pore lining helix, where the ions entering or exiting the cell are transported.

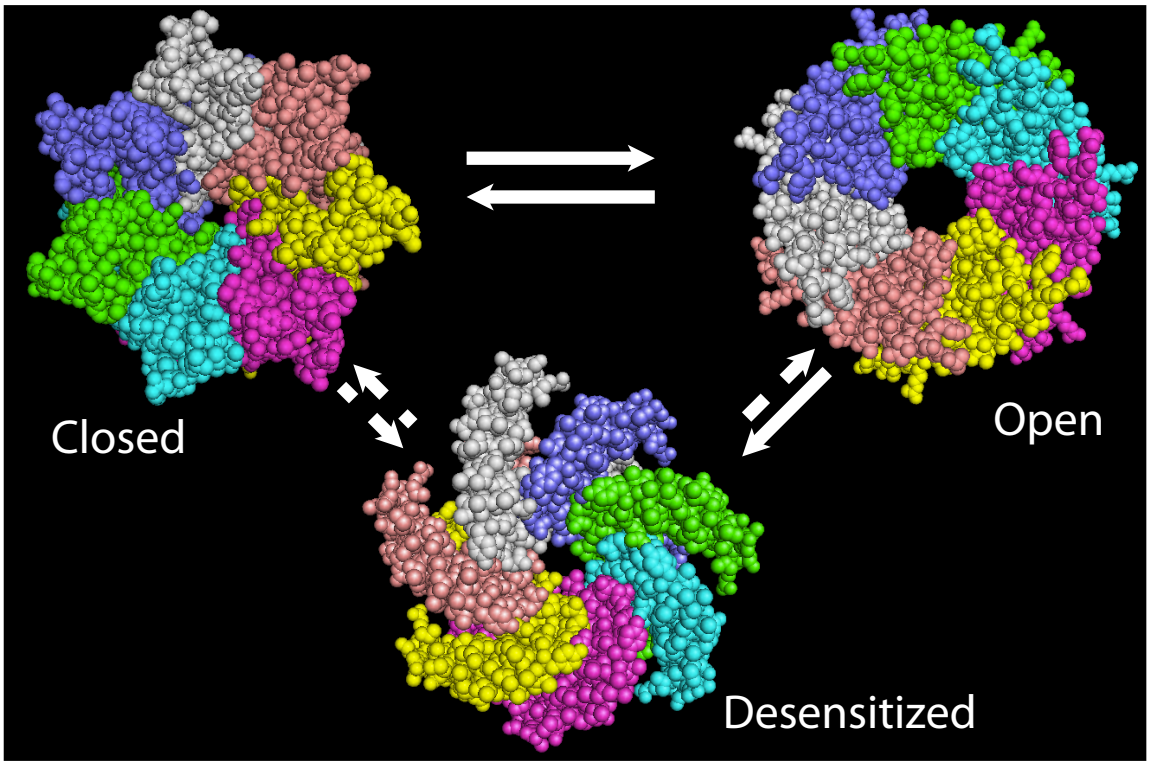


**Figure 1.1.4:** Known gating transitions of Ec-MscS. The known states are shown as spacefilling to emphasize pore size. The open state and the desensitized/inactivated structures are crystal structures and the closed state structure is based on a MD simulation.

Based on electrophysiology, MscS is known to have at least three unique kinetic states: closed, open, and desensitized/inactive (Figure 1.1.4) (Sukharev et al. 1993). These electrophysiological experiments have shown that MscS can transition between the closed and open states (Wang et al. 2008; Bass et al. 2002; Steinbacher et al. 2007). Upon the application of tension for an extended period of time, MscS inactivates. This shows that the gating transitions of MscS are from the closed state to the open state and the reverse of this pathway as well as from the open state to the desensitized state. However,

once MscS reaches the desensitized it is unclear how the channel transitions back to the closed state; does the channel return to the closed state through the open state or is there a direct transition between the desensitized state and the closed state.

Two domains of Ec-MscS consisting of approximately 90 amino acids are used to identify members of the MscS superfamily (Kloda and Martinac 2001b, a, 2002). These two regions are the pore lining helix and the upper vestibule domain. Homology to these regions has identified fifteen different subfamilies within the MscS superfamily. Members of several of these subfamilies have been cloned and characterized with some of these subfamilies have evolved to be non-mechanosensitive (Haswell 2007; Malcolm et al. 2012).

### 1.1.2 References

Anishkin A, Sukharev S (2009) State-stabilizing Interactions in Bacterial Mechanosensitive Channel Gating and Adaptation. The Journal of biological chemistry 284 (29):19153-19157. doi:10.1074/jbc.R109.009357

Bass RB, Strop P, Barclay M, Rees DC (2002) Crystal structure of Escherichia coli MscS, a voltage-modulated and mechanosensitive channel. Science 298 (5598):1582-1587. doi:10.1126/science.1077945

Berrier C, Coulombe A, Szabo I, Zoratti M, Ghazi A (1992) Gadolinium ion inhibits loss of metabolites induced by osmotic shock and large stretch-activated channels in bacteria. European journal of biochemistry / FEBS 206 (2):559-565

Chang G, Spencer RH, Lee AT, Barclay MT, Rees DC (1998) Structure of the MscL homolog from Mycobacterium tuberculosis: a gated mechanosensitive ion channel. Science 282 (5397):2220-2226

Elmore DE, Dougherty DA (2003) Investigating lipid composition effects on the mechanosensitive channel of large conductance (MscL) using molecular dynamics simulations. Biophysical journal 85 (3):1512-1524. doi:10.1016/S0006-3495(03)74584-6

Haswell ES (2007) MscS-like proteins in plants. Curr Top Membr 58:329-359. doi:Doi 10.1016/S1063-5823(06)58013-5

Hille B (2001) Ion Channels of Excitable Membranes. 3rd edn. Sinauer, Sunderland, Mass

Iscla I, Wray R, Blount P (2011) An in vivo screen reveals protein-lipid interactions crucial for gating a mechanosensitive channel. FASEB journal : official publication of the Federation of American Societies for Experimental Biology 25 (2):694-702. doi:10.1096/fj.10-170878

Kloda A, Martinac B (2001a) Mechanosensitive channels in Archaea. Cell Biochem Biophys 34 (3):349-381

Kloda A, Martinac B (2001b) Molecular identification of a mechanosensitive channel in archaea. Biophysical journal 80 (1):229-240

Kloda A, Martinac B (2002) Common evolutionary origins of mechanosensitive ion channels in Archaea, Bacteria and cell-walled Eukarya. Archaea 1 (1):35-44

Leitgeb B, Szekeres A, Manczinger L, Vagvolgyi C, Kredics L (2007) The history of alamethicin: a review of the most extensively studied peptaibol. Chemistry & biodiversity 4 (6):1027-1051. doi:10.1002/cbdv.200790095

Malcolm HR, Elmore DE, Maurer JA (2012) Mechanosensitive behavior of bacterial cyclic nucleotide gated (bCNG) ion channels: Insights into the mechanism of channel gating in the mechanosensitive channel of small conductance superfamily. Biochemical and biophysical research communications 417 (3):972-976. doi:10.1016/j.bbrc.2011.12.049

Maurer JA, Dougherty DA (2003) Generation and evaluation of a large mutational library from the Escherichia coli mechanosensitive channel of large conductance, MscL: implications for channel gating and evolutionary design. The Journal of biological chemistry 278 (23):21076-21082. doi:10.1074/jbc.M302892200

Maurer JA, Elmore DE, Clayton D, Xiong L, Lester HA, Dougherty DA (2008) Confirming the revised C-terminal domain of the MscL crystal structure. Biophysical journal 94 (12):4662-4667. doi:10.1529/biophysj.107.127365

Maurer JA, Elmore DE, Lester HA, Dougherty DA (2000) Comparing and contrasting Escherichia coli and Mycobacterium tuberculosis mechanosensitive channels (MscL). New gain of function mutations in the loop region. The Journal of biological chemistry 275 (29):22238-22244. doi:10.1074/jbc.M003056200

Milac A, Anishkin A, Fatakia SN, Chow CC, Sukharev S, Guy HR (2011) Structural models of TREK channels and their gating mechanism. Channels (Austin) 5 (1):23-33

Schumann U, Edwards MD, Rasmussen T, Bartlett W, van West P, Booth IR (2010) YbdG in Escherichia coli is a threshold-setting mechanosensitive channel with MscM activity. Proceedings of the National Academy of Sciences of the United States of America 107 (28):12664-12669. doi:Doi 10.1073/Pnas.1001405107

Steinbacher S, Bass R, Strop P, Rees DC (2007) Structures of the prokaryotic mechanosensitive channels MscL and MscS. Mechanosensitive Ion Channels, Part A 58:1-24. doi:Doi 10.1016/S1063-5823(06)58001-9

Sukharev SI, Blount P, Martinac B, Blattner FR, Kung C (1994) A large-conductance mechanosensitive channel in E. coli encoded by mscL alone. Nature 368 (6468):265-268. doi:10.1038/368265a0

Sukharev SI, Blount P, Martinac B, Kung C (1997) Mechanosensitive channels of Escherichia coli: the MscL gene, protein, and activities. Annual review of physiology 59:633-657. doi:10.1146/annurev.physiol.59.1.633

Sukharev SI, Martinac B, Arshavsky VY, Kung C (1993) Two types of mechanosensitive channels in the Escherichia coli cell envelope: solubilization and functional reconstitution. Biophysical journal 65 (1):177-183. doi:10.1016/S0006-3495(93)81044-0

Unwin N (1993) Nicotinic acetylcholine receptor at 9 A resolution. J Mol Biol 229 (4):1101-1124

Wang W, Black SS, Edwards MD, Miller S, Morrison EL, Bartlett W, Dong C, Naismith JH, Booth IR (2008) The structure of an open form of an E. coli mechanosensitive channel at 3.45 A resolution. Science 321 (5893):1179-1183. doi:321/5893/1179 [pii]

10.1126/science.1159262

# 1.2 The Mechanosensitive Channel of Small Conductance (MscS) Superfamily: Not Just Mechanosensitive Channels Anymore.

---

### *1.2.1 Introduction*

The mechanosensitive channel of small conductance (MscS) from *Escherichia coli* (*E. coli,* Ec) was first identified electrophysiologically (Martinac et al. 1987; Delcour et al. 1989; Sukharev et al. 1993; Martinac et al. 1990). Several years later, the gene that encoded for Ec-MscS, YggB, was cloned by Booth and co-workers (Levina et al. 1999). Since the identification of the gene encoding for MscS, many highly homologous channels have been identified based on homology to the pore lining helix and upper vestibule domain of Ec-MscS (Kloda and Martinac 2002a, b; Borngen et al. 2010; Caldwell et al. 2010; Haswell et al. 2008; Haswell and Meyerowitz 2006). The initial homologues identified were highly similar to Ec-MscS in both structure and function,

however recently several new members of the MscS superfamily have been identified that have unique domains and novel functions.

The MscS superfamily includes genes that encode for channels with large variations at the N-terminus and C-terminus of the MscS-like channel domain. It is likely that many of these domains lead to channels that are non-mechanosensitive and instead are involved in signaling pathways. While these channels exhibit conservation in the pore region they have significant variations in their outer transmembrane domains that are known to be important in Ec-MscS for tension response (Malcolm et al. 2011). Analysis of gene sequences with significant homology to Ec-MscS in the National Center for the Biotechnology Information (NCBI) database (Altschul et al. 1997; Altschul et al. 2005) using the conserved domain architecture tool (Marchler-Bauer and Bryant 2004; Marchler-Bauer et al. 2009; Marchler-Bauer et al. 2011) and other bioinformatical tools (Krogh et al. 2001; Cserzo et al. 2002) provides significant insight into the diversity within the MscS superfamily.

### *1.2.2 Ec-MscS: the Godfather of the MscS Superfamily*

Ec-MscS is by far the best characterized member of the MscS superfamily and is the basis of the superfamily. This channel gates directly in response to membrane tension *in vivo* and protects *E. coli* from hypoosmotic shock (Anishkin et al. 2008; Sukharev 2002; Vasquez et al. 2008; Levina et al. 1999). In response to tension, Ec-MscS opens a pore in the membrane allowing ions to pass and equilibrate osmotic pressure. In chapter six, we show that hydrophobic interactions between the lipid tails and amino acids in the

transmembrane domains stabilize the closed state of the channel, these interactions are not present in the open and desensitized states of the channel. Furthermore, we demonstrate in chapter seven that that lipid interactions are not important in the open state of the channel, which leads to the hypothesis that Ec-MscS gates via a Jack-In-The-Box mechanism.

The pore lining helix of Ec-MscS is critical to channel function and has been extensively characterized by mutagenesis. In this helix, there is a highly conserved $G(X)_2G(X)_3GLAXQ(X)_4N(X)_3G(X)_5$ motif that is important for channel function (Balleza and Gomez-Lagunas 2009; Akitake et al. 2007). The glycines and alanines in the motif are predicted to interact in a knob and hole mechanism that assist in the packing of the pore lining helices (Edwards et al. 2005) and are thus critical to formation of a functional pore. The last glycine in the conserved pore lining motif is thought to be important for channel kinetics, with the mutation to alanine creating a channel that is unable to inactivate (Akitake et al. 2007).

The C-terminal vestibule domain in Ec-MscS is also critical to channel function. If a C-terminal His-tag is appended to the Ec-MscS gene, $Ni^{2+}$ is able to chelate with the His-tag and rendered the channel inactive (Koprowski and Kubalski 2003). This chelation locks the vestibule domain in the closed conformation, which implies that movement of the vestibule domain is essential for gating in response to mechanical tension. Additionally, it is known that complete removal of the vestibule domain leads to complete inactivation of Ec-MscS (Schumann et al. 2004).

Due to the functional significance of the pore lining helix and the C-terminus, these regions have been designated as hallmarks for channels to be included in the MscS superfamily. All of the members of the superfamily described in the following sections contain significant homology to these regions (Figure 1.2.1).

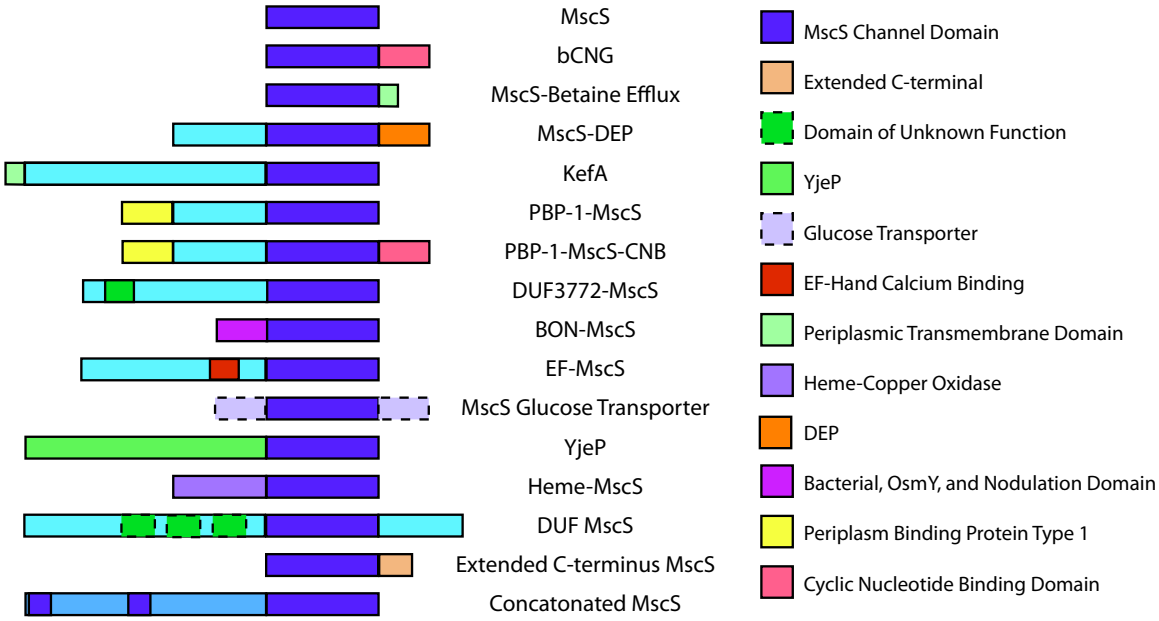


**Figure 1.2.1:** Predicted domains of members of the MscS superfamily.

### *1.2.3 Three-transmembrane Domain MscS Homologues*

Thousands of Ec-MscS homologous are found in the NCBI non-redundant protein database (Altschul et al. 1997). The majority of these genes encode for genes that are highly homologous to Ec-MscS and are predicted to have three transmembrane domains (approximately 7,000 genes). Homologues from a number of different bacteria species have been shown to successfully gate in response to mechanical tension (Kloda and

Martinac 2001; Borngen et al. 2010). This suggests that three transmembrane domain MscS homologues are a universal group of mechanosensitive ion channels that are found in the majority of prokaryotes.

### *1.2.4 Multi-transmembrane domain Homologues*

The second largest subfamily of the MscS superfamily is composed of channels with onr or more additional N-terminal transmembrane domains. This subfamily consists of approximately 700 genes. A number of these channels have been identified, cloned, and experimentally characterized including some that are predicted to encode as many as ten transmembrane domains (Haswell and Meyerowitz 2006; Sukharev et al. 1999; Schumann et al. 2010; Berrier et al. 1992). While all of these large channels may not be tension responsive, in some cases these multi-transmembrane domain homologues are known to gate in response to osmotic pressure. In these cases, the significant distance from the exterior lipid interacting regions and the pore lining helix could make direct signal transduction from the mechanical tension in the membrane difficult, and therefore provides additional credence to the Jack-In-The-Box gating mechanism proposed for Ec-MscS gating in chapter seven.

Additionally, the conserved domain architecture tool identifies several different domains of unknown function (DUF) appended to the N-terminus of MscS. The function of these genes is unknown but they are often clustered in similar bacterial strains. Many of these domains, which are from 50 to 200 amino acids in length, are located in intracellular or extracellular loop regions.

### *1.2.5 MscK homologues*

MscK, previously known as KefA, is a mechanosensitive channel from *E. coli* that spans the periplasmic space and anchors in the periplasmic membrane (Cui and Adler 1996; Li et al. 2007; Li et al. 2002; McLaggan et al. 2002). These channels are known to gate in response to mechanical tension from osmotic downshock. Moreover, both the full-length channel and a construct that does not span the periplasm are functional (Miller et al. 2003). In addition, MscK is a known potassium efflux protein and was originally thought to release potassium after hypoosmotic shock, but not be involved in mechanosensation. From an architectural standpoint, MscK homologues are predicted to have ten transmembrane domains in the inner membrane, a single helix in the periplasmic membrane, and several large loop regions. There are approximately 645 MscK homologous in the MscS superfamily, these homologues are highly identical to Ec-MscK even though they are isolated from many unique bacterial strains that are evolutionarily distant. This is surprising in that many of the other subfamilies of the MscS superfamily are restricted to bacterial strains that are closely related. The broad range of bacteria that contain MscK channels suggest that this is a physiologically an extremely important ion channel.

### *1.2.6 DUF3772-MscS*

A branch of the MscS superfamily, containing approximately 240 members, is predicted to encode for a highly conserved N-terminal domain of unknown function (DUF) that is sixty amino acids in length. These channels are found exclusively in proteobacteria like the multi-transmembrane variants of MscS and MscK, these genes have an extended

number of transmembrane domains. They are predicted to encode for twelve transmembrane domains in the inner membrane and encode for a significant DUF domain that is found in an extracellular loop between the first and second transmembrane domains. In general, these sequences are distinct from the other multi-transmembrane domain channels and represent a cross between Ec-MscS and Ec-MscK.

### *1.2.7 bCNG Channels*

The bacterial cyclic nucleotide gated (bCNG) channel subfamily contains 180 known members from over 90 different bacterial strains. These channels are highly homologous to Ec-MscS in the pore lining helix and upper vestibule domain. In addition, these genes encode for a C-terminal cyclic adenosine monophosphate (cAMP) binding domain. Within the bCNG subfamily there is significant variation in the N-terminal channel domain, as bCNG channels are predicted to have between one and six transmembrane domains. This N-terminal variation suggests that bCNG channels have evolved away from functioning as mechanosensitive channels. It has been shown experimentally that the majority of bCNG channels are unable to gate in response to mechanosensation in osmotic downshock experiments (Malcolm et al. 2012). However, upon removal of the cAMP binding domain limited mechanosensation is restored to the channel. Moreover, these channels have been shown to gate in response to cAMP alone in planar lipid bilayer experiments (Caldwell et al. 2010). Characterization of this family of channels is described in chapters two, three, four, and five.

### *1.2.8 BON-MscS*

A large branch of the MscS superfamily (approximately 55 channels) encodes for channels with a N-terminal "bacterial, OsmY, and nodulation" (BON) domain (Yeats and Bateman 2003). These channels are predicted to have four transmembrane domains with the BON domain located in the extracellular loop between the first and second transmembrane domains. The BON domain in *E.* coli OsmY is predicted to bind to the phospholipids and prevent shrinkage of the inner membrane during osmotic shocks by interacting with both the inner and outer membranes. In these channels, the BON domain is correctly positioned to play this role as it is located in the periplasmic space and, thus, could "reach up" and interact with the periplasmic membrane during osmotic shock.

### *1.2.9 EF-MscS*

EF-MscS is a subset of the MscS superfamily with approximately 50 members that encode for an EF-hand calcium binding motif upstream of the pore lining helix. These channels are predicted to have five transmembrane domains with the EF-hand calcium binding domain falling in the extracellular loop between the fourth and fifth transmembrane domains, just upstream up the pore lining helix. Additionally, along with the previously identified plant channels (Haswell and Meyerowitz 2006; Haswell et al. 2008), these channels represent some of the only eukaryotic members of the MscS superfamily and are found primarily in fungal genomes. We postulate that the EF-hand domain serves as an extracellular calcium sensor and allows these channels to gate in response to calcium.

### *1.2.10 MscCG*

Martinac and co-workers have identified the MscCG, MscS variant in *Corynebacterium glutamicum* (Borngen et al. 2010; Nottebrock et al. 2003). MscCG gates in response to hypoosmotic shifts and during gating MscCG channels efflux betaine, a zwitterionic organic molecule, in addition to ions. Betaine efflux works in concert with the BetP influx and this regulation has been postulated to allow for a tight control over of the osmotic pressure in cells. There are approximately forty channels in this subfamily and they are predicted to have a channel domain very similar to Ec-MscS, which is connected through a linker to a fourth transmembrane domain that places the C-terminus of the channel on the extracellular side. All of the channels in this subfamily are found in different species of *Corynebacterium*, which suggests that these channels preform a very specific function within this genus.

### *1.2.11 Extended C-terminus MscS*

A small subset of the MscS superfamily, approximately 20 channels, contains a C-terminal extension of approximately sixty amino acids. These channels are predicted to have three transmembrane domains and a complete vestibule domain. The C-terminal extension could be important for signal transduction by gating in response to a protein-protein interaction or by serving as a unidentified ligand binding domain. In it likely that this C-terminal extension could inhibit mechanosensation since it is known that the movement of the vestibule domain is essential for Ec-MscS function.

### *1.2.12 MscS-DEP*

Approximately 12 channels encode for an extended N-terminal domain prior to the channel domain and containing a C-terminal DEP domain. A DEP domain is a region of 90 amino acids that was first identified in Dishevelled, EGL-10, and mammalian Plextrin proteins (Chen and Hamm 2006; Ballon et al. 2006). In mammalian channels the plextrin domain interacts with the cytoskeleton, however in bacteria the function is unclear. It is thought that DEP domains are important for association and signal transduction through different receptors, such as G-protein coupled receptors. Based on sequence analysis these channels are predicted to encode for six transmembrane domains with a large intracellular loop between the first and second transmembrane domains. This branch of the MscS superfamily is found exclusively within cyanobacteria, which suggests that they may play a role in photosynthetic regulation.

### *1.2.13 YjeP*

YjeP is a known MscS homologue in *E. coli*, but the function of this channel is as of yet undefined (Schumann et al. 2010; Sukharev et al. 1997; Berrier et al. 1992). These channels are highly conserved throughout many bacterial strains, with approximately 11 members in the subfamily. In some cases, these channels are predicted to encode for a N-terminal BAR domain. BAR domains are thought to be involved in detecting membrane curvature, lipid interactions, and in some cases could act as a dimerization domains (Rao and Haucke 2011).

### *1.2.14 MscS Glucose Transporter*

The glucose transporter MscS is a highly conserved subgroup of the MscS superfamily with approximately 11 members. In this group of channels, a glucose transporter domain is either encoded prior to the channel domain or after the channel domain. The channels that encode for a C-terminal glucose transporter are found only in different strains of *Corynebacterium diphtheria*. It is possible that these channels work in a similar manner to the MscCG channels found in a wider subset of the *Corynebacterium* genus. The channels that encode for a N-terminal glucose transporter are found in a wider subset of bacterial species, however, only a few channels have been identified.

### *1.2.15 PBP-1-MscS*

Seven genes have been identified that encode for proteins that have an N-terminal periplasmic binding protein type 1 (PBP-1) domain and a C-terminal MscS channel domain. The PBP-1 domain is predicted to interact with the ATP-binding cassette (ABC) transporter system in the periplasm (Tomii and Kanehisa 1998; Tam and Saier 1993; Nikaido and Saier 1992), and is thought to scavenge small molecules in the periplasmic space and transport them to the extracellular gate of the ABC transporter. The presence of the PBP-1 domain suggests that these channels span the periplasmic space and are most likely anchored in the periplasmic membrane with at least one transmembrane domain. These channels are predicted to have five transmembrane domains in the inner membrane and at least one anchoring transmembrane domain in the periplasmic membrane. *Azospirillum sp.* B510 contains a unique MscS homologue containing a PBP-1 domain and a cyclic nucleotide binding domain. This channel is highly homologous to the PBP-1-

MscS branch of the MscS superfamily, with the exception of the C-terminal cyclic nucleotide binding domain.

### *1.2.16 Heme-Copper Oxidase MscS*

A small subset of channels (approximately 6) encode for a heme-copper oxidase upstream of the MscS-channel domain. These channels are found in a variety of bacterial species. The heme-copper oxidase is found in an intracellular loop between the first and second transmembrane domains. This oxidase is most likely involved in sensing the redox environment of the cytosol and is likely involved in regulation of this environment. Two of these channels are also predicted to contain an N-terminal EF-Hand domain, between the heme-copper oxidase and the MscS-channel domain, just upstream of the pore lining helix. Unlike the EF-MscS channels, both the EF-hand domain and the heme-copper oxidase domain are predicted to be intracellular.

### *1.2.17 Concatenated MscS*

A rare cluster of MscS superfamily members, containing approximately five channels, encode for proteins that are predicted to have three pore lining helices. These pore lining helices are sequentially oriented such that they should be correctly oriented to form a single pore and are predicted to have a total of eleven transmembrane domains. The pore lining helices are transmembrane domains one, six, and eleven. Architecturally, these channels resembled concatenated channels that have been used to study potassium channel function (Preisig-Muller et al. 2002; Sokolov et al. 2007). *In vivo* these channels could form a dimer to give a channel with six pore lining helices, however they would be

unable to form a heptamer in a manner similar to Ec-MscS (Bass et al. 2002; Steinbacher et al. 2007), unless they form heteromultimeric complexes with different MscS homologues. However, the inability to form a heptamer may not limit channel function, since channels such as the mechanosensitive channel of large conductance (MscL) have been able to form stable assemblies with different numbers of subunits (Dorwart et al. 2010; Liu et al. 2009).

### *1.2.18 Conclusions*

Although there is significant structural variety within the MscS superfamily (Figure 1.2) all of these channels have high homology in the regions needed for inclusion within the MscS superfamily. Variations of Ec-MscS with extensions in the C- and N-terminal domains that may significantly alter channel function are common. On the N-terminus the addition of a perisplamic spanning domains that anchor in the outer membrane are found in the MscK subfamily and the PBP-1-MscS subfamily. Many of the domains added to members of the MscS superfamily seemed to be involved in signal transduction suggesting that the extended MscS superfamily may play a critical role in signal pathways.

### *1.2.19 References*

Akitake B, Anishkin A, Liu N, Sukharev S (2007) Straightening and sequential buckling of the pore-lining helices define the gating cycle of MscS. Nature structural & molecular biology 14 (12):1141-1149. doi:10.1038/nsmb1341

Altschul SF, Madden TL, Schaffer AA, Zhang J, Zhang Z, Miller W, Lipman DJ (1997) Gapped BLAST and PSI-BLAST: a new generation of protein database search programs. Nucleic Acids Res 25 (17):3389-3402. doi:gka562 [pii]

Altschul SF, Wootton JC, Gertz EM, Agarwala R, Morgulis A, Schaffer AA, Yu YK (2005) Protein database searches using compositionally adjusted substitution matrices. Febs J 272 (20):5101-5109. doi:10.1111/j.1742-4658.2005.04945.x

Anishkin A, Akitake B, Sukharev S (2008) Characterization of the resting MscS: modeling and analysis of the closed bacterial mechanosensitive channel of small conductance. Biophysical journal 94 (4):1252-1266. doi:10.1529/biophysj.107.110171

Balleza D, Gomez-Lagunas F (2009) Conserved motifs in mechanosensitive channels MscL and MscS. Eur Biophys J Biophy 38 (7):1013-1027. doi:Doi 10.1007/S00249-009-0460-Y

Ballon DR, Flanary PL, Gladue DP, Konopka JB, Dohlman HG, Thorner J (2006) DEP-domain-mediated regulation of GPCR signaling responses. Cell 126 (6):1079-1093. doi:Doi 10.1016/J.Cell.2006.07.030

Bass RB, Strop P, Barclay M, Rees DC (2002) Crystal structure of Escherichia coli MscS, a voltage-modulated and mechanosensitive channel. Science 298 (5598):1582-1587

Berrier C, Coulombe A, Szabo I, Zoratti M, Ghazi A (1992) Gadolinium Ion Inhibits Loss of Metabolites Induced by Osmotic Shock and Large Stretch-Activated Channels in Bacteria. Eur J Biochem 206 (2):559-565

Borngen K, Battle AR, Moker N, Morbach S, Marin K, Martinac B, Kramer R (2010) The properties and contribution of the Corynebacterium glutamicum MscS variant to fine-tuning of osmotic adaptation. Biochimica et biophysica acta 1798 (11):2141-2149. doi:10.1016/j.bbamem.2010.06.022

Caldwell DB, Malcolm HR, Elmore DE, Maurer JA (2010) Identification and experimental verification of a novel family of bacterial cyclic nucleotide-gated (bCNG) ion channels. Biochimica et biophysica acta 1798 (9):1750-1756. doi:10.1016/j.bbamem.2010.06.001

Chen SH, Hamm HE (2006) DEP domains: More than just membrane anchors. Dev Cell 11 (4):436-438. doi:Doi 10.1016/J.Devcel.2006.09.011

Cserzo M, Eisenhaber F, Eisenhaber B, Simon I (2002) On filtering false positive transmembrane protein predictions. Protein Eng 15:745-752

Cui C, Adler J (1996) Effect of mutation of potassium-efflux system, kefA on mechanosensitive channels in the cytoplasmic membrane of Escherichia coli. J Membrane Biol 150 (2):143-152

Delcour AH, Martinac B, Adler J, Kung C (1989) Modified Reconstitution Method Used in Patch-Clamp Studies of Escherichia-Coli Ion Channels. Biophysical journal 56 (3):631-636

Dorwart MR, Wray R, Brautigam CA, Jiang YX, Blount P (2010) S. aureus MscL Is a Pentamer In Vivo but of Variable Stoichiometries In Vitro: Implications for Detergent-Solubilized Membrane Proteins. Plos Biol 8 (12). doi:Artn E1000555 Doi 10.1371/Journal.Pbio.1000555

Edwards MD, Li Y, Kim S, Miller S, Bartlett W, Black S, Dennison S, Iscla I, Blount P, Bowie JU, Booth IR (2005) Pivotal role of the glycine-rich TM3 helix in gating the MscS mechanosensitive channel. Nature structural & molecular biology 12 (2):113-119. doi:10.1038/nsmb895

Haswell ES, Meyerowitz EM (2006) MscS-like proteins control plastid size and shape in Arabidopsis thaliana. Curr Biol 16 (1):1-11. doi:Doi 10.1016/J.Cub.2005.11.044

Haswell ES, Peyronnet R, Barbier-Brygoo H, Meyerowitz EM, Frachisse JM (2008) Two MscS homologs provide mechanosensitive channel activities in the Arabidopsis root. Curr Biol 18 (10):730-734. doi:Doi 10.1016/J.Cub.2008.04.039

Kloda A, Martinac B (2001) Structural and functional differences between two homologous mechanosensitive channels of Methanococcus jannaschii. Embo Journal 20 (8):1888-1896

Kloda A, Martinac B (2002a) Common evolutionary origins of mechanosensitive ion channels in Archaea, Bacteria and cell-walled Eukarya. Archaea 1 (1):35-44

Kloda A, Martinac B (2002b) Mechanosensitive channels of bacteria and archaea share a common ancestral origin. European biophysics journal : EBJ 31 (1):14-25

Koprowski P, Kubalski A (2003) C termini of the Escherichia coli mechanosensitive ion channel (MscS) move apart upon the channel opening. The Journal of biological chemistry 278 (13):11237-11245. doi:10.1074/jbc.M212073200

Krogh A, Larsson B, von Heijne G, Sonnhammer EL (2001) Predicting transmembrane protein topology with a hidden Markov model: application to complete genomes. J Mol Biol 305:567-580

Levina N, Totemeyer S, Stokes NR, Louis P, Jones MA, Booth IR (1999) Protection of Escherichia coli cells against extreme turgor by activation of MscS and MscL mechanosensitive channels: identification of genes required for MscS activity. The EMBO journal 18 (7):1730-1737. doi:10.1093/emboj/18.7.1730

Li C, Edwards MD, Jeong H, Roth J, Booth IR (2007) Identification of mutations that alter the gating of the Escherichia coli mechanosensitive channel protein, MscK. Molecular microbiology 64 (2):560-574. doi:Doi 10.1111/J.1365-2958.2007.05672.X

Li YZ, Moe PC, Chandrasekaran S, Booth IR, Blount P (2002) Ionic regulation of MscK, a mechanosensitive channel from Escherichia coli. Embo Journal 21 (20):5323-5330

Liu ZF, Gandhi CS, Rees DC (2009) Structure of a tetrameric MscL in an expanded intermediate state. Nature 461 (7260):120-U132. doi:Doi 10.1038/Nature08277

Malcolm HR, Elmore DE, Maurer JA (2012) Mechanosensitive behavior of bacterial cyclic nucleotide gated (bCNG) ion channels: Insights into the mechanism of channel gating in the mechanosensitive channel of small conductance superfamily. Biochemical and biophysical research communications 417 (3):972-976. doi:10.1016/j.bbrc.2011.22.049

Malcolm HR, Heo YY, Elmore DE, Maurer JA (2011) Defining the role of the tension sensor in the mechanosensitive channel of small conductance. Biophysical journal 101 (2):345-352. doi:10.1016/j.bpj.2011.05.058

Marchler-Bauer A, Anderson JB, Chitsaz F, Derbyshire MK, DeWeese-Scott C, Fong JH, Geer LY, Geer RC, Gonzales NR, Gwadz M, He S, Hurwitz DI, Jackson JD, Ke

Z, Lanczycki CJ, Liebert CA, Liu C, Lu F, Lu S, Marchler GH, Mullokandov M, Song JS, Tasneem A, Thanki N, Yamashita RA, Zhang D, Zhang N, Bryant SH (2009) CDD: specific functional annotation with the Conserved Domain Database. Nucleic Acids Research 37:D205-D210. doi:Doi 10.1093/Nar/Gkn845

Marchler-Bauer A, Bryant SH (2004) CD-Search: protein domain annotations on the fly. Nucleic Acids Research 32:W327-W331. doi:Doi 10.1093/Nar/Gkh454

Marchler-Bauer A, Lu SN, Anderson JB, Chitsaz F, Derbyshire MK, DeWeese-Scott C, Fong JH, Geer LY, Geer RC, Gonzales NR, Gwadz M, Hurwitz DI, Jackson JD, Ke ZX, Lanczycki CJ, Lu F, Marchler GH, Mullokandov M, Omelchenko MV, Robertson CL, Song JS, Thanki N, Yamashita RA, Zhang DC, Zhang NG, Zheng CJ, Bryant SH (2011) CDD: a Conserved Domain Database for the functional annotation of proteins. Nucleic Acids Research 39:D225-D229. doi:Doi 10.1093/Nar/Gkq1189

Martinac B, Adler J, Kung C (1990) Mechanosensitive Ion Channels of Escherichia-Coli Activated by Amphipaths. Nature 348 (6298):261-263

Martinac B, Buechner M, Delcour AH, Adler J, Kung C (1987) Pressure-Sensitive Ion Channel in Escherichia-Coli. Proceedings of the National Academy of Sciences of the United States of America 84 (8):2297-2301

McLaggan D, Jones MA, Gouesbet G, Levina N, Lindey S, Epstein W, Booth IR (2002) Analysis of the kefA2 mutation suggests that KefA is a cation-specific channel involved in osmotic adaptation in Escherichia coli. Molecular microbiology 43 (2):521-536

Miller S, Bartlett W, Chandrasekaran S, Simpson S, Edwards M, Booth IR (2003) Domain organization of the MscS mechanosensitive channel of Escherichia coli. The EMBO journal 22 (1):36-46. doi:10.1093/emboj/cdg011

Nikaido H, Saier MH (1992) Transport Proteins in Bacteria - Common Themes in Their Design. Science 258 (5084):936-942

Nottebrock D, Meyer U, Kramer R, Morbach S (2003) Molecular and biochemical characterization of mechanosensitive channels in Corynebacterium glutamicum. Fems Microbiol Lett 218 (2):305-309

Preisig-Muller R, Schlichthorl G, Goerge T, Heinen S, Bruggemann A, Rajan S, Derst C, Veh RW, Daut J (2002) Heteromerization of Kir2.x potassium channels contributes to the phenotype of Andersen's syndrome. Proceedings of the National Academy of Sciences of the United States of America 99 (11):7774-7779. doi:Doi 10.1073/Pnas.102609499

Rao YJ, Haucke V (2011) Membrane shaping by the Bin/amphiphysin/Rvs (BAR) domain protein superfamily. Cell Mol Life Sci 68 (24):3983-3993. doi:Doi 10.1007/S00018-011-0768-5

Schumann U, Edwards MD, Li C, Booth IR (2004) The conserved carboxy-terminus of the MscS mechanosensitive channel is not essential but increases stability and activity. FEBS letters 572 (1-3):233-237. doi:10.1016/j.febslet.2004.07.045

Schumann U, Edwards MD, Rasmussen T, Bartlett W, van West P, Booth IR (2010) YbdG in Escherichia coli is a threshold-setting mechanosensitive channel with MscM activity. Proceedings of the National Academy of Sciences of the United States of America 107 (28):12664-12669. doi:Doi 10.1073/Pnas.1001405107

Sokolov MV, Shamotienko O, Dhochartaigh SN, Sack JT, Dolly JO (2007) Concaterners of brain Kv1 channel alpha subunits that give similar K+ currents yield pharmacologically distinguishable heteromers. Neuropharmacology 53 (2):272-282. doi:Doi 10.1016/J.Neuropharm.2007.05.008

Steinbacher S, Bass R, Strop P, Rees DC (2007) Structures of the prokaryotic mechanosensitive channels MscL and MscS. Curr Top Membr 58:1-24. doi:Doi 10.1016/S1063-5823(06)58001-9

Sukharev S (2002) Purification of the small mechanosensitive channel of Escherichia coli (MscS): the subunit structure, conduction, and gating characteristics in liposomes. Biophysical journal 83 (1):290-298. doi:10.1016/S0006-3495(02)75169-2

Sukharev SI, Blount P, Martinac B, Kung C (1997) Mechanosensitive channels of Escherichia coli: The MscL gene, protein, and activities. Annu Rev Physiol 59:633-657

Sukharev SI, Martinac B, Arshavsky VY, Kung C (1993) 2 Types of Mechanosensitive Channels in the Escherichia-Coli Cell-Envelope - Solubilization and Functional Reconstitution. Biophysical journal 65 (1):177-183

Sukharev SI, Sigurdson WJ, Kung C, Sachs F (1999) Energetic and spatial parameters for gating of the bacterial large conductance mechanosensitive channel, MscL. The Journal of general physiology 113 (4):525-540

Tam R, Saier MH (1993) Structural, Functional, and Evolutionary Relationships among Extracellular Solute-Binding Receptors of Bacteria. Microbiol Rev 57 (2):320-346

Tomii K, Kanehisa M (1998) A comparative analysis of ABC transporters in complete microbial genomes. Genome Research 8 (10):1048-1059

Vasquez V, Sotomayor M, Cordero-Morales J, Schulten K, Perozo E (2008) A structural mechanism for MscS gating in lipid bilayers. Science 321 (5893):1210-1214. doi:321/5893/1210 [pii]

10.1126/science.1159674

Yeats C, Bateman A (2003) The BON domain: a putative membrane-binding domain. Trends Biochem Sci 28 (7):352-355. doi:Doi 10.1016/S0968-0004(03)00115-4

# 1.3 An Introduction to the Study of Mechanosensitive Ion Channels.

---

### *1.3.1 Introduction*

Bacterial mechanosensitive channels gate in response to tension in the cell membrane and act as pressure relief valves to equilibrate the increase in internal pressure due to hypoosmotic shock (Booth and Louis 1999; Sukharev and Corey 2004). Two of the best studied mechanosensitive channels are the mechanosensitive channel of large conductance (MscL) and the mechanosensitive channel of small conductance (MscS) from *Escherichia coli* (*E. coli*) (Edwards et al. 2004; Corry and Martinac 2008; Kung and Blount 2004). These two channels have been studied using many different methods: osmotic downshock, gain of function assays, and electrophysiology. (Rasmussen et al. 2010; Akitake et al. 2007; Malcolm et al. 2011; Maurer et al. 2000). Osmotic downshock and gain of function assays compare mutations to wildtype channel, a relative difference is determined. Electrophysiology determines the exact gating tension of a channel, giving an absolute difference from the wildtype channel.

To determine the function of different regions in the channels point mutations have been utilized (Maurer and Dougherty 2003). Osmotic downshock, gain of function assays, and electrophysiology were used to study the wildtype channel and can be utilized to determine the effect that a mutation has on the channel. Point mutations in MscS and MscL are classified as wildtype, loss of function, or gain of function. Wildtype mutations have no measureable effect on channel function. Loss of function mutations gate at a higher membrane tension, than the wildtype channel (Belyy et al. 2010). Gain of function mutations gate at a lower gating threshold, in comparison with the wildtype channel, or spontaneously (Li et al. 2004).

Loss of function mutations gate at a higher tension, thus they are unable to gate in response to the tension that opens the wildtype channel. These mutations are easily identified in osmotic downshock experiments, where they are unable to rescue cells from a shift in hypoosmotic shock to the same degree as the wildtype channel (Malcolm et al. 2011). Their ability to gate in response to mechanical tension is determined by the severity of the loss of function mutation; more severe mutations are completely unable to rescue bacteria while a partial loss of function phenotype displays some recovery. In this assay, cells expressing a loss of function mutant are subjected to a shift in osmotic strength (Figure 1.3.1). During this shift, a loss of function mutant is unable to rescue the cells to the same degree as the wildtype channel, since the tension created by the osmotic shock is lower than the tension necessary for channel function. In Figure 1.3.1, the cells are grown in a high salt media prior to being diluted into a low salt media, causing a

hypoosmotic shock. The loss of function mutant does not gate in response to this tension causing the cell to burst in response to the increase in internal pressure, thus decreasing the percent recovery.

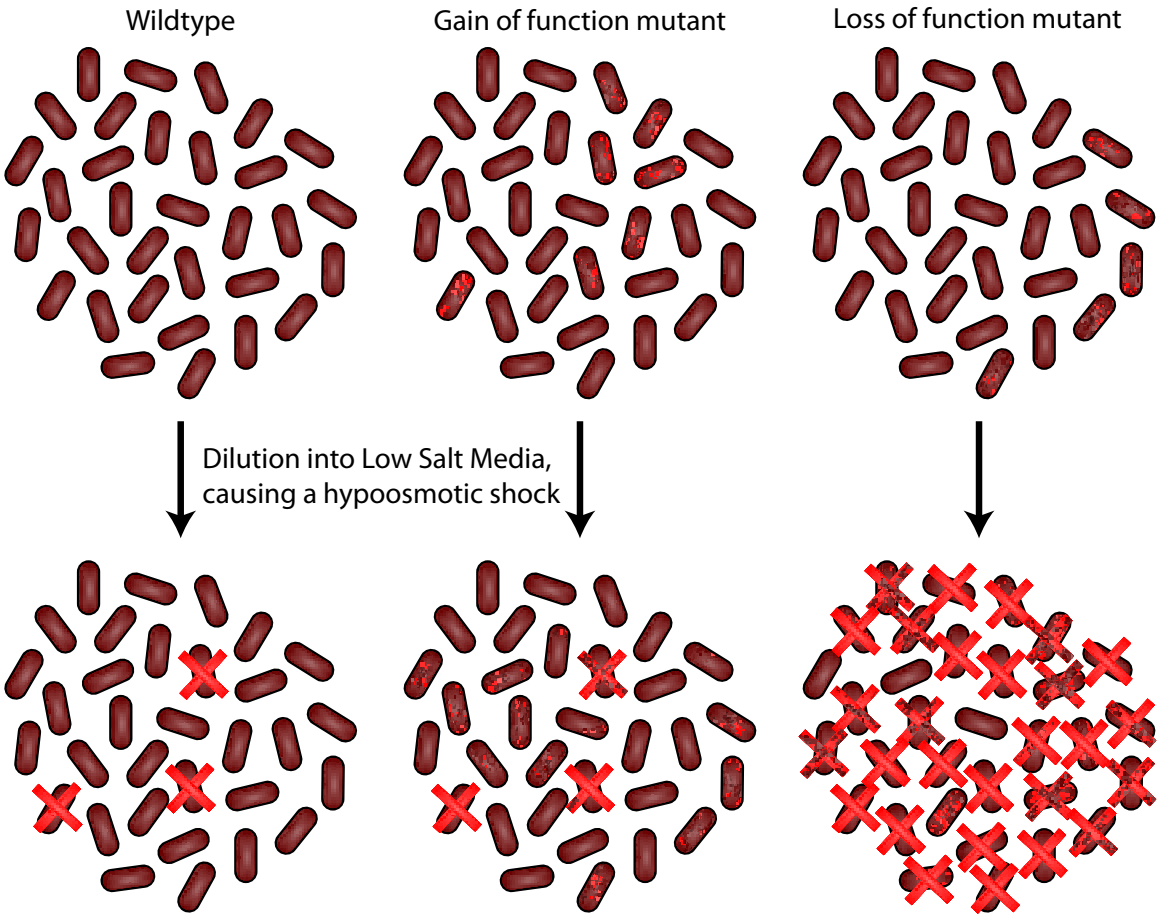


**Figure 1.3.1**: Schematic of different phenotypes in osmotic downshock assays. Bacteria expressing a severe loss of function mutant are completely unable to rescue bacteria upon dilution into a low salt media causing a hypoosmotic shift.

Gain of function mutations gate at a lower gating threshold or spontaneously in comparison to the wildtype channel. Often these mutations are considered 'leaky' channels in that the channel frequently flutters between open and closed states (Maurer et al. 2000). These mutations also affect the viability of the cells. In response to these spontaneous channel openings, the cells divert much of their energy to maintaining their

membrane potential and thus grow at a significantly reduced rate (Figure 1.3.2). Gain of function mutations are typically identified in growth based assays, where decreased growth is observed.

By combining gain and loss of function assays the change in a mutant's phenotype in compared to the wildtype channel can be determined. A gain of function mutation is often silent in osmotic downshock assays and a loss of function mutation is typically silent in the gain of function growth assays. The combination of the two assays allows for the identification for the correct phenotype of a mutant in respect to the wildtype channel.

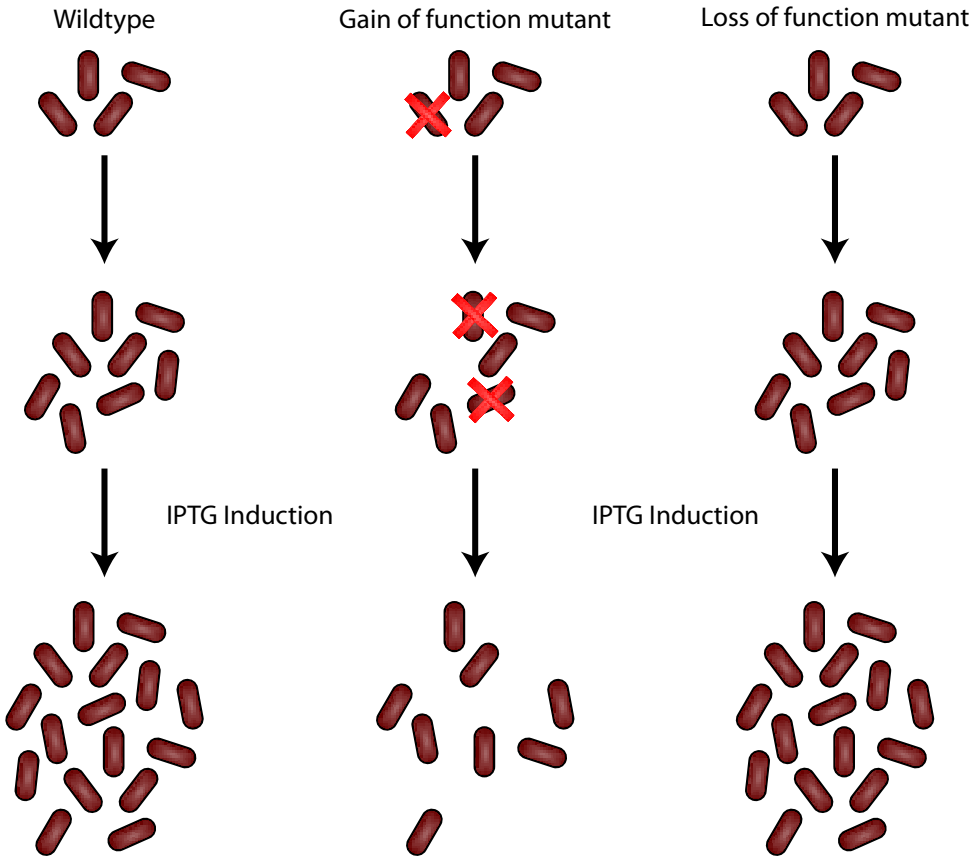


**Figure 1.3.2**: Schematic of different phenotypes in growth assays. Bacteria expressing a gain of function mutant are less viable than wildtype expressing cells and upon channel expression with IPTG induction display decreased growth.

### *1.3.2 Methods*

#### *1.3.2.1 Osmotic Downshock*

Osmotic downshock experiments are used to determine if a point mutation is a loss of function mutation (Levina et al. 1999). In this assay, cells are grown in a high salt media and then diluted into a low salt media. Upon hypoosmotic downshock the bacteria swells, due to an influx of water in an attempt to equilibrate the osmolytes within the cell with the osmolytes in the media. This swelling causes the curvature of the cell membrane to change inducing tension in the membrane (Booth and Louis 1999). Mechanosensitive channels, like MscL, sense membrane tension and open a pore allowing small molecules, ions, and even some small proteins out of the cell (Chang et al. 1998). Osmotic downshock experiments need to be conducted in an *E. coli* strain that exhibits limited recovery from hypoosmotic shock. The *E. coli* MJF465 strain is null MscS, MscL, and MscK, three of the seven known *E. coli* mechanosensitive channels (Levina et al. 1999; Wild et al. 1992) and the removal of these three channels is sufficient to eliminate the wildtype recovery in osmotic downshock experiments.

Several possible phenotypes are identified in the percent recovery plot in Figure 1.3.3: partial loss of function, loss of function, and complete loss of function. The two commonly run controls are also shown in Figure 1.3.3: wildtype channel and empty vector, a null control. To determine the percent recovery for a mutation of interest, the colony forming units (CFU) for the isotonic and hypoosmotic dilutions are calculated. The CFU is the number of viable colonies per milliliter of cells, which is calculated by counting the colonies that survive the shock from a series of dilution plates. Percent

recovery is defined as the CFU of the hypoosmotic culture divided by the CFU of the isotonic dilution. Since loss of function mutations gate at a higher membrane tension, the channels are unable to open in response to the tension and the cells die. In osmotic downshock experiments, gain of function mutations are not observed, therefore these must be identified using other methods (Figure 1.3.1).

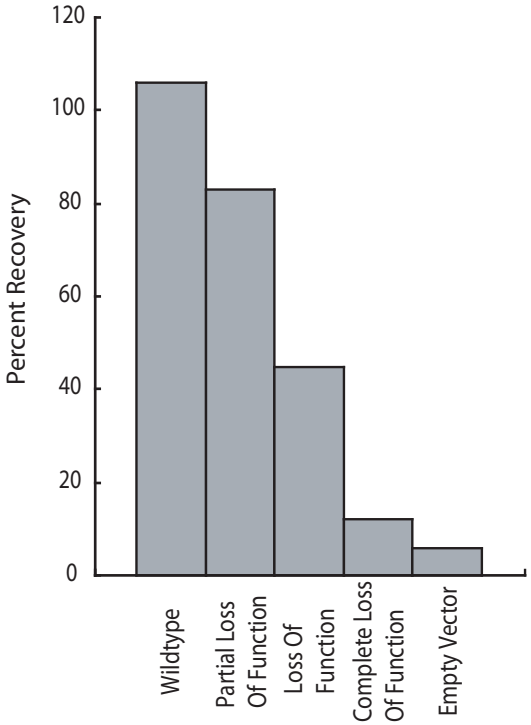


**Figure 1.3.3**: Typical osmotic downshock plot: Loss of function mutations are unable to rescue bacteria upon dilution into hypoosmotic shock and therefore display a lower percent recovery. The severity of the loss of function mutation determines the percent recovery.

*1.3.2.2 Gain of Function Assays*

There are two different assays that are commonly used to determine if a mutation is a gain of function mutation: steady state analysis and a gain of function plate assay. Gain of function mutations effect cell viability. To determine if a mutant is gain of function, a culture of the cells is often induced for several hours at low isopropyl-beta-D-

thiogalactopyranoside (IPTG) concentrations, to induce protein production. A low IPTG concentration is used to prevent over population of the cell membrane with the gain of function mutation, which could effectively depolarize the cell membrane leading to cell death.

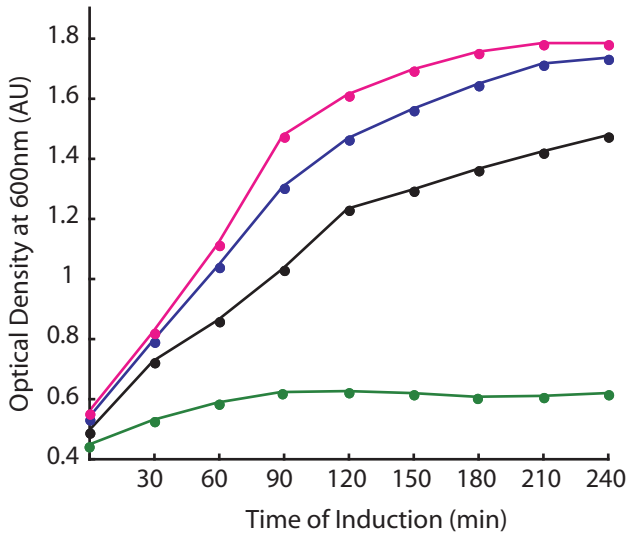


**Figure 1.3.4**: Typical Growth Curves: Wildtype bacteria display sigmoidal growth curves and grow to an $OD_{600}$ >1.5AU when grown in LB. Gain of function mutants display altered growth curves and typically grow to a decreased $OD_{600}$. Wildtype growth is shown as a pink line, a wildtype mutant is the dark blue line, a partial gain of function mutant is shown as the black line, and a severe gain of function mutant is shown in green.

One gain of function assay is a steady state growth assay (Iscla et al. 2008), in this assay a bacteria with wildtype channels will show exponential growth in LB media and grow to an OD greater than 1.5AU when measured at 600 nm, (Figure 1.3.4). Gain of function mutants typically grow at a slower rate and often reach a lower steady state density. Either a growth curve, points taken every thirty minutes for four hours of induction, or the steady state optical density, measured after eight hours of induction, is used to qualify

a mutant as gain of function. In this assay, loss of function mutants are indistinguishable from wildtype, since they are only affected by changes in osmotic strength.

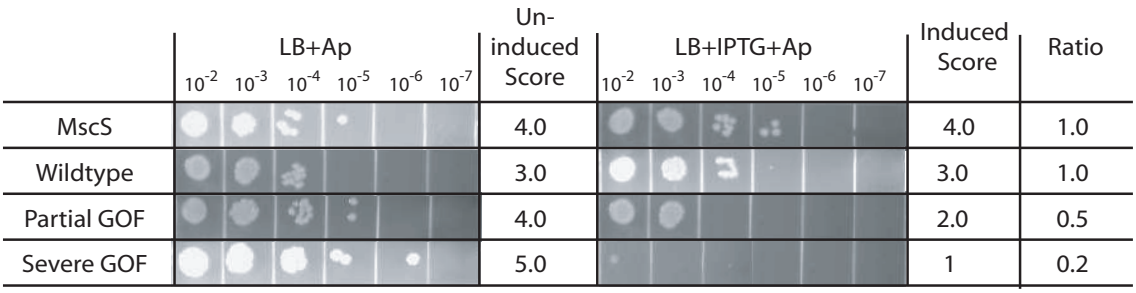


**Figure 1.3.5**: Typical Gain of Function Plate Analysis. Cells expressing the wildtype channel grow equally well on inducing and non-inducing plates, giving a ratio of ~1. Gain of function mutants show decreased growth on inducing plates giving a ratio <<1.

A plate based gain of function assay determines the severity of a gain of function mutant (Maurer et al. 2000). In this assay, cells are grown to mid-log phase and then diluted to a lower optical density. This low density culture is serially diluted prior to being plated on media with 1mM IPTG and media without IPTG. Since gain of function mutants decrease the viability of the cells, the relative amount of growth indicates the severity of a gain of function phenotype. The wildtype channel has an induced versus uninduced ratio of one and a gain of function mutant would have a much lower ratio (Figure 1.3.5). There are some mutants that are unable to be created due to the severity of the gain of function phenotype. In these mutations, basal expression is lethal, and the mutation is typically named a lethal mutation.

*1.3.2.3 Patch Clamp Electrophysiology*

To further study the ability of a point mutation to gate in response to tension, patch clamp electrophysiology can be used (Hurst et al. 2008). To conduct a patch clamp experiment, cells expressing the mutant channel are converted to spheroplasts using lysozyme and Cephalexin (Corry and Martinac 2008). Electrophysiology measurements in spheroplasts extract a small portion of the membrane from the spheroplast using a patch pipette. Upon excising the patch, pressure is applied to the membrane and the response of the channel to tension is measured. It is difficult to determine the exact tension applied to the membrane unless the curvature of the patch can be measured (Chiang et al. 2004).

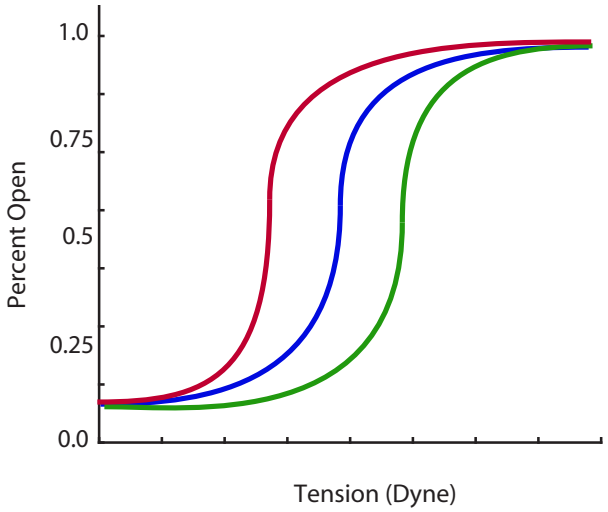


**Figure 1.3.6:** Theoretical Patch Clamp data. The wildtype channel is shown in blue. The gain of function mutant is shown in red and gates at a lower tension. The loss of function mutant is shown in green and gates at a higher tension

Since, it is difficult to determine the curvature of the patch, the tension at which MscS, MscL, or a mutant gates at is often expressed as a ratio to the gating tension of an internal standard (either wildtype MscS or MscL). Patch clamp allows for a tight regulation of the pressure applied to the patch. This tight regulation of pressure allows the $P_{50}$ of the

mutant or wildtype channel to be determined (Figure 1.3.6). Patch clamp experiments give an in depth understanding of a mechanosensitive channel's response to mechanical tension by studying the channel's response to a variety of pressures. These experiments give a deeper insight into a single mutation. In the case of slight gain or loss of function phenotypes, osmotic downshock assays and gain of function assays may not be able to determine if these mutations are statistically different from wildtype but patch clamp will detect slight variations in the $P_{50}$ from the wildtype channel.

Recent research has shown that MscS can be expressed in oocytes for use in patch clamp (Maksaev and Haswell 2011). This is exciting in that bacterial ion channels could be studied using two electrode voltage clamp. Using two electrode voltage clamp on the bacterial cyclic nucleotide gated ion channels will allow for their ability to function as a ligand gated ion channel to be easily assessed. Additionally, there are many different commercial automated two electrode voltage clamp instruments, which could be used to screen for potential agonists or antagonists of these channels.

### *1.3.3 References*

Akitake B, Spelbrink RE, Anishkin A, Killian JA, de Kruijff B, Sukharev S (2007) 2,2,2-Trifluoroethanol changes the transition kinetics and subunit interactions in the small bacterial mechanosensitive channel MscS. Biophysical journal 92 (8):2771-2784. doi:10.1529/biophysj.106.098715

Belyy V, Anishkin A, Kamaraju K, Liu N, Sukharev S (2010) The tension-transmitting 'clutch' in the mechanosensitive channel MscS. Nature structural & molecular biology 17 (4):451-458. doi:10.1038/nsmb.1775

Booth IR, Louis P (1999) Managing hypoosmotic stress: aquaporins and mechanosensitive channels in Escherichia coli. Current opinion in microbiology 2 (2):166-169

Chang G, Spencer RH, Lee AT, Barclay MT, Rees DC (1998) Structure of the MscL homolog from Mycobacterium tuberculosis: a gated mechanosensitive ion channel. Science 282 (5397):2220-2226

Chiang CS, Anishkin A, Sukharev S (2004) Gating of the large mechanosensitive channel in situ: estimation of the spatial scale of the transition from channel population responses. Biophysical journal 86 (5):2846-2861. doi:10.1016/S0006-3495(04)74337-4

Corry B, Martinac B (2008) Bacterial mechanosensitive channels: experiment and theory. Biochimica et biophysica acta 1778 (9):1859-1870. doi:10.1016/j.bbamem.2007.06.022

Edwards MD, Booth IR, Miller S (2004) Gating the bacterial mechanosensitive channels: MscS a new paradigm? Current opinion in microbiology 7 (2):163-167. doi:10.1016/j.mib.2004.02.006

Hurst AC, Petrov E, Kloda A, Nguyen T, Hool L, Martinac B (2008) MscS, the bacterial mechanosensitive channel of small conductance. The international journal of biochemistry & cell biology 40 (4):581-585. doi:10.1016/j.biocel.2007.03.013

Iscla I, Wray R, Blount P (2008) On the structure of the N-terminal domain of the MscL channel: helical bundle or membrane interface. Biophysical journal 95 (5):2283-2291. doi:10.1529/biophysj.107.127423

Kung C, Blount P (2004) Channels in microbes: so many holes to fill. Molecular microbiology 53 (2):373-380. doi:10.1111/j.1365-2958.2004.04180.x

Levina N, Totemeyer S, Stokes NR, Louis P, Jones MA, Booth IR (1999) Protection of Escherichia coli cells against extreme turgor by activation of MscS and MscL mechanosensitive channels: identification of genes required for MscS activity. The EMBO journal 18 (7):1730-1737. doi:10.1093/emboj/18.7.1730

Li Y, Wray R, Blount P (2004) Intragenic suppression of gain-of-function mutations in the Escherichia coli mechanosensitive channel, MscL. Molecular microbiology 53 (2):485-495. doi:10.1111/j.1365-2958.2004.04150.x

Maksaev G, Haswell ES (2011) Expression and characterization of the bacterial mechanosensitive channel MscS in Xenopus laevis oocytes. The Journal of general physiology 138 (6):641-649. doi:10.1085/jgp.201110723

Malcolm HR, Heo YY, Elmore DE, Maurer JA (2011) Defining the role of the tension sensor in the mechanosensitive channel of small conductance. Biophysical journal 101 (2):345-352. doi:10.1016/j.bpj.2011.05.058

Maurer JA, Dougherty DA (2003) Generation and evaluation of a large mutational library from the Escherichia coli mechanosensitive channel of large conductance, MscL: implications for channel gating and evolutionary design. The Journal of biological chemistry 278 (23):21076-21082. doi:10.1074/jbc.M302892200

Maurer JA, Elmore DE, Lester HA, Dougherty DA (2000) Comparing and contrasting Escherichia coli and Mycobacterium tuberculosis mechanosensitive channels (MscL). New gain of function mutations in the loop region. The Journal of biological chemistry 275 (29):22238-22244. doi:10.1074/jbc.M003056200

Rasmussen T, Edwards MD, Black SS, Rasmussen A, Miller S, Booth IR (2010) Tryptophan in the pore of the mechanosensitive channel MscS: assessment of pore conformations by fluorescence spectroscopy. The Journal of biological chemistry 285 (8):5377-5384. doi:10.1074/jbc.M109.071472

Sukharev S, Corey DP (2004) Mechanosensitive channels: multiplicity of families and gating paradigms. Science's STKE : signal transduction knowledge environment 2004 (219):re4. doi:10.1126/stke.2192004re4

Wild J, Altman E, Yura T, Gross CA (1992) DnaK and DnaJ heat shock proteins participate in protein export in Escherichia coli. Genes & development 6 (7):1165-1172

# Chapter Two

# Identification and Experimental Verification of a Novel Family of Bacterial Cyclic Nucleotide Gated (bCNG) Ion Channels.

*Collaboration with David B. Caldwell.

---

### *2.1 Introduction*

Bacterial ion channels provide useful models for exploring channel structure-function relationships using biochemical and structural techniques that are typically not available for mammalian channels due to the increased difficulty of overexpressing eukaryotic ion channels. For example, bacterial channels that gate in response to protons, membrane tension, voltage, and metal ions have provided significant insights into these types of channels (Martinac et al. 2008). Thus, bacterial model systems for ligand-gated ion channels (LGIC) are desirable, since LGICs represent a central component of both inter- and intracellular signaling in higher organisms (Hucho and Weise 2001; Li and Lester 2001).

A number of putative bacterial ligand-gated ion channels (LGICs) have been identified based on sequence similarity to mammalian nicotinic channels (Bocquet et al. 2007; Tasneem et al. 2005). However, it has not been possible to determine what, if any, small molecules are capable of gating these channels, and in some cases gating by other stimuli, such as protons, has been observed (Bocquet et al. 2007; Hilf and Dutzler 2009). This inability to look at function reduces the value of these channels as a model system and prevents the type of significant structure-function studies that have been possible for voltage-gated and mechanosensitive bacterial channels (Martinac et al. 2008). Other work has discovered a prokaryotic homologue of ionotropic glutamate receptors (Chen et al. 1999), GluR0, which has led to interesting insights into the ligand binding interactions in that family of channels (Mayer et al. 2001).

A ligand modulated bacterial ion channel, MloK1 (also called MlotiK1), that was recently cloned and characterized has provided detailed insights into how ligand binding can modulate channel activity (Altieri et al. 2008; Chiu et al. 2007; Clayton et al. 2004; Nimigean et al. 2004). MloK1 is a voltage-gated potassium channel that exhibits increased activity upon binding cyclic adenosine monophosphate (cAMP) in vesicle flux assays (Clayton et al. 2004; Nimigean and Pagel 2007; Nimigean et al. 2004). This interplay of multiple gating mechanisms is extremely important in complex mammalian channels. In fact, several mammalian channels exhibit cyclic nucleotide modulation in a mechanism similar to that observed for MloK1 (Finn et al. 1996). Unfortunately, despite extensive biochemical and crystallographic characterization of MloK1 (Altieri et al. 2008; Chiu et al. 2007; Clayton et al. 2004; Nimigean et al. 2004), researchers have not

been able to directly measure channel activity using electrophysiology. Moreover, MloK1 apparently is not gated by ligand alone.

Bacterial ion channels that are gated by a small molecule ligand and are amenable to electrophysiological characterization provide unique opportunities for considering LGIC structure-function relationships. Moreover, the existence of two families of bacterial ion channels, one gated by cyclic nucleotides and one modulated by cyclic nucleotides, would parallel the roles of cyclic nucleotide mediated channel responses in higher organisms (Finn et al. 1996).

Here we report the identification of a novel family of bacterial ligand-gated gated ion channels using bioinformatic methods. We have named this family the bacterial cyclic nucleotide gated (bCNG) ion channels, since we provide initial electrophysiological results demonstrating that these channels directly gate in response to cAMP binding. We also use osmotic downshock assays to demonstrate that these channels do not respond to membrane tension despite their significant homology to the mechanosesntive channel of small conductance (MscS). Since both MloK1 and bCNG channels are found in *M. loti*, the discovery of bCNG channels shows that bacteria may have channels that parallel the distinct classes of cyclic nucleotide gated and cyclic nucleotide modulated channels observed in Eukaryotes (Finn et al. 1996).

## *2.2 Methods*

### *2.2.1 Database mining*

An open reading frame in *Synechocystis sp.* PCC 6803, which displayed homology to both MscS and a cyclic nucleotide binding domain, was used as a starting point for database analysis. Open reading frames with significant sequence similarity to the *Synechocystis sp.* PCC 6803 open reading frame were identified using successive Blastp searches against the National Center for the Biotechnology Information (NCBI) nonredundant protein database (Altschul et al. 1997). The Blastp search parameters employed the BLOSUM 62 matrix, adjusted by a conditional compositional score matrix, with a gap existence penalty of 11 and a gap extension penalty of 1. Additionally, an expected threshold of 10 and a word size of 3 were utilized. The identified putative proteins were named according to their species name e.g.: *Azorhizobium caulinodans* ORS 571- bacterial Cyclic Nucleotide Gated Channel a (Ac-bCNGa). In these abbreviations, letters after names refer to different channels found in a single bacteria sub-species while numbers refer to channels found in different sub-species.

The initial search was conducted using the translated amino acid sequence from open reading frame NP_442904 (Ss-bCNGa). This resulted in ten putative proteins that had very similar sequences to both the channel domain and the binding domain of the search target. A secondary search of the NCBI database was then performed using the sequence from YP_553212 (Bx-bCNGa). This search gave an additional fifty-three proteins with sequence similarity to both the channel and binding domains of Ss-bCNGa. The NCBI database was also queried using the following target sequences, which displayed unique

features when compared to Ss-bCNGa and Bx-bCNGa: Te-bCNGa (NP_682526), Te-bCNGb (NP_681619), Ml-bCNG (NP_102658), Se-bCNG (YP_399683), Ss-bCNGb (NP_442515), Cw-bCNG (ZP_00513624), Cv-bCNG (NP_902000), Pf-bCNGa (YP_347599), Pf-bCNGb (YP_347700), and Rr-bCNG (NP_356350). However, these searches did not identify additional proteins in the bCNG family. Table 1 contains the channel name, accession number, species, numbers of amino acids, and predicted number of transmembrane domains for each channel.

| **Channel Identifier** | **NCBI Accession Number** | **Species Name** | **Number of Amino Acids** | **Predicted Number of Trans-membrane domains** |
|---|---|---|---|---|
| Ac-bCNGa | YP_001524558 | Azorhizobium caulinodans ORS 571 | 507 | 5 |
| Ac-bCNGb | YP_001526880 | Azorhizobium caulinodans ORS 571 | 473 | 5 |
| Ah-bCNG | YP_855012 | Aeromonas hydrophila subsp. hydrophila ATCC 7966 | 508 | 5 |
| Am-bCNGa | YP_001518669 | Acaryochloris marina MBIC11017 | 575 | 5 |
| Am-bCNGb | YP_001515745 | Acaryochloris marina MBIC11017 | 483 | 5 |
| As-bCNG | YP_001143394 | Aeromonas salmonicida subsp. salmonicida A449 | 508 | 5 |
| Bc-bCNG | YP_001774631 | Burkholderia cenocepacia MC0-3 | 493 | 5 |
| Bc-bCNG-2 | YP_621339 | Burkholderia cenocepacia AU 1054 | 493 | 5 |
| Bg-bCNGa | ZP_02883689 | Burkholderia graminis C4D1M | 489 | 5 |
| Bg-bCNGb | ZP_02882214 | Burkholderia graminis C4D1M | 485 | 5 |
| Bp-bCNG-2 | ZP_01503018 | Burkholderia phymatum STM815 | 528 | 5 |
| Bp-bCNGa | ZP_01507801 | Burkholderia phytofirmans PsJN | 485 | 5 |
| Bp-bCNGb | ZP_01507334 | Burkholderia phytofirmans PsJN | 489 | 5 |
| Bs-bCNG | ZP_02001194 | Beggiatoa sp. PS | 564 | 5 |
| Bx-bCNGa | YP_553214 | Burkholderia xenovorans LB400 | 489 | 4 |
| Bx-bCNGb | YP_555532 | Burkholderia xenovorans LB400 | 492 | 5 |

| | | | | |
|---|---|---|---|---|
| Bx-bCNGc | YP_552952 | Burkholderia xenovorans LB400 | 490 | 5 |
| Cs-bCNGa | ZP_01727527 | Cyanothece sp. CCY0110 | 493 | 3 |
| Cs-bCNGa-2 | YP_001803854 | Cyanothece sp. ATCC 51142 | 493 | 4 |
| Cs-bCNGb-2 | YP_001801906 | Cyanothece sp. ATCC 51142 | 480 | 3 |
| Cs-bCNGb-3 | EDT61489 | Cyanothece sp. PCC 8801 | 484 | 3 |
| Cv-bCNG | NP_902000 | Chromobacterium violaceum ATCC 12472 | 510 | 5 |
| Cw-bCNG | ZP_00513624 | Crocosphaera watsonii WH 8501 (Synechocystis sp. WH 8501) | 527 | 1 |
| Ha-bCNG | YP_001545478 | Herpetosiphon aurantiacus ATCC 23779 | 507 | 5 |
| Ls-bCNGa | ZP_01620793 | Lyngbya sp. PCC 8106 | 478 | 3 |
| Ls-bCNGb | ZP_01619992 | Lyngbya sp. PCC 8106 | 486 | 3 |
| Ma-bCNG | YP_882384 | Mycobacterium avium 104 | 473 | 5 |
| Me-bCNG | EDT54596 | Methylocella silvestris BL2 | 509 | 5 |
| Mg-bCNG | CAM74945 | Magnetospirillum gryphiswaldense MSR-1 | 482 | 3 |
| Ml-bCNG | NP_102658 | Mesorhizobium loti MAFF303099 | 410 | 2 |
| Mm-bCNGa | ZP_01688324 | Microscilla marina ATCC 23134 | 487 | 4 |
| Mm-bCNGb | ZP_01692178 | Microscilla marina ATCC 23134 | 525 | 5 |
| Ms-bCNG | YP_887882 | Mycobacterium smegmatis str. MC2 155 | 464 | 5 |
| Mu-bCNGa | YP_907297 | Mycobacterium ulcerans Agy99 | 466 | 5 |
| Mu-bCNGb | YP_907295 | Mycobacterium ulcerans Agy99 | 464 | 5 |
| Mx-bCNG | YP_631016 | Myxococcus xanthus DK 1622 | 525 | 5 |
| Pe-bCNG | YP_610798 | Pseudomonas entomophila L48 | 475 | 5 |
| Pf-bCNG-1 | YP_261168 | Pseudomonas fluorescens Pf-5 | 480 | 5 |
| Pf-bCNGa | YP_347599 | Pseudomonas fluorescens PfO-1 | 480 | 5 |
| Pf-bCNGb | YP_347700 | Pseudomonas fluorescens PfO-1 | 475 | 5 |
| Pm-bCNGa | NP_895973 | Prochlorococcus marinus str. MIT 931 | 496 | 5 |
| Pp-bCNG | NP_747357 | Pseudomonas putida KT2440 | 475 | 5 |
| Rd-bCNG | YP_682620 | Roseobacter denitrificans OCh 114 | 540 | 5 |
| Re-bCNGa | YP_470272 | Rhizobium etli CFN 42 | 493 | 5 |
| Rl-bCNGa | YP_771266 | Rhizobium leguminosarum bv. viciae 3841 | 506 | 5 |
| Rl-bCNGb | YP_768809 | Rhizobium leguminosarum bv. viciae 3841 | 493 | 5 |
| Rl-bCNGb-3 | ZP_02854402 | Rhizobium leguminosarum bv. trifolii WSM2304 | 492 | 5 |
| Rl-bCNGc-2 | ZP_02293400 | Rhizobium leguminosarum bv. trifolii WSM1325 | 501 | 5 |
| Rr-bCNG | NP_356350 | Agrobacterium tumefaciens str. C58 | 496 | 5 |
| Sa-bCNG | ZP_01463816 | Stigmatella aurantiaca DW4/3-1 | 502 | 4 |
| Sc-bCNG-1 | ZP_01079338 | Synechococcus sp. RS9917 | 489 | 5 |
| Sc-bCNG-2 | ZP_01083597 | Synechococcus sp. WH 5701 | 492 | 5 |
| Sc-bCNG-3 | ZP_01471350 | Synechococcus sp. RS9916 | 494 | 5 |

| | | | | |
|---|---|---|---|---|
| Sc-bCNG-4 | YP_001226119 | Synechococcus sp. WH 7803 | 465 | 4 |
| Se-bCNG | YP_399683 | Synechococcus elongatus PCC 7942 | 449 | 3 |
| Ss-bCNGa | NP_442904 | Synechocystis sp. PCC 6803 | 479 | 3 |
| Ss-bCNGb | NP_442515 | Synechocystis sp. PCC 6803 | 505 | 3 |
| Tb-bCNG | NP_216950 | Mycobacterium tuberculosis H37Rv | 481 | 5 |
| Te-bCNGa | NP_682526 | Thermosynechococcus elongatus BP-1 | 475 | 4 |
| Te-bCNGb | NP_681619 | Thermosynechococcus elongatus BP-1 | 594 | 6 |

**Table 2.1:** bCNG channels with sequence similarity to the third transmembrane domain (TM3) of MscS and known cyclic nucleotide binding domains identified in our bioinformatic analysis. The number of transmembrane domains for each putative bCNG channel was predicted using TMHMM (Krogh et al. 2001), DAS-TMFinder (Hofmann and Stoffel 1993), TMPred (Cserzo et al. 2002), and SOSUI (Hirokawa et al. 1998), as discussed in the text.

*2.2.2 Sequence selection*

Predicted proteins were compared to the *E. coli* MscS (NP_289491) and the binding domain of MloK1 (NP_104392, residues 235-341) (Wilbur and Lipman 1983; Myers and Miller 1988) using ClustalW2 to ensure that the sequences contained both a channel and binding domain. Sequences that did not contain a region analogous to the pore lining helix (TM3) of MscS or a complete cAMP binding cassette were eliminated. A complete cAMP binding cassette was defined by previously identified conserved domains (Marchler-Bauer et al. 2005; Marchler-Bauer et al. 2007) and the criteria outlined by Taylor and co-workers (Berman et al. 2005) and LaFranzo *et al* (LaFranzo et al. 2010).

In several cases, multiple channels were identified from different bacterial sub-species (eg. *Synechococcus sp.* WH 5701 and *Synechococcus sp.* WH 7803). While in some cases these represented unique channels, often the sub-species variants contained minimal

perturbations. As a result AMPS pairwise sequence alignments were used to eliminate channels with greater than 95% identity to other channels of the same species (Table 2.2).

Additionally, ZP_02295598 was eliminated since it is 95% identical to Rl-bCNGb (YP_768809) in the first 400 amino acids. The significant differences observed in the binding domain of this channel (residues 388-435) are potentially the result of sequencing errors. A pairwise alignment of the two nucleotide sequences showed several single base insertions, typically in guanosine rich regions (at nucleotides 1171, 1206, 1233, and 1263). If these mutations are not the result of a sequence error, then these mutations would likely render the binding domain non-functional.

| NCBI Accession Number | Similar Channel | Percent Identity | Species Name | Number of Amino Acids |
|---|---|---|---|---|
| YP_171574 | Se-bCNG | 100% | Synechococcus elongatus PCC 6301 (Synechococcus leopoliensis SAG 1402-1) | 450 |
| YP_001671525 | Pp-bCNG | 90.4 | Pseudomonas putida GB-1 | 508 |
| YP_001270468 | Pp-bCNG | 98.5 | Pseudomonas putida F1 | 475 |
| ZP_02297645 | Rl-bCNGa | 95.06 | Rhizobium leguminosarum bv. trifolii WSM1325 | 506 |
| ZP_02295598 | Rl-bCNGb | 89.02 | Rhizobium leguminosarum bv. trifolii WSM1325 | 435 |

**Table 2.2:** bCNG channels eliminated from analyses because of high percent identity with another sequence from the same bacterial strain.

Finally, YP_001671525 was eliminated due to 96.6% identity in a 475 amino acid overlapping segment with Pp-bCNG. However, YP_001671525 contains an additional

thirty-three amino acids on the N-terminus of the protein, which is not observed in Pp-bCNG and is not homologous with other bCNG channels.

In the case of YP_553214, Bx-bCNGa, we altered the encoded protein domain. In the NCBI database, the protein is 489 amino acids, however, there is no ATG start codon at the 5' end of the gene. To compensate for this, the first 9 amino acids were eliminated from the N-terminus of the gene to give the use the first infame ATG startcodon.

*2.2.3 Sequence analysis*

A final sequence alignment of all bCNG channels, MscS, and the binding domain of MloK1 (Figure 2.1) was prepared using AMPS (Alignment of Multiple Protein Sequences) (Barton 1990). The AMPS alignment was carried out with 100 iterations using the BLOSUM 62 matrix and a gap existence penalty of 10. A MEME analysis of all sequences in the AMPS alignment was conducted to determine regions of high sequence similarity (Bailey and Elkan 1994). MEME parameters were as follows: a maximum of 10 motifs, a minimum of 6 residues per motif, a maximum of 50 residues per motif, and either zero or one repeat motif per sequence. Slight adjustments to the AMPS alignment were made manually based on the MEME results. Additionally, the TREE function of AMPS was used to examine the evolutionary distance between MloK1 and the bCNG family of ion channels (Figure 2.3).

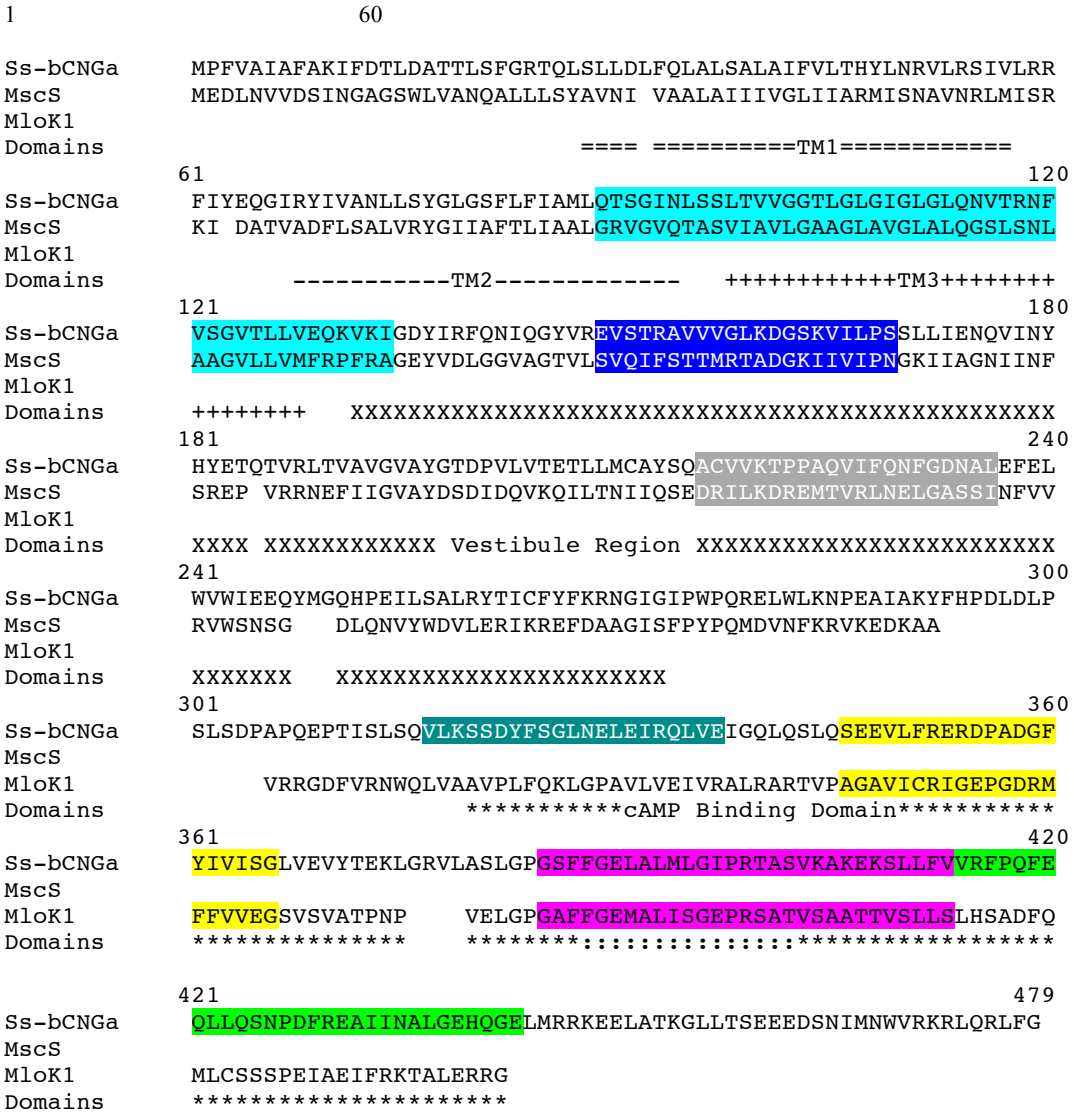


**Figure 2.1**. Alignment of Ss-bCNGa with MscS and the cNMP binding domain of MloK1. The three transmembrane domains of MscS (=,-,+), the vestibule region of MscS (X), the cAMP binding domain (*), and phosphate binding cassette (:) are indicated on the alignment. Highlighted regions of the alignment depict the MEME blocks in these sequences that were found in the analysis of all bCNG sequences given in Figure 2.2. Note that three of the ten conserved MEME blocks found in other members of the family were not present in these sequences.


1
120
Pp-bCNG MLAFIQSSPLLLGCALILLDLVLWQLIPIQ RHAWRISARLVI FLLFSSVLMAAGMSPLQP
Pe-bCNG MLAFIQSSPLLLGTALIFLDLLLWHLIPLE RRAWRIASRLAI FLLFSWVLLAAGMSPLQP
Pf-bCNGb MSLFSAHLLSWSALLLVLDTLLWHLAPFK HRAQRVAVRLVL FLAFNALAINAGVSPLQA
Pf-bCNGa MLSLLTDHPLFCALILILVDLGLWRLISAH GSAWKLLVRVLI FALFSILLFNEGLNPMEP
Pf-bCNG-1 MSSLFSDHPLLAALFLLFLDMLLWRLIGSR GDYWKLAVRVLI FSLYSLMLFNQGMNPMQA
Bp-bCNG-2 MCSDGCMGRAVMPRDGGRATVAANALHVLSTVQPRYGVCVNNPLIFGFALVAFDVAIWRCAIPK NEVARLLVRLCV YAALSSLLFNSGLSPFSK
Bg-bCNGb MSDSLVFGYAVVLIDVALWRFKVPK QDVSRLLLRLAI FAVFTASIFTAGLSPFRQ
Bp-bCNGa MSDSLVFGYAVVVIDVALWRFKVPK KDASRLLLRLTI FAVFTASIFAAGFSPFRQ
Bg-bCNGa MPTLTDGVLYGLGILVLDFLAWRFMGRR SEQARLALRALM FGLSSYVLFSHGMNPLRE
Bx-bCNGc MPTLTDGVLFGLAILVLDFLAWRFMSRK SDQTRLVFRALM FALSSYVLFSYGMNPLRA
Bp-bCNGb MPTLNDGVLYGLGILVLDFLAWRFMTRK TDKGRLALRALM FGLSTYVLFSHGMNPLRA
Bc-bCNG MLNFSDTALYGAPIVLADLAAWRLFGRD RSVARAIRRCAA FAALSAVLFATGVSPLAV
Bc-bCNG-2 MLNFSDTALYGAPIVLADLAAWRLVGRD RAVARAIRRCAA FAALTAVLFATGVSPLAV
Bx-bCNGb MPANLLLHMAPSCLAAALNLLLVLLGMPN RLVIRTIGRCAA FALLTAAMLHDGMVPTQA
Rl-bCNGa MLDNVTWSGVLADPVVQAGTLAVVGAIVTRIALRP FPSWKLAGQVFF FAALTVLLLYHDIVPYEV
Re-bCNGa MIYDALFGKPLISLIVVGFAGILVWYFLSSQ RPTTRLVVQILF FAVMTLILVGSGIEPHRF
Rl-bCNGb MIDDALFGKPLISLITVGFAGIVVWHLLSRH RPTTRLVVQILF FAVMTLILVGSGIEPHRF
Rl-bCNGb-3 MIYDALFGKPLISLITVGFAGIVVWHLLSRQ RPTTRLVVQIVF FGLMTLILVGSGIEPHRF
Rr-bCNG MLQAYMGEIAAAPLAWLIILGLAGMAVWKRIGSQ RSNLRLVVQIAF FGAMTSVLVLGKIPLGPP
Rl-bCNGc-2 MVGFSSIVGDPIAQFAALVALTMIARLLARG HSATRFAANVMF FALLTVLLVANKVAPWNG
Ac-bCNGa MISGGTGLADELRLLIADPMVPTAVAALAVALGLRLALRDRPWPHLIGQVAL LTLLTALLTSEGIVPYEA
Me-bCNG MTMAEMQPAQLFSLIAEHSDIAVMAAALGLGCISLAILALRRDAMWRLAGRIGS FVALTAALASQGIQPYQP
Ml-bCNG
Bx-bCNGa MNLTLLSAAMLVAITLVGVLGLRRFP DKVRITFDVCC FLVISFYFHKQGIFFPVF
Bs-bCNG MLNPTLGWSVEKIGFFQAIAERYSLGDPDYLNVQNGKVEYSQFNVVVHIKRNELTPRGKIDPKYAYYLMILSSIFILLLNIISKKFRQWSKWVWFFQVILAIILLLSGEVLLV
Sa-bCNG MERLGQSFRALLPFLQSNVSLVVGVVLALLLAGA RALSADKDFRRD LLGAFRFLLAFFVFRIAA
Mx-bCNG MARVSPLTRHASTAALTPMEMAGDIPPALLPFLQSNLSLAVGALLIVVLMGVRAAAQDADLRQ DLKSANRLLIAFIVLRLAT
Sc-bCNG-1 MALLLSLFAIGSLLGLQRVCRTRNLTP PPLRLPLIAA IAIPVLTLMVAILEQSRL
Sc-bCNG-3 MTLLLSLVAIVSLLALHRVCKRQKLSP PPLRMPLIAA VAIPALTLISERVSFSGL
Pm-bCNGa MTFGLRLITTILITLLLTVSHQRNLLSSRWP KPPVRLPVLALL LWVGTALPFLEKIISKQA
Sc-bCNG-2 MPLLEVWVTAIVTMVLLLPLQLLIRRLRLP KLPIQMATLAI LSWAVVRTLPLILLPAHY
Cv-bCNG MDTPPAVGWLEKLIPAVWYGSLTVFVAVTAA FSILLYLTRADS RKRVLRTQLIVLIALLVV
Ah-bCNG MFSDNLVALPTLLWIGEHPFWTLLTLFLLFTHFL RSPGRRRELVSE LGFVMISLVVILLIQFEG
As-bCNG MFSDNFVALPTLQWIGEHPFWTLLTLFLLITHFL RSPGRRRELISE LGFVMMSMVVILLIQFEG
Rd-bCNG MLNRATRGINPEPHSVVSMKDAIDRGRFGKGTLVNFLSSFEMLDGNFAISLSIALLTIAWLGLKLFFRKVPLGERYPKLAVTADLVVLPLATLLVG
Am-bCNGb MTSSLLQQSWFLWSCGLMVGFPCLMLVLNESI VYTQKQGKPLVHT LRILRNLVLPIFVGFIVL
Mu-bCNGb MSVFGSAWFYWAVGIAAALPVLVVILTEVQRLLR RRQSALARQVGL LRNYVLPLGALLLLLVNA
Mu-bCNGa MNVLGASWFHWAIGIAIGVPVDLILLTELHNSLA RRNSHLARQVTL LRNFLLPLGALLLFLVKA
Tb-bCNG MNLLDSTWFYWAVGIAIGLPAGLIVLTELHNILV RRNSHLARQASL LRNYLLPLGAVLLLLVKA
Ma-bCNG MSTFDSSSLYWATAVVFGLPLLLIVLTEWHQSLV RKHSPLARPAFL LRSYLIPLGALLVLLVNV
Ms-bCNG MRSVLEANWFYWALSVAVGLPIGLVLLTELHNTLA RHGSYLARPVSL LRNYILPLAALLILLVKG
Ac-bCNGb MLSAQIAQEVPWTILIVLGFPLLTVLLIELTRRF AGPDSAARRP IKALQMIVVPAGAVWIIV
Mm-bCNGa MKTSKLHQFVLPVLLTASFVISWLIRNEI IHYAGLPKAKL WLEIADDILLTGLWLSTA
Mg-bCNG MRSSARVLAPLVLRLGFPLALLAVMVVVRLR WEAQAWASQWD AAILESIETGLAIGQWIA
Te-bCNGb MTKYLGLFLAAAPASILIAQVARTQRLWVAFIEAVQIMGIVAIAILADWLLLNLGIHQLQQRLHQKASQQSQPWLSLGASLLRLTLRILLWS FVLSWILQSAQSLSPWHE
Am-bCNGa MTLFAVDVHFLKNLFIVVGILGGAAISDWLMGRWMQGRLRTAPKKGRAIYPLLRRCLLFGLRLGIWLVAFYNILTLIPALQPIRQLFI
Se-bCNG MDLFDRLEQWTSTPLLRLGSSQIS LGSLILLAVLAGLLLYLM

```
Ls-bCNGb                                    MKIIENILQFLSRVFTQPIFLGGI                SISLSSI            FTILVAFFAVVISSRYLS
Cs-bCNGa-2                                    MFNLQGIFNNLISILDSITFSI                GKNEVTLTYL           FQVIAYLIIIAILANYLN
Cs-bCNGa                                      MFNLQGIFNNIISILDSITFSI                GKNEVTLTYF           FQVIFYLIIIAILASYLN
Ss-bCNGa                                      MPFVAIAFAKIFDTLDATTLSF                GRTQLSLLDL           FQLALSALAIFVLTHYLN
Te-bCNGa                                    MPSQVIELWSLFIGIVDAPLFRL                 GRETISLRWL           LQVVLLLILVAILARFFK
Cs-bCNGb-2                                  MPAYWSLFKQWFHSTFSTPLFNI                 GGEAISILWM           LKAILLLILVSILARSIK
Cs-bCNGb-3                                MPNSISWSIIQAWFSQTLTTPLFTI                 GVENISLLWI           IQVIVLLIIVSIIARAIK
Ss-bCNGb                                   MIAQINPPPQGPGPQAIANVLEQ                    WHFLNIWL           FETLNTPIFKLGTESITL
Cw-bCNG                                 MLEQGIHLISTDEMTGIQALERLFPNKRIKPKQVEKIEFEYERHGTLSLIAN           WDVARGKVVSPSIGPTRT
Ls-bCNGa                                    MLFANIGELAVNFSFLSEPLFKI                 GNKPISSLAV           INLTISLLIAILISRLFK
Ha-bCNG                                   MLSVIEHIIQPMLWAIGTYAVLRLLIRL            GRRIGLISGLSI           LGQFLALSSAGLIGLWSD
Sc-bCNG-4                                   MLFFRIALTAAVLSRLLLMFE                  QQGEVLVW             LRLVESAALYVAFVEFSL
Mm-bCNGb                                MELSTFYSLLMIAGFYAMVVVILYIMWSIAQKL          KVPQKSKRIVFL           FFILLGLAVASPLREIWF
MscS                                        MEDLNVVDSINGAGSWLVANQAL                 LLSYAVNI            VAALAIIIVGLIIARMIS
MloK1
MscS Domains                                                                          ====                ==========TM1=====
```

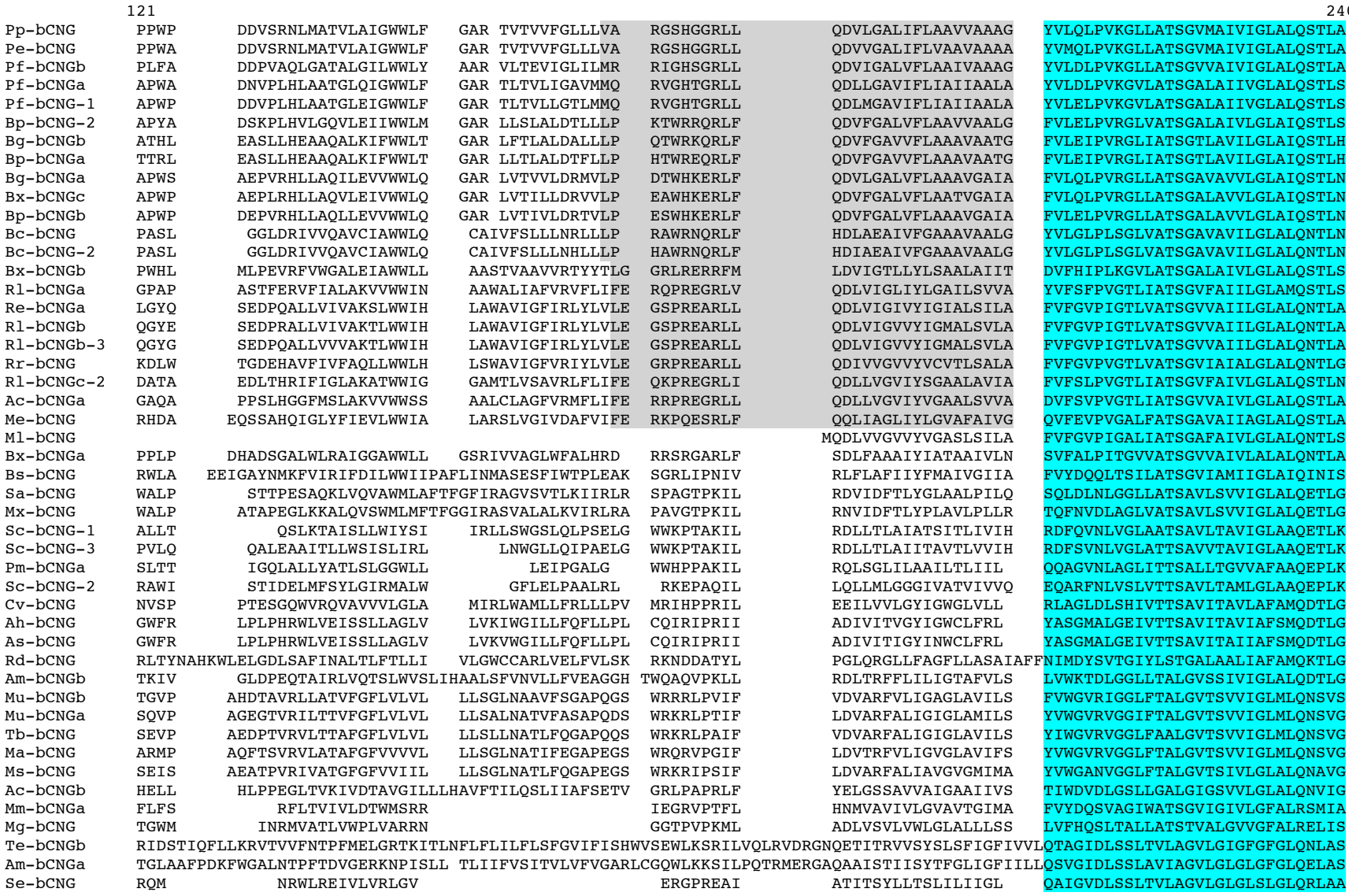
121
240
Pp-bCNG PPWP DDVSRNLMATVLAIGWWLF GAR TVTVVFGLLLVA RGSHGGRLL QDVLGALIFLAAVVAAAG YVLQLPVKGLLATSGVMAIVIGLALQSTLA
Pe-bCNG PPWA DDVSRNLMATVLAIGWWLF GAR TVTVVFGLLLVA RGSHGGRLL QDVVGALIFLVAAVAAAA YVMQLPVKGLLATSGVMAIVIGLALQSTLA
Pf-bCNGb PLFA DDPVAQLGATALGILWWLY AAR VLTEVIGLILMR RIGHSGRLL QDVIGALVFLAAIVAAAG YVLDLPVKGLLATSGVVAIVIGLALQSTLA
Pf-bCNGa APWA DNVPLHLAATGLQIGWWLF GAR TLTVLIGAVMMQ RVGHTGRLL QDLLGAVIFLIAIIAALA YVLDLPVKGVLATSGALAIIVGLALQSTLS
Pf-bCNG-1 APWP DDVPLHLAATGLEIGWWLF GAR TLTVLLGTLMMQ RVGHTGRLL QDLMGAVIFLIAIIAALA YVLELPVKGVLATSGALAIIVGLALQSTLS
Bp-bCNG-2 APYA DSKPLHVLGQVLEIIWWLM GAR LLSLALDTLLLP KTWRRQRLF QDVFGALVFLAAVVAALG FVLELPVRGLVATSGALAIVLGLAIQSTLS
Bg-bCNGb ATHL EASLLHEAAQALKIFWWLT GAR LFTLALDALLLP QTWRKQRLF QDVFGAVVFLAAAVAATG FVLEIPVRGLIATSGTLAVILGLAIQSTLH
Bp-bCNGa TTRL EASLLHEAAQALKIFWWLT GAR LLTLALDTFLLP HTWREQRLF QDVFGAVVFLAAAVAATG FVLEIPVRGLIATSGTLAVILGLAIQSTLH
Bg-bCNGa APWS AEPVRHLLAQILEVVWWLQ GAR LVTVVLDRMVLP DTWHKERLF QDVLGALVFLAAAVGAIA FVLQLPVRGLLATSGAVAVVLGLAIQSTLN
Bx-bCNGc APWP AEPLRHLLAQVLEIVWWLQ GAR LVTILLDRVVLP EAWHKERLF QDVFGALVFLAATVGAIA FVLQLPVRGLLATSGALAVVLGLAIQSTLN
Bp-bCNGb APWP DEPVRHLLAQLLEVVWWLQ GAR LVTIVLDRTVLP ESWHKERLF QDVFGALVFLAAAVGAIA FVLELPVRGLLATSGALAVVLGLAIQSTLN
Bc-bCNG PASL GGLDRIVVQAVCIAWWLQ CAIVFSLLLNRLLLP RAWRNQRLF HDLAEAIVFGAAAVAALG YVLGLPLSGLVATSGAVAVILGLALQNTLN
Bc-bCNG-2 PASL GGLDRIVVQAVCIAWWLQ CAIVFSLLLNHLLLP HAWRNQRLF HDIAEAIVFGAAAVAALG YVLGLPLSGLVATSGAVAVILGLALQNTLN
Bx-bCNGb PWHL MLPEVRFVWGALEIAWWLL AASTVAAVVRTYYTLG GRLRERRFM LDVIGTLLYLSAALAIIT DVFHIPLKGVLATSGALAIVLGLALQSTLS
Rl-bCNGa GPAP ASTFERVFIALAKVVWWIN AAWALIAFVRVFLIFE RQPREGRLV QDLVIGLIYLGAILSVVA YVFSFPVGTLIATSGVFAIILGLAMQSTLS
Re-bCNGa LGYQ SEDPQALLVIVAKSLWWIH LAWAVIGFIRLYLVLE GSPREARLL QDLVIGIVYIGIALSILA FVFGVPIGTLVATSGVVAIILGLALQNTLA
Rl-bCNGb QGYE SEDPRALLVIVAKTLWWIH LAWAVIGFIRLYLVLE GSPREARLL QDLVIGVVYIGMALSVLA FVFGVPIGTLVATSGVVAIILGLALQNTLA
Rl-bCNGb-3 QGYG SEDPQALLVVVAKTLWWIH LAWAVIGFIRLYLVLE GSPREARLL QDLVIGVVYIGMALSVLA FVFGVPIGTLVATSGVVAIILGLALQNTLA
Rr-bCNG KDLW TGDEHAVFIVFAQLLWWLH LSWAVIGFVRIYLVLE GRPREARLL QDIVVGVVYVCVTLSALA FVFGVPVGTLVATSGVIAIALGLALQNTLG
Rl-bCNGc-2 DATA EDLTHRIFIGLAKATWWIG GAMTLVSAVRLFLIFE QKPREGRLI QDLLVGVIYSGAALAVIA FVFSLPVGTLIATSGVFAIVLGLALQSTLN
Ac-bCNGa GAQA PPSLHGGFMSLAKVVWWSS AALCLAGFVRMFLIFE RRPREGRLL QDLLVGVIYVGAALSVVA DVFSVPVGTLIATSGVVAIVLGLALQSTLA
Me-bCNG RHDA EQSSAHQIGLYFIEVLWWIA LARSLVGIVDAFVIFE RKPQESRLF QQLIAGLIYLGVAFAIVG QVFEVPVGALFATSGAVAIIAGLALQSTLA
Ml-bCNG MQDLVVGVVYVGASLSILA FVFGVPIGALIATSGAFAIVLGLALQNTLS
Bx-bCNGa PPLP DHADSGALWLRAIGGAWWLL GSRIVVAGLWFALHRD RRSRGARLF SDLFAAAIYIATAAIVLN SVFALPITGVVATSGVVAIVLALALQNTLA
Bs-bCNG RWLA EEIGAYNMKFVIRIFDILWWIIPAFLINMASESFIWTPLEAK SGRLIPNIV RLFLAFIIYFMAIVGIIA FVYDQQLTSILATSGVIAMIIGLAIQINIS
Sa-bCNG WALP STTPESAQKLVQVAWMLAFTFGFIRAGVSVTLKIIRLR SPAGTPKIL RDVIDFTLYGLAALPILQ SQLDLNLGGLLATSAVLSVVIGLALQETLG
Mx-bCNG WALP ATAPEGLKKALQVSWMLMFTFGGIRASVALALKVIRLRA PAVGTPKIL RNVIDFTLYPLAVLPLLR TQFNVDLAGLVATSAVLSVVIGLALQETLG
Sc-bCNG-1 ALLT QSLKTAISLLWIYSI IRLLSWGSLQLPSELG WWKPTAKIL RDLLTLAIATSITLIVIH RDFQVNLVGLAATSAVLTAVIGLAAQETLK
Sc-bCNG-3 PVLQ QALEAAITLLWSISLIRL LNWGLLQIPAELG WWKPTAKIL RDLLTLAIITAVTLVVIH RDFSVNLVGLATTSAVVTAVIGLAAQETLK
Pm-bCNGa SLTT IGQLALLYATLSLGGWLL LEIPGALG WWHPPAKIL RQLSGLILAAILTLIIL QQAGVNLAGLITTSALLTGVVAFAAQEPLK
Sc-bCNG-2 RAWI STIDELMFSYLGIRMALW GFLELPAALRL RKEPAQIL LQLLMLGGGIVATVIVVQ EQARFNLVSLVTTSAVLTAMLGLAAQEPLK
Cv-bCNG NVSP PTESGQWVRQVAVVVLGLA MIRLWAMLLFRLLLPV MRIHPPRIL EEILVVLGYIGWGLVLL RLAGLDLSHIVTTSAVITAVLAFAMQDTLG
Ah-bCNG GWFR LPLPHRWLVEISSLLAGLV LVKIWGILLFQFLLPL CQIRIPRII ADIVITVGYIGWCLFRL YASGMALGEIVTTSAVITAVIAFSMQDTLG
As-bCNG GWFR LPLPHRWLVEISSLLAGLV LVKVWGILLFQFLLPL CQIRIPRII ADIVITIGYINWCLFRL YASGMALGEIVTTSAVITAIIAFSMQDTLG
Rd-bCNG RLTYNAHKWLELGDLSAFINALTLFTLLI VLGWCCARLVELFVLSK RKNDDATYL PGLQRGLLFAGFLLASAIAFFNIMDYSVTGIYLSTGALAALIAFAMQKTLG
Am-bCNGb TKIV GLDPEQTAIRLVQTSLWVSLIHAALSFVNVLLFVEAGGH TWQAQVPKLL RDLTRFFLILIGTAFVLS LVWKTDLGGLLTALGVSSIVIGLALQDTLG
Mu-bCNGb TGVP AHDTAVRLLATVFGFLVLVL LLSGLNAAVFSGAPQGS WRRRLPVIF VDVARFVLIGAGLAVILS FVWGVRIGGLFTALGVTSVVIGLMLQNSVS
Mu-bCNGa SQVP AGEGTVRILTTVFGFLVLVL LLSALNATVFASAPQDS WRKRLPTIF LDVARFALIGIGLAMILS YVWGVRVGGIFTALGVTSVVIGLMLQNSVG
Tb-bCNG SEVP AEDPTVRVLTTAFGFLVLVL LLSLLNATLFQGAPQQS WRKRLPAIF VDVARFALIGIGLAVILS YIWGVRVGGLFAALGVTSVVIGLMLQNSVG
Ma-bCNG ARMP AQFTSVRVLATAFGFVVVVL LLSGLNATIFEGAPEGS WRQRVPGIF LDVTRFVLIGVGLAVIFS YVWGVRVGGLFTALGVTSVVIGLMLQNSVG
Ms-bCNG SEIS AEATPVRIVATGFGFVVIIL LLSGLNATLFQGAPEGS WRKRIPSIF LDVARFALIAVGVGMIMA YVWGANVGGLFTALGVTSIVLGLALQNAVG
Ac-bCNGb HELL HLPPEGLTVKIVDTAVGILLLHAVFTILQSLIIAFSETV GRLPAPRLF YELGSSAVVAIGAAIIVS TIWDVDLGSLLGALGIGSVVLGLALQNVIG
Mm-bCNGa FLFS RFLTVIVLDTWMSRR IEGRVPTFL HNMVAVIVLGVAVTGIMA FVYDQSVAGIWATSGVIGIVLGFALRSMIA
Mg-bCNG TGWM INRMVATLVWPLVARRN GGTPVPKML ADLVSVLVWLGLALLLSS LVFHQSLTALLATSTVALGVVGFALRELIS
Te-bCNGb RIDSTIQFLLKRVTVVFNTPFMELGRTKITLNFLFLILFLSFGVIFISHWVSEWLKSRILVQLRVDRGNQETITRVVSYSLSFIGFIVVLQTAGIDLSSLTVLAGVLGIGFGFGLQNLAS
Am-bCNGa TGLAAFPDKFWGALNTPFTDVGERKNPISLL TLIIFVSITVLVFVGARLCGQWLKKSILPQTRMERGAQAAISTIISYTFGLIGFIILLQSVGIDLSSLAVIAGVLGLGLGFGLQELAS
Se-bCNG RQM NRWLREIVLVRLGV ERGPREAI ATITSYLLTSLILIIGL QAIGVDLSSLTVLAGVLGLGLSLGLQRLAA

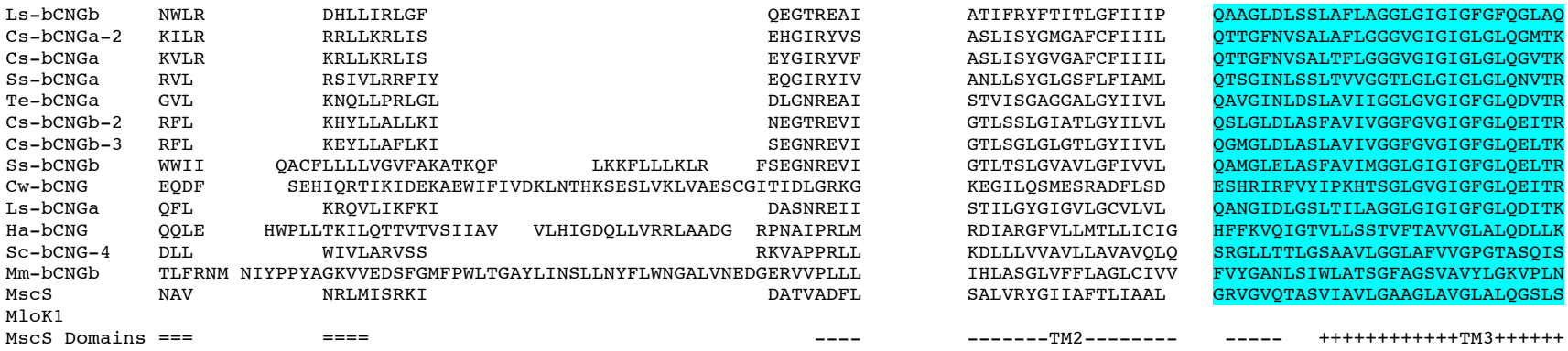
Ls-bCNGb NWLR DHLLIRLGF QEGTREAI ATIFRYFTITLGFIIIP QAAGLDLSSLAFLAGGLGIGIGFGFQGLAQ
Cs-bCNGa-2 KILR RRLLKRLIS EHGIRYVS ASLISYGMGAFCFIIIL QTTGFNVSALAFLGGGVGIGIGLGLQGMTK
Cs-bCNGa KVLR KRLLKRLIS EYGIRYVF ASLISYGVGAFCFIIIL QTTGFNVSALTFLGGGVGIGIGLGLQGVTK
Ss-bCNGa RVL RSIVLRRFIY EQGIRYIV ANLLSYGLGSFLFIAML QTSGINLSSLTVVGGTLGLGIGLGLQNVTR
Te-bCNGa GVL KNQLLPRLGL DLGNREAI STVISGAGGALGYIIVL QAVGINLDSLAVIIGGLGVGIGFGLQDVTR
Cs-bCNGb-2 RFL KHYLLALLKI NEGTREVI GTLSSLGIATLGYILVL QSLGLDLASFAVIVGGFGVGIGFGLQEITR
Cs-bCNGb-3 RFL KEYLLAFLKI SEGNREVI GTLSGLGLGTLGYIIVL QGMGLDLASLAVIVGGFGVGIGFGLQELTK
Ss-bCNGb WWII QACFLLLLVGVFAKATKQF LKKFLLLKLR FSEGNREVI GTLTSLGVAVLGFIVVL QAMGLELASFAVIMGGLGIGIGFGLQELTR
Cw-bCNG EQDF SEHIQRTIKIDEKAEWIFIVDKLNTHKSESLVKLVAESCGITIDLGRKG KEGILQSMESRADFLSD ESHRIRFVYIPKHTSGLGVGIGFGLQEITR
Ls-bCNGa QFL KRQVLIKFKI DASNREII STILGYGIGVLGCVLVL QANGIDLGSLTILAGGLGIGIGFGLQDITK
Ha-bCNG QQLE HWPLLTKILQTTVTVSIIAV VLHIGDQLLVRRLAADG RPNAIPRLM RDIARGFVLLMTLLICIG HFFKVQIGTVLLSSTVFTAVVGLALQDLLK
Sc-bCNG-4 DLL WIVLARVSS RKVAPPRLL KDLLLVVAVLLAVAVQLQ SRGLLTTLGSAAVLGGLAFVVGPGTASQIS
Mm-bCNGb TLFRNM NIYPPYAGKVVEDSFGMFPWLTGAYLINSLLNYFLWNGALVNEDGERVVPLLL IHLASGLVFFLAGLCIVV FVYGANLSIWLATSGFAGSVAVYLGKVPLN
MscS NAV NRLMISRKI DATVADFL SALVRYGIIAFTLIAAL GRVGVQTASVIAVLGAAGLAVGLALQGSLS
MloK1
MscS Domains === ==== ---- -------TM2-------- ----- ++++++++++TM3++++++

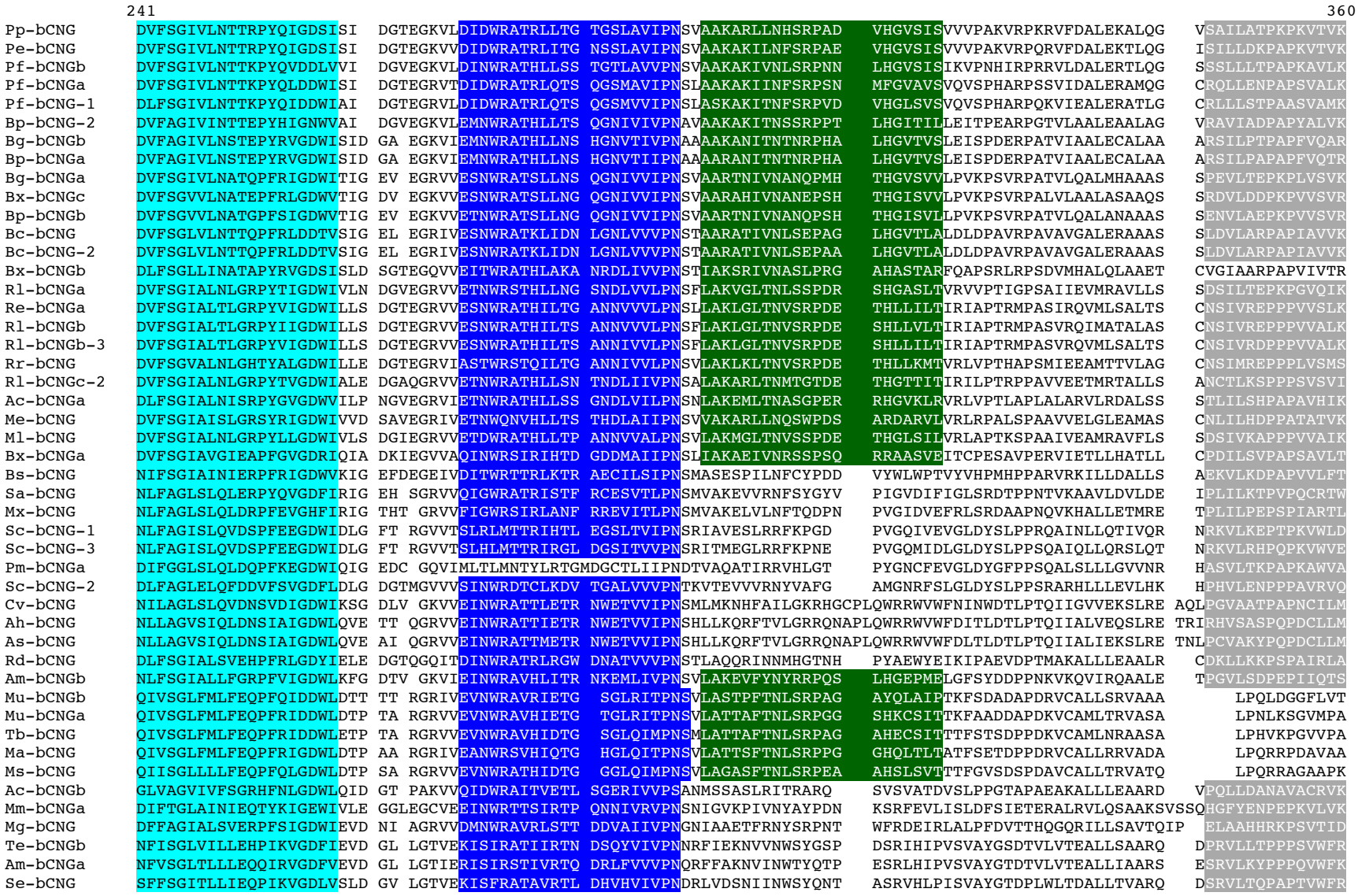
241
360
Pp-bCNG DVFSGIVLNTTRPYQIGDSISI DGTEGKVLDIDWRATRLLTG TGSLAVIPNSVAAKARLLNHSRPAD VHGVSISVVVPAKVRPKRVFDALEKALQG VSAILATPKPKVTVK
Pe-bCNG DVFSGIVLNTTRPYQIGDSISI DGTEGKVVDIDWRATRLITG NSSLAVIPNSVAAKAKILNFSRPAE VHGVSISVVVPAKVRPQRVFDALEKTLQG ISILLDKPAPKVTVK
Pf-bCNGb DVFSGIVLNTTKPYQVDDLVVI DGVEGKVLDINWRATHLLSS TGTLAVVPNSVAAKAKIVNLSRPNN LHGVSISIKVPNHIRPRRVLDALERTLQG SSSLLLTPAPKAVLK
Pf-bCNGa DVFSGIVLNTTKPYQLDDWISI DGTEGRVTDIDWRATRLQTS QGSMAVIPNSLAAKAKIINFSRPSN MFGVAVSVQVSPHARPSSVIDALERAMQG CRQLLENPAPSVALK
Pf-bCNG-1 DLFSGIVLNTTKPYQIDDWIAI DGTEGRVLDIDWRATRLQTS QGSMVVIPNSLASKAKITNFSRPVD VHGLSVSVQVSPHARPQKVIEALERATLG CRLLLSTPAASVAMK
Bp-bCNG-2 DVFAGIVINTTEPYHIGNWVAI DGVEGKVLEMNWRATHLLTS QGNIVIVPNAVAAKAKITNSSRPPT LHGITILLEITPEARPGTVLAALEAALAG VRAVIADPAPYALVK
Bg-bCNGb DVFAGIVLNSTEPYRVGDWISID GA EGKVIEMNWRATHLLNS HGNVTIVPNAAAAKANITNTNRPHA LHGVTVSLEISPDERPATVIAALECALAA ARSILPTPAPFVQAR
Bp-bCNGa DVFAGIVLNSTEPYRVGDWISID GA EGKVIEMNWRATHLLNS HGNVTIIPNAAAARANITNTNRPHA LHGVTVSLEISPDERPATVIAALECALAA ARSILPAPAPFVQTR
Bg-bCNGa DVFSGIVLNATQPFRIGDWITIG EV EGRVVESNWRATSLLNS QGNIVVIPNSVAARTNIVNANQPMH THGVSVVLPVKPSVRPATVLQALMHAAAS SPEVLTEPKPLVSVK
Bx-bCNGc DVFSGVVLNATEPFRLGDWVTIG DV EGKVVESNWRATSLLNG QGNIVVIPNSVAARAHIVNANEPSH THGISVVLPVKPSVRPALVLAALASAAQS SRDVLDDPKPVVSVR
Bp-bCNGb DVFSGVVLNATGPFSIGDWVTIG EV EGKVVETNWRATSLLNG QGNIVVIPNSVAARTNIVNANQPSH THGISVLLPVKPSVRPATVLQALANAAAS SENVLAEPKPVVSVR
Bc-bCNG DVFSGLVLNTTQPFRLDDTVSIG EL EGRIVESNWRATKLIDN LGNLVVVPNSTAARATIVNLSEPAG LHGVTLALDLDPAVRPAVAVGALERAAAS SLDVLARPAPIAVVK
Bc-bCNG-2 DVFSGLVLNTTQPFRLDDTVSIG EL EGRIVESNWRATKLIDN LGNLVVVPNSTAARATIVNLSEPAA LHGVTLALDLDPAVRPAVAVGALERAAAS SLDVLARPAPIAVVK
Bx-bCNGb DLFSGLLINATAPYRVGDSISLD SGTEGQVVEITWRATHLAKA NRDLIVVPNSTIAKSRIVNASLPRG AHASTARFQAPSRLRPSDVMHALQLAAET CVGIAARPAPVIVTR
Rl-bCNGa DVFSGIALNLGRPYTIGDWIVLN DGVEGRVVETNWRSTHLLNG SNDLVVLPNSFLAKVGLTNLSSPDR SHGASLTVRVVPTIGPSAIIEVMRAVLLS SDSILTEPKPGVQIK
Re-bCNGa DVFSGIALTLGRPYVIGDWILLS DGTEGRVVESNWRATHILTG ANNVVVLPNSLLAKLGLTNVSRPDE THLLILTIRIAPTRMPASIRQVMLSALTS CNSIVREPPPVVSLK
Rl-bCNGb DVFSGIALTLGRPYIIGDWILLS DGTEGRVVESNWRATHILTS ANNVVVLPNSFLAKLGLTNVSRPDE SHLLVLTIRIAPTRMPASVRQIMATALAS CNSIVREPPPVVALK
Rl-bCNGb-3 DVFSGIALTLGRPYVIGDWILLS DGTEGRVVESNWRATHILTS ANNIVVLPNSFLAKLGLTNVSRPDE SHLLILTIRIAPTRMPASVRQVMLSALTS CNSIVRDPPPVVALK
Rr-bCNG DVFSGVALNLGHTYALGDWILLE DGTEGRVIASTWRSTQILTG ANNIVVLPNSVLAKLKLTNVSRPDE THLLKMTVRLVPTHAPSMIEEAMTTVLAG CNSIMREPPPLVSMS
Rl-bCNGc-2 DVFSGIALNLGRPYTVGDWIALE DGAQGRVVETNWRATHLLSN TNDLIIVPNSALAKARLTNMTGTDE THGTTITIRILPTRPPAVVEETMRTALLS ANCTLKSPPPSVSVI
Ac-bCNGa DLFSGIALNISRPYGVGDWVILP NGVEGRVIETNWRATHLLSS GNDLVILPNSNLAKEMLTNASGPER RHGVKLRVRLVPTLAPLALARVLRDALSS STLILSHPAPAVHIK
Me-bCNG DVFSGIAISLGRSYRIGDWIVVD SAVEGRIVETNWQNVHLLTS THDLAIIPNSVVAKARLLNQSWPDS ARDARVLVRLRPALSPAAVVELGLEAMAS CNLILHDPPATATVK
Ml-bCNG DVFSGIALNLGRPYLLGDWIVLS DGIEGRVVETDWRATHLLTP ANNVVALPNSVLAKMGLTNVSSPDE THGLSILVRLAPTKSPAAIVEAMRAVFLS SDSIVKAPPPVVAIK
Bx-bCNGa DVFSGIAVGIEAPFGVGDRIQIA DKIEGVVAQINWRSIRIHTD GDDMAIIPNSLIAKAEIVNRSSPSQ RRAASVEITCPESAVPERVIETLLHATLL CPDILSVPAPSAVLT
Bs-bCNG NIFSGIAINIERPFRIGDWVKIG EFDEGEIVDITWRTTRLKTR AECILSIPNSMASESPILNFCYPDD VYWLWPTVYVHPMHPPARVRKILLDALLS AEKVLKDPAPVVLFT
Sa-bCNG NLFAGLSLQLERPYQVGDFIRIG EH SGRVVQIGWRATRISTF RCESVTLPNSMVAKEVVRNFSYGYV PIGVDIFIGLSRDTPPNTVKAAVLDVLDE IPLILKTPVPQCRTW
Mx-bCNG NLFAGLSLQLDRPFEVGHFIRIG THT GRVVFIGWRSIRLANF RREVITLPNSMVAKELVLNFTQDPN PVGIDVEFRLSRDAAPNQVKHALLETMRE TPLILPEPSPIARTL
Sc-bCNG-1 NLFAGISLQVDSPFEEGDWIDLG FT RGVVTSLRLMTTRIHTL EGSLTVIPNSRIAVESLRRFKPGD PVGQIVEVGLDYSLPPRQAINLLQTIVQR NRKVLKEPTPKVWLD
Sc-bCNG-3 NLFAGISLQVDSPFEEGDWIDLG FT RGVVTSLHLMTTRIRGL DGSITVVPNSRITMEGLRRFKPNE PVGQMIDLGLDYSLPPSQAIQLLQRSLQT NRKVLRHPQPKVWVE
Pm-bCNGa DIFGGLSLQLDQPFKEGDWIQIG EDC GQVIMLTLMNTYLRTGMDGCTLIIPNDTVAQATIRRVHLGT PYGNCFEVGLDYGFPPSQALSLLLGVVNR HASVLTKPAPKAWVA
Sc-bCNG-2 DLFAGLELQFDDVFSVGDFLDLG DGTMGVVVSINWRDTCLKDV TGALVVVPNTKVTEVVVRNYVAFG AMGNRFSLGLDYSLPPSRARHLLLEVLHK HPHVLENPPPAVRVQ
Cv-bCNG NILAGLSLQVDNSVDIGDWIKSG DLV GKVVEINWRATTLETR NWETVVIPNSMLMKNHFAILGKRHGCPLQWRRWVWFNINWDTLPTQIIGVVEKSLRE AQLPGVAATPAPNCILM
Ah-bCNG NLLAGVSIQLDNSIAIGDWLQVE TT QGRVVEINWRATTIETR NWETVVIPNSHLLKQRFTVLGRRQNAPLQWRRWVWFDITLDTLPTQIIALVEQSLRE TRIRHVSASPQPDCLLM
As-bCNG NLLAGVSIQLDNSIAIGDWLQVE AI QGRVVEINWRATTMETR NWETVVIPNSHLLKQRFTVLGRRQNAPLQWRRWVWFDLTLDTLPTQIIALIEKSLRE TNLPCVAKYPQPDCLLM
Rd-bCNG DLFSGIALSVEHPFRLGDYIELE DGTQGQITDINWRATRLRGW DNATVVVPNSTLAQQRINNMHGTNH PYAEWYEIKIPAEVDPTMAKALLLEAALR CDKLLKKPSPAIRLA
Am-bCNGb NLFSGIALLFGRPFVIGDWLKFG DTV GKVIEINWRAVHLITR NKEMLIVPNSVLAKEVFYNYRRPQS LHGEPMELGFSYDDPPNKVKQVIRQAALE TPGVLSDPEPIIQTS
Mu-bCNGb QIVSGLFMLFEQPFQIDDWLDTT TT RGRIVEVNWRAVRIETG SGLRITPNSVLASTPFTNLSRPAG AYQLAIPTKFSDADAPDRVCALLSRVAAA LPQLDGGFLVT
Mu-bCNGa QIVSGLFMLFEQPFRIDDWLDTP TA RGRVVEVNWRAVHIETG TGLRITPNSVLATTAFTNLSRPGG SHKCSITTKFAADDAPDKVCAMLTRVASA LPNLKSGVMPA
Tb-bCNG QIVSGLFMLFEQPFRIDDWLETP TA RGRVVEVNWRAVHIDTG SGLQIMPNSMLATTAFTNLSRPAG AHECSITTTFSTSDPPDKVCAMLNRAASA LPHVKPGVVPA
Ma-bCNG QIVSGLFMLFEQPFRIGDWLDTP AA RGRIVEANWRSVHIQTG HGLQITPNSVLATTSFTNLSRPPG GHQLTLTATFSETDPPDRVCALLRRVADA LPQRRPDAVAA
Ms-bCNG QIISGLLLLFEQPFQLGDWLDTP SA RGRVVEVNWRATHIDTG GGLQIMPNSVLAGASFTNLSRPEA AHSLSVTTTFGVSDSPDAVCALLTRVATQ LPQRRAGAAPK
Ac-bCNGb GLVAGVIVFSGRHFNLGDWLQID GT PAKVVQIDWRAITVETL SGERIVVPSANMSSASLRITRARQ SVSVATDVSLPPGTAPAEAKALLLEAARD VPQLLDANAVACRVK
Mm-bCNGa DIFTGLAINIEQTYKIGEWIVLE GGLEGCVEEINWRTTSIRTP QNNIVRVPNSNIGVKPIVNYAYPDN KSRFEVLISLDFSIETERALRVLQSAAKSVSSQHGFYENPEPKVLVK
Mg-bCNG DFFAGIALSVERPFSIGDWIEVD NI AGRVVDMNWRAVRLSTT DDVAIIVPNGNIAAETFRNYSRPNT WFRDEIRLALPFDVTTHQGQRILLSAVTQIP ELAAHHRKPSVTID
Te-bCNGb NFISGLVILLEHPIKVGDFIEVD GL LGTVEKISIRATIIRTN DSQYVIVPNNRFIEKNVVNWSYGSP DSRIHIPVSVAYGSDTVLVTEALLSAARQ DPRVLLTPPPSVWFR
Am-bCNGa NFVSGLTLLLEQQIRVGDFVEVD GL LGTIERISIRSTIVRTQ DRLFVVVPNQRFFAKNVINWTYQTP ESRLHIPVSVAYGTDTVLVTEALLIAARS ESRVLKYPPPQVWFK
Se-bCNG SFFSGITLLIEQPIKVGDLVSLD GV LGTVEKISFRATAVRTL DHVHVIVPNDRLVDSNIINWSYQNT ASRVHLPISVAYGTDPLWLTDALLTVARQ DSRVLTQPAPTVWFR

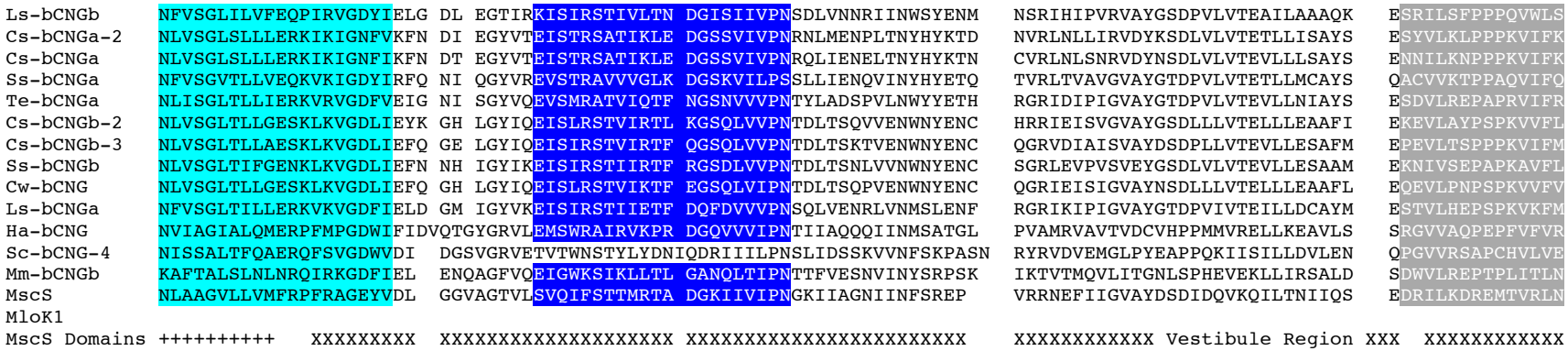
Ls-bCNGb NFVSGLILVFEQPIRVGDYIELG DL EGTIRKISIRSTIVLTN DGISIIVPNSDLVNNRIINWSYENM NSRIHIPVRVAYGSDPVLVTEAILAAAQK ESRILSFPPPQVWLS
Cs-bCNGa-2 NLVSGLSLLLERKIKIGNFVKFN DI EGYVTEISTRSATIKLE DGSSVIVPNRNLMENPLTNYHYKTD NVRLNLLIRVDYKSDLVLVTETLLISAYS ESYVLKLPPPKVIFK
Cs-bCNGa NLVSGLSLLLERKIKIGNFIKFN DT EGYVTEISTRSATIKLE DGSSVIVPNRQLIENELTNYHYKTN CVRLNLSNRVDYNSDLVLVTEVLLLSAYS ENNILKNPPPKVIFK
Ss-bCNGa NFVSGVTLLVEQKVKIGDYIRFQ NI QGYVREVSTRAVVVGLK DGSKVILPSSLLIENQVINYHYETQ TVRLTVAVGVAYGTDPVLVTETLLMCAYS QACVVKTPPAQVIFQ
Te-bCNGa NLISGLTLLIERKVRVGDFVEIG NI SGYVQEVSMRATVIQTF NGSNVVVPNTYLADSPVLNWYYETH RGRIDIPIGVAYGTDPVLVTEVLLNIAYS ESDVLREPAPRVIFR
Cs-bCNGb-2 NLVSGLTLLGESKLKVGDLIEYK GH LGYIQEISLRSTVIRTL KGSQLVVPNTDLTSQVVENWNYENC HRRIEISVGVAYGSDLLLVTELLLEAAFI EKEVLAYPSPKVVFL
Cs-bCNGb-3 NLVSGLTLLAESKLKVGDLIEFQ GE LGYIQEISIRSTVIRTF QGSQLVVPNTDLTSKTVENWNYENC QGRVDIAISVAYDSDPLLVTEVLLESAFM EPEVLTSPPPKVIFM
Ss-bCNGb NLVSGLTIFGENKLKVGDLIEFN NH IGYIKEISIRSTIIRTF RGSDLVVPNTDLTSNLVVNWNYENC SGRLEVPVSVEYGSDLVLVTEVLLESAAM EKNIVSEPAPKAVFL
Cw-bCNG NLVSGLTLLGESKLKVGDLIEFQ GH LGYIQEISLRSTVIKTF EGSQLVIPNTDLTSQPVENWNYENC QGRIEISIGVAYNSDLLLVTELLLEAAFL EQEVLPNPSPKVVFV
Ls-bCNGa NFVSGLTILLERKVKVGDFIELD GM IGYVKEISIRSTIIETF DQFDVVVPNSQLVENRLVNMSLENF RGRIKIPIGVAYGTDPVIVTEILLDCAYM ESTVLHEPSPKVKFM
Ha-bCNG NVIAGIALQMERPFMPGDWIFIDVQTGYGRVLEMSWRAIRVKPR DGQVVVIPNTIIAQQQIINMSATGL PVAMRVAVTVDCVHPPMMVRELLKEAVLS SRGVVAQPEPFVFVR
Sc-bCNG-4 NISSALTFQAERQFSVGDWVDI DGSVGRVETVTWNSTYLYDNIQDRIIILPNSLIDSSKVVNFSKPASN RYRVDVEMGLPYEAPPQKIISILLDVLEN QPGVVRSAPCHVLVE
Mm-bCNGb KAFTALSLNLNRQIRKGDFIEL ENQAGFVQEIGWKSIKLLTL GANQLTIPNTTFVESNVINYSRPSK IKTVTMQVLITGNLSPHEVEKLLIRSALD SDWVLREPTPLITLN
MscS NLAAGVLLVMFRPFRAGEYVDL GGVAGTVLSVQIFSTTMRTA DGKIIVIPNGKIIAGNIINFSREP VRRNEFIIGVAYDSDIDQVKQILTNIIQS EDRILKDREMTVRLN
MloK1
MscS Domains ++++++++++ XXXXXXXXX XXXXXXXXXXXXXXXXXXXX XXXXXXXXXXXXXXXXXXXXXXX XXXXXXXXXXXX Vestibule Region XXX XXXXXXXXXXX


361
480
Pp-bCNG ASTLESVEYEASGFVADAG AKGDARNQLFDLAHRHLEASGVMWN VDLAVPPRSRQRE VLDEVRVFRSLSDEERDALS
Pe-bCNG ASTLESVEYEASGFIADMS RKTEVRNQLFDLAHRHLEASGVIWN VETGVPARSRQRE LLEEVRVFRSLTSDERDSLS
Pf-bCNGb EAGDEMSEYVASGFIAELG KKSEVRNQLFDLAHRHLEAAGISRH PDGVIEPSTRARA LLDEVKIFRSLSHEERDRLA
Pf-bCNGa SSSSAGTEYEISGFVASMS EKRVVRNQLFDLAYRHLQASGVNLL SSDEPGVPSNLSRPRA LLDSSPIFSTLRQEEKETFS
Pf-bCNG-1 STSSSGAEYEISGFVADMG HKREVRNQLFDLAFRHLQASGIGLL SAAEPVQAATLSRPRA LLDASSIFSTLRQDEKDTFS
Bp-bCNG-2 RTSAISVTYEATAYVDDMS KKLAVTNELYDLCYRQLEAAGVALRP LGAGYAQPLAAAAPETDPRMH LLRRVEMFAALTQDELKRLA
Bg-bCNGb KSTIHSIQYEATAFVDDTA KKTPLTNELYDLCYRHLTAAGVALRPP GVPSVTAIVANAEER LLRRIELFAAISDDELKMLS
Bp-bCNGa KATVDSIQYEATAFVDDTA KKTPLTNELYDLCYRHLTAAGVDLRP RGVPSVTAIVDKAEER LLRRIELFTTIGDEELKMLS
Bg-bCNGa RATNDAIEYEIVCYVDAWT KKIGVRNDLYDLAHRHLLSRGVVLRP LSVAEPIGEPADEKQR LLRNVLIFQTLDDGEIAELA
Bx-bCNGc RATNDAIEYEIVCYVSELG KKIAVRNDLFDLAHRHLLSRGVVLRP LSVPEPVTGGTADEKLR LLRNVLIFQTLARDELAELA
Bp-bCNGb RATNDAIEYEIVCYVDSLG EKIEVRNELFDLAHRHLSSRGVVLHP LSVSEPANEATDEKQR LLRSVLIFQTLDDSGIAELA
Bc-bCNG AFRANAIQYELVCYVDALQ KKITVRNALYDLAHRHLAAAGVAWRP LAGSAPVSVSTSQGQPVSRRLL LLRAVELFARVDDDDLVVLA
Bc-bCNG-2 AFRANAIQYELVCYVDALQ KKITVRNALYDLAHRHLAAAGVAWRP LAGSAPASVSTSPGQPVSRRLL LLRAVELFARVDDDDLAVLA
Bx-bCNGb SVGLDATDYEVSFFASERW QADEALNSFYDAAHRHLESFHALISP AAQADDASAGTLEYQ LIAGIRVFGLLAREERIKLA
Rl-bCNGa SLTSDAMEVELSFRVRDIG QAGPAKNEIFDLIYRHIKAAGLTLARPL DAAGPPPEQLQSEEMTKPHRPTPL KLLDAIPLFFSLTEDEKETLA
Re-bCNGa GLDATALEVELQFRVTSPS QRVTARNEVLDLVYRHCKSAGLLLAVP PAAQVLTADLPTEENAKPPTVTPL ALIEAIPVFATLTSDERQKLA
Rl-bCNGb GLDATALEVELWFRVTSPS QRVTARNEVLDLVYRHCKSAGLLLAIP PSATVLTADLPTEESAKPPSVTPL ALIEAIPVFTTLTSDEKRRLA
Rl-bCNGb-3 GLDATALEVELQFRVASPS RRVQARNEVLDLVYRHCKSAGLLLAVP AAASVLTGDLPTEESARPPRVTPL ELIEAIPIFATLTTDEKQKLA
Rr-bCNG GLDATALEIHLFFRVSNPM LRIKAQNEVIDRFYRHCRSIGLQLAMP PSAIAIMNGVASTEISRRAEATL QEVIDENPILSRLTRAEREKLA
Rl-bCNGc-2 GLDASAIEVELAFKVSSLS RTSVAKNEIYDLVFRHAKAAGLQLGAP YGAQADGIQSSEGVKHPGTPWR LLSSIALFSTLTEDEMESLA
Ac-bCNGa TLDAQAVDLELSFHVAELG ASSAAKDEMFDLVYRHAKAAGLHLAAP AGAGGDSVPRSEVSQRPLSLR LLDSVALFSSLSEEEKAALA
Me-bCNG SLNGSAIEVELKCRVHDRT LVDGATNEVFDRFFRHAVAAGLSFAP DAGDSYAPDIEFETAAAAAGR LTMRLPLFASLAKEDRAALA
Ml-bCNG GLDADAIVIELSFRAPNIG QRIAARNDVFDLVYRHAKSAGLHLAT QSSSISAASLPNRETWPFTAIE LIEGTALFSALTDQEREALA
Bx-bCNGa QLGARRNAYKISFFVGNTR HLSSTKDILLRAARRQLHYAGFLDQD RRDDTATPNLSDEALTVRR LLRDITLFECLDERQLDSLA
Bs-bCNG GINEWAASYWIAFCADDYG DKNFILEDVWTRVWFHLNRGGITPAVQ RQEIHLFKGVKERGGEEATKPLT LLQEVDIFKPFSDDAKLHLS
Sa-bCNG AYDGSSIRYQIRYWVSDFS QADNAMEQIYTQLWYRLRRERIEIPYP QQTVHLRQGMDHAEVSQETVRD LLKAVDLFSVLDDSELHQVH
Mx-bCNG GYEDSAIRYMVRFFIGDYG LADAVKEDLHSRLWYRLRRANIEIPYA QRTVHVRQEMARTELSEDTIRS LLGAVDLFQSLDTEELDRLR
Sc-bCNG-1 AFADSSINYRLLTWQNSAL EQLQLKSDLLEQIWYALQRIGQSIPFPIR DIRSEPSPALLPSDTVSEEAKQQ LLASLEIFSHLTADQLQRLA
Sc-bCNG-3 AFADSSITYRLLTWQGSAP EMPQLKSDVLEQVWYALHRIDQSIPYPVR DIRTEPVPARLPSSAVNPGQKQR LLACTDIFGHLSDQQLGALA
Pm-bCNGa SFEDSYICYGIQVWHKDISDVKRLSIRGELMEQIWYALERIGQSIPFRV RLGSPKPQTLAADDPMCADTQRKV QWLTSNALFTDLSQAQLDALA
Sc-bCNG-2 AFADSAITYDIIAFQPPGNFGDMLDLRSELLEQIWFSLERTGQSVPYPV RELREKRTVLDAGHPDQRGLDQRR ALLIRNPLFGDLSEEEMLQLA
Cv-bCNG GFENGFTRYAVRYWLTDLA ADDYTDSIVRTHIDAALRRHNLRMASPYY NVLTIKENEKYIEARMKRHLEERV LALRKVELLSALNDEEMVVLA
Ah-bCNG NVENGIARYAVRYWLTDLA VDDPTDSAVRTLIDAALRRNDRRLTPPI FNVFMTTDQDHKDQRHKRHTAERT DTLRRLPLFAMLQEEELLRLA
As-bCNG NEGGIARYAVRYWLTDLA RDDPTDSMVRSLIDAALRRNDRRLTPPI FNVFMAKEKQHQDARHKRHTVERT ATLRKLPLFAMLQEDELIQLA
Rd-bCNG DATTIPYVYTVWVHFPNFL SMFAGREQLFREIHYALKNAGIQIAP ETYELHSRRADVIKVEPPTALV TLKKLDIANFLTDEELEQLV
Am-bCNGb AYGDSSINYYVRLYLRDYD RVPEIRDAFMTRVWYAAQRHGLTIPFP IRTLIHERPPKPELNGGTNRII TELRSLPCFITTHTEVLEKLV
Mu-bCNGb TEPVGGTEYCTTIGLRSPA EESAARATFLRWIWYAARREGLHLN GADDDFSTTERVQHAL KTVVAPVMRLSDTDQQALL
Mu-bCNGa TVALGGAEYRTTVRIKSPA EDGAAQDTFLRWVWYAARREGLALD GAGDSYSTPQRVQDA LRAVSPELKLSLLDQQSLA
Tb-bCNG TIARGAAEYRTTVRLTSPA DEGPTQATFLRWVWYAARREGLHLD EADDEFSTAERVESAL RTVVGPELRLSSSDQQSLA
Ma-bCNG AVPAGGGEYHVTIGLTSPA DDSAAQATLLRWLWYGARREGLRLD GAEDDISTPERIERAL RMVVAPALRLGPPDQQALV
Ms-bCNG AIPLGAGEYKTSIPLRTPA DDSAARAVFLRWLWYAARRAELHLD GETDDFSTPERLTKA VRQMAPTLRLSHTEQQEVL
Ac-bCNGb QLGGTAIVYGVSFPVADAS QVVKARDAFLHRLWYVGQRHGVSVAE GVSAEELYGTDTPQTRLAA LAGTGAFGAVSD DLRVVA
Mm-bCNGa NINEIGVEYEIHYWINSWKGVSPPVARSRVLASVLEQLRHAGISIAYP KQDIYHEKMPTRHLDSATGDDCI PLLRKVELFKPLGESELAVLG
Mg-bCNG GYDDRGILWRLLYWAPDFE RLSSLRFAVHSNILRNLHMSGLRLPVP IEEIRVMRSTLGSELGSIER MLRTSPVFSALTDEELSLLA
Te-bCNGb GFGESAYLFELLVWINRPQ DSEPIKSALNFLIEQELRQRQIEVPFPQLDLRLRDLGELRSLAHY YHRCAASVPQTSAVTAPAAPEMAKAEPSLTN LLRNISCFSRCSNAELQMLI
Am-bCNGa SFGDDAYKFELLAWINQPC DFEPIKSSLNFLIEQELNRKNIQIPFPQRELWLKNPEALAQALQPQ PEAAAPLPTVASGEGLKLKTGIKVTKNSTLRV LLRKVSYFENCTNAQLRVLI
Se-bCNG SFGDSTLNFELLFWTDRPE LIEPIKSDLNFRIASEFERREIQIPFP QLVLHRHRSVTTSELPDDYLPS LLRRVDLFRDYDDSQIRWLI

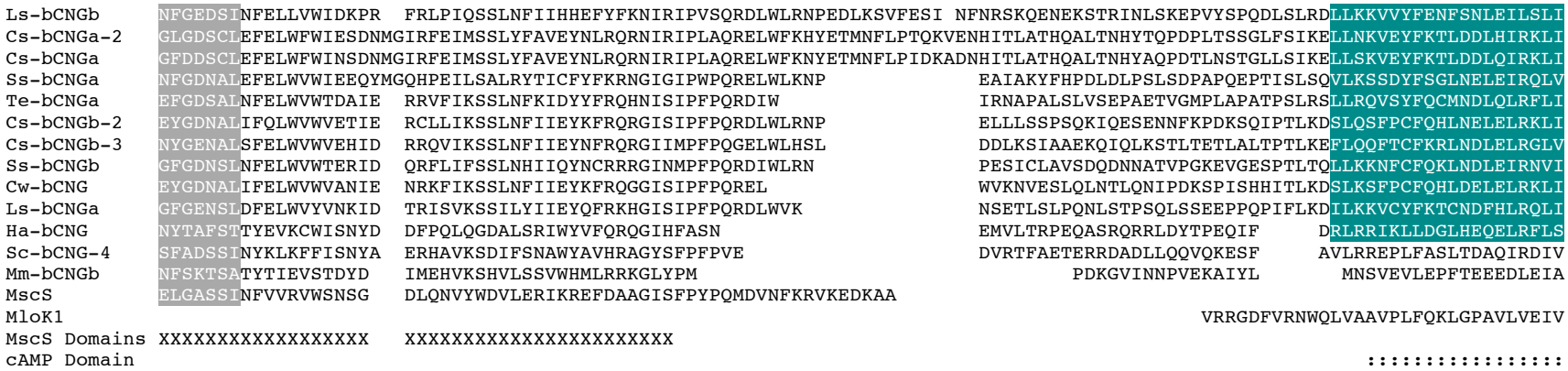
Ls-bCNGb NFGEDSINFELLVWIDKPR FRLPIQSSLNFIIHHEFYFKNIRIPVSQRDLWLRNPEDLKSVFESI NFNRSKQENEKSTRINLSKEPVYSPQDLSLRDLLKKVVYFENFSNLEILSLI
Cs-bCNGa-2 GLGDSCLEFELWFWIESDNMGIRFEIMSSLYFAVEYNLRQRNIRIPLAQRELWFKHYETMNFLPTQKVENHITLATHQALTNHYTQPDPLTSSGLFSIKELLNKVEYFKTLDDLHIRKLI
Cs-bCNGa GFDDSCLEFELWFWINSDNMGIRFEIMSSLYFAVEYNLRQRNIRIPLAQRELWFKNYETMNFLPIDKADNHITLATHQALTNHYAQPDTLNSTGLLSIKELLSKVEYFKTLDDLQIRKLI
Ss-bCNGa NFGDNALEFELWVWIEEQYMGQHPEILSALRYTICFYFKRNGIGIPWPQRELWLKNP EAIAKYFHPDLDLPSLSDPAPQEPTISLSQVLKSSDYFSGLNELEIRQLV
Te-bCNGa EFGDSALNFELWVWTDAIE RRVFIKSSLNFKIDYYFRQHNISIPFPQRDIW IRNAPALSLVSEPAETVGMPLAPATPSLRSLLRQVSYFQCMNDLQLRFLI
Cs-bCNGb-2 EYGDNALIFQLWVWVETIE RCLLIKSSLNFIIEYKFRQRGISIPFPQRDLWLRNP ELLLSSPSQKIQESENNFKPDKSQIPTLKDSLQSFPCFQHLNELELRKLI
Cs-bCNGb-3 NYGENALSFELWVWVEHID RRQVIKSSLNFIIEYNFRQRGIIMPFPQGELWLHSL DDLKSIAAEKQIQLKSTLTETLALTPTLKEFLQQFTCFKRLNDLELRGLV
Ss-bCNGb GFGDNSLNFELWVWTERID QRFLIFSSLNHIIQYNCRRRGINMPFPQRDIWLRN PESICLAVSDQDNNATVPGKEVGESPTLTQLLKKNFCFQKLNDLEIRNVI
Cw-bCNG EYGDNALIFELWVWVANIE NRKFIKSSLNFIIEYKFRQGGISIPFPQREL WVKNVESLQLNTLQNIPDKSPISHHITLKDSLKSFPCFQHLDELELRKLI
Ls-bCNGa GFGENSLDFELWVYVNKID TRISVKSSILYIIEYQFRKHGISIPFPQRDLWVK NSETLSLPQNLSTPSQLSSEEPPQPIFLKDILKKVCYFKTCNDFHLRQLI
Ha-bCNG NYTAFSTTYEVKCWISNYD DFPQLQGDALSRIWYVFQRQGIHFASN EMVLTRPEQASRQRRLDYTPEQIF DRLRRIKLLDGLHEQELRFLS
Sc-bCNG-4 SFADSSINYKLKFFISNYA ERHAVKSDIFSNAWYAVHRAGYSFPFPVE DVRTFAETERRDADLLQQVQKESF AVLRREPLFASLTDAQIRDIV
Mm-bCNGb NFSKTSATYTIEVSTDYD IMEHVKSHVLSSVWHMLRRKGLYPM PDKGVINNPVEKAIYL MNSVEVLEPFTEEEDLEIA
MscS ELGASSINFVVRVWSNSG DLQNVYWDVLERIKREFDAAGISFPYPQMDVNFKRVKEDKAA
MloK1 VRRGDFVRNWQLVAAVPLFQKLGPAVLVEIV
MscS Domains XXXXXXXXXXXXXXXXXX XXXXXXXXXXXXXXXXXXXXXX
cAMP Domain ::::::::::::::::

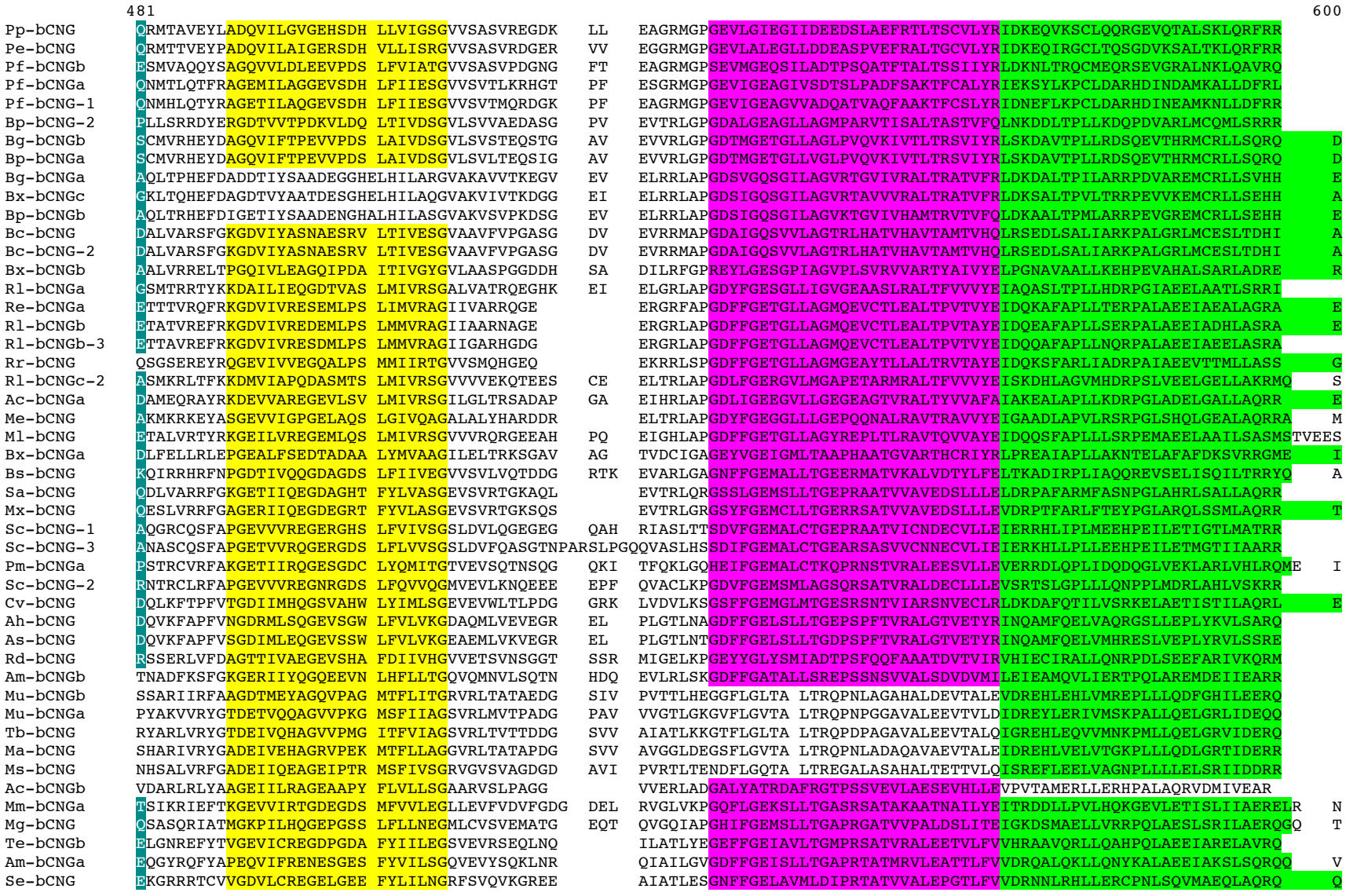
481
600
Pp-bCNG QRMTAVEYLADQVILGVGEHSDH LLVIGSGVVSASVREGDK LL EAGRMGPGEVLGIEGIIDEEDSLAEFRTLTSCVLYRIDKEQVKSCLQQRGEVQTALSKLQRFRR
Pe-bCNG QRMTTVEYPADQVILAIGERSDH VLLISRGVVSASVRDGER VV EGGRMGPGEVLALEGLLDDEASPVEFRALTGCVLYRIDKEQIRGCLTQSGDVKSALTKLQRFRR
Pf-bCNGb ESMVAQQYSAGQVVLDLEEVPDS LFVIATGVVSASVPDGNG FT EAGRMGPSEVMGEQSILADTPSQATFTALTSSIIYRLDKNLTRQCMEQRSEVGRALNKLQAVRQ
Pf-bCNGa QNMTLQTFRAGEMILAGGEVSDH LFIIESGVVSVTLKRHGT PF ESGRMGPGEVIGEAGIVSDTSLPADFSAKTFCALYRIEKSYLKPCLDARHDINDAMKALLDFRL
Pf-bCNG-1 QNMHLQTYRAGETILAQGEVSDH LFIIESGVVSVTMQRDGK PF EAGRMGPGEVIGEAGVVADQATVAQFAAKTFCSLYRIDNEFLKPCLDARHDINEAMKNLLDFRR
Bp-bCNG-2 PLLSRRDYERGDTVVTPDKVLDQ LTIVDSGVLSVVAEDASG PV EVTRLGPGDALGEAGLLAGMPARVTISALTASTVFQLNKDDLTPLLKDQPDVARLMCQMLSRRR
Bg-bCNGb SCMVRHEYDAGQVIFTPEVVPDS LAIVDSGVLSVSTEQSTG AV EVVRLGPGDTMGETGLLAGLPVQVKIVTLTRSVIYRLSKDAVTPLLRDSQEVTHRMCRLLSQRQ D
Bp-bCNGa SCMVRHEYDAGQVIFTPEVVPDS LAIVDSGVLSVLTEQSIG AV EVVRLGPGDTMGETGLLVGLPVQVKIVTLTRSVIYRLSKDAVTPLLRDSQEVTHRMCRLLSQRQ D
Bg-bCNGa AQLTPHEFDADDTIYSAADEGGHELHILARGVAKAVVTKEGV EV ELRRLAPGDSVGQGSGILAGVRTGVIVRALTRATVFRLDKDALTPILARRPDVAREMCRLLSVHH E
Bx-bCNGc GKLTQHEFDAGDTVYAATDESGHELHILAQGVAKVIVTKDGG EI ELRRLAPGDSIGQGSGILAGVRTAVVVRALTRATVFRLDKSALTPVLTRRPEVVKEMCRLLSEHH A
Bp-bCNGb AQLTRHEFDIGETIYSAADENGHALHILASGVAKVSVPKDSG EV ELRRLAPGDSIGQGSGILAGVKTGVIVHAMTRVTVFQLDKAALTPMLARRPEVGREMCRLLSEHH E
Bc-bCNG DALVARSFGKGDVIYASNAESRV LTIVESGVAAVFVPGASG DV EVRRMAPGDAIGQSVVLAGTRLHATVHAVTAMTVHQLRSEDLSALIARKPALGRLMCESLTDHI A
Bc-bCNG-2 DALVARSFGKGDVIYASNAESRV LTIVESGVAAVFVPGASG DV EVRRMAPGDAIGQSVVLAGTRLHATVHAVTAMTVHQLRSEDLSALIARKPALGRLMCESLTDHI A
Bx-bCNGb AALVRRELTPGQIVLEAGQIPDA ITIVGYGVLAASPGGDDH SA DILRFGPREYLGESGPIAGVPLSVRVVARTYAIVYELPGNAVAALLKEHPEVAHALSARLADRE R
Rl-bCNGa GSMTRRTYKKDAILIEQGDTVAS LMIVRSGALVATRQEGHK EI ELGRLAPGDYFGESGLLIGVGEAASLRALTFVVVYEIAQASLTPLLHDRPGIAEELAATLSRRI
Re-bCNGa ETTTVRQFRKGDVIVRESEMLPS LIMVRAGIIVARRQGE ERGRFAPGDFFGETGLLAGMQEVCTLEALTPVTVYEIDQKAFAPLLTERPALAEEIAEALAGRA E
Rl-bCNGb ETATVREFRKGDVIVREDEMLPS LMMVRAGIIAARNAGE ERGRLAPGDFFGETGLLAGMQEVCTLEALTPVTAYEIDQEAFAPLLSERPALAEEIADHLASRA E
Rl-bCNGb-3 ETTAVREFRKGDVIVRESDMLPS LMMVRAGIIGARHGDG ERGRLAPGDFFGETGLLAGMQEVCTLEALTPVTVYEIDQQAFAPLLNQRPALAEEIAEELASRA
Rr-bCNG QSGSEREYRQGEVIVVEGQALPS MMIIRTGVVSMQHGEQ EKRRLSPGDFFGETGLLAGMGEAYTLLALTRVTAYEIDQKSFARLIADRPAIAEEVTTMLLASS G
Rl-bCNGc-2 ASMKRLTFKKDMVIAPQDASMTS LMIVRSGVVVVEKQTEES CE ELTRLAPGDLFGERGVLMGAPETARMRALTFVVVYEISKDHLAGVMHDRPSLVEELGELLAKRMQ S
Ac-bCNGa DAMEQRAYRKDEVVAREGEVLSV LMIVRSGILGLTRSADAP GA EIHRLAPGDLIGEEGVLLGEGEAGTVRALTYVVAFAIAKEALAPLLKDRPGLADELGALLAQRR E
Me-bCNG AKMKRKEYASGEVVIGPGELAQS LGIVQAGALALYHARDDR ELTRLAPGDYFGEGGLLLGEPQQNALRAVTRAVVYEIGAADLAPVLRSRPGLSHQLGEALAQRRA M
Ml-bCNG ETALVRTYRKGEILVREGEMLQS LMIVRSGVVVRQRGEEAH PQ EIGHLAPGDFFGETGLLAGYREPLTLRAVTQVVAYEIDQQSFAPLLLSRPEMAEELAAILSASMSTVEES
Bx-bCNGa DLFELLRLEPGEALFSEDTADAA LYMVAAGILELTRKSGAV AG TVDCIGAGEYVGEIGMLTAAPHAATGVARTHCRIYRLPREAIAPLLAKNTELAFAFDKSVRRGME I
Bs-bCNG KQIRRHRFNPGDTIVQQGDAGDS LFIIVEGVVSVLVQTDDG RTK EVARLGAGNFFGEMALLTGEERMATVKALVDTYLFELTKADIRPLIAQQREVSELISQILTRRYQ A
Sa-bCNG QDLVARRFGKGETIIQEGDAGHT FYLVASGEVSVRTGKAQL EVTRLQRGSSLGEMSLLTGEPRAATVVAVEDSLLLELDRPAFARMFASNPGLAHRLSALLAQRR
Mx-bCNG QESLVRRFGAGERIIQEGDEGRT FYVLASGEVSVRTGKSQS EVTRLGRGSYFGEMCLLTGERRSATVVAVEDSLLLEVDRPTFARLFTEYPGLARQLSSMLAQRR T
Sc-bCNG-1 AQGRCQSFAPGEVVVREGERGHS LFVIVSGSLDVLQGEGEG QAH RIASLTTSDVFGEMALCTGEPRAATVICNDECVLLEIERRHLIPLMEEHPEILETIGTLMATRR
Sc-bCNG-3 ANASCQSFAPGETVVRQGERGDS LFLVVSGSLDVFQASGTNPARSLPGQQVASLHSSDIFGEMALCTGEARSASVVCNNECVLIEIERKHLLPLLEEHPEILETMGTIIAARR
Pm-bCNGa PSTRCVRFAKGETIIRQGESGDC LYQMITGTVEVSQTNSQG QKI TFQKLGQHEIFGEMALCTKQPRNSTVRALEESVLLEVERRDLQPLIDQDQGLVEKLARLVHLRQME I
Sc-bCNG-2 RNTRCLRFAPGEVVVREGNRGDS LFQVVQGMVEVLKNQEEE EPF QVACLKPGDVFGEMSMLAGSQRSATVRALDECLLLEVSRTSLGPLLLQNPPLMDRLAHLVSKRR
Cv-bCNG DQLKFTPFVTGDIIMHQGSVAHW LYIMLSGEVEVWLTLPDG GRK LVDVLKSGSFFGEMGLMTGESRSNTVIARSNVECLRLDKDAFQTILVSRKELAETISTILAQRL E
Ah-bCNG DQVKFAPFVNGDRMLSQGEVSGW LFVLVKGDAQMLVEVEGR EL PLGTLNAGDFFGELSLLTGEPSPFTVRALGTVETYRINQAMFQELVAQRGSLLEPLYKVLSARQ
As-bCNG DQVKFAPFVSGDIMLEQGEVSSW LFVLVKGEAEMLVKVEGR EL PLGTLNTGDFFGELSLLTGDPSPFTVRALGTVETYRINQAMFQELVMHRESLVEPLYRVLSSRE
Rd-bCNG RSSERLVFDAGTTIVAEGEVSHA FDIIVHGVVETSVNSGGT SSR MIGELKPGEYYGLYSMIADTPSFQQFAAATDVTVIRVHIECIRALLQNRPDLSEEFARIVKQRM
Am-bCNGb TNADFKSFGKGERIIYQGQEEVN LHFLLTGQVQMNVLSQTN HDQ EVLRLSKGDFFGATALLSREPSSNSVVALSDVDVMILEIEAMQVLIERTPQLAREMDEIIEARR
Mu-bCNGb SSARIIRFAAGDTMEYAGQVPAG MTFLITGRVRLTATAEDG SIV PVTTLHEGGFLGLTA LTRQPNLAGAHALDEVTALEVDREHLEHLVMREPLLLQDFGHILEERQ
Mu-bCNGa PYAKVVRYGTDETVQQAGVVPKG MSFIIAGSVRLMVTPADG PAV VVGTLGKGVFLGVTA LTRQPNPGGAVALEEVTVLDIDREYLERIVMSKPALLQELGRLIDEQQ
Tb-bCNG RYARLVRYGTDEIVQHAGVVPMG ITFVIAGSVRLTVTTDDG SVV AIATLKKGTFLGLTA LTRQPDPAGAVALEEVTALQIGREHLEQVVMNKPMLLQELGRVIDERQ
Ma-bCNG SHARIVRYGADEIVEHAGRVPEK MTFLLAGGVRLTATAPDG SVV AVGGLDEGSFLGVTA LTRQPNLADAQAVAEVTALEIDREHLVELVTGKPLLLQDLGRTIDERR
Ms-bCNG NHSALVRFGADEIIQEAGEIPTR MSFIVSGRVGVSVAGDGD AVI PVRTLTENDFLGQTA LTREGALASAHALTETTVLQISREFLEELVAGNPLLLLELSRIIDDRR
Ac-bCNGb VDARLRLYAAGEIILRAGEAAPY FLVLLSGAARVSLPAGG VVERLADGALYATRDAFRGTPSSVEVLAESEVHLLEVPVTAMERLLERHPALAQRVDMIVEAR
Mm-bCNGa TSIKRIEFTKGEVVIRTGDEGDS MFVVLEGLLEVFVDVFGDG DEL RVGLVKPGQFLGEKSLLTGASRSATAKAATNAILYEITRDDLLPVLHQKGEVLETISLIIAERELR N
Mg-bCNG QSASQRIATMGKPILHQGEPGSS LFLLNEGMLCVSVEMATG EQT QVGQIAPGHIFGEMSLLTGAPRGATVVPALDSLITEIGKDSMAELLVRRPQLAESLSRILAERQGQ T
Te-bCNGb ELGNREFYTVGEVICREGDPGDA FYIILEGSVEVRSEQLNQ ILATLYEGEFFGEIAVLTGMPRSATVRALEETVLFVVHRAAVQRLLQAHPQLAEEIARELAVRQ
Am-bCNGa EQGYRQFYAPEQVIFRENESGES FYVILSGQVEVYSQKLNR QIAILGVGDFFGEISLLTGAPRTATMRVLEATTLFVVDRQALQKLLQNYKALAEEIAKSLSQRQQ V
Se-bCNG EKGRRRTCVVGDVLCREGELGEE FYLILNGRFSVQVKGREE AIATLESGNFFGELAVMLDIPRTATVVALEPGTLFVVDRNNLRHLLERCPNLSQVMAEQLAQRQ Q

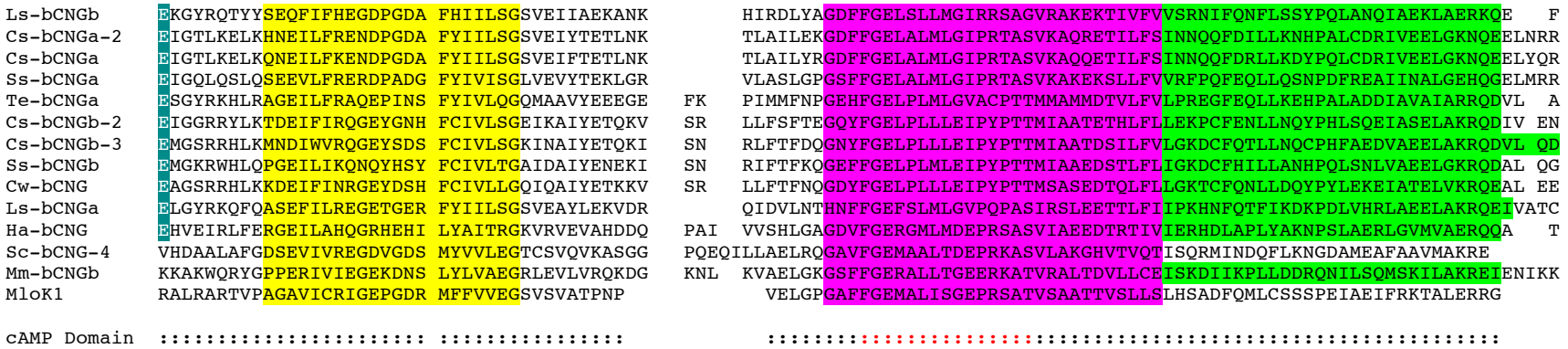
Ls-bCNGb EKGYRQTYYSEQFIFHEGDPGDA FHIILSGSVEIIAEKANK HIRDLYAGDFFGELSLLMGIRRSAGVRAKEKTIVFVVSRNIFQNFLSSYPQLANQIAEKLAERKQE F
Cs-bCNGa-2 EIGTLKELKHNEILFRENDPGDA FYIILSGSVEIYTETLNK TLAILEKGDFFGELALMLGIPRTASVKAQRETILFSINNQQFDILLKNHPALCDRIVEELGKNQEELNRR
Cs-bCNGa EIGTLKELKQNEILFKENDPGDA FYIILSGSVEIFTETLNK TLAILYRGDFFGELALMLGIPRTASVKAQQETILFSINNQQFDRLLKDYPQLCDRIVEELGKNQEELYQR
Ss-bCNGa EIGQLQSLQSEEVLFRERDPADG FYIVISGLVEVYTEKLGR VLASLGPGSFFGELALMLGIPRTASVKAKEKSLLFVVRFPQFEQLLQSNPDFREAIINALGEHQGELMRR
Te-bCNGa ESGYRKHLRAGEILFRAQEPINS FYIVLQGQMAAVYEEEGE FK PIMMFNPGEHFGELPLMLGVACPTTMMAMMDTVLFVLPREGFEQLLKEHPALADDIAVAIARRQDVL A
Cs-bCNGb-2 EIGGRRYLKTDEIFIRQGEYGNH FCIVLSGEIKAIYETQKV SR LLFSFTEGQYFGELPLLLEIPYPTTMIAATETHLFLLEKPCFENLLNQYPHLSQEIASELAKRQDIV EN
Cs-bCNGb-3 EMGSRRHLKMNDIWVRQGEYSDS FCIVLSGKINAIYETQKI SN RLFTFDQGNYFGELPLLLEIPYPTTMIAATDSILFVLGKDCFQTLLNQCPHFAEDVAEELAKRQDVL QD
Ss-bCNGb EMGKRWHLQPGEILIKQNQYHSY FCIVLTGAIDAIYENEKI SN RIFTFKQGEFFGELPLMLEIPYPTTMIAAEDSTLFLIGKDCFHILLANHPQLSNLVAEELGKRQDAL QG
Cw-bCNG EAGSRRHLKKDEIFINRGEYDSH FCIVLLGQIQAIYETKKV SR LLFTFNQGDYFGELPLLLEIPYPTTMSASEDTQLFLLGKTCFQNLLDQYPYLEKEIATELVKRQEAL EE
Ls-bCNGa ELGYRKQFQASEFILREGETGER FYIILSGSVEAYLEKVDR QIDVLNTHNFFGEFSLMLGVPQPASIRSLEETTLFIIPKHNFQTFIKDKPDLVHRLAEELAKRQEIVATC
Ha-bCNG EHVEIRLFERGEILAHQGRHEHI LYAITRGKVRVEVAHDDQ PAI VVSHLGAGDVFGERGMLMDEPRSASVIAEEDTRTIVIERHDLAPLYAKNPSLAERLGVMVAERQQA T
Sc-bCNG-4 VHDAALAFGDSEVIVREGDVGDS MYVVLEGTCSVQVKASGG PQEQILLAELRQGAVFGEMAALTDEPRKASVLAKGHVTVQTISQRMINDQFLKNGDAMEAFAAVMAKRE
Mm-bCNGb KKAKWQRYGPPERIVIEGEKDNS LYLVAEGRLEVLVRQKDG KNL KVAELGKGSFFGERALLTGEERKATVRALTDVLLCEISKDIIKPLLDDRQNILSQMSKILAKREIENIKK
MloK1 RALRARTVPAGAVICRIGEPGDR MFFVVEGSVSVATPNP VELGPGAFFGEMALISGEPRSATVSAATTVSLLSLHSADFQMLCSSSPEIAEIFRKTALERRG
cAMP Domain :::::::::::::::::::::: ::::::::::::::: ::::::::::::::::::::::::::::::::::::::::::::::::::::::::::::

```
                601
Pp-bCNG      QSRESLLLQKPASIKKGGFLSWLHK
Pe-bCNG      QKRESLLLQKPTVVKKGGFLSWLHK
Pf-bCNGb     QNSRLALMAKPAPVKKGGFLGWLQKR
Pf-bCNGa     HKAQSLTEDTPAVVPKKGFLQWLRNRV
Pf-bCNG-1    HMAQTLSQAAPKPVPRKGFLQWLRSRT
Bp-bCNG-2    DTLDKLGTPTPVAQSEQSVFQWLLDGMRKLHDLTF
Bg-bCNGb     MLHKMAMKNAAHADDEHASFHWLLDKIHRLHALKF
Bp-bCNGa     MLHKMAMKNTDHADDEHASFHWFLEKIHRLHALKF
Bg-bCNGa     SEKMLLAPSANADAGSGGLLQWIRDGVRRFHELAL
Bx-bCNGc     TEEMLLASPASLDENTGGLLQWIRDGVRRFHELTL
Bp-bCNGb     TEKLLLASPDNADAGPGGLLQWIRDGVRRIHDLAL
Bc-bCNG      TEERMMIPPVEKAHAGFSLIGWLEKEMKRLHDSLG
Bc-bCNG-2    TEERMMIPPVEKAHAGFSLIGWLEKEMKRLHDSLG
Bx-bCNGb     EGRALMQPQAEMPVTRHGLASWIASCIRALHQGHREP
Rl-bCNGa      FTGQHSFAPEGATLNGRSMSSLVTRIRHLFQVPQ
Re-bCNGa     RFRDGAALPPEQASNAHAILKTIRTIFRA
Rl-bCNGb     RFRNGASLPPEHARSAHAILKTIRTIFKA
Rl-bCNGb-3   ERFRDAALPPEPAHSAHAILKTIRTIFRG
Rr-bCNG      NVSQLPLTQAKHERNASAFLKSIRTIFST
Rl-bCNGc-2   EEHLGAINDKAAGSRPTSLAARIRHLFEVPHIPRK
Ac-bCNGa     TAHLEAAAPCDREWGRSRLAEGIRAFMQVHRGRG
Me-bCNG      EQKNEVDVKHHTGHTAKRFADRIMELFQLDLTSAR
Ml-bCNG      GLNRQRHPISKSALREAIHTAFRAVPFRRVVGGPDRAQKKRESHGHLAE
Bx-bCNGa     LHREVAVRASPDIGPQGQLLQRIRSIFHFGSD
Bs-bCNG      TQSVKTHVEEDGEIEKEAVYKRFLNRIEQFFGLKEEQ
Sa-bCNG      TQLRAVAANSSGSVDPTPEAGRILDRLRHIFGITG
Mx-bCNG      QLRAVAEASGTSNDAIPAEVGRILGRLRQIFGLNATHE
Sc-bCNG-1     KELRTLSQRRSETRRRALIGRMQRLFNLASDTP
Sc-bCNG-3     QELKALKENRAENRRLALIARMQRLFSLTGQDE
Pm-bCNGa     GSLNQQQSHSSKLHSQRRLIRSMHRLYKVIRGD
Sc-bCNG-2     GELEGMEREKVKQHENQLLKRMKQLFETLTL
Cv-bCNG      EQRNRVPDALLDAEGEMPKRAELVDRVRSFFGLNKH
Ah-bCNG      QEQQELLAREAEAMKQITPPRDLLDKLMALFGGR
As-bCNG      QEQQTLLAKEAESMKQPPQQRDLLNKLMKLFSGG
Rd-bCNG       DNAQAVRLGADKTPARLTFQDIMRRLDALMR
Am-bCNGb        KAIQIAQQTYA
Mu-bCNGb      SKVRRVGGLN
Mu-bCNGa      MKVRQVTQRERVA
Tb-bCNG         RKAQQAIRRDLHQSPAAAGEHRGPARR
Ma-bCNG         ALVHRAVTAEPTPSREPVS
Ms-bCNG           SAARAALTAD
Ac-bCNGb        TAALADSLAGNGGAAA
Mm-bCNGa     SSIFEKASKELRASETSSLSKQILVKMKDLFSDF
Mg-bCNG      AARMAAETNDVEHCDDQGATRLMLGRIRSFFNMPG
Te-bCNGb     QVLQELGLVNSQEIKSLPPLHWIRHRLKTLFDV
Am-bCNGa     LEELGLTQINPSESAGDDPFIWIRRRIQTLFGI
Se-bCNG      VLTNAGLLTPTANQSRPDQLRGILRRVLRL
```

```
Ls-bCNGb      IERKKELGLSDDEDLENNPLVWIRKRMKTLFNI
Cs-bCNGa-2    REELKEKGLLKAEEEESNIIDWVRHRLQSILTL
Cs-bCNGa      REELKEKGLLKAEEEESNIIDWVRHRLQSMLTL
Ss-bCNGa      KEELATKGLLTSEEEDSNIMNWVRKRLQRLFG
Te-bCNGa      QHQQELQQLSRQESDPSRPMNWIRDRLQKLLNW
Cs-bCNGb-2    YQQTLQEMGLIDEKSLKDPVTWIRQRLSQIFRL
Cs-bCNGb-3    YQQQLKKMGLMDEEDLKNPVAWIRQRLGQIFNLKL
Ss-bCNGb      YEQKLKEMGLLEEADLKNPVEWIRQRINKIFGVSQESAYR
Cw-bCNG       HQNSLKEMGLIDDEYLKNPVVWIRKRLSQIFNLS
Ls-bCNGa      QIKLKELGLIEESENNQNPVVWIRKRIQKIFDRC
Ha-bCNG       HNYLEQQRSVNQNPTPSPAARSITERIRDVLLDLSK
Sc-bCNG-4      ARRREFSVDQTQTYELDLIERMRKTFARLFAAS
Mm-bCNGb      SREYAQEVEEKEKDTVARRLLDLMKNFFKNDNVDDDDDDDLDKDAHKKMTI
MscS
MloK1
```

**Figure 2.2:** Sequence alignment of all identified bCNG channels. The three transmembrane domains of MscS (=,-,+), the vestibule region of MscS (X), the cAMP binding domain (:), and phosphate binding cassette (:) are indicated on the alignment. Highlighted regions of the alignment depict the MEME blocks that were found in the analysis of all bCNG sequences.

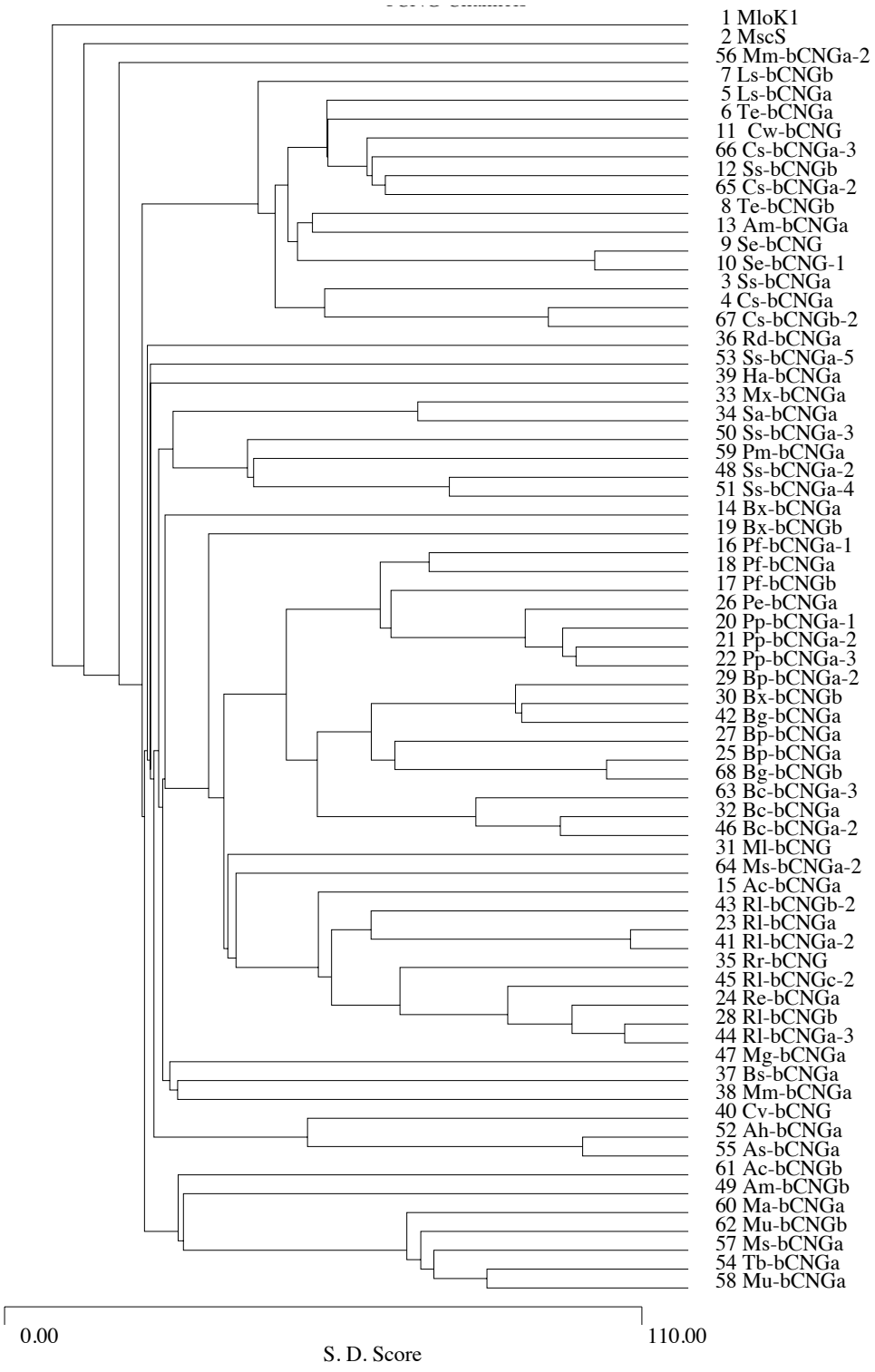


**Figure 2.3**: Homology Tree of bCNG channels.

*2.2.4 Cloning and expression*

Genomic DNA from *Thermosynechococcus elongates* BP-1 (Te) and *Mesorhizobium loti* MAFF303099 (Ml) was obtained from KAZUSA and genomic DNA from *Chromobacterium violaceum* (Cv) was obtained the American Type Culture Collection. Cloning was carried out using a ligation independent cloning (LIC) strategy (Aslanidis and de Jong 1990; Haun and Moss 1992), which allowed genomic DNA to be directly incorporated into the pET46 vector (Novagen) without the use of an intermediate cloning vector and the introduction of additional enzymatic restriction sites. All genes were cloned into pET46 such that the methionine start codon for the gene immediately follows the sequence for the LIC site, and the native stop codon for the gene is included within the construct. In this process, an N-terminal His-Tag was incorporated into the gene. Cloned sequences were verified by automated DNA sequencing (Big Dye v3.1; Applied Biosystems).

Protein expression was carried out in the BL21(dE3) stain of *E. coli* (Novagen). Single colonies were used to inoculate 5 mL of Luria Bertani Broth (LB) with 50 µg/mL ampicillin. The cultures were grown overnight at 37°C with shaking. LB cultures were used to inoculate 500 mL of TB media with ampicillin. The resulting terrific broth (TB) cultures were grown to mid-log phase and induced with 1 mM isopropyl-beta-D-thiogalactopyranoside (IPTG). After induction, the cultures were grown for an additional 2 hours at 37°C or in some cases for 3 hours at 30°C. Bacteria were then pelleted and resuspended in 50 mM Tris / 75 mM NaCl / 1% Fos-Choline 14 (Anatrace) at pH 7.5 (10 mL) with complete protease inhibitor cocktail (Roche). The suspensions were then probe

sonicated (4 x 30 s) on ice, pelleted at 45,000 x g for 45 min, and the resulting supernatant was passed through a 0.2 μm filter. Affinity Chromatography was carried out on a HPLC with diode array detector (Shimadzu) using a POROS metal chelate affinity column (Applied Biosystems) charged with cobalt chloride. Elution from the metal chelate column was achieved using an imidazole gradient (0.25 mM - 1 M at pH 7.5) with 0.05% n-Octyl-ß-D-Glucopyranoside (Anatrace). The purified protein was reconstituted into lipid vesicles prepared from a lipid mixture containing 5:3:2 DOPE:DOPS:DOPC (Avanti Polar Lipids) in 400 mM KCl with 5 mM 4-(2-hydroxyethyl)-1-piperazineethanesulfonic acid (HEPES) pH 7.5.

*2.2.5 Planar Lipid Bilayer Electrophysiology*

Electrophysiology measurements were recorded using an Axiopatch 200B, Digidata 1321, pClamp 9 (Molecular Devices) and a planar lipid bilayer workstation, consisting of a Faraday cage, active pneumatic vibration isolation table, low noise lamp, and low noise stirrer (Warner Instruments). Recordings were obtained in 400 mM KCl with 5 mM HEPES at pH 7.5. Bilayers were formed over a 150 μm aperture in a delrin chamber (Warner Instruments) using a lipid mixture containing 5:3:2 DOPE:DOPS:DOPC in decane, and bilayer formation was monitored by capacitance. Lipid vesicles containing reconstituted bCNG channels were then fused to the lipid bilayer in the presence of calcium. Vesicle fusion was observed as conductance spikes in the electrical trace. After several minutes, fusion was stopped by the addition of EDTA. Initial recordings were then made on the bilayer to confirm that it was electrically silent. A given concentration

of cAMP was then added to the bilayer and channel activity was recorded. Channel activity was only observed after the addition of cAMP.

*2.2.6 Subcloning into pB10b*

The bCNG channel genes in pET46 were sub-cloned into the pB10b (Wild et al. 1992; Sukharev et al. 1994) vector using a variant of Stratagene's QuikChange method and the QuikChange Lightning Kit (Stratagene) (Geiser et al. 2001). Primers for cloning contained two domains of approximately 25 bases each: one priming to the gene and one priming to the flanking region of the target pB10b plasmid. This strategy allowed for direct insertion in the pB10b vector without the addition of enzymatic sites. All genes were sub-cloned at their start codon, eliminating the His-Tag introduced by the pET46 vector, into the pB10b vector by replacement of the Ec-MscL gene. Sub-cloned products were screened enzymatically and final sequences were verified by automated sequencing with Big Dye v3.1 (Applied Biosystems).

*2.2.7 Osmotic Downshock*

Osmotic Downshock experiments were carried out in the MJF465 (MscS, MscL, and MscK null) bacterial strain (Levina et al. 1999), as previously described (Booth et al. 2007). A 2 mL culture of Luria Bertami (LB) Broth Lennox (BD Biosystems) with ampicillin (100 μg/mL) was inoculated with a single colony and grown overnight at 37 °C. The culture was diluted 1:20 into LB Broth supplemented with ampicillin (100 μg/mL) and 250 mM NaCl. Cultures were grown to an optical density at 600 nm ($OD_{600}$) of 0.5-0.7 and induced by addition of Isopropyl β-D-1-thiogalactopyranoside (IPTG) to a

final concentration of 0.1 mM IPTG (10 μL of 100 mM IPTG, Shelton Scientific). The cultures were grown for 60 minutes and downshocked by a 1:40 dilution into a low osmolyte medium (1:1 LB: water) and isotonic media. After dilution the cultures were incubated with shaking at 37°C for 30 minutes. Cultures were serially diluted into like media (1:10, 1:100, 1:1000, 1:10000, 1:100000), and 50 μL of each dilution was plated onto LB agar Miller (BD Biosystems) plates supplemented with ampicillin and grown at 37°C for 12 hours. Plates containing between 50 and 250 colonies were used for the calculation of colony forming units (CFU) per milliliter of media. Percent recovery was subsequently calculated by dividing the CFU/mL for bacteria exposed to osmotic downshock by the CFU/mL for the isotonic media. Six trials were conducted for each channel on at least two different days.

## *2.3 Results and Discussion*

### *2.3.1 Defining the bCNG family*

An open reading frame, Slr1575, was initially assigned as a putative bacterial LGIC during genome annotation of *Synechocystis sp*. PCC 6803 (Kaneko et al. 1995). A secondary bioinformatics analysis of the PCC 6803 genome noted very weak similarity between Slr1575 and the pore lining region of several potassium channels (Ochoa de Alda and Houmard 2000). While the similarity of Slr1575 to potassium channels is relatively weak, our bioinformatic analysis showed that the channel domain had significant sequence similarity with the *E. coli* MscS (Figures 2.1 and 2.2). MscS is part of a larger superfamily of ion channels that share significant sequence similarity in their pore-lining region and includes channels from bacteria, archaea, and eukaryotes (Pivetti

et al. 2003). While the amino-terminal region of Slr1575 shares significant similarity with MscS, the carboxyl-terminal region of the putative protein product shares significant similarity with known cyclic nucleotide monophosphate (cNMP) binding domains. Figure 2.1 shows the similarity between this region and the cNMP binding domain of MloK1. This binding domain is attached to the carboxyl-terminal end of the channel via a linker domain. Since rearrangements of the carboxyl-terminal end of the MscS channel domain have been observed in MscS gating (Wang et al. 2008; Vásquez et al. 2008), conformational changes induced by cNMP binding could feasibly lead to gating in this MscS-related channel. Thus, we hypothesized that Slr1575 encodes a bacterial cyclic nucleotide gated ion channel from *Synechocystis sp*., which we will refer to as Ss-bCNGa.

Starting with the Ss-bCNGa sequence, we carried out a series of iterative searches of the non-redundant protein database and identified fifty-nine potential homologues of Ss-bCNGa (Table 1). Each homologue in the family contains a channel region similar to the pore lining helix from MscS and a binding domain containing critical elements for cyclic nucleotide binding (Berman et al. 2005; LaFranzo et al. 2010). These putative channels span thirty-seven different bacterial species. Moreover, significant sequence differences are observed in the putative channel sequences from some subspecies of bacteria, such as *Cyanothece sp*. CCY0110, ATCC 51142, and PCC 8801 (Table 2.1). In several cases, bacterial subspecies showed strong similarities to each other, and in these cases nearly identical sequences were eliminated from further analysis (Table 2.2).

The genomes of eleven species contained two distinct putative bCNG channels with significant sequence differences, and the genome of one species contained three putative bCNG channels. This suggests that some bCNG channels may exist as heteromultimers *in vivo*. The potential for the existence of heteromultimers is consistent with mammalian LGICs where heteromultimeric assemblies are observed quite frequently. However, to our knowledge this represents the first example of bioinformatics data that suggest bacterial ion channels may form complex assemblies similar to their mammalian counterparts.

Many bCNG channels are found in bacterial strains that represent parasitic, symbiotic, and photosynthetic bacteria. Photosynthetic bacteria regulate their cAMP level in response to light, and it previously has been suggested that a cyclic nucleotide gated channel might play a role in energy cycle regulation for these bacteria (Ochoa de Alda and Houmard 2000). We hypothesize that bCNG channels may be involved in host-bacteria signaling pathways in parasitic and symbiotic bacterial strains. While we postulate that the binding domains of these channels are intracellular based on the MscS architecture, cAMP is known to exhibit some membrane permeability (Kumar 1976).

*2.3.2 Sequence conservation within the bCNG family*

A multiple sequence alignment of the fifty-nine putative bCNG channels was created using AMPS (Barton 1990), and the sequences were further analyzed using MEME (Grundy et al. 1997) to highlight regions with high sequence similarity (Figure 2.3). The MEME analysis identified ten conserved blocks that highlight both differences and

similarity of these fifty-nine proteins. One of the universally conserved blocks corresponds to the third transmembrane (TM3) domain of MscS (turquoise). The pore lining region of these channels exhibits significant sequence similarity with other channels and likely represents the distinguishing feature for an ion channel superfamily with members in all phylogenic kingdoms (Haswell et al. 2008; Pivetti et al. 2003). Additionally, there are two almost completely conserved domains that correspond to the vestibule region of MscS (blue and dark gray). The high conservation in this region coupled with the observation that rearrangements of the vestibule region of MscS are coincident with channel gating (Wang et al. 2008; Vásquez et al. 2008) suggest that the vestibule regions of bCNG channels are intimately involved in signal transduction and gating.

Despite the distinct similarities between the pore-lining domains of these channels, the bCNG channels appear to have different numbers of TM domains. Using the TM prediction methods TMHMM (Krogh et al. 2001), DAS-TMFinder (Hofmann and Stoffel 1993), TMPred (Cserzo et al. 2002), and SOSUI (Hirokawa et al. 1998), we predict that the number of TM domains in the fifty-nine identified bCNG channels ranges from two to six (Table 2.1). Differences in the number of TM domains may play a significant role in the function of bCNG channels as they would lead to different interactions between adjacent TM domains. Since the exact definition of TM domains can be difficult based solely on sequence analyses, we plan to experimentally investigate the TM topology of bCNG channels in future studies.

All identified bCNG channels contain a conserved phosphate-binding cassette (PBC), highlighted by the magenta block from the MEME analysis. However, the sequence of the PBC is not perfectly conserved, since bCNG channels that do not contain the MEME block also contain a binding domain based on the presence of particular conserved cationic residues that are shifted in position by a residue or two in the protein sequence. This type of charged residue conservation without total sequence identity is not surprising based on the bioinformatics analysis of Taylor and co-workers (Berman et al. 2005) and our own characterization (LaFranzo et al. 2010) of cyclic nucleotide binding domains.

Moreover, in the binding and linking domains of the protein, some of the conserved regions identified by the MEME analysis (teal and light green blocks) represent regions of high sequence similarity within the bCNG family that are not observed in MscS or MloK1. The teal MEME group represents a highly conserved linker region at the start of the binding domain that shows little sequence similarity with the MloK1 linking region. This is important, since this similarity with MscS suggests that bCNG channels may exist as heptamers, while the MloK1 channel has been assigned a tetrameric structure. As a result, one would expect the binding transduction domains to vary greatly in these channels.

A phylogenetic sequence analysis of the bCNG family of ion channels and the MloK1 channel was carried out to examine the evolutionary distance between these protein families (Figure 2.3). This analysis clearly indicates that the bCNG family of ion channels is not closely related to the MloK1 ion channel. Despite similarities between the

binding domains of MloK1 and the bCNG family of ion channels, the transmembrane regions of these channels are quite divergent. While they are all more closely related to one another than to MloK1, there is significant diversity within the ion channel domain of members of the bCNG family.

### *2.3.3 Channel cloning and functional verification*

Our analyses above showed significant homology between regions of bCNG channels with cyclic nucleotide binding domains and the mechanosensitive ion channel MscS. As an initial test of whether the putative bCNG channel family is in fact a family of bacterial LGICs or exhibits mechanosensitive properties, we cloned three channels from genomic bacterial DNA: Ml-bCNG, Cv-bCNG, and Te-bCNGb. These particular channels were chosen to initially consider putative function since they are diverse members of the bCNG family that have various numbers of predicted transmembrane helices and exhibit significant sequence differences.

### *2.3.4 Electrophysiological measurements*

Bilayer electrophysiology experiments were carried out to perform an initial verification that bCNG channels respond to cyclic nucleotides. The Ml-bCNG, Cv-bCNG, and Te-bCNGb channels were cloned into a pET expression vector, overexpressed in *E. coli*, purified by affinity chromatography, and reconstituted into lipid vesicles. Overexpression and purification of bacterial ion channels from *E. coli* is a well-established technique for the determination a bacterial ion channel's functional role, and *E. coli* can properly fold and assemble ion channels from other bacterial species (Rees et al. 2000).

Representative measurements of Te-bCNGb at 50 mV as a function of cAMP concentration are shown in Figure 2.4A. All of the traces in Figure 2.4A contain multiple bCNG channels. As expected for a cAMP LGIC, no channel activity is observed in the absence of cAMP, and addition of cAMP to the recording solution results in channel activity. Furthermore, increased open probability is observed as a function of concentration. In addition to the fully open state, Te-bCNGb has a clear sub-conductance state, which is minimally conductive.

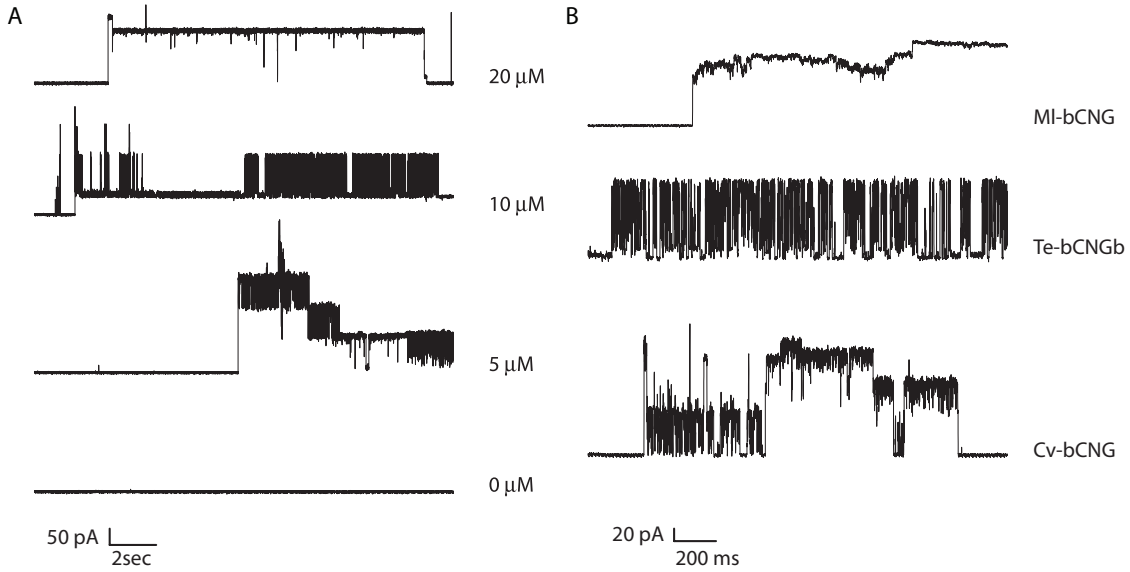


**Figure 2.4:** Representative planar lipid bilayer electrophysiological traces of bCNG channels. **A**) Electrophysiology of Te-bCNGb as a function of cAMP concentration at 50 mV. **B**) Representative electrophysiological traces of Ml-bCNG, Te-bCNGb, and Cv-bCNG at 10 μM cAMP and 50 mV.

Figure 2.4B shows representative electrophysiological traces for Ml-bCNG, Cv-bCNG, and Te-bCNGb at 10 $\mu$M cAMP and 50 mV. For all three channels, no activity was observed in the absence of cAMP. A similar single channel conductance is observed for

all three channels, which is also consistent with the single channel conductance reported for Ec-MscS (Sukharev 2002). Additionally, all three channels exhibit at least one sub-conductance state. These observations suggest that despite the significant sequence differences between these channels, they all function as ligand-gated ion channels with similar pore regions.

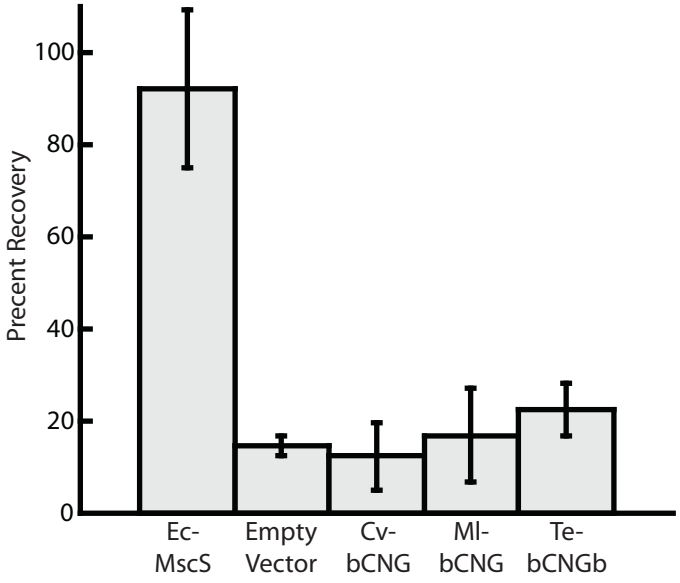


**Figure 2.5**: Osmotic downshock data for bCNG channels. Error bars are the standard deviation of the six trials for each construct. Only MscS is statistically different from the empty vector control (at <99.99% confidence).

*2.3.5 Osmotic downshock assays*

To determine if the bCNG channels were mechanosensitive, osmotic downshock experiments were conducted on the three channels and the results were compared to osmotic downshock experiments carried out with Ec-MscS and an empty vector control (Figure 2.5). Analogous osmotic downshock methods have been used extensively to

characterize the ability of MscL and MscS channels to respond to membrane tension (Blount et al. 1997; Maurer and Dougherty 2003; Vásquez et al. 2007). In these experiments, none of the bCNG channels mediated significant rescue from osmotic downshock, implying that these bCNG channels likely do not gate in response to membrane tension. All channels were statistically similar to the empty vector control and statistically different from MscS. This suggests that while these channels share sequence homology with MscS, they do not exhibit functional homology to MscS. Although MscS and bCNG channels share sequence homology, this homology is concentrated in the pore lining helix (Figure 2.1 and 2.2) that does not interact with lipid tails or head groups. As a result, it is not surprising that these channels are not capable of directly sensing lipid bilayer tension, since it has previously been demonstrated that tension in bacterial mechanosensitive channels is transduced through direct interactions with the lipid bilayer (Sukharev 2002; Sukharev et al. 1999).

### *2.4 Conclusion*

Here we have identified a new family of bacterial ligand-gated ion channels. Although these channels contain significant sequence homology to MscS, they are not capable of rescuing bacteria from osmotic downshock. The existence of cyclic nucleotide gated ion channels *in M. loti* that also express MloK1, a cyclic nucleotide modulated channel, suggests that, like mammalian cells, bacteria make use of both cyclic nucleotide *gated* and cyclic nucleotide *modulated* ion channels. The identification of bCNG ion channels will form the basis for interesting structure-function studies of LGICs. Moreover, this family of ion channels represents an intriguing structural target, since the crystal structure

of the homologous channel MscS has been solved in different conformations (Bass et al. 2002; Wang et al. 2008).

### *2.5 References*


Altieri SL, Clayton GM, Silverman WR, Olivares AO, De la Cruz EM, Thomas LR, Morais-Cabral JH (2008) Structural and energetic analysis of activation by a cyclic nucleotide binding domain. J Mol Biol 381 (3):655-669

Altschul SF, Madden TL, Schaffer AA, Zhang J, Zhang Z, Miller W, Lipman DJ (1997) Gapped BLAST and PSI-BLAST: a new generation of protein database search programs. Nucleic Acids Res 25 (17):3389-3402. doi:gka562 [pii]

Aslanidis C, de Jong PJ (1990) Ligation-independent cloning of PCR products (LIC-PCR). Nucleic Acids Res 18 (20):6069-6074

Bailey TL, Elkan C (1994) Fitting a mixture model by expectation maximization to discover motifs in biopolymers. Proc Int Conf Intell Syst Mol Biol 2:28-36

Barton GJ (1990) Protein multiple sequence alignment and flexible pattern matching. Methods Enzymol 183:403-428

Bass RB, Strop P, Barclay M, Rees DC (2002) Crystal structure of Escherichia coli MscS, a voltage-modulated and mechanosensitive channel. Science 298 (5598):1582-1587. doi:10.1126/science.1077945

298/5598/1582 [pii]

Berman HM, Ten Eyck LF, Goodsell DS, Haste NM, Kornev A, Taylor SS (2005) The cAMP binding domain: an ancient signaling module. Proc Natl Acad Sci U S A 102 (1):45-50. doi:0408579102 [pii]

10.1073/pnas.0408579102

Blount P, Schroeder MJ, Kung C (1997) Mutations in a bacterial mechanosensitive channel change the cellular response to osmotic stress. J Biol Chem 272 (51):32150-32157

Bocquet N, Prado de Carvalho L, Cartaud J, Neyton J, Le Poupon C, Taly A, Grutter T, Changeux JP, Corringer PJ (2007) A prokaryotic proton-gated ion channel from the nicotinic acetylcholine receptor family. Nature 445 (7123):116-119. doi:nature05371 [pii]

10.1038/nature05371

Booth IR, Edwards MD, Black S, Schumann U, Bartlett W, Rasmussen T, Rasmussen A, Miller S (2007) Physiological analysis of bacterial mechanosensitive channels. Methods Enzymol 428:47-61. doi:S0076-6879(07)28003-6 [pii]

10.1016/S0076-6879(07)28003-6

Chen GQ, Cui C, Mayer ML, Gouaux E (1999) Functional characterization of a potassium-selective prokaryotic glutamate receptor. Nature 402 (6763):817-821. doi:10.1038/45568

Chiu PL, Pagel MD, Evans J, Chou HT, Zeng X, Gipson B, Stahlberg H, Nimigean CM (2007) The structure of the prokaryotic cyclic nucleotide-modulated potassium channel MloK1 at 16 A resolution. Structure 15 (9):1053-1064

Clayton GM, Silverman WR, Heginbotham L, Morais-Cabral JH (2004) Structural basis of ligand activation in a cyclic nucleotide regulated potassium channel. Cell 119 (5):615-627. doi:S0092867404010359 [pii]

10.1016/j.cell.2004.10.030

Cserzo M, Eisenhaber F, Eisenhaber B, Simon I (2002) On filtering false positive transmembrane protein predictions. Protein Eng 15:745-752

Finn JT, Grunwald ME, Yau KW (1996) Cyclic nucleotide-gated ion channels: An extended family with diverse functions. Annual Review of Physiology 58:395-426

Geiser M, Cebe R, Drewello D, Schmitz R (2001) Integration of PCR fragments at any specific site within cloning vectors without the use of restriction enzymes and DNA ligase. Biotechniques 31 (1):88-90, 92

Grundy WN, Bailey TL, Elkan CP, Baker ME (1997) Meta-MEME: motif-based hidden Markov models of protein families. Comput Appl Biosci 13 (4):397-406

Haswell ES, Peyronnet R, Barbier-Brygoo H, Meyerowitz EM, Frachisse JM (2008) Two MscS homologs provide mechanosensitive channel activities in the Arabidopsis root. Curr Biol 18 (10):730-734

Haun RS, Moss J (1992) Ligation-independent cloning of glutathione S-transferase fusion genes for expression in Escherichia coli. Gene 112 (1):37-43

Hilf RJ, Dutzler R (2009) Structure of a potentially open state of a proton-activated pentameric ligand-gated ion channel. Nature 457 (7225):115-118. doi:nature07461 [pii]

10.1038/nature07461

Hirokawa T, Boon-Chieng S, Mitaku S (1998) SOSUI: classification and secondary structure prediction system for membrane proteins. Bioinformatics 14:378-379

Hofmann K, Stoffel W (1993) TMbase—A database of membrane spanning proteins segments. Biol Chem Hoppe-Seyler 374:166

Hucho F, Weise C (2001) Ligand-gated ion channels. Angewandte Chemie-International Edition 40 (17):3101-3116

Kaneko T, Tanaka A, Sato S, Kotani H, Sazuka T, Miyajima N, Sugiura M, Tabata S (1995) Sequence analysis of the genome of the unicellular cyanobacterium Synechocystis sp. strain PCC6803. I. Sequence features in the 1 Mb region from map positions 64% to 92% of the genome. DNA Res 2 (4):153-166, 191-158

Krogh A, Larsson B, von Heijne G, Sonnhammer EL (2001) Predicting transmembrane protein topology with a hidden Markov model: application to complete genomes. J Mol Biol 305:567-580

Kumar S (1976) Properties of adenyl cyclase and cyclic adenosine 3',5'-monophosphate receptor protein-deficient mutants of Escherichia coli. J Bacteriol 125 (2):545-555

LaFranzo NL, Strulson MK, Yanker DM, Dang L, Maurer JA (2010) Sequence or Structure: Using Bioinformatics and Homology Modeling to Understand Functional Relationships in cAMP/cGMP Binding Domains. Mol Biosyst 6:894-901

Levina N, Totemeyer S, Stokes NR, Louis P, Jones MA, Booth IR (1999) Protection of Escherichia coli cells against extreme turgor by activation of MscS and MscL mechanosensitive channels: identification of genes required for MscS activity. EMBO J 18 (7):1730-1737. doi:10.1093/emboj/18.7.1730

Li M, Lester HA (2001) Ion channel diseases of the central nervous system. CNS Drug Rev 7 (2):214-240

Marchler-Bauer A, Anderson JB, Cherukuri PF, DeWeese-Scott C, Geer LY, Gwadz M, He S, Hurwitz DI, Jackson JD, Ke Z, Lanczycki CJ, Liebert CA, Liu C, Lu F,

Marchler GH, Mullokandov M, Shoemaker BA, Simonyan V, Song JS, Thiessen PA, Yamashita RA, Yin JJ, Zhang D, Bryant SH (2005) CDD: a Conserved Domain Database for protein classification. Nucleic Acids Res 33 (Database issue):D192-196. doi:33/suppl_1/D192 [pii]

10.1093/nar/gki069

Marchler-Bauer A, Anderson JB, Derbyshire MK, DeWeese-Scott C, Gonzales NR, Gwadz M, Hao L, He S, Hurwitz DI, Jackson JD, Ke Z, Krylov D, Lanczycki CJ, Liebert CA, Liu C, Lu F, Lu S, Marchler GH, Mullokandov M, Song JS, Thanki N, Yamashita RA, Yin JJ, Zhang D, Bryant SH (2007) CDD: a conserved domain database for interactive domain family analysis. Nucleic Acids Res 35 (Database issue):D237-240. doi:gkl951 [pii]

10.1093/nar/gkl951

Martinac B, Saimi Y, Kung C (2008) Ion channels in microbes. Physiol Rev 88 (4):1449-1490

Maurer JA, Dougherty DA (2003) Generation and evaluation of a large mutational library from the Escherichia coli mechanosensitive channel of large conductance, MscL: implications for channel gating and evolutionary design. J Biol Chem 278 (23):21076-21082. doi:10.1074/jbc.M302892200

M302892200 [pii]

Mayer ML, Olson R, Gouaux E (2001) Mechanisms for ligand binding to GluR0 ion channels: crystal structures of the glutamate and serine complexes and a closed apo state. J Mol Biol 311 (4):815-836. doi:10.1006/jmbi.2001.4884

S0022-2836(01)94884-3 [pii]

Myers EW, Miller W (1988) Optimal alignments in linear space. Comput Appl Biosci 4 (1):11-17

Nimigean CM, Pagel MD (2007) Ligand binding and activation in a prokaryotic cyclic nucleotide-modulated channel. J Mol Biol 371 (5):1325-1337

Nimigean CM, Shane T, Miller C (2004) A cyclic nucleotide modulated prokaryotic K+ channel. J Gen Physiol 124 (3):203-210. doi:10.1085/jgp.200409133

jgp.200409133 [pii]

Ochoa de Alda JA, Houmard J (2000) Genomic survey of cAMP and cGMP signalling components in the cyanobacterium Synechocystis PCC 6803. Microbiology 146 Pt 12:3183-3194

Pivetti CD, Yen M-R, Miller S, Busch W, Tseng Y-H, Booth IR, Saier MH, Jr. (2003) Two families of mechanosesitive channel proteins. Microbiol Mol Biol Rev 67 (1):66-85

Rees DC, Chang G, Spencer RH (2000) Crystallographic analyses of ion channels: lessons and challenges. J Biol Chem 275 (2):713-716

Sukharev S (2002) Purification of the small mechanosensitive channel of Escherichia coli (MscS): the subunit structure, conduction, and gating characteristics in liposomes. Biophys J 83 (1):290-298

Sukharev SI, Blount P, Martinac B, Blattner FR, Kung C (1994) A large-conductance mechanosensitive channel in E. coli encoded by mscL alone. Nature 368 (6468):265-268. doi:10.1038/368265a0

Sukharev SI, Sigurdson WJ, Kung C, Sachs F (1999) Energetic and spatial parameters for gating of the bacterial large conductance mechanosensitive channel, MscL. J Gen Physiol 113 (4):525-540

Tasneem A, Iyer LM, Jakobsson E, Aravind L (2005) Identification of the prokaryotic ligand-gated ion channels and their implications for the mechanisms and origins of animal Cys-loop ion channels. Genome Biol 6 (1):R4

Vásquez V, Cortes DM, Furukawa H, Perozo E (2007) An optimized purification and reconstitution method for the MscS channel: strategies for spectroscopical analysis. Biochemistry 46 (23):6766-6773. doi:10.1021/bi700322k

Vásquez V, Sotomayor M, Cordero-Morales J, Schulten K, Perozo E (2008) A structural mechanism for MscS gating in lipid bilayers. Science 321:1210-1214

Wang W, Black SS, Edwards MD, Miller S, Morrison EL, Bartlett W, Dong C, Naismith JH, Booth IR (2008) The structure of an open form of an E. coli mechanosensitive channel at 3.45 A resolution. Science 321 (5893):1179-1183

Wilbur WJ, Lipman DJ (1983) Rapid similarity searches of nucleic acid and protein data banks. Proc Natl Acad Sci U S A 80 (3):726-730

Wild J, Altman E, Yura T, Gross CA (1992) DnaK and DnaJ heat shock proteins participate in protein export in Escherichia coli. Genes Dev 6 (7):1165-1172

# Chapter Three

# Mechanosensitive Behavior of Bacterial Cyclic Nucleotide Gated (bCNG) Ion Channels: Insights into the Mechanism of Channel Gating in the Mechanosensitive Channel of Small Conductance (MscS) Superfamily.

---

### *3.1. Introduction*

We previously identified a novel class of ligand-gated bacterial ion channels, the bacterial cyclic nucleotide gated (bCNG) ion channel family (Caldwell et al.). These channels are composed of three domains: a channel domain, a linker domain, and a cyclic nucleotide binding domain (Figure 3.1). The pore lining helix of the channel domain has significant homology to the mechanosensitive channel of small conductance from *Escherichia coli* (*E. coli*) (Ec-MscS) and the cyclic nucleotide monophosphate (cNMP) binding domain has high homology to known cNMP binding domains, including the cNMP binding domain of MloK1, a bacterial cyclic nucleotide regulated potassium

channel (Nimigean et al. 2004; Chiu et al. 2007; LaFranzo et al.). The linker domain is not highly conserved within the family and does not exhibit significant homology to known protein sequences. In previous studies, we demonstrated that three members of this channel family gate in response to cyclic adenosine monophosphate (cAMP) (Caldwell et al.).

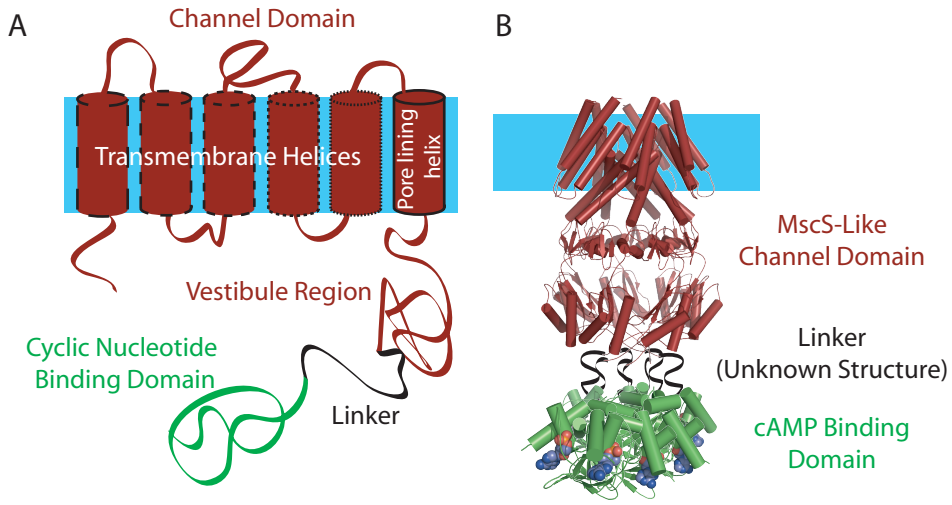


**Figure 3.1**: A) Graphical representation of bCNG channels labeling the various channel domains and regions. Relative helix conservation across the bCNG family is indicated by dashed lines around each helix with the totally conserved pore lining helix shown as a solid line and the poorly conserved sixth helix shown with the largest spacing between dashes. B) Schematic representation of a three transmembrane domain bCNG channel based on the MscS structure (2OAU) (Bass et al. 2002; Steinbacher et al. 2007) and the binding domain of MloK1 (IVP6) (Clayton et al. 2004).

The strong homology of bCNG channels to Ec-MscS indicates that these channels are members of the MscS superfamily of ion channels, which is primarily composed of mechanosensitive channels from all phylogenetic kingdoms (Pivetti et al. 2003; Kloda and Martinac 2002a, b). However, we have previously demonstrated that three members of the family do not gate in response to mechanical stress (Caldwell et al.). The inability

of bCNG channels to gate in response to mechanical stress is surprising, due to their significant similarity to the pore lining helix and upper vestibule domain of Ec-MscS (Figure 3.2). Previously, sequence homology in these regions has been used as a benchmark for the identification of ion channels that gate in response to membrane tension (Pivetti et al. 2003; Haswell et al. 2008). Using this approach a broad range of mechanosensitive ion channels, across all phylogenetic kingdoms, have been identified that include mechanosensitive ion channels in plants, bacteria, and archea (Kloda and Martinac 2002a, b; Pivetti et al. 2003).

Here we examine the ability of a larger subset of the bCNG ion channel family to rescue *E. coli* from osmotic downshock. Strikingly, we find that none of the channels examined are capable of rescuing *E. coli*, suggesting that the bCNG ion channel family has evolved to be non-mechanosensitive. To further examine the structural source of this decreased mechanosensitivity, we removed the cyclic nucleotide binding domain and linker region (Figure 3.1) from four of these channels to determine if these domains interfered with the channels' ability to respond to mechanical stress. The removal of the C-terminal cyclic nucleotide binding domain produced bCNG channels that were slightly mechanosensitive. The increased mechanosensation of these truncated channels provides insight into the gating mechanism of bCNG ion channels.

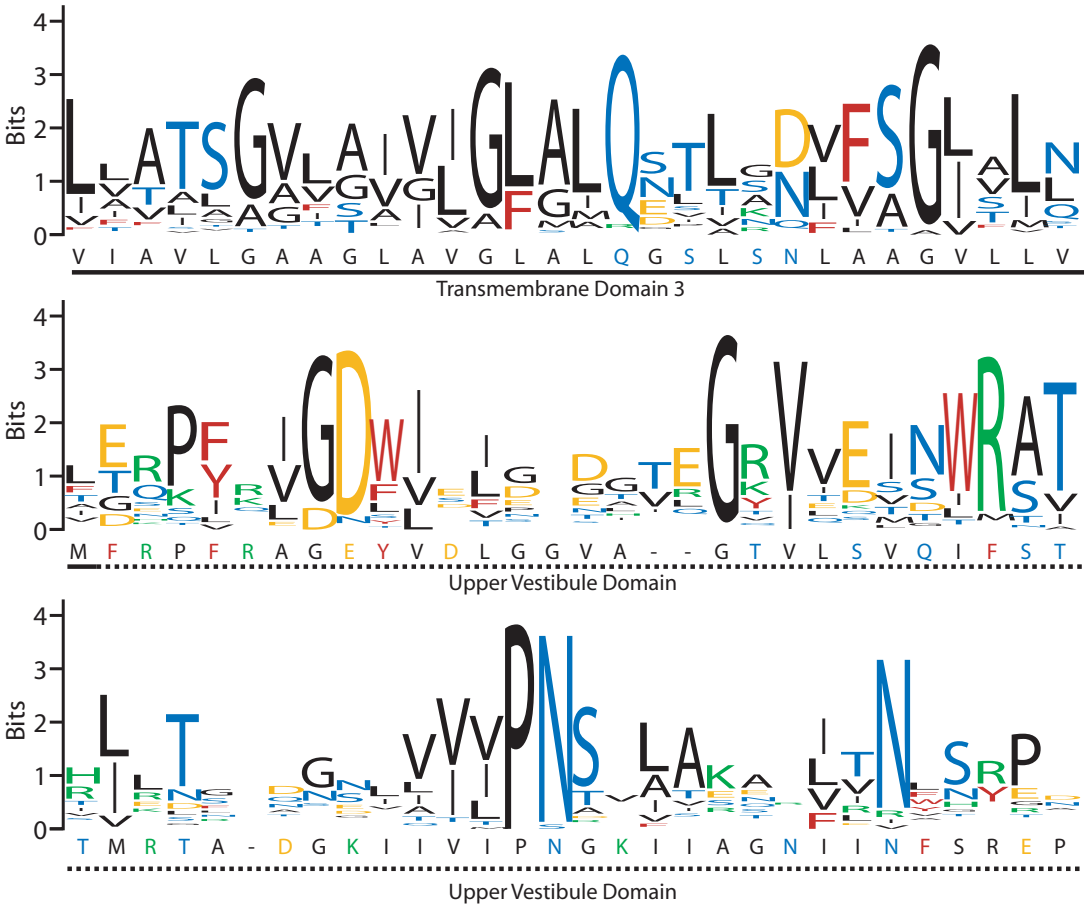


**Figure 3.2**: Conservation of amino acids in the pore lining helix and the upper vestibule domain for the entire bCNG channels is shown using WebLogos (Crooks et al. 2004; Schneider and Stephens 1990). The corresponding residues in MscS are indicated below each logo. Hydrophobic residues (I,P,L,M,V,A,G), are colored black; aromatic residues (F,W,Y) are colored red; polar residues (S,T,Q,N,C) are colored blue; basic residues (K,R,H) are colored green; and acidic residues (D,E) are colored yellow. The Y-axis, in bits, gives the maximum sequence conservation, $\log_2(20)=4.13$ (Crooks et al. 2004; Schneider and Stephens 1990), larger letters indicate higher conservation of that residue.

## *3.2. Materials and Methods*

### *3.2.1 Strains and Plasmids*

The *E. coli* strain MJF465 (*MscS, MscL, MscK* null) was used for osmotic downshock assays (Wild et al. 1992; Sukharev et al. 1994). Cloning was conducted using the

Top10F` *E. coli* strain (Invitrogen). Channels were initially cloned into pET46 vector (Novagen), before being subcloned into the pB10b vector for osmotic downshock assays (Levina et al. 1999; Ou et al. 1998).

*3.2.2 Cloning and Subcloning into pB10b*

Ac-bCNGa, Ac-bCNGb, Bg-bCNGa, Bx-bCNGa, Bx-bCNGb, Bx-bCNGc, Rr-bCNG, Se-bCNG, and Ss-bCNGb were cloned from genomic DNA into pET46 as previously described for Cv-bCNG, Ml-bCNG, and Te-bCNGb by Caldwell *et. al* (Caldwell et al.). Primers used for genomic cloning are given in Table 3.1. Bacterial genomic DNA was obtained from the following sources: *Azorhizobium caulinodas* ORS 571 (Ac) from T. Aono at U. Tokyo, *Burkholderia graminis* C4D1M (Bg) from S. Brady at Rockefeller University, *Burkholderia xenovorans* LB400 (Bx) from J. Tiedje at Michigan State University, *Agrobacterium tumefaciens str*. C58 (Rr) was purchased from ATCC, *Synechococcus elongatus* PCC 7942 (Se) from S.S. Golden at UCSD, *Synechocystis sp.* PCC6803 (Ss) from KAZUZA. Channels were subsequently subcloned into pB10b for osmotic downshock assays, as previously described (Caldwell et al.). Primers used for subcloning are given in Table 3.2. Constructs were verified by enzymatic digestion and sequences confirmed using automated sequencing (Big Dye v3.1, Applied Biosystems).

| | pET46 Forward | pET46 Reverse |
|---|---|---|
| Ac-bCNGa | GACGACGACAAGATGATCTCGGGCGGAAC | GAGGAGAAGCCCGGTCCGGTCGCCTACCCTCG |
| Ac-bCNGb | GACGACGACAAGATGCTCAGCGCG | GAGGAGAAGCCCGGTAAGCTGGTGAAGAGAGT |
| Bg-bCNGa | GACGACGACAAGATGCCGACTCTGACC | GAGGAGAAGCCCGGTTCACAGCGCGAGTTCGTGAAAA |
| Bx-bCNGa | GACGACGACAAGATGCTGGTGGCGATCACACTCGTGGG | GAGGAGAAGCCCGGTCGCATCGAACTCAATCGGAGCCG |
| Bx-bCNGb | GACGACGACAAGATGCCTGCCAATCTATTGTTGC | GAGGAGAAGCCCGGTCAGGGCTCCCGATGTC |
| Bx-bCNGc | GACGACGACAAGATGCCGACCCTGACTG | GAGGAGAAGCCCGGTCAAAGCGTCAGTTCATGG |
| Cv-bCNG | GAAAAAAGCTTGGCGGAGCAAGCATGGACACCCC | AGCAGGCTCGAGCCTGCCGCATTTCAGAAATGGGCGATCG |
| Ml-bCNG | GACGACGACAAGATGCAGGACCTCGTCGTTGGCG | GAGGAGAAGCCCGGTGGCTTCATTCTGCAAGATGGCC |
| Rr-bCNG | GACGACGACAAGATGCTGCAGGCATATATGGGTGAAATCGCCGC | GAGGAGAAGCCCGGTGCTATTCAGGTACTGAAGATCGTCCGG |
| Se-bCNG | GACGACGACAAGATGGATCTTTTTGATCGCC | GAGGAGAAGCCCGGTTTAGAGGCGCAGGACGCGGCGC |
| Ss-bCNGb | GACGACGACAAGATGATTGCACAAATTAATCCACCACC | GAGGAGAAGCCCGGTGGTTTAACGATATGCAGATTCTTGACTGACACC |
| Te-bCNGb | GACGACGACAAGATGACGAAGTACCTCGG | GAGGAGAAGCCCGGTCGCCCTAAACCTTCTAAACATCAAAGAGGG |

**Table 3.1**: PCR primers for cloning of bCNG channels from genomic DNA into the pET46 vector.

*3.2.3 Inserting N-terminal His-tags into full-length pB10b constructs*

To determine if bCNG channels were membrane expressed during osmotic downshock experiments, a N-terminal His-tag was inserted into the bCNG channels. His-Ml-bCNG

pB10b was cloned as previously described (Caldwell et al.). His-Ac-bCNGa, His-Ac-bCNGb, His-Bg-bCNGb, His-Bx-bCNGa, His-Bx-bCNGb, His-Bx-bCNGc His-Cv-bCNG, His-Rr-bCNG, His-Se-bCNG, His-Ss-bCNGb, and His-Te-bCNGb were sub-cloned from pET46 into the His-Ml-bCNG pB10b using enzymatic cut sites in the multiple cloning region. Sequences were confirmed using automated sequencing (Big Dye v3.1, Applied Biosystems).

| | pB10b Forward | pB10B Reverse |
|---|---|---|
| Ac-bCNGa | CCGAGATCTCATAGGGAGAATAACATGATCTCGGGCGGAAC | TCGAGCTGCTTTCAGGCGCTTCCGGTCGCCTACCCTCG |
| Ac-bCNGb | CCGAGATCTCATAGGGAGAATAACATGCTCAGCGCG | TCGAGCTGCTTTCAGGCGCTTCTGGTGAAGAGAGTC |
| Bg-bCNGa | CCGAGATCTCATAGGGAGAATAACATGCCGACTCTGACC | CGCCTCGAGCTGCTTTCAGGCGCTTCGAGATTTGAGGAGAAGCCCG |
| Bx-bCNGa | CCGAGATCTCATAGGGAGAATAACATGCTGGTGGCGATCACACTCG | CGCCTCGAGCTGCTTTCAGGCGCTTGCGAGATTTGAGGAGAAGC |
| Bx-bCNGb | CCGAGATCTCATAGGGAGAATAACATGCCTGCCAATCTATTGTTGCA | CGCCTCGAGCTGCTTTCAGGCGCTTGTCAGGGCTCCCGATGT |
| Bx-bCNGc | CCGAGATCTCATAGGGAGAATAACATGCCGACCCTGACTGA | CGCCTCGAGCTGCTTTCAGGCGCTTGTCAAAGCGTCAGTTCAT |
| Cv-bCNG | CCGAGATCTCATAGGGAGAATAACATGGACACCCCTCCCGCTGTCGGC | CGCCTCGAGCTGCTTTCAGGCGCTTGGGCGATCGGCCATCCCTACGG |
| Ml-bCNG | CCGAGATCTCATAGGGAGAATAACATGCAGGACCTCGTCGTTGGCGTCG | CGCCTCGAGCTGCTTTCAGGCGCTTGTCATTCTGCAAGATGGCCATGGCTTTCTCTCTTC |
| Rr-bCNG | CCGAGATCTCATAGGGAGAATAACATGCTGCAGGCATATATGGGTGAAATCG | CCTCGAGCTGCTTTCAGGCGCTTGGGTACTGAAGATCGTCCGG |
| Se-bCNG | CCGAGATCTCATAGGGAGAATAACATGGATCTTTTTGATCGCCTCG | CGCCTCGAGCTGCTTTCAGGCGCTTGTTAGAGGCGCAGGACGCGGCGC |

| | | |
|---|---|---|
| Ss-bCNGb | CCGAGATCTCATAGGG AGAATAACATGATTGC ACAAATTAATCCACCA CC | CCTCGAGCTGCTTTCAGG CGCTTGTTAACGATATGC AGATTCTTGACTG |
| Te-bCNGb | CCGAGATCTCATAGGG AGAATAACATGACGAA GTACCTCGGTTTATTTT TAGCAGCAGCC | CGCCTCGAGCTGCTTTCA GGCGCTTGCTAAACATCA AAGAGGGTTTTCAAACGG TGGCG |

**Table 3.2**: PCR primers for subcloning of bCNG channels from pET46 into pB10b.

*3.2.4 Truncation of bCNG channels*

Cv-bCNG, Ml-bCNG, Rr-bCNG, Se-bCNG, and their His-tag variants were truncated by inserting two in frame stop codons into the gene using either Megaprimer mutagenesis (Yoshimura et al. 1999) or QuikChange mutagenesis (Stratagene). Primers for insertion of stop codons were designed using Stratagene's QuikChange Primer design (primers can be found in Table 6.3). Insertion of stop codons was verified by enzymatic digestion and sequences confirmed using automated sequencing (Big Dye v3.1, Applied Biosystems).

*3.2.5 Osmotic downshock assays*

Downshock experiments on un-tagged bCNG channels were conducted as previously described (Booth et al. 2007; Caldwell et al.) without modification. For each construct six trials were carried out.

| | Forward | Reverse |
|---|---|---|
| Cv-bCNG | CCACCTGGAGTAACGGG TGTAAGCGCTGCGC | GCGCAGCGCTTACACC CGTTACTCCAGGTGG |
| Ml-bCNG | ACCTGGCCCTTTACCGC GATAAAATAGATCGATT AAACGGCGTTGTTT | AAACAACGCCGTTTAA TCGATCTATTTTATCGC GGTAAAGGGCCAGGT |
| Rr-bCNG | CTGAAGCCACCTTGCAG TAAGTCATCTAAGAAAA TCCGATCGTCTC | GAGACGATCGGATTTT CTTAGATGACTTACTGC AAGGTGGCTTCAG |

| | | |
|---|---|---|
| Se-bCNG | CCCTTCCCTCAATAAGT CCTGCATTGACATCGCT CGGGGACAAC | GTTGTCCCCGAGCGAT GTCAATGCAGGACTTA TTGAGGGAAGGG |

**Table 3.3**: PCR primers for the insertion of two in frame stop codons into bCNG channels.

*3.2.6 Bacterial Expression Analysis*

Expression analysis on N-terminally His-tagged bCNG channels was carried out as previously described without modification (Malcolm et al.).

## *3.3 Results*

*3.3.1 Osmotic downshock of full-length bCNG*

Osmotic downshock assays of full-length bCNG channels indicate that bCNG channels, unlike Ec-MscS, are ineffective at rescuing *E. coli* from hypoosmotic stress, with most showing no significant difference from empty vector (Figure 3.3). All bCNG channels are greater than 99.99% statistically different ($p < 0.001$) from Ec-MscS when analyzed using a Student's T-test (Table 3.4). Additionally, all channels are expressed and trafficked to the membrane, as seen by Western blot analysis of the solublized membrane fraction (Figure 3.3). Moreover, none of the channels exhibit gain of function mechanosensitive phenotypes, as seen by steady-state optical density measurements (Table 3.5). This indicates that these channels are not "leaky" and do not gate at low membrane tensions, since it has been shown for other members of the MscS superfamily that channels exhibiting a gain of function phenotype can be identified by a lower steady-state optical density due to growth inhibition (Maurer and Dougherty 2001). Taken together, these results suggest that none of the bCNG channels are mechanosensitive.

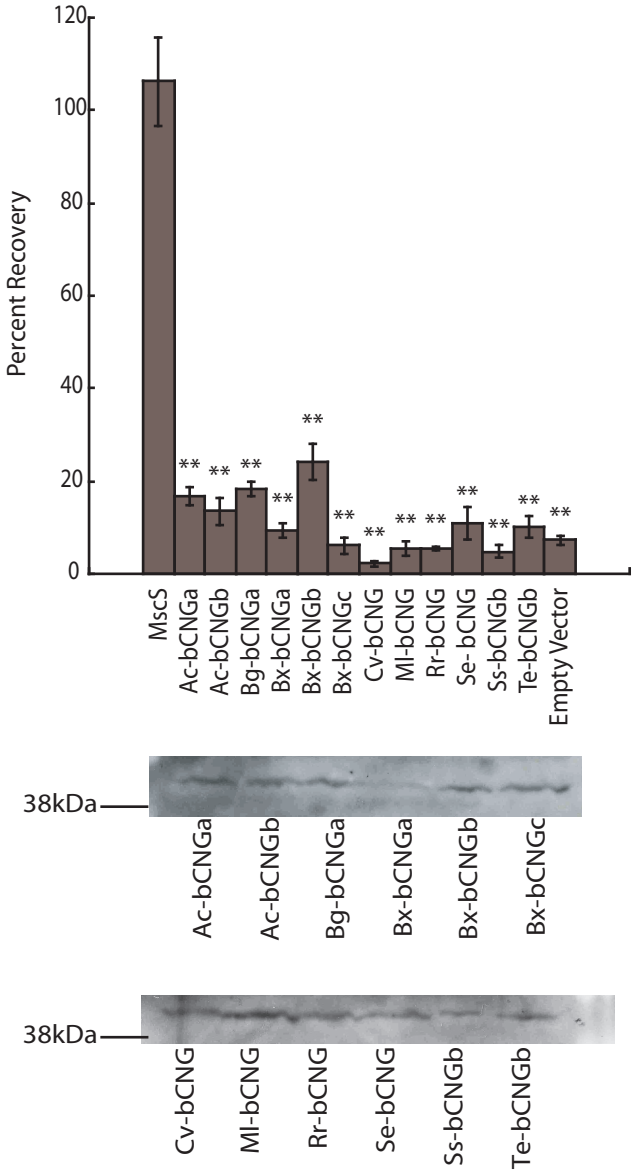


**Figure 3.3**: Funcational Assays of full-length bCNG channels. Osmotic downshock results for bCNG channels. Error bars are standard error of the mean based on six replicates. All bCNG channels are >99.99% statistically different from MscS (** = $p<0.0001$). Western Blot analysis of protein expression levels of full-length bCNG channels under expression conditions identical to those used for the osmotic downshock assays.

| | Percent Recovery | Difference from MscS (p-value) |
|---|---|---|
| MscS | 106 ± 10 | N/A |
| Ac-bCNGa | 17 ± 2 | $3.4x10^{-6}$ |
| Ac-bCNGb | 14 ± 3 | $3.2x10^{-6}$ |
| Bg-bCNGa | 18 ± 2 | $3.9x10^{-6}$ |
| Bx-bCNGa | 9 ± 1 | $1.6x10^{-5}$ |
| Bx-bCNGb | 24 ± 4 | $1.2x10^{-5}$ |
| Bx-bCNGc | 6 ± 2 | $1.3x10^{-6}$ |
| Cv-bCNG | 10 ± 5 | $7.4x10^{-7}$ |
| Ml-bCNG | 5 ± 1 | $1.1x10^{-6}$ |
| Rr-bCNG | 5.5 ± 0.5 | $9.9x10^{-7}$ |
| Se-bCNG | 11 ± 4 | $3.0x10^{-6}$ |
| Ss-bCNGb | 5 ± 1 | $1.0x10^{-6}$ |
| Te-bCNGb | 10 ± 2 | $1.9x10^{-4}$ |
| Empty Vector | 7 ± 1 | $1.2x10^{-6}$ |

**Table 3.4**: Percent Recovery data for full-length bCNG channels, the standard error of the mean for six trials is shown. The p-values for the difference from MscS was calculated using a Student's T-test.

### *3.3.2 Truncation of bCNG channels*

Since none of the channels exhibited mechanosensitive behavior, four bCNG channels were truncated to remove the cyclic nucleotide binding domain. A sequence alignment of all 59 punitive bCNG channels and MscS (Caldwell et al.) was used to define the channel and binding domains of these bCNG channels. Two in-frame stop codons were inserted in the linker between the channel domain and the binding domain. Based on the sequence alignment, stop codons were inserted as close to the residue aligned with the C-terminus of MscS as possible to give truncated proteins encoding primarily for the channel domain upon overexpression. Stop codons were inserted at residue 342 for Cv-bCNG, residue 228 for Ml-bCNG, residue 343 for Rr-bCNG, and residue 273 for Se-bCNG. An alignment of the truncated channels with MscS is given in Figure 3.4.

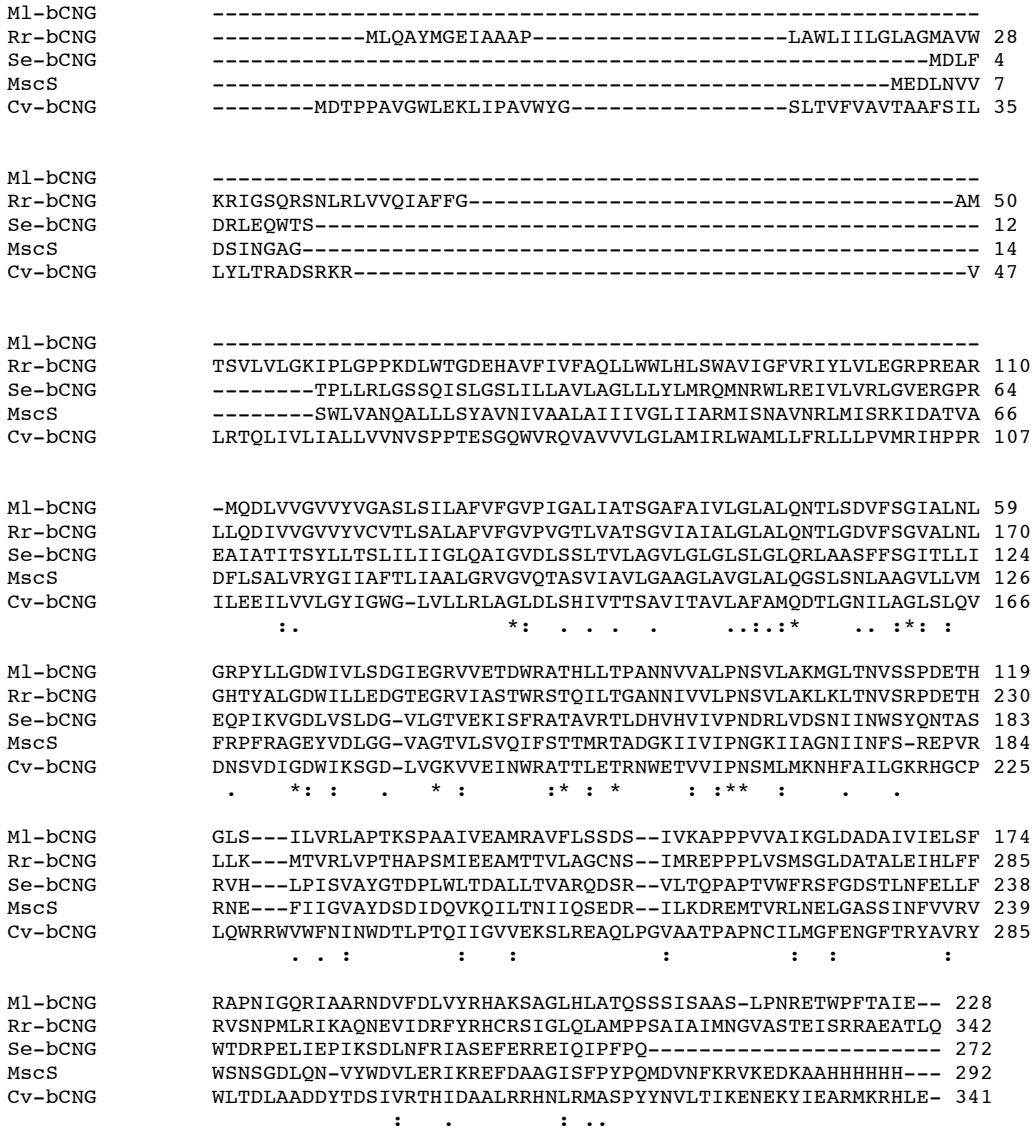


**Figure 3.4**: Alignment of truncated bCNG channels with MscS created using ClustalW (Chenna et al. 2003).

Osmotic downshock assays of the truncated bCNG channels show that removal of the cyclic nucleotide binding domain dramatically increases the ability of these channels to rescue *E. coli* from hypoosmotic stress when compared to full-length bCNG channels (Figure 3.5, Table 3.6). All of the truncated mutants have a statistical difference of

greater than 99.9% ($p<0.001$) when compared with the full-length channel using a Student's T-test. All truncated channels are expressed to the membrane in equivalent levels (Figure 3.6). Additionally, truncated channels and full-length channels are expressed in similar levels so increased mechanosensation is not due to a variation in protein levels. Despite a significant increase their in mechanosensitivity, these channels are still less mechanosensitive than Ec-MscS. The observed rescue from osmotic downshock by the truncated bCNG channels was typically only around 20% compared to close to 100% for Ec-MscS. Moreover, all truncated bCNG channels were confirmed to not be gain of function by measuring their steady-state optical densities (Table 3.4).

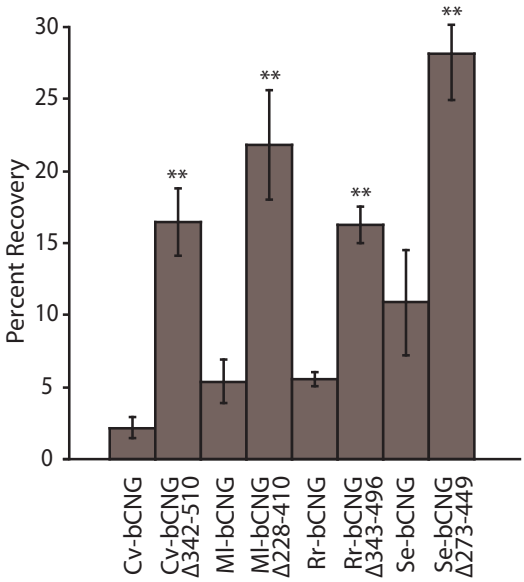


**Figure 3.5**: Osmotic downshock results for truncated bCNG channels. Error bars are standard error of the mean based on six replicates. All truncated channels are statistically different from their full-length counter part (** = $p<0.001$)

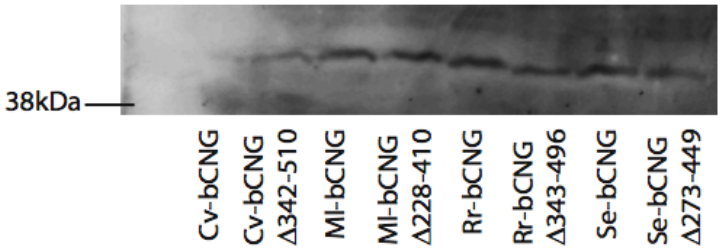


**Figure 3.6**: Western Blot analysis of protein expression levels of truncated bCNG channels and their full-length bCNG counterparts under expression conditions identical to those used for the osmotic downshock assays.

| | Stationary Phase Optical Density ($OD_{600}$) |
|---|---|
| MscS | 1.7 |
| Ac-bCNGa | 1.5 |
| Ac-bCNGb | 1.6 |
| Bg-bCNGa | 1.5 |
| Bx-bCNGa | 1.5 |
| Bx-bCNGb | 1.5 |
| Bx-bCNGc | 1.5 |
| Cv-bCNG | 1.5 |
| Cv-bCNG Δ342-510 | 1.5 |
| Ml-bCNG | 1.7 |
| Ml-bCNG Δ228-410 | 1.5 |
| Rr-bCNG | 1.6 |
| Rr-bCNG Δ343-496 | 1.5 |
| Se-bCNG | 1.4 |
| Se-bCNG Δ273-449 | 1.4 |
| Ss-bCNGb | 1.7 |
| Te-bCNGb | 1.4 |
| Empty Vector | 1.5 |

**Table 3.5**: Stationary phase optical densities for bCNG channels, full-length and truncated channels. Stationary phase optical densities were obtained by growing a single colony to an $OD_{600}$ of approximately 0.5 in LB media, followed by induction with 0.1 mM IPTG for 8 hours.

| Truncated bCNG channels | Percent Recovery | Difference from full-length (p-value) |
|---|---|---|
| Cv-bCNG | 16 ± 2 | $1.5x10^{-4}$ |
| Ml-bCNG | 22 ± 4 | $2.5x10^{-3}$ |
| Rr-bCNG | 16 ± 1 | $1.4x10^{-5}$ |
| Se-bCNG | 28 ± 3 | $4.9x10^{-3}$ |

**Table 3.6**: Percent Recovery data for truncated bCNG channels, the standard error of the mean for six trials is given. The p-values from the corresponding full-length bCNG channel was calculated using a Student's T-test.

### *3.4. Discussion*

Tension gated ion channels in bacteria, plants, and archea have been successfully identified based on their homology to the pore lining helix and upper vestibule region of Ec-MscS (Pivetti et al. 2003; Kloda and Martinac 2002a, b). The recently identified bCNG ion channel family is highly homologous to Ec-MscS in the pore lining helix and upper vestibule domain (Figure 3.2). This homology identifies the bCNG channel family as being a subset of the MscS superfamily. However, we have previously shown that while three bCNG homologues gate in response to cAMP alone, they are incapable of rescuing *E. coli* from osmotic downshock.

Osmotic downshock assays of twelve full-length bCNG channels demonstrated that none of these channels are capable of rescuing *E. coli* from hypoosmotic shock (Figure 3.3). The inability to respond to mechanical stress is not due to problems with protein expression and trafficking, since all channels are expressed to the membrane (Figure 3.4). We would have expected these channels to display a mechanosensitive phenotype, since phylogenic tree analysis of the bCNG channel family suggest that these channels are a

subset of the MscS superfamily (Caldwell et al.) and it seems plausible that they evolved from the same progenitor as Ec-MscS through the appendage of a cyclic nucleotide binding domain to the C-terminus of a MscS-like protein (Figure 3.1). While some bCNG channels have little overall homology to Ec-MscS, all of these channels exhibit significant homology in both the pore lining helix and the upper vestibule domain (Figure 3.2, Table 3.7). Furthermore, the channel domain of Se-bCNG is very similar to that of Ec-MscS and is predicted to be composed of three transmembrane domains. However, even Se-bCNG fails to rescue *E. coli* from hypoosmotic downshock. Thus, it seems that bCNG channels have likely evolved to be non-mechanosensitive.

| | Percent Identity of full-length bCNG in comparison with *E. coli* MscS | Percent Identity of bCNG channel domain in comparison with *E. coli* MscS | Percent Identity of bCNG TM3 and upper vestibule in comparison with *E. coli* MscS |
|---|---|---|---|
| Ac-bCNGa | 12.0% | 15.5% | 29.5% |
| Ac-bCNGb | 10.7% | 15.0% | 27.3% |
| Bg-bCNGa | 11.9% | 17.3% | 32.2% |
| Bx-bCNGa | 11.7% | 17.1% | 26.1% |
| Bx-bCNGb | 11.2% | 16.2% | 35.2% |
| Bx-bCNGc | 12.9% | 18.8% | 35.2% |
| Cv-bCNG | 9.2% | 13.7% | 20.7% |
| Ml-bCNG | 10.1 % | 16.3% | 29.5% |
| Rr-bCNG | 11.1% | 16.0% | 30.7% |
| Se-bCNG | 15.4% | 23.6% | 32.2% |
| Ss-bCNGb | 11.8% | 18.5% | 24.1% |
| Te-bCNGb | 11.2% | 15.3% | 28.7% |

**Table 3.7**: Percent identity scores of full-length bCNG, bCNG channel domain, and bCNG TM3 and upper vestibule domains were aligned with MscS. Pairwise alignments of individual channels with MscS were prepared and scored using ALIGN (Myers and Miller 1989).

In Figure 3.3, all bCNG channels are observed to run at the same molecular weight, since there is not a large variance in molecular weight between bCNG channels (Caldwell et al.). Moreover, all channels are observed to run at a lower molecular weight than expected, which is attributed to the inability of membrane proteins to be full denatured in SDS-Loading dye (Tulumello and Deber). Previous work with Ec-MscS, which has related TM segments, demonstrated that it runs with a lower effective molecular weight than predicted (Machiyama et al. 2009; Malcolm et al. ; Schumann et al. 2004; Akitake et al. 2007; Nomura et al. 2006).

The most striking difference between bCNG channels and Ec-MscS is the presence of a C-terminal cyclic nucleotide binding domain that is connected to the MscS-like channel domain by a linker (Figure 3.1). Previous research has indicated that the C-terminus of Ec-MscS is essential for channel function (Miller et al. 2003) and expands upon channel opening (Machiyama et al. 2009). Machiyama and co-workers showed that the vestibule domain of Ec-MscS swells in response to mechanical tension by examining the distances between residues using fluorescence resonance energy transfer (FRET) (Machiyama et al. 2009). Additionally, it has been shown through nickel (II) coordination to C-terminal His-tags in Ec-MscS that hampering the movement of the C-terminus in MscS hinders the ability of MscS to gate in response to mechanical stress (Koprowski and Kubalski 2003). This coordination interferes with the movement of the vestibule domain, which in turn interferes with the ability of MscS to gate in response to mechanical stress (Koprowski et al. ; Koprowski and Kubalski 2003). Hence, one might expect the addition of a C-terminal nucleotide binding domain, as seen in the bCNG channel family, to

eliminate the mechanosensitive behavior of these channels by blocking the C-terminal rearrangement required for channel opening in the absence of cyclic nucleotide ligand.

To test the hypothesis that the binding domain of bCNG channels blocks the C-terminal rearrangement required for gating, we removed the cyclic nucleotide binding domains of four bCNG homologues with differing numbers of transmembrane helices. Truncations of the bCNG channels were made in the early region of the linker, so as to best preserve the entire C-terminal region of the MscS-like channel domain while eliminating the majority of the binding domain and linker (Figure 3.4).

In Figure 3.6, the full-length bCNG channels and their truncated partners are observed to run at similar molecular weights, despite the fact that truncation removes a significant portion of the protein. This can be attributed to incomplete denaturation of the membrane portion of the protein altering the apparent molecular weight of both the truncated and non-truncated channels (Tulumello and Deber).

Removal of the binding domain and the majority of the linker resulted in channels capable of rescuing *E. coli* from hypoosmotic stress (Figure 3.5). These results indicate that the nucleotide-binding domain in bCNG channels inhibits the movement of the vestibule domain and prevents bCNG channels from gating in response to mechanical stress. Thus, it seems likely that the binding of cAMP to the binding domain of bCNG channels induces rearrangement of the vestibule domain, which in turn leads to channel opening. This suggests that the rearrangement of the pore lining helix of bCNG channels

leading to channel opening is functionally analogous to the rearrangement that occurs in Ec-MscS, but is achieved by a different gating stimuli.

Although, truncated bCNG channels are membrane expressed (Figure 3.6) and are able to rescue *E. coli* from hypoosmotic shock (Figure 3.5), they do not rescue to the same degree as Ec-MscS. This is likely attributable to the evolution of the lipid lining region away from Ec-MscS. This is highlighted by the fact that these channels do not all have three transmembrane domains akin to Ec-MscS and instead are predicted to have varying numbers of transmembrane domains, between one and six (Caldwell et al.). In light of this, it is interesting that extent of rescue observed for the truncated channels is not dependent on the number of transmembrane domains that make up the bCNG channel domain. Even the channel domain of Se-bCNG, which is very similar to Ec-MscS has clearly undergone significant evolution to reduce its mechanosensitivity. This is a result of changes in the critical residues for tension sensation, which have previously been identified in Ec-MscS (Malcolm et al.).

While bCNG channels are a subset of the larger MscS superfamily and the transition between the closed and open state likely involves similar molecular level motions, bCNG channels have evolved to be non-mechanosensitive. This evolution involves changes in the lipid lining residues that are important for tension sensation and changes to the C-terminus of the protein. The appendage of a binding domain onto the C-terminus of an MscS-like channel domain blocks the rearrangements of the C-terminal region required for mechanosensitive gating, as seen in our osmotic downshock and truncation assays.

Based on these observations it is likely that gating in response to cAMP by full-length bCNG channels occurs through C-terminal rearrangement of the vestibule domain of the channel. These data suggest the MscS superfamily of ion channels is not simply a mechanosensitive ion channel family, and members of this superfamily may play diverse functional roles in prokaryotic and eukaryotic physiology.

### *3.5 References*


Akitake B, Spelbrink RE, Anishkin A, Killian JA, de Kruijff B, Sukharev S (2007) 2,2,2-Trifluoroethanol changes the transition kinetics and subunit interactions in the small bacterial mechanosensitive channel MscS. Biophysical journal 92 (8):2771-2784. doi:S0006-3495(07)71082-2 [pii]

10.1529/biophysj.106.098715

Bass RB, Strop P, Barclay M, Rees DC (2002) Crystal structure of Escherichia coli MscS, a voltage-modulated and mechanosensitive channel. Science 298 (5598):1582-1587. doi:10.1126/science.1077945

298/5598/1582 [pii]

Booth IR, Edwards MD, Black S, Schumann U, Bartlett W, Rasmussen T, Rasmussen A, Miller S (2007) Physiological analysis of bacterial mechanosensitive channels. Methods Enzymol 428:47-61. doi:S0076-6879(07)28003-6 [pii]

10.1016/S0076-6879(07)28003-6

Caldwell DB, Malcolm HR, Elmore DE, Maurer JA Identification and experimental verification of a novel family of bacterial cyclic nucleotide-gated (bCNG) ion

channels. Biochim Biophys Acta 1798 (9):1750-1756. doi:S0005-2736(10)00185-9 [pii]

10.1016/j.bbamem.2010.06.001

Chenna R, Sugawara H, Koike T, Lopez R, Gibson TJ, Higgins DG, Thompson JD (2003) Multiple sequence alignment with the Clustal series of programs. Nucleic Acids Res 31 (13):3497-3500

Chiu PL, Pagel MD, Evans J, Chou HT, Zeng X, Gipson B, Stahlberg H, Nimigean CM (2007) The structure of the prokaryotic cyclic nucleotide-modulated potassium channel MloK1 at 16 A resolution. Structure 15 (9):1053-1064. doi:S0969-2126(07)00277-8 [pii]

10.1016/j.str.2007.06.020

Clayton GM, Silverman WR, Heginbotham L, Morais-Cabral JH (2004) Structural basis of ligand activation in a cyclic nucleotide regulated potassium channel. Cell 119 (5):615-627. doi:S0092867404010359 [pii]

10.1016/j.cell.2004.10.030

Crooks GE, Hon G, Chandonia JM, Brenner SE (2004) WebLogo: a sequence logo generator. Genome Res 14 (6):1188-1190. doi:10.1101/gr.849004

14/6/1188 [pii]

Haswell ES, Peyronnet R, Barbier-Brygoo H, Meyerowitz EM, Frachisse JM (2008) Two MscS homologs provide mechanosensitive channel activities in the Arabidopsis root. Curr Biol 18 (10):730-734. doi:S0960-9822(08)00525-3 [pii]

10.1016/j.cub.2008.04.039

Kloda A, Martinac B (2002a) Common evolutionary origins of mechanosensitive ion channels in Archaea, Bacteria and cell-walled Eukarya. Archaea 1 (1):35-44

Kloda A, Martinac B (2002b) Mechanosensitive channels of bacteria and archaea share a common ancestral origin. Eur Biophys J 31 (1):14-25

Koprowski P, Grajkowski W, Isacoff EY, Kubalski A Genetic screen for potassium leaky small mechanosensitive channels (MscS) in e. coli: recognition of cytoplasmic beta domain as a new gating element. J Biol Chem. doi:M110.176131 [pii]

10.1074/jbc.M110.176131

Koprowski P, Kubalski A (2003) C termini of the Escherichia coli mechanosensitive ion channel (MscS) move apart upon the channel opening. J Biol Chem 278 (13):11237-11245. doi:10.1074/jbc.M212073200

M212073200 [pii]

LaFranzo NA, Strulson MK, Yanker DM, Dang LT, Maurer JA Sequence or structure: using bioinformatics and homology modeling to understand functional relationships in cAMP/cGMP binding domains. Mol Biosyst 6 (5):894-901. doi:10.1039/b922562e

Levina N, Totemeyer S, Stokes NR, Louis P, Jones MA, Booth IR (1999) Protection of Escherichia coli cells against extreme turgor by activation of MscS and MscL mechanosensitive channels: identification of genes required for MscS activity. EMBO J 18 (7):1730-1737. doi:10.1093/emboj/18.7.1730

Machiyama H, Tatsumi H, Sokabe M (2009) Structural changes in the cytoplasmic domain of the mechanosensitive channel MscS during opening. Biophys J 97 (4):1048-1057. doi:S0006-3495(09)01025-X [pii]

10.1016/j.bpj.2009.05.021

Malcolm HR, Heo YY, Elmore DE, Maurer JA Defining the role of the tension sensor in the mechanosensitive channel of small conductance. Biophys J 101 (2):345-352. doi:S0006-3495(11)00660-6 [pii]

10.1016/j.bpj.2011.05.058

Maurer JA, Dougherty DA (2001) A high-throughput screen for MscL channel activity and mutational phenotyping. Biochim Biophys Acta 1514 (2):165-169. doi:S000527360100390X [pii]

Miller S, Bartlett W, Chandrasekaran S, Simpson S, Edwards M, Booth IR (2003) Domain organization of the MscS mechanosensitive channel of Escherichia coli. EMBO J 22 (1):36-46. doi:10.1093/emboj/cdg011

Myers, Miller (1989). CABIOS 4:11-17

Nimigean CM, Shane T, Miller C (2004) A cyclic nucleotide modulated prokaryotic K+ channel. J Gen Physiol 124 (3):203-210. doi:10.1085/jgp.200409133

jgp.200409133 [pii]

Nomura T, Sokabe M, Yoshimura K (2006) Lipid-protein interaction of the MscS mechanosensitive channel examined by scanning mutagenesis. Biophysical journal 91 (8):2874-2881. doi:S0006-3495(06)72001-X [pii]

10.1529/biophysj.106.084541

Ou X, Blount P, Hoffman RJ, Kung C (1998) One face of a transmembrane helix is crucial in mechanosensitive channel gating. Proc Natl Acad Sci U S A 95 (19):11471-11475

Pivetti CD, Yen MR, Miller S, Busch W, Tseng YH, Booth IR, Saier MH, Jr. (2003) Two families of mechanosensitive channel proteins. Microbiol Mol Biol Rev 67 (1):66-85, table of contents

Schneider TD, Stephens RM (1990) Sequence logos: a new way to display consensus sequences. Nucleic Acids Res 18 (20):6097-6100

Schumann U, Edwards MD, Li C, Booth IR (2004) The conserved carboxy-terminus of the MscS mechanosensitive channel is not essential but increases stability and activity. FEBS Lett 572 (1-3):233-237. doi:10.1016/j.febslet.2004.07.045

S0014579304009214 [pii]

Steinbacher S, Bass R, Strop P, Rees DC (2007) Structures of the prokaryotic mechanosensitive channels MscL and MscS. Mechanosensitive Ion Channels, Part A 58:1-24. doi:Doi 10.1016/S1063-5823(06)58001-9

Sukharev SI, Blount P, Martinac B, Blattner FR, Kung C (1994) A large-conductance mechanosensitive channel in E. coli encoded by mscL alone. Nature 368 (6468):265-268. doi:10.1038/368265a0

Tulumello DV, Deber CM Positions of polar amino acids alter interactions between transmembrane segments and detergents. Biochemistry 50 (19):3928-3935. doi:10.1021/bi200238g

Wild J, Altman E, Yura T, Gross CA (1992) DnaK and DnaJ heat shock proteins participate in protein export in Escherichia coli. Genes Dev 6 (7):1165-1172

Yoshimura K, Batiza A, Schroeder M, Blount P, Kung C (1999) Hydrophilicity of a single residue within MscL correlates with increased channel mechanosensitivity. Biophys J 77 (4):1960-1972. doi:S0006-3495(99)77037-2 [pii]

10.1016/S0006-3495(99)77037-2

# Chapter Four

# Ss-bCNGa: a Unique Member of the Bacterial Cyclic Nucleotide Gated (bCNG) Channel Family that Gates in Response to Mechanical Tension.

*Collaboration with David B. Caldwell, Ryann C. Guayasamin, Jessica F. Hawkins, Yoon-Young Heo, and John K. McConnell

---

### *4.1 Introduction*

Bacterial cyclic nucleotide gated (bCNG) channels are a subfamily of the mechanosensitive channel of small conductance (MscS) superfamily (Caldwell et al. 2010). These channels are characterized by high sequence homology to the pore lining helix and the upper vestibule domain of *Escherichia coli* (*E. coli*) MscS (Ec-MscS), which have been defined as hallmarks for mechanosensation and inclusion in the MscS superfamily (Pivetti et al. 2003; Kloda and Martinac 2002b, a; Haswell et al. 2008). Several bCNG channels have been shown to gate in response to cyclic adenosine monophosphate (cAMP) alone in a dose dependent manner, although these channels do not respond to osmotic downshock.

While members of the bCNG subfamily show significant sequence similarity to mechanosensitive ion channels from all phylogenetic kingdoms, we previously demonstrated, based on osmotic downshock assays, that many of these channels are unable to gate in response to mechanical tension (Malcolm et al. 2012). However, removal of the C-terminal cAMP binding domain restores limited mechanosensation to many bCNG channels. In particular, Se-bCNG, a bCNG channel from *Synechococcus elongatus* PCC 7942, is unable to gate in response to mechanical tension unless the binding domain has been removed. This is surprising, in that the channel domain of Se-bCNG is highly identical to Ec-MscS and is predicted to be composed of three transmembrane domains (Table 4.1). Furthermore, the third transmembrane domain and upper vestibule regions, of Se-bCNG and Ec-MscS are highly conserved (Figure 1). These regions of the MscS superfamily have previously been identified as critical for mechanosensation (Pivetti et al. 2003; Haswell et al. 2008; Kloda and Martinac 2002a, b). As a result of this conservation, the inability of Se-bCNG to gate in response to mechanical tension was very unexpected.

| | TM1 | TM2 | TM3 |
|---|---|---|---|
| Ss-bCNGa | 27.59% | 32.0% | 37.50% |
| Se-bCNG | 13.79% | 24.00% | 25.00% |

**Table 4.1:** Sequence Identity of Ss-bCNGa and Se-bCNG as compared to Ec-MscS calculated from an alignment created using ClustalW (Chenna et al. 2003).

Another bCNG channel with significant sequence homology to Ec-MscS is Ss-bCNGa from *Synechocystis sp.* PCC 6803 (Figure 4.1, Table 4.1). Ss-bCNGa was the first bCNG channel identified in the original bioinformatical analysis due to its extreme similarity to

Ec-MscS (Caldwell et al. 2010), and this protein had been previously assigned as a putative cyclic nucleotide gated ion channel based on weak homology to several potassium channels (de Alda and Houmard 2000). Like Se-bCNG, this channel is highly homologous to Ec-MscS throughout the entire channel domain, is predicted to have three transmembrane domains, and displays high conservation with Ec-MscS in the third transmembrane domain and upper vestibule region. Compared to Se-bCNG, Ss-bCNGa has slightly higher identity to Ec-MscS in all of the transmembrane domains (Table 4.1).

```
Ss-bCNGa        MPFVAIAFAKIFDTLDATTLSFGRTQLSLLDLFQLALSALAIFVLTHYLNRVLRSIVLRR 60
Se-bCNG         ----MDLFDRLEQWTSTPLLRLGSSQISLGSLILLAVLAGLLLYLMRQMNRWLREIVLVR 56
MscS            -----MEDLNVVDSINGAGSWLVANQALLLSYAVNIVAALAIIIVGLIIARMISNAVNRL 55
Domains                                        ==============TM1============
                         .: :  . .   :  .*  * .     : *  :: :   : * : . *

Ss-bCNGa        FI---YEQGIRYIVANLLSYGLGSFLFIAMLQTSGINLSSLTVVGGTLGLGIGLGLQNVT 117
Se-bCNG         LG---VERGPREAIATITSYLLTSLILIIGLQAIGVDLSSLTVLAGVLGLGLSLGLQRLA 113
MscS            MISRKIDATVADFLSALVRYGIIAFTLIAALGRVGVQTASVIAVLGAAGLAVGLALQGSL 115
Domains         =         -----------TM2-------------   ++++++++++TM3+++++
                :     :      :: :  * : :: :*  *   *:: :*: .: *. **.:.*.**

Ss-bCNGa        RNFVSGVTLLVEQKVKIGDYIRFQNIQGYVREVSTRAVVVGLKDGSKVILPSSLLIENQV 177
Se-bCNG         ASFFSGITLLIEQPIKVGDLVSLDGVLGTVEKISFRATAVRTLDHVHVIVPNDRLVDSNI 173
MscS            SNLAAGVLLVMFRPFRAGEYVDLGGVAGTVLSVQIFSTTMRTADGKIIVIPNGKIIAGNI 175
Domains         ++++++++++   XXXXXXXXXXXXXXXXXXXXXXXXXXXXXXXXXXXXXXXXXXXXX
                 .: :*: *:: : .: *: : : .: * * .:.  :..:   *   :::*.. :: .::

Ss-bCNGa        INYHYETQTVRLTVAVGVAYGTDPVLVTETLLMCAYSQACVVKTPPAQVIFQNFGDNALE 237
Se-bCNG         INWSYQNTASRVHLPISVAYGTDPLWLTDALLTVARQDSRVLTQPAPTVWFRSFGDSTLN 233
MscS            INFSRE-PVRRNEFIIGVAYDSDIDQVKQILTNIIQSEDRILKDREMTVRLNELGASSIN 234
Domains         XXXXXX XXXXXXXXXXXXX Vestibule Region XXXXXXXXXXXXXXXXXXXXX
                **:  :  . *  . :.***.:*   :.: *     .:  ::.     * :..:* .:::

Ss-bCNGa        FELWVWIEEQYMGQHPEILSALRYTICFYFKRNGIGIPWPQRELWLKNPEAIAKYFHPDL 297
Se-bCNG         FELLFWTDRPELIEP--IKSDLNFRIASEFERREIQIPFPQ--LVLHRHRSVTTSELPDD 289
MscS            FVVRVWSNS---GDLQNVYWDVLERIKREFDAAGISFPYPQMDVNFKRVKEDKAA----- 286
Domains         XXXXXXXXX   XXXXXXXXXXXXXXXXXXXXXXX
                * : .* :     :   :   :   *   *.   * :*:**  : ::. .

Ss-bCNGa        DLPSLSDPAPQEPTISLSQVLKSSDYFSGLNELEIRQLVEIGQLQSLQSEEVLFRERDPA 357
Se-bCNG         YLPSL----------------LRRVDLFRDYDDSQIRWLIEKGRRRTCVVGDVLCREGELG 334
MscS            ------------------------------------------------------------
Domains                            ***********cAMP Binding Domain*********

Ss-bCNGa        DGFYIVISGLVEVYTEKLGRVLASLGPGSFFGELALMLGIPRTASVKAKEKSLLFVVRFP 417
Se-bCNG         EEFYLILNGRFSVQVKGREEAIATLESGNFFGELAVMLDIPRTATVVALEPGTLFVVDRN 394
MscS            ------------------------------------------------------------
Domains         ************************************************************


Ss-bCNGa        QFEQLLQSNPDFREAIINALGEHQGELMRRKEELATKGLLTSEEEDS--NIMNWVRKRLQ 475
Se-bCNG         NLRHLLERCPNLSQVMAEQLAQRQ-------QVLTNAGLLTPTANQSRPDQLRGILRRVL 447
MscS            ------------------------------------------------------------
Domains         ************************

Ss-bCNGa        RLFG 479
Se-bCNG         RL-- 449
MscS            ----
```

**Figure 4.1:** ClustalW alignment of Ec-MscS, Ss-bCNGa, and Se-bCNG (Chenna et al. 2003). Significant protein regions are labeled on the alignment.

Here we examine how Ss-bCNGa fits into the MscS superfamily of ion channels. The mechanosensitive abilities of Ss-bCNGa, Se-bCNG, and Ec-MscS are compared using osmotic downshock experiments and gain of function assays. Ss-bCNGa is shown to gate in response to mechanical tension in osmotic downshock assays, but at much lower levels than Ec-MscS. This places Ss-bCNGa squarely between Se-bCNG and Ec-MscS in terms of relative recovery in osmotic downshock assays. To assess why Ss-bCNGa displays intermediate activity, we have explored the changes in mechanosensation that occur upon the removal of the C-terminal cAMP binding domain, examined the effect of expression level on osmotic downshock, and employed molecular dynamic simulations to understand lipid-protein interactions in Ss-bCNGa.

### *4.2 Materials and Methods*

#### *4.2.1 Strains and Plasmids*

The *E. coli* strain, MJF465 (*MscS, MscL, MscK* null), was used for osmotic downshock assays and expression experiments (Levina et al. 1999; Wild et al. 1992). Cloning was conducting using the Top10F` *E. coli* strain (Invitrogen, Carlsbad, CA). Ss-bCNGa was initially cloned into pET46 vector (Novagen), before being subcloned into the pB10b vector for osmotic downshock assays and expression analysis (Levina et al. 1999; Ou et al. 1998).

### *4.2.2 Genomic Cloning*

Genomic DNA from *Synechocystis sp.* PCC 6803 (Ss) was obtained from KAZUZA. Cloning was carried out using a ligation independent cloning (LIC) strategy (Aslanidis and de Jong 1990; Haun and Moss 1992), which allowed genomic DNA to be directly incorporated into the pET46 vector (Novagen) without the use of an intermediate cloning vector or the introduction of additional enzymatic restriction sites. Primer sequences can be found in Table 4.2. Ss-bCNGa was cloned into pET46 such that the methionine start codon for the gene immediately follows the sequence for the LIC site, and the native stop codon for the gene is included within the construct. In this process, an N-terminal His-Tag was incorporated into the gene. Cloned sequences were verified by automated DNA sequencing (Big Dye v3.1; Applied Biosystems).

| | Forward | Reverse |
|---|---|---|
| Ss-bCNGa pET46 | GACGACGACAAGATGCCCTTG TTGCCATTGCTTTCGCC | GAGGAGAAGCCCGGTCCCTAA CCAAATAGCCGCTGGAGCCGTT TACGC |
| Ss-bCNGa pB10b | CCGAGATCTCATAGGGAGAA TAACATGCCCTTTGTTGCCAT TGCTTT CGCC | CGCCTCGAGCTGCTTTCAGGCG CTTGCTAACCAAATAGCCGCTG GA GCCG |
| Ss-bCNGa Δ287-479 | TCTGGCTTAAAAATCCCGAG TAAATCGCCTAATATTTTCAC CCGGATTTG | CAAATCCGGGTGAAAATATTA GGCGATTTACTCGGGATTTTTA AGCCAGA |
| Outer cloning primers | CAATTTCACACAGGAAACAG GC | TACACGGAGGCATCAGTGAC CAAA |

**Table 4.2:** Primers used in cloning of Ss-bCNGa into pET46 and pB10b.

### *4.2.3 Subcloning into pB10b*

The Ss-bCNGa gene in pET46 was subcloned into the pB10b (Sukharev et al. 1994; Wild et al. 1992) vector as previously described (Caldwell et al. 2010) with the following

modifications. Primers for cloning contained two domains of approximately 25 bases each; one priming to the gene and one priming to the flanking region of the target pB10b plasmid. Primer sequences can be found in Table 4.2. This strategy allowed for direct insertion in the pB10b vector without the addition of enzymatic sites. All genes were sub-cloned at their start codon, eliminating the His-Tag introduced by the pET46 vector, into the pB10b vector by replacement of the Ec-MscL gene. Sub-cloned products were screened enzymatically and final sequences were verified by automated sequencing with Big Dye v3.1 (Applied Biosystems).

### *4.2.4 Inserting N-terminal His-Tag*

To determine if Ss-bCNGa was membrane expressed during osmotic downshock experiments, a N-terminal His-tag was inserted into the Ss-bCNGa construct. His-Ss-bCNGa was sub-cloned from pET46 into His-Ml-bCNG pB10b using enzymatic cut sites in the multiple cloning region as previously described (Malcolm et al. 2012). Primer sequences can be found in Table 4.2. Sequences were confirmed using automated sequencing (Big Dye v3.1, Applied Biosystems).

### *4.2.5 Truncation of Ss-bCNGa*

Ss-bCNGa and His-Ss-bCNGa were truncated by inserting two in frame stop codons into the gene using Megaprimer mutagenesis (Yoshimura et al. 1999). Primers for insertion of stop codons were designed using Stratagene's QuikChange Primer design (See Table 4.2 for primers). Insertion of stop codons was verified by enzymatic digestion and sequences confirmed using automated sequencing (Big Dye v3.1, Applied Biosystems).

### *4.2.6 Osmotic Downshock*

Downshock experiments were conducted as previously described (Booth et al. 2007; Caldwell et al. 2010), with the following modifications. A single colony was used to inoculate an overnight culture in Luria-Bertani Broth (LB Broth, BD Biosciences, San Jose, CA) supplemented with ampicillin (100µg/mL), and this overnight culture was subsequently used to inoculate (1:20) a culture in LB Broth with 250 mM NaCl and ampicillin. The resulting culture was grown to an $OD_{600}$ of approximately 0.5 and induced with 0.1 mM isopropyl-beta-D-thiogalactopyranoside (IPTG) for 90 min. Following 0, 30, 60, 90 min of induction, the culture was diluted (1:40) into 1:1 LB Broth and deionized water or isotonically into LB Broth with 250 mM NaCl, and allowed to recover for 30 min in a shaking incubator. After hypoosmotic downshock or isotonic dilution, bacterial cultures were serially diluted and plated on LB plates supplemented with ampicillin (100µg/mL). Plates containing between 25 and 250 colonies were used to determine the colony forming units (CFU) per millimeter of media. Percent recovery was defined as the CFU of the downshocked culture divided by the CFU of the isotonic dilution. Six trials for each construct were conducted.

### *4.2.7 Osmotic Time Course Bacterial Expression Analysis*

To verify bacterial expression of bCNG channels, cultures were grown as described above and pelleted for 15 min at 16,000 x g after 0, 30, 60, 90 min of induction. The supernatant was removed and the pellet resuspended in a buffer containing 50 mM Tris, 75 mM NaCl, 0.1% Fos-Choline-14 (Anatrace, Maumee, OH), and protease complete inhibitor (Roche, Basel, Switzerland) at 10µL of buffer per 10mg of bacteria. Samples

were detergent-solubilized using a probe sonicator for three cycles of 15 s on and 45 s off. After lysis and solubilization, insoluble material was removed by pelleting for 30 min at 16,000 x g. The supernatant was combined with sodium dodecyl sulfate polyacrylamide-gel electrophoresis (SDS-PAGE) loading dye, and the samples were boiled for 5 min. Samples were then run on a 12.5% poly-acrylamide gel using a TRIS-glycine running buffer. Equivalent volumes of the supernatant were loaded to allow for comparisons of protein expression levels. Proteins were transferred to a 0.2-µm nitrocellulose membrane using a semidry transfer system and Cashini's Buffer (0.1 M Tris, 0.02% SDS, 0.2 M glycine, 5% methanol). The protein expression of the N-terminally 6-His-tagged bCNG channels was probed using a primary mouse-anti-His monoclonal IgG antibody (Covance, Emeryville, CA) and a secondary HRP-conjugated goat anti-mouse antibody (Jackson ImunoResearch Laboratories, West Grove, PA).

### *4.2.8 Gain of Function Plate Assay*

Gain of function analysis was carried out as previously described (Maurer et al. 2000), with the following modifications. A single colony was used to inoculate an overnight culture in LB Broth supplemented with ampicillin (100µg/mL), the overnight culture was subsequently used to inoculate (1:75) a culture in LB Broth with ampicillin. The resulting culture was grown to an $OD_{600}$ between 0.5 and 0.8 and diluted to an $OD_{600}$ of 0.2±0.02. This culture was serially diluted into prewarmed LB with ampicillin, 5µL of the $10^{-2}$, $10^{-3}$, $10^{-4}$, $10^{-5}$, $10^{-6}$, and $10^{-7}$ dilutions were plated onto LB agar plates supplemented with ampicillin and LB agar plates supplemented with ampicillin and IPTG to a final concentration of 1mM. The resulting plates were scored after 20 hours of growth by

giving a score of one for each concentration containing growth (maximum score of 6). Four trials for each mutation were carried out.

### *4.2.9 Molecular Dynamics Simulations*

MODELLER 9.1 (Madhusudhan et al. 2005; Sali and Blundell 1993) was used to construct an all-atom structure of Ss-bCNGa based on the three-dimensional carbon alpha (Cα) model of the Ec-MscS channel in its closed state developed by Perozo and co-workers (Vasquez et al. 2008). Since this Ec-Mscs model does not represent the entire protein only the channel domain of Ss-bCNGa was modeled. Sequence alignments for modeling were produced using the ALIGN feature of MODELLER and the Perozo structure was used as the modeling template. Three hundred models were produced, and the model with the lowest DOPE energy was used as a starting structure for molecular dynamics (MD) simulations.

MD simulations of Ss-bCNGa were performed using the GROMACS suite (Lindahl et al. 2001). The channel model was embedded in a preequilibrated palmitoyloleoyl-phosphatidylethanolamine (POPE) membrane using the method of Kandt and co-workers (Kandt et al. 2007). Briefly, the all-atom Ss-bCNGa structure obtained from MODELLER was superimposed onto a pre-equilibrated POPE bilayer with the desired orientation relative to the membrane, such that the structure overlapped with lipids. The bilayer was then expanded by translating lipid molecules and scaling the lateral dimensions of the box size by a factor of four, and the protein was centered in the new bilayer plane. A series of compression steps were performed using a scaling factor of 0.95 to slowly reequilibrate

the lipid density and properly embed the channel in the bilayer. During this process, the protein was constrained and the system energy was minimized after each scaling step. The area per lipid was calculated at each step with scaling and minimization steps performed until the area per lipid reached 0.4990 $nm^2$/lipid, the reference value of a POPE membrane (Rand and Parsegian 1989). Following reequilibration of the membrane, the system was hydrated, sufficient chloride ions were added to neutralize the net charge on the protein, sodium and chloride ions were added to yield an ionic strength of 100 mM, and the system was minimized using 50 steps of steepest descents minimization. Any lipids that had significant overlap with the channel after the steepest descents minimization were removed. The final system was composed of the protein, 433 POPE lipids, 23,918 water molecules, 95 sodium ions and 137 chloride ions, for a total of 107,053 atoms.

A MD simulation was carried out starting from the minimized system. The system was initially heated to 310 K over 20 ps with the alpha carbons of the protein restrained with a force constant of 1000 kJ/mol□$nm^2$. These restraints were maintained for an additional 480 ps at which time the restraints were removed and the trajectories were extended for a total of 50 ns. Simulations were carried out using a 2 fs time-step with water geometries constrained using SETTLE (Miyamoto and Kollman 1992) and all other bonds constrained using LINCS (Hess et al. 1997). Temperature was held constant using a time constant ($\tau_t$) of 0.1 ps for three groups: protein, lipid and water/ions. Pressure was maintained at 1.0 atm using a time constant ($\tau_p$) of 1.0 ps with anisotropic coupling. Short-range electrostatics and Lennard-Jones interactions were cutoff at 1.0 nm and long-

range electrostatics were calculated with PME (Darden et al. 1993), using a grid spacing of 0.10 nm and cubic interpolation. The Berger et al. force field parameters for POPE lipids were used with GROMOS parameters for the oleoyl double bond (Berger et al. 1997), and GROMACS parameters were used for the protein, ions, and water. Fluctuations and lipid interaction energies were obtained as an average of the last 10 ns of the simulations, and protein-lipid interaction energies were calculated as described previously for Ec-MscS (Malcolm et al. 2011). Analyses were performed using tools in the GROMACS suite, and figures were made using Pymol (DeLano 2002).

### *4.3 Results and Discussion*

#### *4.3.1 Functional Characterization*

It has previously been shown that while Ec-MscS is capable of rescuing *E. coli* from hypoosmotic shock, Se-bCNG is incapable of rescue (Malcolm et al. 2012). Using a typical induction time for osmotic downshock assays of thirty minutes, Ss-bCNGa showed partial osmotic rescue that was statistically different from both Ec-MscS and Se-bCNG (Figure 4.2A). To further analyze this response we examined osmotic rescue as a function of induction time for Se-bCNG, Ss-bCNGa, and Ec-MscS. *E. coli* rescue, and hence channel response, was examined in thirty minute intervals from uninduced to ninety minutes post induction (Figure 4.2A).

Ec-MscS shows nearly 100% recovery at all time points, including uninduced. This suggests that even the extremely low protein levels, that result from leak through the pB10b lacoperon controlled promoter, are sufficient for bacterial rescue. This is

consistent with the observation that Ec-MscS is found in very low copy numbers *in vivo* (Stokes et al. 2003; Ishihama et al. 2008) and is similar to previous Ec-MscS rescue data collected by different groups using different induction times (Nomura et al. 2006; Malcolm et al. 2011; Wang et al. 2008; Koprowski et al. 2011; Boer et al.). In contrast to Ec-MscS, Se-bCNG shows essentially no recovery at the uninduced, thirty minutes post-induction, and sixty minutes post-induction time points and is statistically similar to empty vector. This is not surprising based on our previous analysis of bCNG channels, which has demonstrated their inability to rescue (Malcolm et al. 2012).

At ninety minutes post-induction Se-bCNG shows significant recovery, however this is not likely a result of Se-bCNG activity, since a corresponding increase in recovery is also observed for bacteria carrying an empty vector (Figure 4.2A). While the MJF465 strain of *E. coli* used in these experiments is MscL, MscS, and MscK null, this recovery may be attributed to additional mechanosensitive channels still present in the strain: YbdG, YjeP, YbiO and YnaI (Berrier et al. 1992; Schumann et al. 2010; Sukharev et al. 1997). Alternatively, this may be an effect of other, yet unidentified, stress response proteins.

The response of Ss-bCNGa is unique amongst the channels, in that its activity increases with induction time. While even uninduced Ss-bCNGa is statistically different from both Ec-MscS and Se-bCNG, this difference becomes even more pronounced at thirty and sixty minutes post-induction. The dependence of percent recovery on induction time is a unique feature of Ss-bCNGa among mechanosensitive channels. At ninety minutes, the

Ss-bCNGa recovery is dominated by the same background recovery observed for Se-bCNGa and the empty vector control.

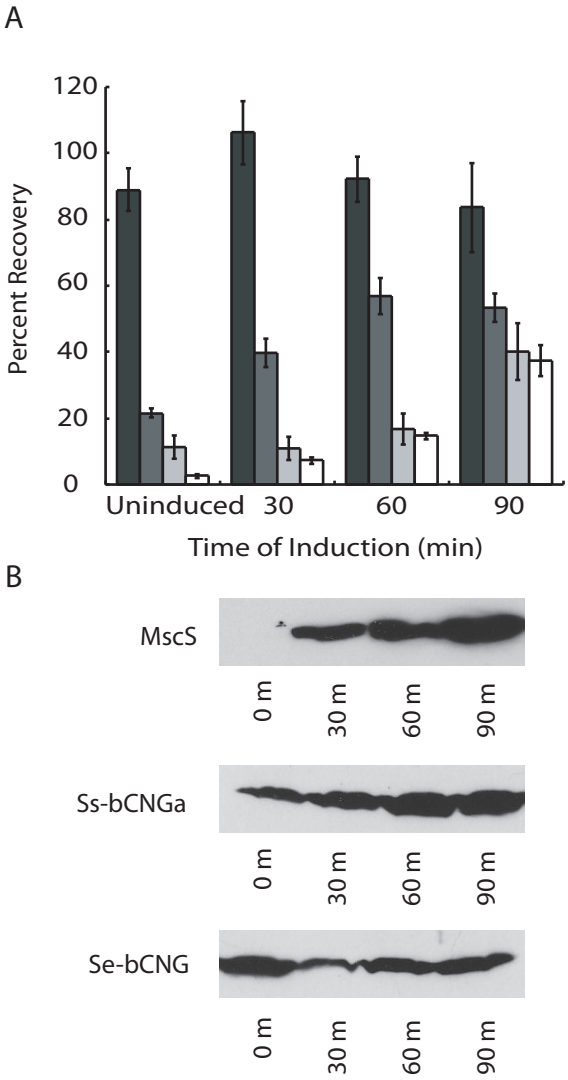


**Figure 4.2:** A) Osmotic downshock of Ec-MscS (black), Ss-bCNGa (dark gray), Se-bCNG (light gray), and empty vector (white) over ninety minutes. Error bars are standard error of the mean based on six replicates. Ec-MscS, Ss-bCNGa, and Se-bCNG are statistically different from one another at all time points with a p-value less than 0.01. B) Western blot analysis of protein expression levels of Ec-MscS, Ss-bCNGa, and Se-bCNG under expression conditions identical to those used in the osmotic downshock assay.

To better understand the behavior observed for Ss-bCNGa, we examined expression level as a function of time for all three channels. Ss-bCNGa showed an increase in protein concentration over time, which correlated with the increased recovery over the 90 minutes (Figure 4.2B). Ec-MscS and Se-bCNG show relatively consistent protein levels through out the induction period, with Ec-MscS showing no detectable expression prior to induction.

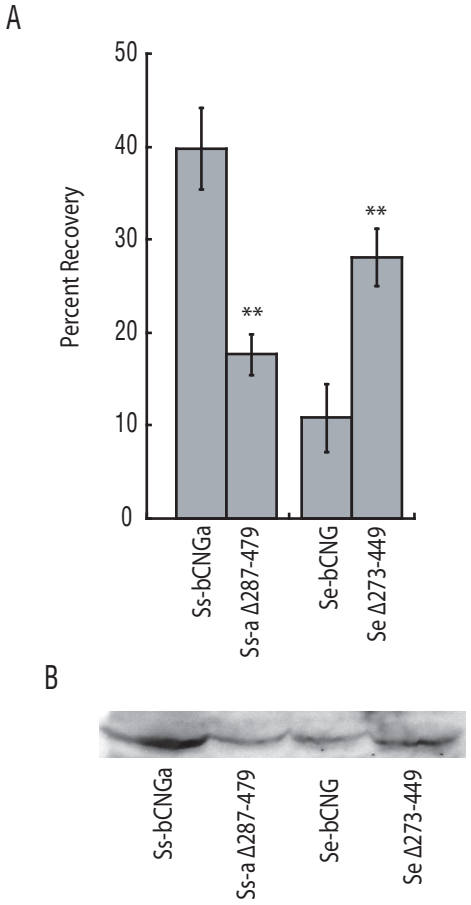


**Figure 4.3:** A) Osmotic downshock of Ss-bCNGa, Ss-bCNGa Δ287-479, Se-bCNG, and Se-bCNG Δ273-479. Error bars are standard error of the mean based on six replicates. (** = $p < 0.01$) B) Western blot analysis of protein expression levels of Ss-bCNGa, Ss-bCNGa Δ287-479, Se-bCNG, and Se-bCNG Δ273-479 under expression conditions identical to those used in the osmotic downshock assay.

We previously found that removal of the C-terminal cAMP binding domain of bCNG channels results in increased recovery in osmotic downshock assays (Malcolm et al. 2012). This trend is observed for Se-bCNG, where the Δ273-449 mutant shows a statistically significant increase in recovery from osmotic downshock in comparison to the full-length channel (Figure 4.3A). Based on this, we postulated that the increase in mechanosensation observed upon truncation of bCNG channels is a result of the C-terminal cAMP binding domain inhibiting channel rearrangement and gating. Ss-bCNGa was truncated in a similar location to produce a Ss-bCNGa Δ287-479 mutant. This mutant displays decreased recovery relative to the full-length channel (Figure 4.3), which suggests that the position of the C-terminal binding domain in Ss-bCNGa does not significantly hinder mechanosensitive gating. However, the higher levels of recovery observed for Ss-bCNGa suggest that there are further differences between Se-bCNG and Ss-bCNGa channels. Based on our previous work, examining the importance of lipid interactions in Ec-MscS (Malcolm et al. 2011), it seems likely that these difference lie in the transmembrane regions.

To verify that the difference observed in osmotic recovery for the three channels and their truncation mutants was not a result of ion leakage through expressed channels, a growth assay that has been previously used to identify gain of function mutations was conducted. In Figure 4.4, Ss-bCNGa and Se-bCNG show similar phenotypical data to Ec-MscS. Additionally, the truncated channels display a phenotype identical to Ec-MscS. These

observations indicate that the differences observed in the osmotic downshock assays result of differences in how the channels response to mechanical stress.

| | LB+Ap $10^{-2}$ $10^{-3}$ $10^{-4}$ $10^{-5}$ $10^{-6}$ $10^{-7}$ | Un-induced Score | LB+IPTG+Ap $10^{-2}$ $10^{-3}$ $10^{-4}$ $10^{-5}$ $10^{-6}$ $10^{-7}$ | Induced Score | Ratio |
|---|---|---|---|---|---|
| MscS |  | 4±0.8 |  | 3.5±0.6 | 0.9±0.2 |
| Ss-bCNGa |  | 3.75±0.5 |  | 4.25±0.5 | 1.1±0.2 |
| Ss-a Δ287-479 | 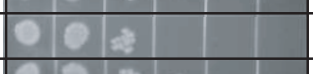 | 4.0±0.0 | 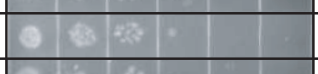 | 3.75±0.5 | 0.9±0.1 |
| Se-bCNG | 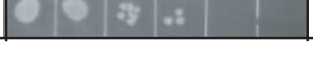 | 3.5±1.0 |  | 4.5±0.6 | 1.3±0.4 |
| Se Δ273-449 | 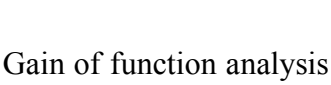 | 4.0±0.0 |  | 3.75±0.5 | 0.9±0.1 |

**Figure 4.4:** Gain of function analysis for Ec-MscS, Ss-bCNGa, Ss-bCNGa Δ287-479, Se-bCNG, and Se-bCNG Δ273-449. Representative plates are shown for all constructs. Plates were scored by counting the number of dilutions with bacterial growth. The ratio was determined by dividing the induced score by the unindued score. The error represents the standard deviation for four independent trials in all cases.

### *4.3.2 Physiochemical Conservation*

To explain the differences observed in channel gating, we examined the sequence differences in the channel domains of the proteins. Ss-bCNGa and Se-bCNG are highly similar to Ec-MscS (Figure 4.1) and both have, as previously noted, significant identity in their transmembrane domains to Ec-MscS (Table 4.1). While, Ss-bCNGa shows slightly higher identity to Ec-MscS in the transmembrane domains, this difference does not seem significant enough to explain the differences observed in osmotic downshock assays.

To further identify the difference between the residues in the first and the second transmembrane domain of Ss-bCNGa and Se-bCNG compared to Ec-MscS, the Grantham index was utilized (Grantham 1974). The Grantham index was selected, as it is a physiochemical matrix that gives a relative 'goodness' for any point mutation. The

reason for using a physiochemical matrix for this analysis is that we have previously observed significant differences in Ec-MscS channel function upon mutation of hydrophobic amino acids to small amino acids in the first and second domains (Malcolm et al. 2011). Typically, low Grantham index values indicate an acceptable mutation (values <50) and high index values indicate mutations that are deleterious to protein function (values >150) (Rudd et al. 2005; Li et al. 1984). In Figure 4.5, the Grantham index values for all residues in first and second transmembrane domains of Se-bCNG (Figure 4.5A) and Ss-bCNGa (Figure 4.5B) compared to the residues of Ec-MscS are colored onto the Ec-MscS closed state structure.

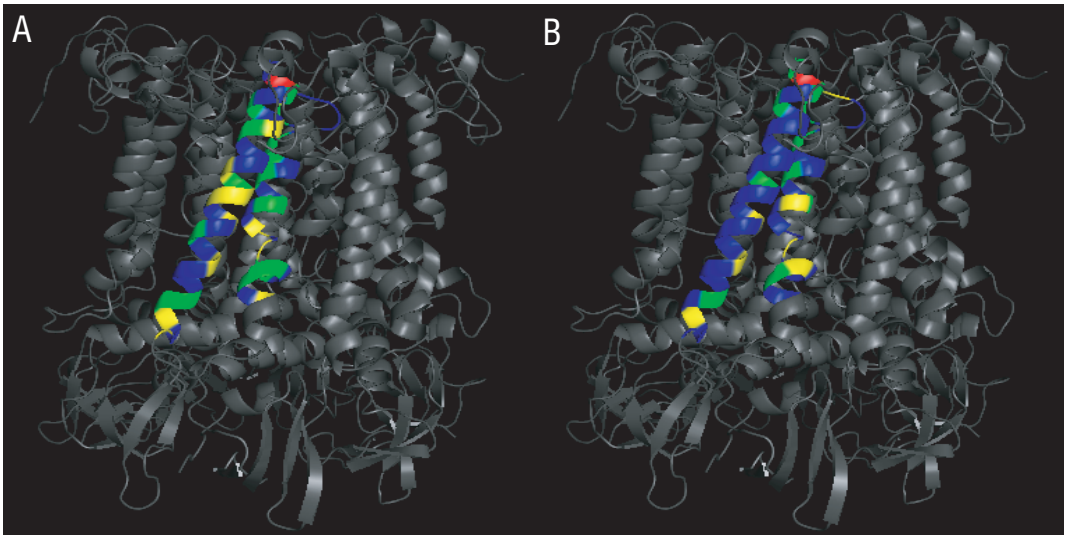


**Figure 4.5:** Homology to Ec-MscS in the first and second transmembrane domains of Se-bCNG (A) and Ss-bCNGa (B). The Grantham Index scores for each amino acid were colored onto the closed state model of Ec-MscS (Malcolm et al. 2011). The color code is a follows: great conservation, (0-50, blue), good conservation (51-100, green), poor conservation (101-150, yellow), and terrible conservation (159-215, red). Ss-bCNGa shows much better conservation than Se-bCNG throughout the transmembrane regions.

Based on the Grantham index, the amino acids in the first and second transmembrane domains of Se-bCNG are a mixture of "great", "good", and "poor" conservation with Ec-MscS. Interestingly, there are no solidly conserved regions, and the lipid exposed residues have varying conservation with some of the residues that we have previously identified as being critical for Ec-MscS tension sensation being poorly conserved (Malcolm et al. 2011). Additionally, Se-bCNG has some "poor" conservation in the non-lipid exposed regions of the transmembrane domains, which are known in Ec-MscS to transmit tension to the gate upon osmotic downshock (Belyy et al. ; Nomura et al. 2008, 2006; Machiyama et al. 2009). The physiochemical differences between Se-bCNG and Ec-MscS are most likely the reason that this channel does not rescue *E. coli* from hypoosmotic shock.

Unlike Se-bCNG, Ss-bCNGa shows strong conservation to Ec-MscS throughout all of the transmembrane domains. This conservation is especially high in the lipid-exposed regions, with most of the residues having a "great" Grantham index value. Based on these observations, we would have expected that Ss-bCNGa and Ec-MscS to exhibit similar responses to mechanical tension.

### *4.3.3 Identification of the Lipid Interactions for Ss-bCNGa*

Since the observed physiological results for Ss-bCNGa compared to Ec-MscS did not correspond with the expected outcome based on the physiochemical analysis of the two channels, we carried out a molecular dynamics simulation on a homology model of Ss-bCNGa to further identify the lipid interacting residues. An all atom homology model of

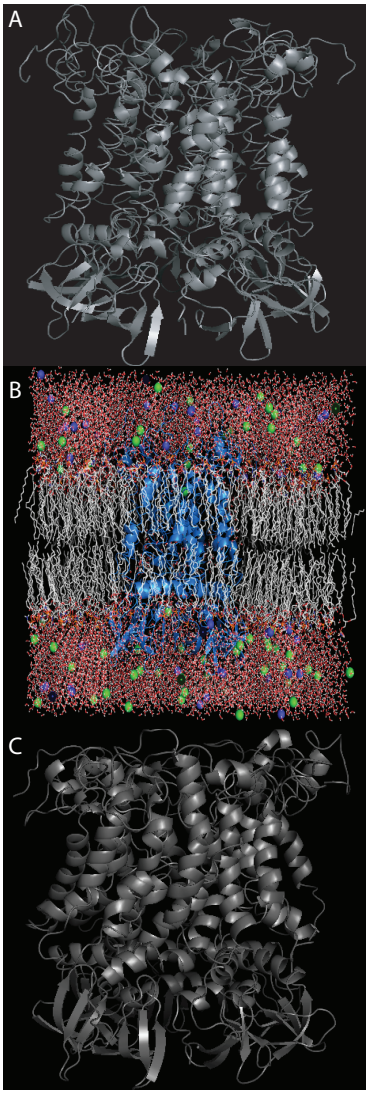


**Figure 4.6:** A) Initial closed state all-atom Ss-bCNGa model generated with MODELLER. B) Closed state Ss-bCNGa model at the start of the MD simulation, as seen from the side with the lipids, chloride ions, sodium ions, and water molecules included in the simulation. C) Ss-bCNGa all-atom closed state model after 50 ns.

Ss-bCNGa was generated from the experimentally determined Cα Ec-MscS closed state structure (Vasquez et al. 2008) using the MODELLER Suite (Madhusudhan et al. 2005; Sali and Blundell 1993). The final homology model was selected from 300 similar

models based on its zDOPE score and used as a starting point for a molecular dynamics simulation with explicit lipid molecules, water molecules, and ions (Figure 4.6). The simulation was carried out as previously described for the closed state of Ec-MscS (Malcolm et al. 2011).

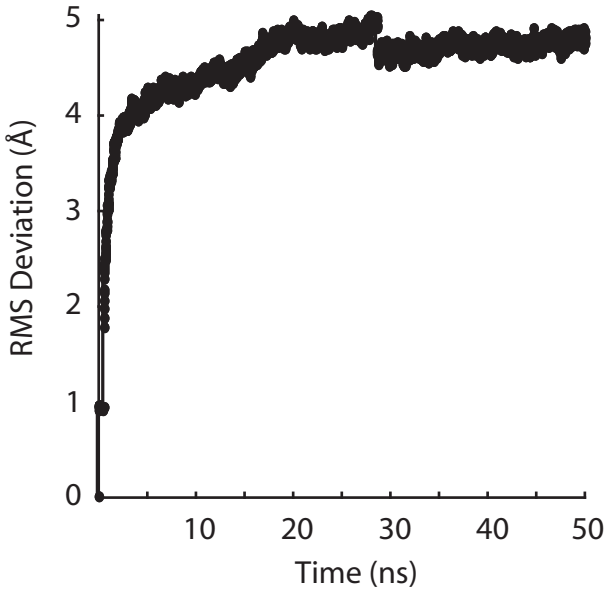


**Figure 4.7:** Structural deviations during the MD simulation. A) RMS deviation of the Ss-bCNGa structure over the course of the MD simulation.

Structural equilibration was observed within the first third of the simulation (Figure 4.7). Additionally, the lipid exposed residues in the first and second transmembrane domains were relatively stable during the final 10 ns of the trajectories, as shown by their low RMS Cα fluctuations (Figure 4.8). At the end of the simulation, the transmembrane domains were more defined and the channel as a whole appeared more compact (Figure 4.6C).

Over the last 10 ns of the simulation, the lipid interactions with each residue in the first and second transmembrane domain were calculated to identify residues with significant interactions (Figure 4.9). In the first transmembrane domain, seven residues were predicted to have lipid interactions, L45, Y48, R51, R54, I56, and R59, (Figure 4.10) and, in the second transmembrane domain, five residues were predicted to interact with the lipids, N73, Y77, S81, F84, and G92 (Figure 4.10).

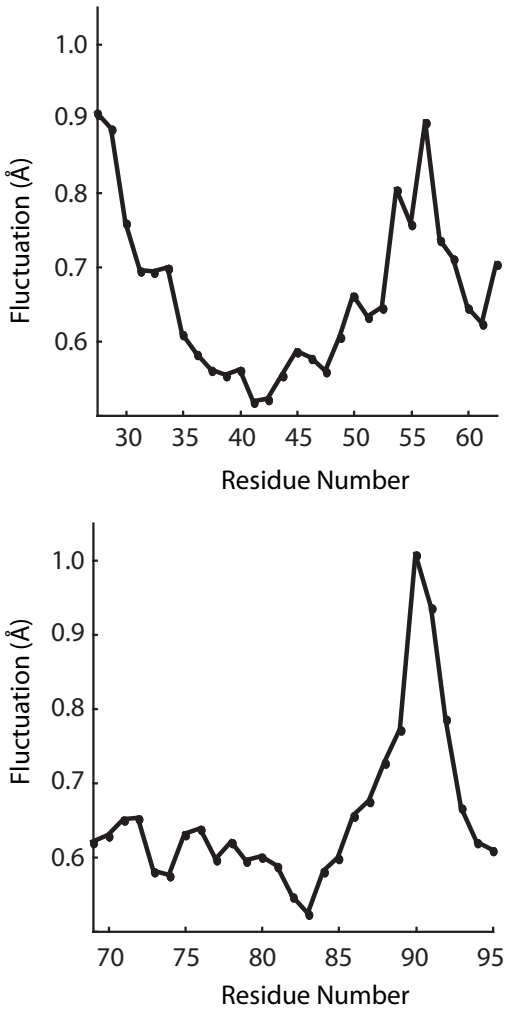


**Figure 4.8:** The average RMS fluctuation per residue over the final 10 ns of the MD simulations for TM1 (A) and TM2 (B).

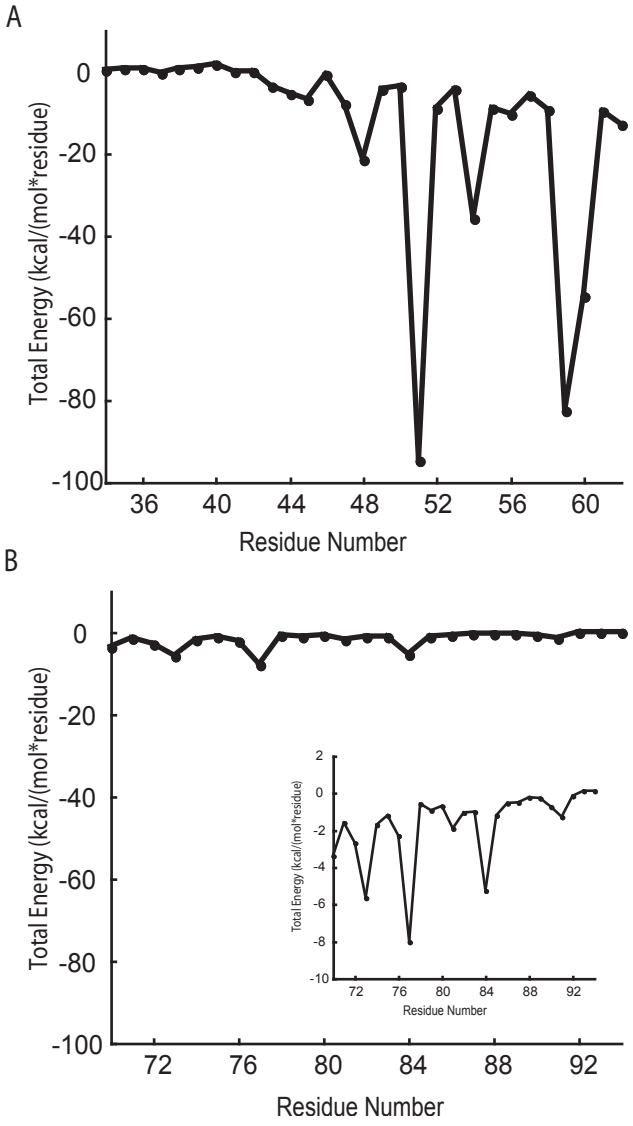


**Figure 4.9:** Protein lipid interaction energies averaged over the final 10 ns of the MD simulation for the first transmembrane domain (A) and the second transmembrane domain (B) of Ss-bCNGa.

In Ec-MscS, the majority of the lipid interacting residues were large hydrophobic amino acids (leucine or valine), while the amino acids identified as lipid interaction in Ss-bCNGa are more diverse including charged, aromatic, and polar residues. These residues

are unlikely to form the strong hydrophobic contacts that we have shown are important for gating in Ec-MscS. However, it is possible that these residues may induce receptor clustering, through cation-π interactions between the lipid-exposed arginine residues and the lipid-exposed tyrosine and phenylalanine residues. Furthermore, increased channel function do to clustering could account for the increased recovery observed as a function of channel expression in Ss-bCNGa (Figure 4.2). Receptor clustering has been postulated to occur within and between Ec-MscS and Ec-MscL *in vivo* and this clustering is postulated to increase channel activity in Ec-MscS (Grage et al. 2011; Ursell et al. 2007; Bialecka-Fornal et al. 2012) Moreover, it is possible that clustering between Ec-MscS and Ec-MscL might be induced by similar cation-π interactions in the transmembrane regions. In our analysis of the closed Ec-MscS lipid interacting residues, we identified several arginine residues that did not induce water columns in the simulation and could be mutated to alanine without inducing a phenotypic change. These residues could form transmembrane cation-π intereactions with the lipid exposed aromatic residues that we previously identified in the closed Ec-MscL.

### *4.4 Conclusions*

Ss-bCNGa represents a unique member of the bCNG subfamily of the MscS superfamily of ion channels that can gate in response to mechanical tension. The osmotic downshock response of Ss-bCNGa is significantly different from that of both Se-bCNG and Ec-MscS and is protein expression level dependent. Detailed analysis of the lipid lining residues in

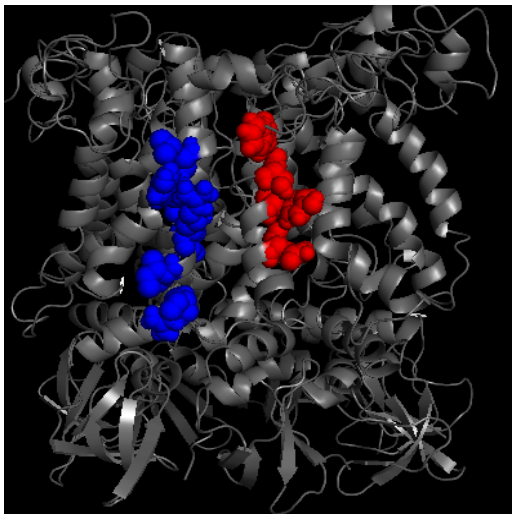

**Figure 4.10:** The closed state model of Ss-bCNGa at the end of the MD simulation as seen from the side. The lipid interacting residues are highlighted in transmembrane domain one (L45, Y48, R51, R54, I56, and R59) shown in blue and the residues in transmembrane domain two (N73, Y77, S81, F84, and G92) shown in red.

Ss-bCNGa indicates significant changes in the critical lipid exposed residues between Ec-MscS and Ss-bCNGa. In Ec-MscS, these residues are mainly large hydrophobics, however, in Ss-bCNGa, these residues are mainly a mixture of positively charged and aromatic residues. Based on this difference, we postulate that these residues might induce channel clustering through cation-π interactions in the membrane. This would account for the observed dependence of channel concentration on hypoosmotic shock recovery rates and fits with recent observations of increased mechanosensation due to channel clustering.

### *4.5 References*

Aslanidis C, de Jong PJ (1990) Ligation-independent cloning of PCR products (LIC-PCR). Nucleic Acids Res 18 (20):6069-6074

Belyy V, Anishkin A, Kamaraju K, Liu N, Sukharev S The tension-transmitting 'clutch' in the mechanosensitive channel MscS. Nat Struct Mol Biol 17 (4):451-458. doi:nsmb.1775 [pii]

10.1038/nsmb.1775

Berger O, Edholm O, Jahnig F (1997) Molecular dynamics simulations of a fluid bilayer of dipalmitoylphosphatidylcholine at full hydration, constant pressure, and constant temperature. Biophys J 72 (5):2002-2013. doi:S0006-3495(97)78845-3 [pii]

10.1016/S0006-3495(97)78845-3

Berrier C, Coulombe A, Szabo I, Zoratti M, Ghazi A (1992) Gadolinium ion inhibits loss of metabolites induced by osmotic shock and large stretch-activated channels in bacteria. European journal of biochemistry / FEBS 206 (2):559-565

Bialecka-Fornal M, Lee HJ, Deberg HA, Gandhi CS, Phillips R (2012) Single-cell census of mechanosensitive channels in living bacteria. PloS one 7 (3):e33077. doi:10.1371/journal.pone.0033077

Boer M, Anishkin A, Sukharev S Adaptive MscS gating in the osmotic permeability response in E. coli: the question of time. Biochemistry 50 (19):4087-4096. doi:10.1021/bi1019435

Booth IR, Edwards MD, Black S, Schumann U, Bartlett W, Rasmussen T, Rasmussen A, Miller S (2007) Physiological analysis of bacterial mechanosensitive channels. Methods Enzymol 428:47-61. doi:S0076-6879(07)28003-6 [pii]

10.1016/S0076-6879(07)28003-6

Caldwell DB, Malcolm HR, Elmore DE, Maurer JA (2010) Identification and experimental verification of a novel family of bacterial cyclic nucleotide-gated (bCNG) ion channels. Biochim Biophys Acta 1798 (9):1750-1756. doi:S0005-2736(10)00185-9 [pii]

10.1016/j.bbamem.2010.06.001

Chenna R, Sugawara H, Koike T, Lopez R, Gibson TJ, Higgins DG, Thompson JD (2003) Multiple sequence alignment with the Clustal series of programs. Nucleic Acids Res 31 (13):3497-3500

Darden T, York D, Pedersen L (1993) Particle mesh Ewald: An N□log(N) method for Ewald sums in large systems. Journal Chemical Physics 98 (12):10089-10092

de Alda JAGO, Houmard J (2000) Genomic survey of cAMP and cGMP signalling components in the cyanobacterium Synechocystis PCC 6803. Microbiol-Uk 146:3183-3194

DeLano WL (2002) The PyMOL Molecular Graphics System.

Grage SL, Keleshian AM, Turdzeladze T, Battle AR, Tay WC, May RP, Holt SA, Contera SA, Haertlein M, Moulin M, Pal P, Rohde PR, Forsyth VT, Watts A, Huang KC, Ulrich AS, Martinac B (2011) Bilayer-mediated clustering and functional interaction of MscL channels. Biophys J 100 (5):1252-1260. doi:10.1016/j.bpj.2011.01.023

Grantham R (1974) Amino acid difference formula to help explain protein evolution. Science 185 (4154):862-864

Haswell ES, Peyronnet R, Barbier-Brygoo H, Meyerowitz EM, Frachisse JM (2008) Two MscS homologs provide mechanosensitive channel activities in the Arabidopsis root. Curr Biol 18 (10):730-734. doi:S0960-9822(08)00525-3 [pii]

10.1016/j.cub.2008.04.039

Haun RS, Moss J (1992) Ligation-independent cloning of glutathione S-transferase fusion genes for expression in Escherichia coli. Gene 112 (1):37-43

Hess B, Bekker H, Berendsen HJC, Fraaiji JGEM (1997) LINCS: A linear constraint solver for molecular simulations. Journal of Computational Chemistry 18 (12):1463-1472

Ishihama Y, Schmidt T, Rappsilber J, Mann M, Hartl FU, Kerner MJ, Frishman D (2008) Protein abundance profiling of the Escherichia coli cytosol. BMC genomics 9:102. doi:10.1186/1471-2164-9-102

Kandt C, Ash WL, Tieleman DP (2007) Setting up and running molecular dynamics simulations of membrane proteins. Methods 41 (4):475-488. doi:S1046-2023(06)00187-3 [pii]

10.1016/j.ymeth.2006.08.006

Kloda A, Martinac B (2002a) Common evolutionary origins of mechanosensitive ion channels in Archaea, Bacteria and cell-walled Eukarya. Archaea 1 (1):35-44

Kloda A, Martinac B (2002b) Mechanosensitive channels of bacteria and archaea share a common ancestral origin. Eur Biophys J 31 (1):14-25

Koprowski P, Grajkowski W, Isacoff EY, Kubalski A (2011) Genetic screen for potassium leaky small mechanosensitive channels (MscS) in Escherichia coli:

recognition of cytoplasmic beta domain as a new gating element. The Journal of biological chemistry 286 (1):877-888. doi:10.1074/jbc.M110.176131

Levina N, Totemeyer S, Stokes NR, Louis P, Jones MA, Booth IR (1999) Protection of Escherichia coli cells against extreme turgor by activation of MscS and MscL mechanosensitive channels: identification of genes required for MscS activity. EMBO J 18 (7):1730-1737. doi:10.1093/emboj/18.7.1730

Li WH, Wu CI, Luo CC (1984) Nonrandomness of point mutation as reflected in nucleotide substitutions in pseudogenes and its evolutionary implications. Journal of molecular evolution 21 (1):58-71

Lindahl E, Hess B, van der Spoel D (2001) GROMACS 3.0: a package for molecular simulation and trajectory analysis. Journal of Molecular Modeling 7 (8):306-317

Machiyama H, Tatsumi H, Sokabe M (2009) Structural changes in the cytoplasmic domain of the mechanosensitive channel MscS during opening. Biophys J 97 (4):1048-1057. doi:10.1016/j.bpj.2009.05.021

Madhusudhan MS, Marti-Renom MA, Eswar N, John B, Pieper U, Karchin R, Shen M-Y, Sali A (2005) Comparative protein structure modeling. In: Walker JM (ed) The Proteomics Protocols Handbook. Humana Press, Totowa, NJ,

Malcolm HR, Elmore DE, Maurer JA (2012) Mechanosensitive behavior of bacterial cyclic nucleotide gated (bCNG) ion channels: Insights into the mechanism of channel gating in the mechanosensitive channel of small conductance superfamily. Biochemical and biophysical research communications 417 (3):972-976. doi:10.1016/j.bbrc.2011.12.049

Malcolm HR, Heo YY, Elmore DE, Maurer JA (2011) Defining the role of the tension sensor in the mechanosensitive channel of small conductance. Biophys J 101 (2):345-352. doi:S0006-3495(11)00660-6 [pii]

10.1016/j.bpj.2011.05.058

Maurer JA, Elmore DE, Lester HA, Dougherty DA (2000) Comparing and contrasting Escherichia coli and Mycobacterium tuberculosis mechanosensitive channels (MscL). New gain of function mutations in the loop region. J Biol Chem 275 (29):22238-22244. doi:10.1074/jbc.M003056200

M003056200 [pii]

Miyamoto S, Kollman PA (1992) Settle: An analytical version of the SHAKE and RATTLE algorithm for rigid water models. Journal of Computational Chemistry 13 (8):952-962

Nomura T, Sokabe M, Yoshimura K (2006) Lipid-protein interaction of the MscS mechanosensitive channel examined by scanning mutagenesis. Biophys J 91 (8):2874-2881. doi:10.1529/biophysj.106.084541

Nomura T, Sokabe M, Yoshimura K (2008) Interaction between the cytoplasmic and transmembrane domains of the mechanosensitive channel MscS. Biophys J 94 (5):1638-1645. doi:10.1529/biophysj.107.114785

Ou X, Blount P, Hoffman RJ, Kung C (1998) One face of a transmembrane helix is crucial in mechanosensitive channel gating. Proc Natl Acad Sci U S A 95 (19):11471-11475

Pivetti CD, Yen MR, Miller S, Busch W, Tseng YH, Booth IR, Saier MH, Jr. (2003) Two families of mechanosensitive channel proteins. Microbiol Mol Biol Rev 67 (1):66-85, table of contents

Rand RP, Parsegian VA (1989) Hydration Forces between phospholipid bilayers. Biochim Biophys Acta 988:351-376

Rudd MF, Williams RD, Webb EL, Schmidt S, Sellick GS, Houlston RS (2005) The predicted impact of coding single nucleotide polymorphisms database. Cancer epidemiology, biomarkers & prevention : a publication of the American Association for Cancer Research, cosponsored by the American Society of Preventive Oncology 14 (11 Pt 1):2598-2604. doi:10.1158/1055-9965.EPI-05-0469

Sali A, Blundell TL (1993) Comparative protein modelling by satisfaction of spatial restraints. J Mol Biol 234 (3):779-815. doi:S0022-2836(83)71626-8 [pii]

10.1006/jmbi.1993.1626

Schumann U, Edwards MD, Rasmussen T, Bartlett W, van West P, Booth IR (2010) YbdG in Escherichia coli is a threshold-setting mechanosensitive channel with MscM activity. Proc Natl Acad Sci U S A 107 (28):12664-12669. doi:10.1073/pnas.1001405107

Stokes NR, Murray HD, Subramaniam C, Gourse RL, Louis P, Bartlett W, Miller S, Booth IR (2003) A role for mechanosensitive channels in survival of stationary phase: regulation of channel expression by RpoS. Proc Natl Acad Sci U S A 100 (26):15959-15964. doi:10.1073/pnas.2536607100

Sukharev SI, Blount P, Martinac B, Blattner FR, Kung C (1994) A large-conductance mechanosensitive channel in E. coli encoded by mscL alone. Nature 368 (6468):265-268. doi:10.1038/368265a0

Sukharev SI, Blount P, Martinac B, Kung C (1997) Mechanosensitive channels of Escherichia coli: the MscL gene, protein, and activities. Annual review of physiology 59:633-657. doi:10.1146/annurev.physiol.59.1.633

Ursell T, Huang KC, Peterson E, Phillips R (2007) Cooperative gating and spatial organization of membrane proteins through elastic interactions. PLoS computational biology 3 (5):e81. doi:10.1371/journal.pcbi.0030081

Vasquez V, Sotomayor M, Cortes DM, Roux B, Schulten K, Perozo E (2008) Three-dimensional architecture of membrane-embedded MscS in the closed conformation. J Mol Biol 378 (1):55-70. doi:10.1016/j.jmb.2007.10.086

Wang W, Black SS, Edwards MD, Miller S, Morrison EL, Bartlett W, Dong C, Naismith JH, Booth IR (2008) The structure of an open form of an E. coli mechanosensitive channel at 3.45 A resolution. Science 321 (5893):1179-1183. doi:10.1126/science.1159262

Wild J, Altman E, Yura T, Gross CA (1992) DnaK and DnaJ heat shock proteins participate in protein export in Escherichia coli. Genes Dev 6 (7):1165-1172

Yoshimura K, Batiza A, Schroeder M, Blount P, Kung C (1999) Hydrophilicity of a single residue within MscL correlates with increased channel mechanosensitivity. Biophys J 77 (4):1960-1972. doi:S0006-3495(99)77037-2 [pii]

10.1016/S0006-3495(99)77037-2

# Chapter Five

# Exploring the Heteromultimerization of the Bacterial Cyclic Nucleotide Gated (bCNG) Channel Family.

---

### *5.1 Introduction*

The bacterial cyclic nucleotide gated (bCNG) channel subfamily is composed of over sixty unique channels from over thirty-seven different bacterial species (Caldwell et al. 2010). Structurally these channels are composed of three domains: a channel domain homologous to the mechanosensitive channel of small conductance (MscS), a non-conserved linker domain, and a cyclic adenosine monophosphate (cAMP) binding domain. Eleven bacterial strains encode for two bCNG homologues and one strain encodes for three bCNG homologues. The presence of multiple bCNG homologous in a single genome suggests that they could form a heteromultimeric channel or that one of the genes may be silent. While many eukaryotic ion channels exist as heteromultimers

there are no identified prokaryotic heteromultimeric channels. However, prokaryotes, like eukaryotes, form many important heteromultimeric protein assemblies, so the lack of identified prokaryotic channels may not be a result of the simplicity of prokaryotes (Bricker et al. 2012; McHenry 2011).

Heteromultimeric channels are common in mammalian cells and changes in the ratio of subunits are known to alter the channel phenotype (Wu and Lukas 2011). In the nicotinic acetylcholine receptor, both the homomeric α7 and the heteromeric α7ß4 form functional channels. One of the main differences between the two channels is their affinity for acetylcholine, the heteromultimer displays higher affinity for the ligand than the homomultimer. Moreover, while homomeric α7 exists as a result of heterologous expression and has been extensive characterized by biophysical techniques, it is likely not formed *in vivo*. In the Shaker channel family, there are instances where the heteromultimer creates a new phenotype: in a heteromultimer of Kv1.4/Kv1.5, the Kv1.5 subunit suppresses Src binding (Nitabach et al. 2001). The consequence of this is that there is increase phosphorylation of the adjacent subunits, leading to regions that are unable to directly bind Src.

In bacteria there are many processes that are facilitated by the formation of multiprotein complexes. For example, the association of KaiA to the KaiC complex is essential for the proper oscillation of the photosynthetic clock in many cyanobacteria (Golden and Canales 2003; Mackey and Golden 2007). In the photosystem II complex over forty different proteins have been identified to be involved (Shi et al. 2012). In the different

photosystem II complexes that have been identified, they are all composed of several different components. These complexes show that bacterial proteins are known to associate with one another.

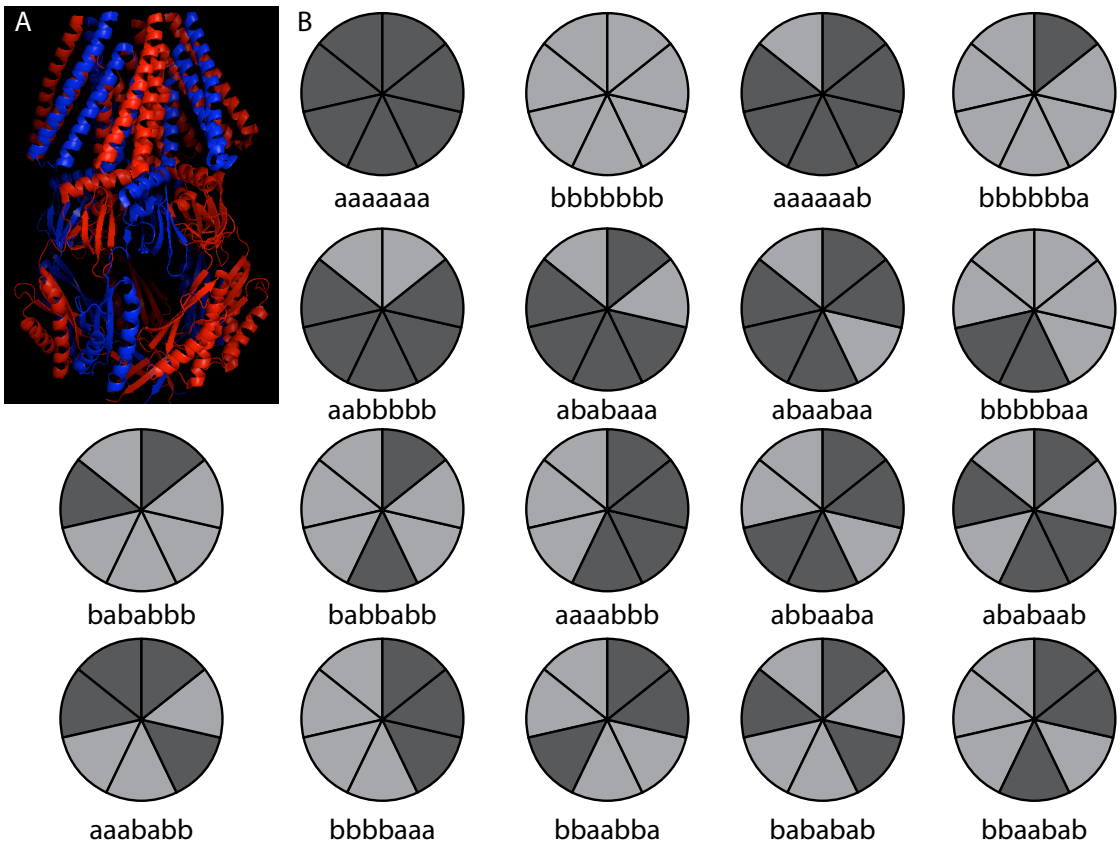


**Figure 5.1:** Potential configurations of two bCNG channels. A) Representation of a heteromultimer shown on the MscS desensitized crystal structure (Bass et al. 2002; Steinbacher et al. 2007) with the subunits colored to represent the abababa multimer. B) Models of the 18 possible configurations for heteromultimers of two bCNG channels.

For bacterial strains that encode for two bCNG homologues, there are eighteen possible configurations of the two unique channel subunits (Figure 5.1) and for the strain that encodes for three unique channels there are one hundred and ninety-eight unique

configurations. These possible configurations result from variations in both subunit copy number and location. Preliminary homology models suggest that several unique conformations of Ss-bCNGa and Ss-bCNGb are structurally possible, and that a heteromultimer of the two channels could form.

To determine if bCNG channels could co-multimerize *in vitro*: two bCNG channels from *Synechocystis sp*. PCC6803 were heterologously co-expressed. The ability of these channels, Ss-bCNGa and Ss-bCNGb, to comultimerize *in vitro* was analyzed using a pull down assay. *In vivo* mRNA levels for four bacterial strains that encode for two bCNG channels and the bacterial strain that encodes for three bCNG channels were analyzed to determine if one or more of these subunits was active *in vivo*. These studies show that upon heterologous expression bCNG channels from the same bacterial species form heteromultimers and that the mRNA levels for bCNG channels are present at similar levels when compared to an internal RpoB standard.

## *5.2 Methods*

### *5.2.1 Strains and Plasmids*

Cloning was conducted using the Top10F` *E. coli* strain (Invitrogen). Channels were initially cloned into pET46 vector (Novagen), before being subcloned into the pET30 vector (Novagen). Protein expression was conducted in the BL21(DE3) *E. coli* strain (Novagen).

*5.2.2 Cloning*

Bg-bCNGb was cloned into pET46 from genomic DNA (*Burkholderia graminis* C4D1M (Bg) from S. Brady at Rockefeller University) as previously described by Caldwell et. al. (Caldwell et al. 2010). Ss-bCNGa, Ss-bCNGb, Bg-bCNGa, and Bg-bCNGb were subcloned into pET30 using a ligation independent cloning (LIC) strategy (Aslanidis and de Jong 1990; Haun and Moss 1992), which allowed DNA to be directly incorporated into the pET30 vector (Novagen) without the use of an intermediate cloning vector. All genes were cloned into pET30 such that the methionine start codon for the gene immediately follows the sequence for the LIC site, and the native stop codon for the gene is included within the construct. In this process, an N-terminal His-Tag and S-tag were incorporated into the gene. (See Table 5.1 for cloning primers) Cloned sequences were verified by automated DNA sequencing (Big Dye v3.1; Applied Biosystems).

| | Forward | Reverse |
|---|---|---|
| Ss-bCNGa | GACGACGACAAGATGCC CTTGTTGCCATTGCTTTC GCC | GAGGAGAAGCCCGGTCCCTA ACCAAATAGCCGCTGGAGCC GTTTACGC |
| Ss-bCNGb | GACGACGACAAGATGA TTGCACAAATTAATCCA CCACC | GAGGAGAAGCCCGGTGGTTT AACGATATGCAGATTCTTGA CTGACACC |
| Bg-bCNGa | GACGACGACAAGATGC CGACTCTGACC | GAGGAGAAGCCCGGTTCACA GCGCGAGTTCGTGAAAA |
| Bg-bCNGb | GACGACGACAAGATGA GCGATT | GAGGAGAAGCCCGGTCGACG CTTAACAATCAG |

**Table 5.1**: Primers for LIC cloning of bCNG channels into pET46 and pET30.

*5.2.3 Insertion of HA-Tag into pET30 vector*

The His-tag and S-tag normally found in pET30 were swapped out for an HA affinity tag (YPYDVPDYA). The pET30 plasmid (containing Ss-bCNGa, Ss-bCNGb, Bg-bCNGa, or

Bg-bCNGb) was digested with KpnI (NEB) and NdeI (Promega) in sequential reactions followed by dephosphorylation. The HA tag insert was prepared for ligation by annealing two oligos containing 5'-phosphate groups (1.0ng of each) in a buffer containing 100mM Tris, 20$MgCl_2$, 1mM ATP, 1mM DTT (Primer Sequences can be found in Table 5.2). Annealing conditions were as follows: 95ºC for two minutes, cool to 50ºC over 7.5 minutes (0.1ºC/sec), 50ºC for 5 minutes, and then cooled to room temperature (Cravchik and Matus 1993; Pati 1992). The resulting linear DNA was ligated under standard conditions with the prepared HA tag insert. Final sequences were verified by enzymatic digestion and automated sequencing using Big Dye v3.1 (Applied Biosystems).

| | |
|---|---|
| Forward | 5'Phos-TATGGCATACCCATACGACGTCCCAGACTACGCTGGTAC |
| Reverse | 5'Phos-CAGCGTAGTCTGGGACGTCGTATGGGTATGCCA |

**Table 5.2**: HA tag Primers. On the 5' end is the NdeI site and on the 3'end of the forward primer is a KpnI site.

*5.2.4 Co-Transforming Two Plasmids into E. coli*

To create a bacterial strain carrying two plasmids: one plasmid was transformed into BL21(dE3) by electroporation. The resulting transformant was used to create quick competent cells in the following manner: 1mL dense culture was pelleted at 8000 x g, the pellet was washed twice with 1mL sterile water, and the pellet was resuspended in 50 µL sterile water. The resulting quick competent cells were then transformed with the second plasmid by electroporation. Transformants carrying both plasmids were selected on plates containing both ampicillin (50 µg/mL) and kanamycin (25 µg/mL).

*5.2.5 Expression and purification of Two Plasmids Strains*

Protein expression was carried out in the BL21(dE3) strain of *E. coli* (Novagen). Single colonies were used to inoculate 50 mL of LB Broth with 50 µg/mL ampicillin and 25 µg/mL Kanamycin. The cultures were grown overnight at 37°C with shaking. The overnight LB culture was used to inoculate 500 mL of Terrific Broth (TB) with ampicillin and kanamycin. The resulting TB culture was grown to mid-log phase and induced with 0.8 mM isopropyl-beta-D-thiogalactopyranoside (IPTG). After induction, the cultures were grown for an additional 3 to 6 hours at 37°C. Bacteria were then pelleted at 10,000 x g for fifteen minutes and resuspended in 25mM Imidazole, 100mM NaCl, 1% Fos-Choline 14 (Anatrace) at pH 7.5 (1 mL/ 1 g of bacterial pellet) with complete protease inhibitor cocktail (Roche). The suspension was then probe sonicated (7 x 30 s) on ice. The resulting suspension was pelleted for one hour at 28,000 x g. The supernatant was filtered using a 0.2 µm filter before being applied to a nickel charged affinity column.

Affinity Chromatography was carried out on a HPLC with diode array detector (Shimadzu) using a POROS MC affinity column (Applied Biosystems). Elution from the nickel chelate column was conducted using an imidazole step gradient (25mM, 60mM, and 1M imidazole) with 0.1% n-Octyl-ß-D-Glucopyranoside (Anatrace), 100mM NaCl at pH 7.5. Fractions were collected thought the wash steps and the elution steps, and the samples were mixed with 2x SDS-PAGE loading buffer containing 4% β-mercaptoethanol and boiled for five minutes prior to being run on a 12.5% SDS-PAGE.

Gels were run until the dye front reached the end of the gel. SDS-PAGE gels were silver stained to determine the purity of the eluted protein samples.

*5.2.6 Anti-HA and Anti-His Westerns*

To confirm co-multimerization of bCNG channels, Western's blots were utilized. Protein samples were run on 12.5% SDS-PAGE. Proteins were transferred to a 0.2-mm nitrocellulose membrane using a semidry transfer system and Cashini's Buffer (0.1 M Tris, 0.02% SDS, 0.2 M glycine, 5% methanol). His-tagged proteins were probed using a primary mouse-anti-His monoclonal IgG antibody (Covance, Emeryville, CA) and HA-tagged proteins were probed using a primary mouse-anti-HA monoclonal IgG antibody (Covance, Emeryville, CA). Both primary antibodies were detected with a secondary HRP-conjugated goat anti-mouse antibody (Jackson ImunoResearch Laboratories, West Grove, PA).

*5.2.7 Growth of Bacterial Strains*

Bacteria used for RT-PCR was grown under the following conditions. *Burkholderia xenovorans* LB400 (J. Tiedje, Michigan State University) was cultured in LB with no salt (10 g Tryptone, 5 g yeast extract per liter) for 12 hours prior to RNA isolation. *Rhizobium leguminosarum bv. viciae* 3841 (Johnny's Selected Seeds company, Product number: 9359) and grown for 12 hours in TY Broth (5 g Tryptone, 3 g yeast extract, 1.2 g calcium chloride dehydrate, per liter) prior to RNA isolation. *Synechocystis sp*. PCC6803 (M. M. Allen, Wellesley College) was grown in BG(II) (Bustos and Golden 1991; Allen 1968) under constant light until a medium optical density was obtained. To synchronize the

photosynthetic clocks, 5 cycles of 12 hours light and 12 hours dark were completed prior to RNA isolation from cultures mid-cycle. A culture of *Acaryochloris marina* MBIC11017 was received from R. Blankenship (WashU) and a culture of *Cyanothece sp. ATCC* 51142 was obtained from H. B. Pakrasi (WashU).

*5.2.8 RNA Isolation and RT-PCR Experiments*

Total RNA was isolated from 2mL of a bacterial culture using the e.Z.N.A. bacterial RNA kit (Omega Bio-tek) following their recommendations. RT-PCR experiments were conducted using iScript One-Step RT-PCR kit with SYBR Green (Bio-Rad) on the Cepheid Smart Cycler (Cepheid). Primers for RT-PCR amplification are shown in Table 5.3. The RT-PCR cycle was as follows: cDNA was synthesized at 50 ˚C 10 minutes, heat inactivation at 95 ˚C 5 minutes, gene of interest amplification 40 cycles of 95 ˚C 15 seconds, 60 ˚C 30 seconds, followed by melt curve analysis at 0.2˚C/second with optical detection. Results were analyzed by calculating the ratio of the normalized cycle threshold for the gene of interest to the normalized cycle threshold of RpoB, the internal standard. To verify expression level and primer specificity PCR samples were run on 2% agarose gels.

| | Forward | Reverse |
|---|---|---|
| Am-bCNGa | GGACTATTGAGCGAATTTCTATT | GACCGCGCTGCAATCAATAAGGC |
| Am-bCNGb | GATACCCTCGGCAACTTGTTTTCAG | GATAGTTATAGAACACTTCCTTGGC |
| Am-RpoB | CCTGAAGGTCCTAACGCGGGTCTAATTG | GACGATAGCGCACAGGCACAATCTCA |
| Bg-bCNGa | CGCATCGGCGACTGGATCACCATCG | CTCGCCGCGGCGTGCATCAGCGCCTGCAATA |
| Bg-bCNGb | GCGGGCATCGTACTCAATTCCACG | GGATTTTCTCGCCTGCACGAAGGGAGC |
| Bg-RpoB | AGTCGCGCGCTTCGACA | CATACGGCCCACCTTGG |

| | | |
|---|---|---|
| | TCACGGAC | ACAGGTCGTATGC |
| Bg-Crp | CGGCGACGGCGACGTG CTCAACGAA | GACGAGCCGCTTTCTGA CATCGTGC |
| Bx-bCNGa | GTCGTCGCGCAGATCAA CTGGC | CGGCGCGGGCACCGAA AGAATATC |
| Bx-bCNGb | GCGCCATATCGTGTGGG CGATTCC | CATCACGTCGGATGGCC GGAGC |
| Bx-bCNGc | GCCGTTTCGACTCGGCG ACTGGGTG | GCTCACGACGGGCTTCG GAT |
| Bx-RpoB | ACGATCTGGATCAAGGT CCGTACATCTCG | CGTCCACTTCGCCCTTG CCGTTA |
| Cs-bCNGa-2 | GGATCTTCCGTGATTGT CCCTAACC | CTAAACAGCTATCGCCC AACCC |
| Cs-bCNGb-2 | CAGTGATACGAACGTTA AAAGGCTCTC | TTAAAGCATTATCTCCG TACTC |
| Cs-RpoB | CGGCGATCGATTATCTC ATTAACC | GGTTTAGGATTCACCAA AGAAGCAG |
| Rl-bCNGa | CTGATCGCCACCTCAGG CGTCTTTGC | CCGACCTTGGCCAGAAA GCTGTTG |
| Rl-bCNGb | CATTCTCGGCCTGGCGC TACAGAACAC | GTTCGGCAGAACGACG ACATTGTTTGCGCTGG |
| Rl-RpoB | GCTGTTCTTCGATGCGG AGCGTTA | CGCGCGCTCCATGCGCA GCAGGCCGAGAC |
| Ss-bCNGa | CCCTTGGGCTAGGGATT GGTTTAGG | GGCAAAATTACTTTGGA GCCATC |
| Ss-bCNGb | GGAATTAACTAGGAATT TAGTCAGTGG | CTGCCATATTCCACA CTAACTGGTACTTC |
| Ss-Crp | GGGCGGCTCAGTTTATT TCGTCATGGA | CGCCATGGGCTCTGTTT GGAGAAAAT |
| Ss-RpoB | CCCGGGAGCGGGCCGG TTTTGCGGTG | CGGCTACATAGTCAACT TGTTCTGGG |

**Table 5.3**: Primers used for RT-PCR analysis of bCNG channels.

## *5.3 Results and Discussion*

### *5.3.1 Heterologous Expression of Ss-bCNGa*

Ss-bCNGa and Ss-bCNGb are two bCNG homologues from the *Synechocystis sp.* PCC 6803 bacterial strain and are both predicted to encode for bCNG channels with three

transmembrane domains. The presence of two bCNG channels in a single bacterial genome suggests that these two channels could form a heteromultimer. If a heteromultimer can be detected in an *in vitro* expression experiment and the mRNA levels for the bCNG homologues are similar, it is likely that the bCNG channels form a heteromultimeric complex *in vivo*.

To determine if two bCNG channels could form a heteromultimer, the genes for these two channels were encoded in different plasmids with different antibiotic resistance cassettes, pET46, ampicillin, and pET30, kanamycin. The different antibiotic resistance cassettes allow the two plasmids to be co-expressed in *E. coli*. In addition to the two antibiotic resistance cassettes, the two plasmids encode for two different N-terminal affinity tags; a His-tag and a HA-tag. To purify the heteromultimer the cell lysate was loaded onto a Ni-affinity column and then eluted with imidazole. By using a Nickel column, the His tagged protein was the only protein bound to the column and is eluted from the column with imidazole. The HA-tagged protein is unable to bind to the column. This pull-down assay allows for the protein to be purified using the His-tag and for

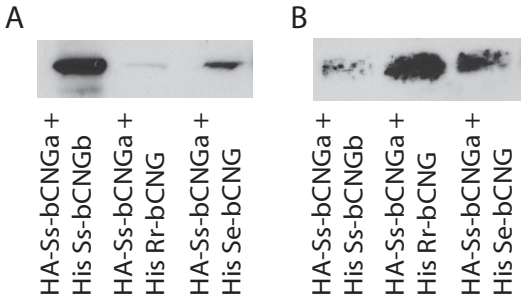


**Figure 5.2:** Westerns of HA-Ss-bCNGa co-multimers. A) Anti-HA western showing that HA-Ss-bCNGa forms co-multimers with His-Ss-bCNGb and His-Se-bCNG. B) Anti-His westerns showing that His-bCNG channels were purified from the column.

complex formation to be monitored by probing for the HA-tag. The presence of the HA-tag in the purified protein indicates that these two channels form heteromultimers.

Since, Ss-bCNGa is able to form a heteromultimer with Ss-bCNGb (Figure 5.3), its ability to form a heteromultimer with other bCNG channels was probed. The heteromultimerization of Ss-bCNGa, a three transmembrane channel, was explored with Se-bCNG, a three transmembrane channel, and Rr-bCNG, a five transmembrane channel. These two channels were selected to determine if the number of transmembrane domains is an important factor for mutlimerization. Ss-bCNGa is able to form heteromultimers with Se-bCNG and is unable to form heteromultimers with Rr-bCNG (Figure 5.2). The presence of both channels in the lysate suggests that there is sufficient protein for the formation of a heteromultimeric complex (Figure 5.3). These results suggest that the number of transmembrane domains is important for the formation of heteromultimeric channels. The number of transmembrane domains is likely essential for the transmembrane domain packing of the channels.

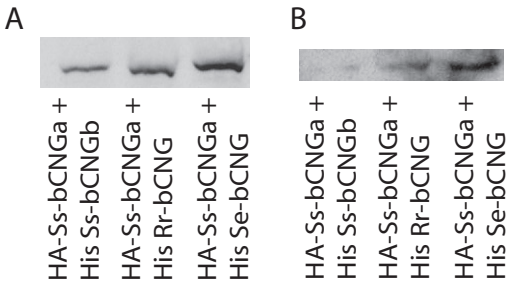


**Figure 5.3:** Westerns of HA-Ss-bCNGa lysates. A) Anti-HA western showing that HA-tagged protein is present in each sample. B) Anti-His western showing that His-tagged protein is present in each sample.

### *5.3.2 RNA Analysis of Synechocystis sp.* PCC 6803 *bCNG Channels*

To determine if heteromultimers are possible *in vivo*, RT-PCR was utilized to verify that mRNA from both bCNG channel subunits were co-transcribed. *Synechocystis sp.* PCC 6803 is a photosynthetic bacteria, so the cultures were subjected to five days of twelve hours light/twelve hours dark to sync their photosynthetic clocks. This syncing allowed for a clock dependence to be determined, since cAMP levels have been shown to oscillate in similar rhythms (de Alda and Houmard 2000; Segovia et al. 2001). mRNA samples were obtained from the middle of a light and dark cycle. Ss-bCNGa and Ss-bCNGb are expressed at similar levels *in vivo*, when compared to RpoB, in both the light and dark (Figure 5.4). These findings indicate that there is no clock dependence for Ss-bCNGa and Ss-bCNGb expression. Moreover, the expression of Ss-bCNGa and Ss-bCNGb at similar levels, taken together with the ability of these channels to form heteromultimers during heterologous expression suggests that these channels would form heteromultimers *in vivo*.

Since, cAMP levels are tightly controlled in response to light in photosynthetic bacteria (de Alda and Houmard 2000; Segovia et al. 2001), it would not have been surprising if the expression of bCNG channels was also tightly tied to the photosynthetic clock. The amount of bCNG mRNA was also compared to crp, the cAMP receptor protein, since Crp is critical for cAMP dependent transcription. The mRNA for Ss-bCNGa, Ss-bCNGb, and Crp was present at similar levels when compared to RpoB. To verify primer specificity the products were run on agarose gels. All gels showed the correct size bands (Figure 5.5).

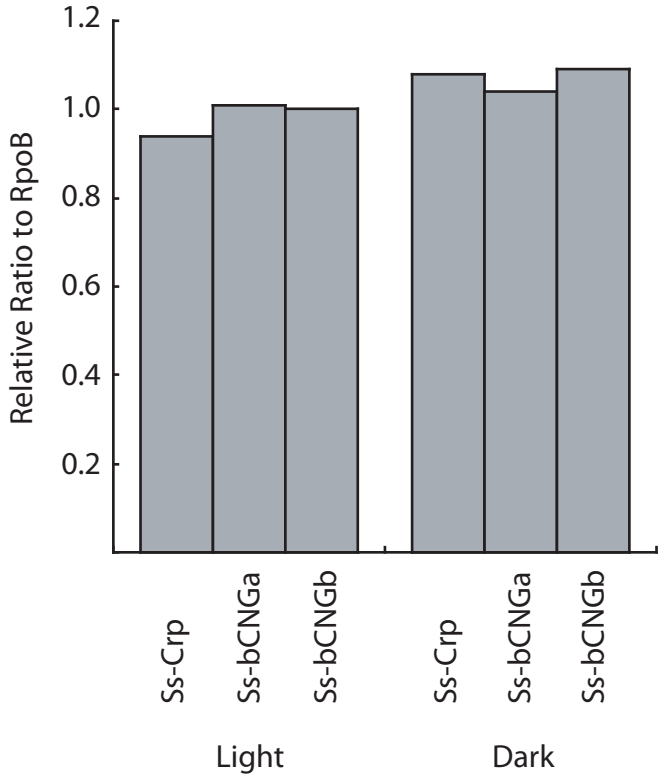


**Figure 5.4:** RT-PCR analysis of Ss PCC 6803 genes. Ss-bCNGa and Ss-bCNGb are found in equivalent levels in both the light and the dark. These genes are also found to be in similar levels as Crp, indicating there is no cAMP dependence for expression of bCNG genes. The similar levels found in the light and dark indicate that there is not a dependence upon the clock for these channels.

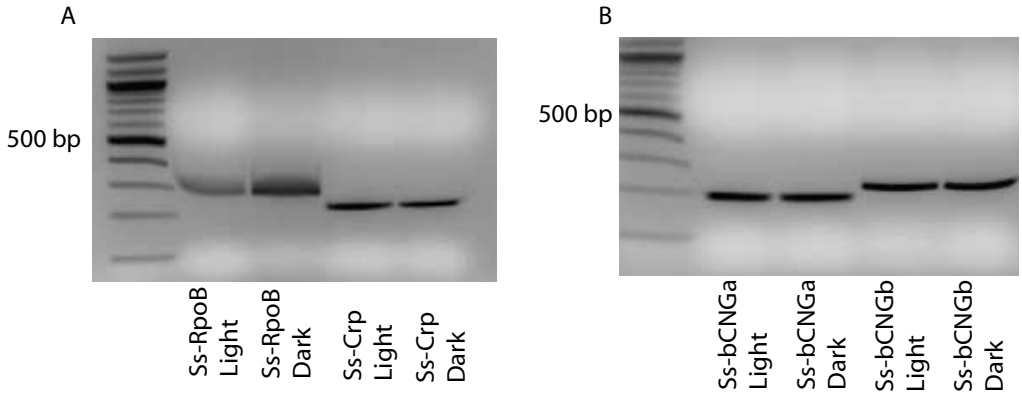


**Figure 5.5:** Agarose gels of Ss PCC6803 genes studied in RT-PCR. All of the reactions show only one product that is at the correct molecular weight (Table 5.4).

*5.3.3 RNA Analysis for additional bCNG channels*

We examined the mRNA levels of bCNG subunits in four other bacterial strains. In *A. marina*, the mRNA for Am-bCNGa and Am-bCNGb is present in similar levels in comparison to RpoB and in *Cyanothece sp.* ATCC 51142 the mRNA levels for Cs-bCNGa-2 and Cs-bCNGb-2 are found in identical levels (Figure 5.6). However, in *R. leguminosarum* the two bCNG channels are expressed at different levels with the mRNA for Rl-bCNGb being detected at a slightly higher level than the mRNA for Rl-bCNGa. In *B. xenovorans* LB400 all three bCNG channels are all expressed at similar levels (Figure 5.6). The final products were run on 2% agarose gels to verify primer affinity; there is only one product for each gene (Figure 5.7).

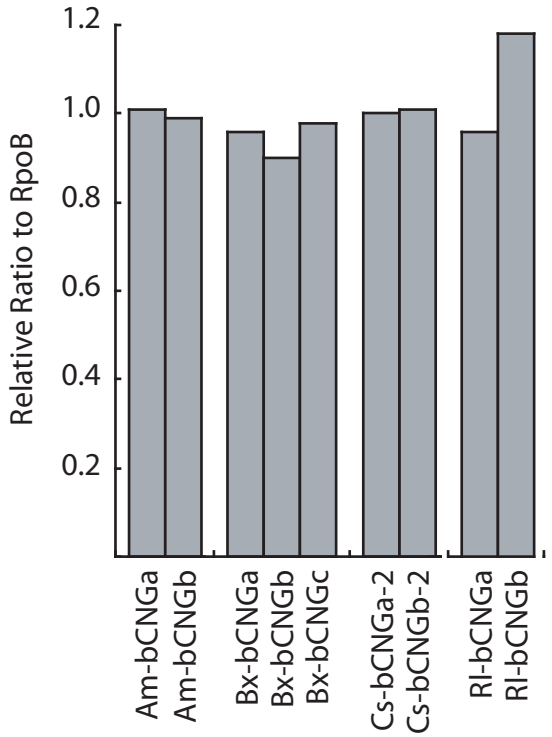


**Figure 5.6:** RT-PCR data of bCNG channels. The genes for the bCNG channels are all expressed at similar levels in ratio to RpoB, the internal standard.

The presence of the mRNA for multiple bCNG homologues at a single time point indicates that it is possible for the bCNG channels to form heteromultimeric ion channels in vivo. These heteromultimeric ion channels would be the first identified in bacteria, the *in vitro* heterologous expression data indicates that two bCNG channels with the same number of transmembrane domains could form a functional heteromultimeric channel *in vivo*.

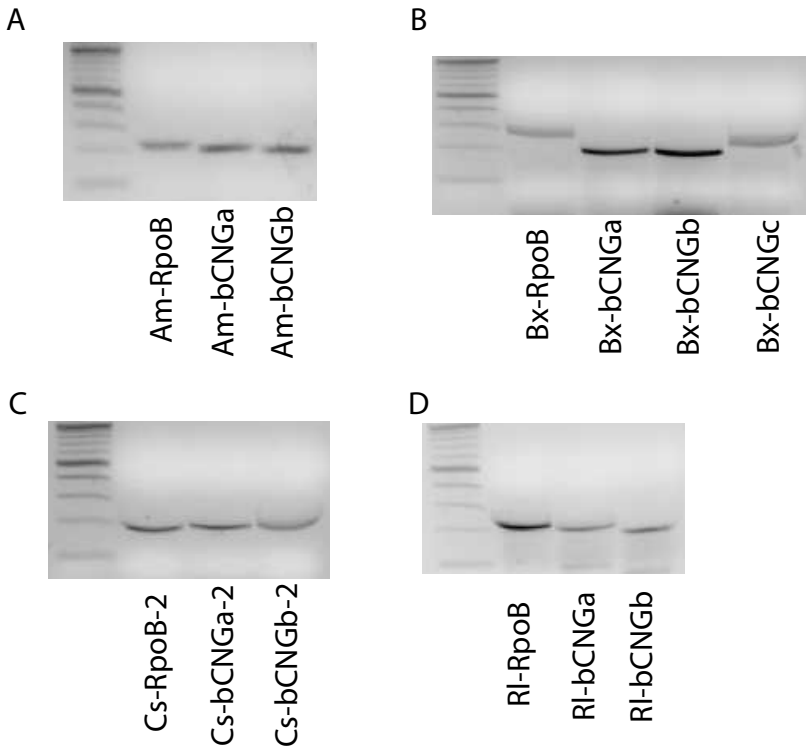


**Figure 5.7:** Agarose gels of bCNG channel RT-PCR reactions. All of the reactions show only one product that is at the correct molecular weight (Table 5.5).

| | Cycle Threshold | Expected Size (bp) |
|---|---|---|
| Am-RpoB | 14.44 | 235 |
| Am-bCNGa | 14.25 | 208 |
| Am-bCNGb | 14.70 | 199 |
| Bx-RpoB | 14.42 | 315 |
| Bx-bCNGa | 15.50 | 237 |
| Bx-bCNGb | 17.08 | 231 |
| Bx-bCNGc | 15.08 | 292 |
| Cs-RpoB-2 | 16.37 | 211 |
| Cs-bCNGa-2 | 16.39 | 226 |
| Cs-bCNGb-2 | 16.18 | 246 |
| Rl-RpoB | 28.05 | 262 |
| Rl-bCNGa | 28.61 | 239 |
| Rl-bCNGb | 25.94 | 190 |
| Ss-RpoB (light) | 17.48 | 354 |
| Ss-RpoB (dark) | 18.36 | |
| Ss-Crp (light) | 18.82 | 229 |
| Ss-Crp (dark) | 16.56 | |
| Ss-bCNGa (light) | 17.30 | 193 |
| Ss-bCNGa (dark) | 16.74 | |
| Ss-bCNGb (light) | 17.42 | 255 |
| Ss-bCNGb (dark) | 16.45 | |

**Table 5.5:** RT-PCR analysis: The cycle threshold values for the genes as determined by the instrument (Cepheid Smart Cycler) and the expected band size for the genes

### *5.4 Conclusions*

Two bCNG channels from the same bacteria when heterologously expressed in *E. coli* form heteromultimeric ion channels. Analysis of mRNA levels for Ss-bCNGa and Ss-bCNGb shows that both channels are expressed at similar levels and that these two genes do not display a dependence upon Crp expression level. In four additional bacterial strains, the genes for the bCNG homologues are expressed at similar levels. Although in some bacterial strains there is a slight preference for one channel over the other. The equivalent expression levels of the bCNG homologues indicate that the presence of

heteromultimeric bCNG channels is possible. These channels represent the first identified heteromultimeric ion channels in bacteria.

### *5.5 References*


Allen MM (1968) Photosynthetic membrane system in Anacystis nidulans. Journal of bacteriology 96 (3):836-841

Aslanidis C, de Jong PJ (1990) Ligation-independent cloning of PCR products (LIC-PCR). Nucleic Acids Res 18 (20):6069-6074

Bass RB, Strop P, Barclay M, Rees DC (2002) Crystal structure of Escherichia coli MscS, a voltage-modulated and mechanosensitive channel. Science 298 (5598):1582-1587

Bricker TM, Roose JL, Fagerlund RD, Frankel LK, Eaton-Rye JJ (2012) The extrinsic proteins of Photosystem II. Biochimica et biophysica acta 1817 (1):121-142. doi:10.1016/j.bbabio.2011.07.006

Bustos SA, Golden SS (1991) Expression of the psbDII gene in Synechococcus sp. strain PCC 7942 requires sequences downstream of the transcription start site. Journal of bacteriology 173 (23):7525-7533

Caldwell DB, Malcolm HR, Elmore DE, Maurer JA (2010) Identification and experimental verification of a novel family of bacterial cyclic nucleotide-gated (bCNG) ion channels. Biochimica et biophysica acta 1798 (9):1750-1756. doi:10.1016/j.bbamem.2010.06.001

Cravchik A, Matus A (1993) A novel strategy for the immunological tagging of cDNA constructs. Gene 137 (1):139-143. doi:0378-1119(93)90262-2 [pii]

de Alda JAGO, Houmard J (2000) Genomic survey of cAMP and cGMP signalling components in the cyanobacterium Synechocystis PCC 6803. Microbiol-Uk 146:3183-3194

Golden SS, Canales SR (2003) Cyanobacterial circadian clocks--timing is everything. Nature reviews Microbiology 1 (3):191-199. doi:10.1038/nrmicro774

Haun RS, Moss J (1992) Ligation-independent cloning of glutathione S-transferase fusion genes for expression in Escherichia coli. Gene 112 (1):37-43

Mackey SR, Golden SS (2007) Winding up the cyanobacterial circadian clock. Trends in microbiology 15 (9):381-388. doi:10.1016/j.tim.2007.08.005

McHenry CS (2011) Bacterial replicases and related polymerases. Current opinion in chemical biology 15 (5):587-594. doi:10.1016/j.cbpa.2011.07.018

Nitabach MN, Llamas DA, Araneda RC, Intile JL, Thompson IJ, Zhou YI, Holmes TC (2001) A mechanism for combinatorial regulation of electrical activity: Potassium channel subunits capable of functioning as Src homology 3-dependent adaptors. Proceedings of the National Academy of Sciences of the United States of America 98 (2):705-710. doi:10.1073/pnas.031446198

Pati UK (1992) Novel vectors for expression of cDNA encoding epitope-tagged proteins in mammalian cells. Gene 114 (2):285-288

Segovia M, Gordillo FJL, Schaap P, Figueroa FL (2001) Light regulation of cyclic-AMP levels in the red macroalga Porphyra leucosticta. J Photoch Photobio B 64 (1):69-74

Shi LX, Hall M, Funk C, Schroder WP (2012) Photosystem II, a growing complex: updates on newly discovered components and low molecular mass proteins. Biochimica et biophysica acta 1817 (1):13-25. doi:10.1016/j.bbabio.2011.08.008

Steinbacher S, Bass R, Strop P, Rees DC (2007) Structures of the prokaryotic mechanosensitive channels MscL and MscS. Curr Top Membr 58:1-24. doi:Doi 10.1016/S1063-5823(06)58001-9

Wu J, Lukas RJ (2011) Naturally-expressed nicotinic acetylcholine receptor subtypes. Biochemical pharmacology 82 (8):800-807. doi:10.1016/j.bcp.2011.07.067

# Chapter Six

# Defining the Role of the Tension Sensor in the Mechanosensitive Channel of Small Conductance (MscS).

*Collaboration with Yoon-Young Heo

---

### *6.1 Introduction*

Bacterial mechanosensitive channels function as pressure relief valves; alleviating the high intracellular pressure caused by hypoosmotic shock and preventing bacterial lysis. In *Escherichia coli* (*E. coli*), four mechanosensitive channels have been identified, cloned, and characterized; the mechanosensitive channel of large conductance (MscL), the mechanosensitive channel of small conductance (MscS), the mechanosensitive channel of potassium-dependant small conductance (MscK), and *YbdG* (Li et al. 2007; Levina et al. 1999; Schumann et al. ; Sukharev et al. 1994). MscS and MscL are the best studied of the bacterial mechanosensitive channels (Hurst et al. 2008; Kloda et al. 2008). These two channels are found in the plasma membrane, activated by mechanical tension on the lipid membrane, and rescue bacteria from cell lysis under hypoosmotic conditions.

Hypoosmotic shock, or downshock, causes bacteria to swell due to an influx of water across the cellular membrane in order to equilibrate the osmotic strength of the internal and external environments. This swelling results in membrane tension and can induce cell lysis. Mechanosensitive channels in bacteria gate in response to this tension and release small osmolytes and even proteins to allow for rapid equilibration of the internal and external osmotic strengths.

The response of MscS to membrane tension has been characterized using osmotic downshock assays (Vasquez et al. 2007; Levina et al. 1999; Rasmussen et al. ; Koprowski et al.) and patch-clamp electrophysiology (Sukharev et al. 1993; Akitake et al. 2005; Nomura et al. 2006). In addition, molecular dynamic simulations of MscS under tension have been carried out in an attempt to understand MscS's tension response (Vasquez et al. 2008a; Anishkin et al. 2008b). Previous work has identified nine residues that are important for MscS gating; I37, A51, D62, F68, L86, L111, L115, R128, R131 (Machiyama et al. 2009; Nomura et al. 2006, 2008; Belyy et al.). Three of these residues, D62, R128, and R131, are postulated to work in concert to stabilize the open state conformation of the channel under tension through electrostatic interactions (Nomura et al. 2008). Removal of one of these two positively charged arginines decreases the stability of the open state conformation. Based on the MscS crystal structures, this cluster of residues is predicted to be located in the loop between the first and second transmembrane domains (TM) and the cytoplasmic vestibule at the protein-lipid-water interface (Nomura et al. 2008; Bass et al. 2002). The remaining residues are within the TM domains and have been postulated to play important roles during the transition

between closed and open states (Machiyama et al. 2009; Nomura et al. 2008, 2006). Two pairs of residues, I37/L86 and A51/ F68, are postulated to be involved with the displacement of TM1 and TM2 from the central axis during gating (Nomura et al. 2006) and are predicted not to interact with the lipid bilayer based on the MscS crystal structures (Bass et al. 2002; Nomura et al. 2006). Mutation of F68, L111, and L115 to serine has suggested that these residues are involved in the desensitization or inactivation of MscS (Belyy et al.). These three residues are thought to transduce mechanical stress to the gate through hydrophobic interactions. The removal of these hydrophobic interactions results in rapid desensitization. Furthermore, these hydrophobic interactions are postulated to be involved in the coupling of TM2 and TM3 as they come into contact with one another during the transduction of the force to the gate. While these nine residues clearly play critical roles in MscS channel function, they are not involved in the tension sensation or response from direct interaction with surrounding lipid.

Using the initial MscS crystal structure solved by Rees and co-workers (1MXM/2OAU) as a starting point (Bass et al. 2002), Nomura and co-workers employed asparagine scanning mutagenesis of the lipid facing amino acid side chains in an attempt to identify the residues critical for tension sensation (Nomura et al. 2006). This study revealed a number of amino acids that phenotypically alter MscS channel function, including I37, A51, F68, and L86. The study of these mutations revealed that these residues take part in important intermolecular interactions that are involved in the open to closed transition state. These four residues interact as two pairs, I37/L86 and A51/ F68, which work in concert to open the channel under mechanical stress. However, few if any of the residues

identified in this study seem to be involved in tension sensation through the lipid bilayer. This may not be surprising since 1MXM (2OAU), the initial MscS crystal structure, is thought to represent a desensitized or inactivated state of MscS (Vasquez et al. 2008a; Martinac 2005; Anishkin and Sukharev 2004). In the desensitized state, the MscS channel is insensitive to tension. This insensitivity is potentially due to occlusion of the tension sensing or tension responsive residues in the desensitized state, leading to decreased interactions with the membrane. This is consistent with the assertion that changes to the lipid membrane can alter the desensitization behavior of MscS as observed upon lysophosphatidylcholine application, MscS reconsitution by the "sucrose method", and in lipid exchange (Battle et al. 2009; Belyy et al. ; Vasquez et al. 2008a).

We have previously used a combination of extensive random mutagenesis and molecular dynamic simulations to show that many MscL residues important for sensing bilayer tension interact strongly with the lipid tail groups (Elmore and Dougherty 2003; Maurer and Dougherty 2003). A large library of MscL mutations, created by random mutagenesis, was used to identify critical residues involved in tension sensation (Maurer and Dougherty 2003). This analysis showed that mutations to the lipid lining residues of MscL had a high propensity of being phenotypically loss of function (LOF) (Maurer and Dougherty 2003). A LOF phenotype has been demonstrated to correspond to an increase in gating tension for bacterial mechanosensitive channels (Maurer and Dougherty 2001). In a subsequent study, we conducted molecular dynamic (MD) simulations on the closed state structure of MscL and analyzed the protein-lipid interaction energies. This analysis indicated that the majority of lipid lining LOF mutations identified in our random

mutagenesis study corresponded to residues with significant lipid interactions. Together, these observations implied that channel residues that interact with lipid are critical in tension sensation (Elmore and Dougherty 2003; Maurer and Dougherty 2003).

Unfortunately, a crystal structure of the closed state of MscS has yet to be determined to allow an analysis of the lipid lining residues in the closed state similar to that carried out for the desensitized state (Nomura et al. 2006). However, an experimentally derived electron paramagnetic resonance (EPR) structure for the carbon-alpha (Cα) chain of MscS has been developed by Perozo and co-workers (Vasquez et al. 2008b). This structure cannot be directly analyzed for lipid bilayer interactions, since it is missing the amino acid side chains. Nonetheless, this structure does provide an excellent starting point for the type of analysis that we have previously carried out on MscL (Elmore and Dougherty 2003).

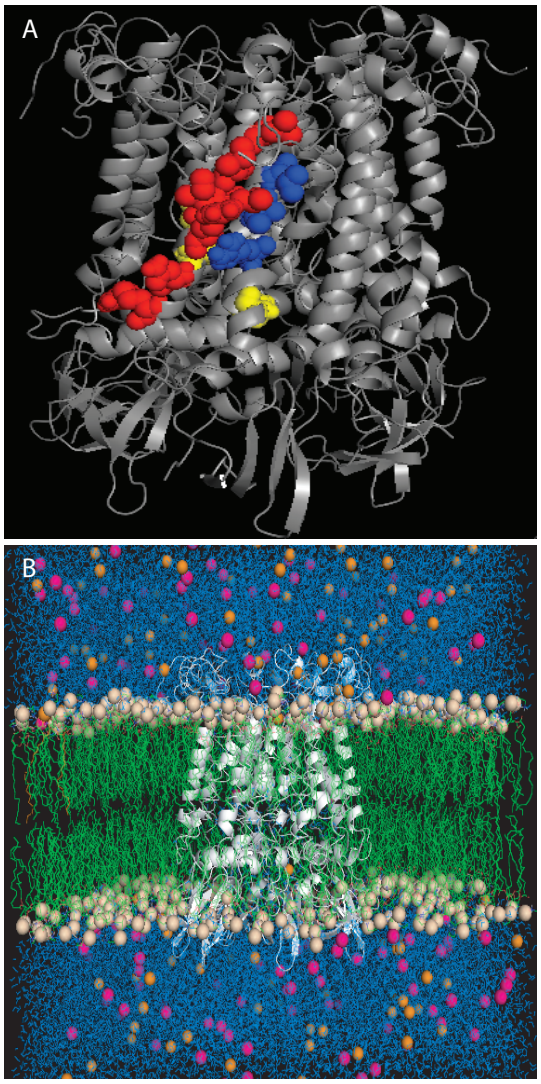


**Figure 6.1**: Closed state MscS model at the end of the MD simulation, as seen from the side and (A) the residues highlighted as space-filling model in A correspond to the predicted lipid interacting residues in TM1 (L35, I39, L42, I43, R46, N50, R54) shown in red, the predicted lipid interacting residues in TM2 (R74, I78, L82) shown in blue, and non-interacting residues used as controls in this study (I44, I48, F68) shown in yellow (B) and with lipids, chloride ions, sodium ions, and water included in the simulation.

Here, we explore the residues critical for tension sensation in MscS and evaluate how these residues move through the closed, open, and desensitized states. Starting from a computational analysis, we identified potentially critical residues in MscS tension sensation based on the closed state of MscS. The central role of these residues for tension

sensation was then confirmed using *in vivo* downshock assays of alanine mutations (Figure 6.1A). Moreover, we note that the seven residues identified here are mostly distinct from those previously identified by Nomura and co-workers (Nomura et al. 2006). By considering these residues and their relative location in the closed, open, and desensitized states of MscS, we gain significant insight into how MscS channels sense and respond to membrane tension.

## *6.2 Materials and Methods*

### *6.2.1 Molecular Dynamics Simulations*

MODELLER 9.1 (Madhusudhan et al. 2005; Sali and Blundell 1993) was used to construct an all-atom structure of MscS based on the three-dimensional Cα model of the channel in its closed state developed by Perozo and co-workers (Vasquez et al. 2008b). Since the model does not represent the entire MscS protein, sequence alignments for modeling were produced using the ALIGN feature of MODELLER and the Perozo structure was used as the modeling template. Three hundred models were produced, and the model with the lowest DOPE energy was used as a starting structure for MD simulations.

Molecular dynamics (MD) simulations of MscS were performed using the GROMACS MD simulations suite and the GROMOS force field (Lindahl et al. 2001). The channel model was embedded in a preequilibrated palmitoyloleoyl-phospha-tidylethanolamine (POPE) membrane using the method of Kandt and co-workers (Kandt et al. 2007). The all-atom MscS structure obtained from MODELLER was superimposed onto a pre-

equilibrated POPE bilayer with the desired orientation relative to the membrane, such that the structure overlapped with lipids. The bilayer was then expanded by translating lipid molecules and scaling the lateral dimensions of the box size by a factor of four and the protein was centered in the new bilayer plane. A series of compression steps were performed using a scaling factor of 0.95 to slowly reequilibrate the lipid density and properly embed the channel in the bilayer. During this process, the protein was constrained and the system energy was minimized after each scaling step. The area per lipid was calculated at each step with scaling and minimization steps performed until the area per lipid reached 0.4990 $nm^2$/lipid, the reference value of a POPE membrane (Rand and Parsegian 1989). Following reequillibration of the membrane, the system was hydrated, sufficient chloride ions were added to neutralize the net charge on the protein, sodium and chloride ions were added to yield an ionic strength of 100 mM, and the system was minimized using 50 steps of steepest descents minimization. Any lipids that had significant overlap with the channel after the steepest descents minimization were removed. The final system was composed of the protein, 451 POPE lipids, 40205 water molecules, 127 sodium ions and 148 chloride ions (Figure 6.1B).

Two MD simulations were carried out starting from the minimized system, using different initial random velocities. In both cases, the systems were initially heated to 310 K over 20 ps with the alpha carbons of the protein restrained with a force constant of 1000 kJ/mol□$nm^2$. These restraints were maintained for an additional 480 ps at which time the restraints were removed and the trajectories were extended for a total of 50 ns. Simulations were carried out using a 2 fs timestep with water geometries constrained

using SETTLE (Miyamoto and Kollman 1992) and all other bonds constrained using LINCS (Hess et al. 1997). Temperature was held constant using a time constant ($\tau_t$) of 0.1 ps for three groups: protein, lipid and water/ions. Pressure was maintained at 1.0 atm using a time constant ($\tau_p$) of 1.0 ps with anisotropic coupling. Short-range electrostatics and Lennard-Jones interactions were cutoff at 1.0 nm and long-range electrostatics were calculated with PME (Darden et al. 1993), using a grid spacing of 0.10 nm and cubic interpolation. The Berger et al. force field parameters for POPE lipids were used with GROMOS parameters for the oleoyl double bond (Berger et al. 1997), and GROMACS parameters were used for the protein, ions, and water. Fluctuations and lipid interaction energies were obtained as an average of the last 10 ns of the simulations, and protein-lipid interaction energies were calculated as described previously for MscL by Elmore and Dougherty (Elmore and Dougherty 2003). Analyses were performed using tools in the GROMACS suite, and figures were made using Pymol (DeLano 2002).

*6.2.2 Strains and Plasmids*

The *E. coli* strain, MJF465 (*MscS, MscL, MscK* null), was used for osmotic downshock assays and expression experiments (Levina et al. 1999; Wild et al. 1992). Mutational cloning was conducting using the Top10F` *E. coli* strain (Invitrogen, Carlsbad, CA). All mutants were created in the pB10b vector with a C-terminal six-His tag (Wild et al. 1992; Sukharev et al. 1994; Ou et al. 1998) under the control of the LacUV5 promoter.

### *6.2.3 Site-Directed Mutagenesis*

Residues predicted to be involved in protein-lipid interactions as well as several controls were mutated to alanine using either Megaprimer mutagenesis (Yoshimura et al. 1999) or QuikChange mutagenesis (Agilent, Santa Clara, CA). All mutations in MscS were made in the pB10B vector. For megaprimer mutagenesis, forward and reverse primers located in the vector were used as the exterior primers and primers for mutagenesis were designed using Stratagene's QuikChange Primer design tool. Primer sequences are given in Table 6.1. Mutations were verified by enzymatic digestion and sequences confirmed using automated sequencing (Big Dye v3.1, Applied Biosystems, Carlsbad, CA).

| | Forward | Reverse |
|---|---|---|
| L35A | AGTAAACATCGTGGCGGCAG CCGCGATCATCATCG | CGATGATGATCGCGGCTGCC GCCACGATGTTTACT |
| I39A | GCGGCACTCGCCATCATCGC CGTTGGTTTGATTATCGC | GCGATAATCAAACCAACGGC GATGATGGCGAGTGCCGC |
| L42A | CGCAATCATCATCGTTGGTG CGATTATCGCGCGGATGATT | AATCATCCGCGCGATAATCG CACCAACGATGATGATTGCG |
| I43A | AATCATCATCGTTGGTTTGGC TATCGCGCGGATGATTTCC | GGAAATCATCCGCGCGATAG CCAAACCAACGATGATGATT |
| L42A/I43A | ACTCGCAATCATCATCGTTG GTGCGGCTATCGCGAG | CTCGCGATAGCCGCACCAAC GATGATGATTGCGAGT |
| R46A | GTTGGTTTGATTATCGCGGC GATGATATCCAACGCGGT | ACCGCGTTGGATATCATCGC CGCGATAATCAAACCAAC |
| N50A | GCGCGGATGATTTCCGCCGC GGTGAATCGCCT | AGGCGATTCACCGCGGCGGA AATCATCCGCGC |
| R54A | GGATGATATCCAACGCGGTG AATGCCCTGATGATCTCC | GGAGATCATCAGGGCATTCA CCGCGTTGGATATCATCC |
| R74A | TGCTGATTTTCTTTCTGCACT AGTCGCTTACGGTATTATCG CCTTT | AAAGGCGATAATACCGTAAG CGACTAGTGCAGAAAGAAAA TCAGCA |
| I78A | CTGCACTAGTCCGTTACGGT ATTGCCGCCTTTACGCTAATC | GATTAGCGTAAAGGCGGCAA TACCGTAACGGACTAGTGCA G |
| L82A | GTATTATCGCCTTTACGGCA ATCGCAGCCCTGGGAC | GTCCCAGGGCTGCGATTGCC GTAAAGGCGATAATAC |
| I44A | CGCGATCATCATCGTTGGTTT GATTGCCGCGCGGATGATA | TATCATCCGCGCGGCAATCA AACCAACGATGATGATCGCG |
| I48A | TTGATTATCGCGCGGATGGC TTCGAACGCGGTGAATCG | CGATTCACCGCGTTCGAAGC CATCCGCGCGATAATCAA |
| F68A | AATAGATGCCACTGTTGCTG ATGCTCTTTCTGCATTAGTCC G | CGGACTAATGCAGAAAGAGC ATCAGCAACAGTGGCATCTA TT |
| Outer cloning primers | CAATTTCACACAGGAAACAG GC | TACACGGAGGCATCAGTGAC CAAA |

**Table 6.1:** PCR primers for MscS alanine point mutations.

*6.2.4 Osmotic Downshock Experiments*

Downshock experiments were conducted as previously described (Booth et al. 2007; Caldwell et al.), with the following modifications. A single colony was used to inoculate an overnight culture in Luria-Bertani Broth (LB Broth, BD Biosciences, San Jose, CA) supplemented with ampicillin (100μg/mL), the overnight culture was subsequently used to inoculate (1:20) a culture in LB Broth with 250 mM NaCl and ampicillin. The resulting culture was grown to an $OD_{600}$ of approximately 0.5 and induced with 0.1 mM isopropyl-beta-D-thiogalactopyranoside (IPTG) for 30 min. Following 30 min of induction, the culture was diluted (1:40) into 1:1 LB Broth and deionized water or isotonically into LB Broth with 250 mM NaCl, and allowed to recover for 30 min in a shaking incubator. After hypoosmotic downshock or isotonic dilution, bacterial cultures were serially diluted and plated on LB plates supplemented with ampicillin (100μg/mL). Plates containing between 25 and 250 colonies were used to determine the colony forming units (CFU) per millimeter of media. Percent recovery was defined as the CFU of the downshocked culture divided by the CFU of the isotonic dilution. Six trials for each mutation were conducted.

*6.2.5 Bacterial Expression Analysis*

To verify bacterial expression of MscS mutants, cultures were grown as described above and pelleted for 15 min at 16000xg after 30 min of induction. The supernatant was removed and the pellets resuspended in a buffer containing 50 mM Tris, 75 mM NaCl, 0.1% Fos-Choline-14 (Anatrace, Maumee, OH), and protease complete inhibitor (Roche,

Basel, Schweiz) at 10 µL buffer per 10 mg bacteria. Samples were detergent solubilized using a probe sonicator for 3 cycles of 15 s on and 45 s off. After lysis and solubilization, insoluble material was removed by pelleting for 30 min at 16000xg. The supernatant was combined with SDS-PAGE loading dye, and the samples were boiled for 5 min. Samples were then run on a 12.5% SDS-PAGE poly-acrylamide gel using a TRIS-glycine running buffer. Equivalent volumes of the supernatant were loaded to allow for comparisons of protein expression levels. Proteins were transferred to a 0.2 µm nitrocellulose membrane using a semi-dry transfer system and Cashini's Buffer (0.1M Tris, 0.02% SDS, 0.2M glycine, 5% methanol). The protein expression of the C-terminally 6-His-tagged MscS mutants was probed using a primary mouse-anti-His monoclonal IgG (Covance, Emeryville, CA) and a secondary HRP-conjugated goat anti-mouse (Jackson ImunoResearch Laboratories, West Grove, PA) antibody.

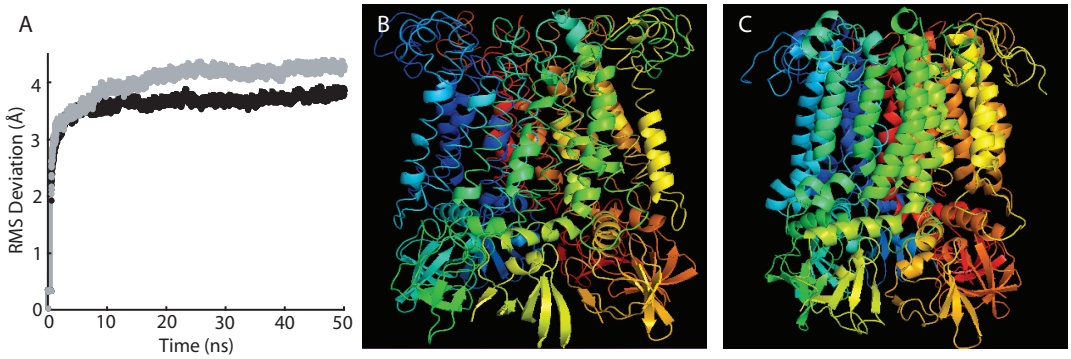


**Figure 6.2**: Structural deviations during the MD simulation. A) RMS deviation of the MscS structure over the course of the MD simulation; simulation 1 is shown in black and simulation 2 is shown in gray. B) Initial closed state all-atom MscS model generated with MODELLER. C) MscS all-atom closed state model from simulation 1 after 50 ns.

## *6.3 Results and Discussion*

### *6.3.1 Computational Analysis*

MD simulations were conducted starting with the closed state model of MscS developed by Vasquez *et al*. from distance constraints obtained by EPR (Vasquez et al. 2008b). This particular model was selected since it was directly based on experimentally obtained constraints (Anishkin et al. 2008a; Vasquez et al. 2008b). However, this closed state model contains only Cα atoms for MscS, which does not allow it to be used directly for the identification of side chain-lipid bilayer interactions. To circumvent this problem, we built side chains into the model using the MODELLER suite (Sali and Blundell 1993; Madhusudhan et al. 2005) and allowed these side chains to equilibrate into a native closed state conformation using MD simulations with an explicit POPE lipid bilayer, water, and ions.

Two 50 ns simulations of MscS embedded in an explicit POPE membrane were performed (Figure 1). POPE lipid was chosen for the membrane because of the prevalence of phosphatidylethanolamine lipids in bacterial membranes (Elmore and Dougherty 2001) and its use in previous simulations considering the lipid interactions of MscL (Elmore and Dougherty 2003). Both simulations gave similar results and showed structural equilibration within the first half of the trajectories (Figure 6.2). As well, the residues in the lipid exposed TM1 and TM2 domains were relatively stable during the final 10 ns of the trajectories, as shown by their low RMS Cα fluctuations (Figure 6.3).

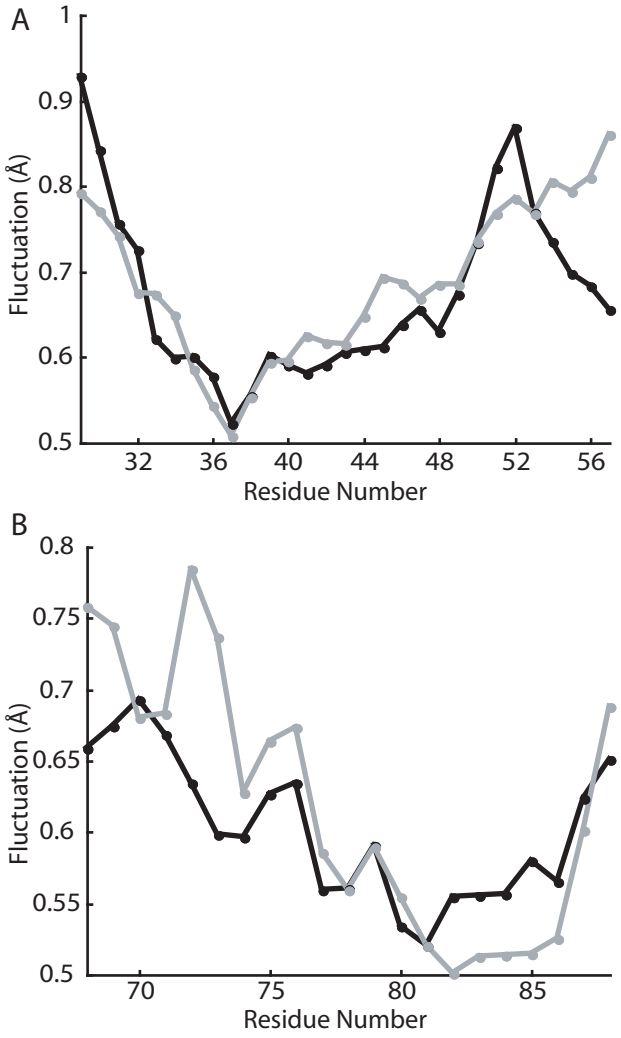


**Figure 6.3**: The average RMS fluctuation per residue over the final 10 ns of the MD simulations for TM1 (A) and TM2 (B); simulation 1 is shown in black and simulation 2 is shown in gray.

The total protein-lipid interaction energy for each residue was calculated over the last 10 ns of each simulation (Fig 6.4). A similar analysis previously conducted for MscL identified eight residues as having significant protein-lipid interactions (Elmore and Dougherty 2003). A comparison with random mutagenesis data showed that mutations to these residues were more likely to cause phenotypic changes in MscL than mutations to

other residues, including residues with significant intersubunit interactions (Maurer and Dougherty 2003; Elmore and Dougherty 2003). Thus, in this study the protein-lipid interaction energy for TM1 and TM2 residues of MscS were analyzed to predict residues involved in tension sensation.

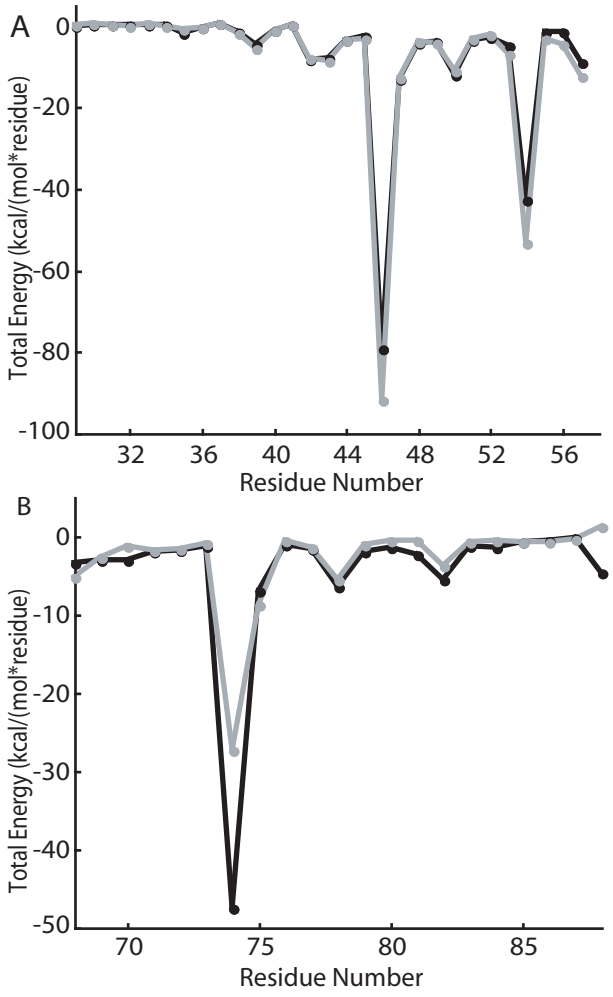


**Figure 6.4**: Protein-lipid interactions energies over the final 10 ns of the MD simulations for TM1 (A) and TM2 (B); simulation 1 is shown in black and simulation 2 is shown in gray.

Based on our previous work with MscL, residues that are involved in tension sensation produce local minima in the protein-lipid interaction analysis (Elmore and Dougherty

2003). Local minima in this analysis correspond to strong-protein lipid interactions. These local minima are important in predicting tension sensation since channel opening involves a global structural rearrangement in which entire helices twist. Thus, these global structural rearrangements would require an entire lipid exposed face of the protein to sense the tension on the lipid membrane. Based on our total protein-lipid interaction energy analysis (Figure 6.4), we predicted residues in TM1 and TM2 to be involved in tension sensation. In TM1 residues that gave local minima in the analysis are L35, I39, L42, I43, R46, N50, and R54 (red residues in Figure 6.1A) and in TM2 residues that gave local minima are R74, I78, and L82 (blue residues in Figure 6.1A). As predicted, these residues lie on the outer face of the MscS channel in the closed state of the structure.

*6.3.2 Functional Analysis*

To determine if the predicted protein-lipid interacting residues were important for tension sensation, we individually mutated each of the residues identified by our protein-lipid interaction energy analysis (Figure 6.4) to alanine. For hydrophobic residues, which could potentially interact with the lipid tails groups via the hydrophobic effect, mutation to alanine should greatly reduce the extent of interaction due to the small size of the alanine side chain. For charged residues, mutation to alanine both decreases the size of the residue and eliminates the possibility of electrostatic interaction (either hydrogen bonding or ion pairs). Thus, alanine mutations were prepared by site-directed mutagenesis for each of the residues identified using our protein-lipid interactions energy analysis.

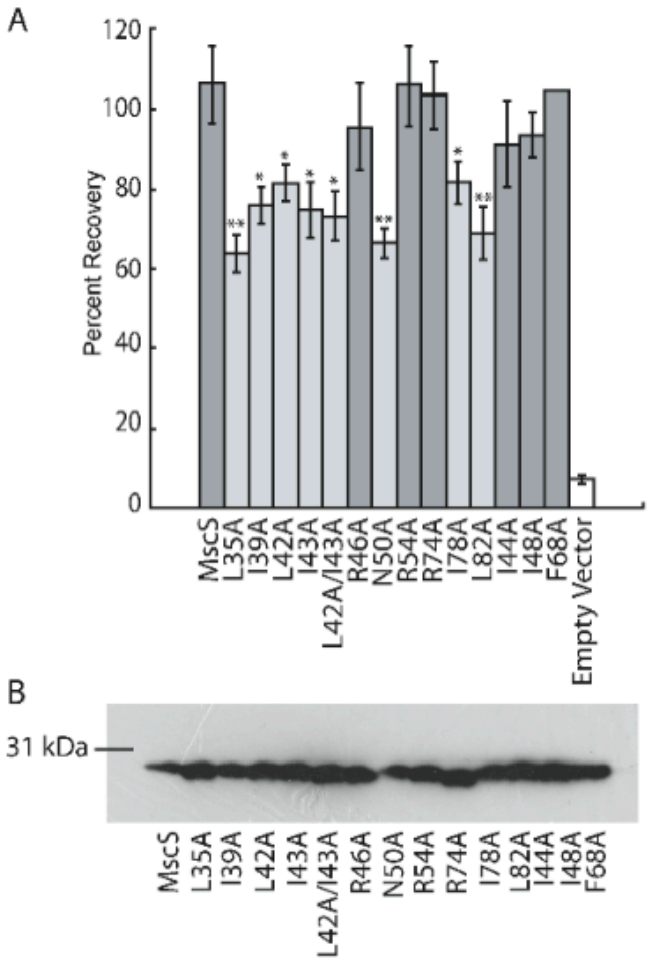


**Figure 6.5**: Functional analysis of MscS alanine mutations. A) Osmotic downshock assay results of wild-type MscS and alanine mutants. Error bars represent the standard error of the mean for 6 independent trials. Light gray bar indicate constructs that are statistically different from wild-type MscS as determined using a Student's T-test (** = $p < 0.01$ and * = $p < 0.05$) B) Western blot analysis of protein expression levels for wildtype MscS and alanine mutants under expression conditions identical to those used for the osmotic downshock assay.

The function of the mutant channels was then tested using an osmotic downshock assay (Figure 6.5). For each mutation six trials were conducted, and percent recovery values were compared using the T-test. A partial LOF phenotype was observed for L35A, I39A,

L42A, I43A, N50A, I78A, and L82A, and R46A, R54A, and R74A were phenotypically wildtype. Mutants were defined as having a partial LOF phenotype if they were statistically different from wildtype MscS at greater that 95% as determined using the Student's T-test. In Figure 6.5A, phenotypically partial LOF mutants are light gray and phenotypically wildtype mutants are dark gray. Additionally, all mutations were confirmed not to be gain of function (GOF) by measuring their stationary phase optical densities (Table 6.2). The partial LOF phenotypic differences were not due to decreased channel expression levels, since all mutants and controls were expressed at levels comparable to wildtype MscS (Figure 6.5B). Thus, an observed partial LOF phenotype corresponds to the inability of a site-directed MscS mutant to gate in response to tension with a comparable gating threshold to wildtype MscS.

| | Stationary Phase Optical Density ($OD_{600}$) |
|---|---|
| Wildtype MscS | 1.8 |
| L35A | 1.3 |
| I39A | 1.8 |
| L42A | 1.3 |
| I43A | 1.7 |
| L42A/I43A | 1.7 |
| R46A | 1.8 |
| N50A | 1.7 |
| R54A | 1.7 |
| R74A | 1.8 |
| I78A | 1.8 |
| L82A | 1.8 |
| I44A | 1.6 |
| I48A | 1.5 |
| F68A | 1.8 |

**Table 6.2**: Stationary phase optical densities for MscS mutations. Stationary phase optical densities were obtained by growing a single colony to an $OD_{600}$ of approximately 0.5 in LB media, followed by induction with 0.1 mM IPTG for 8 hours.

Similar trends are observed in the MscS and MscL residues that are necessary for tension sensation. In this study of MscS, six of the seven alanine mutations that produced a partial LOF phenotype were very hydrophobic residues, and the three charged residues with significant protein-lipid interactions in MD simulations were insensitive to mutation (R46, R54 and R74). This trend is similar to that observed in MscL (Yoshimura and Sokabe). In the analogous series of studies on MscL comparing MD simulations with random mutagenesis data we also identified several LOF mutations upon substitutions of hydrophobic amino acids (Maurer and Dougherty 2003; Elmore and Dougherty 2003). Moreover, analyses of the effects of lipid composition on MscL have implied that specific electrostatic interactions, such as hydrogen bonding, with lipid headgroups is generally less important for MscL mechanosensation than hydrophobic interactions with lipid tail groups (Moe and Blount 2005). As well, almost all mutations that led to a significant reduction in channel function for MscS were clustered near the periplasmic interface of the channel as observed for MscL (Elmore and Dougherty 2003). This suggests that the tension sensor for both channels is located in hydrophobic lipid-interacting residues at the periplasmic interface. These regions of TM1 and TM2 also had lower RMS fluctuations than the cytoplasmic sides of the helices (Figure 6.3), implying that these important lipid interactions lead to increased structural stability in this region of the channel.

In order to determine whether the effects observed for mutation of hydrophobic residues were specific to lipid-interacting residues, we also studied three additional MscS alanine mutations (I44A, I48A, and F68A) (Figure 6.5). For these control mutations, we selected

residues I44 and I48 in TM1 and F68 in TM2 (yellow residues in Figure 6.1A). All of these residues are very hydrophobic, akin to many of the residues that were identified as important lipid interacting residues, but these residues are not predicted by our computational analysis of lipid interactions to be important in tension sensation (Figure 6.4). None of these mutations led to a significant effect on channel function, as they were phenotypically wildtype (Figure 6.5A). These observations provide further evidence that lipid-interacting residues are particularly central to tension sensation in MscS and that in order to interact with the lipids the amino acid side chains must be on the exterior side of the transmembrane helix. The non-tension sensing hydrophobic residues in the transmembrane helices are rotated slightly outward in the open and desensitized crystal structures and therefore likely play a role in stabilizing these states through hydrophobic interactions with the lipid tail groups. This is reflected in the physiological differences observed for I48N and F68N by Yoshimura and co-workers (Nomura et al. 2006).

One pair of lipid interacting residues, L42 and I43, is particularly interesting as they are adjacent in the structure. Alanine mutations at both sites are statistically different from MscS (Figure 6.5A). A double mutant of L42A/I43A was created to determine if the removal of two adjacent lipid interacting residues would create a unique phenotypic mutant with different properties from the single mutation. Interestingly, the double-mutation showed behavior similar to that of the two single mutations, implying that a disruption one of these interactions is sufficient to disrupt channel function.

### *6.3.3 Role of Lipid-Interacting Residues in Tension Sensation*

The data presented above demonstrates that a series of hydrophobic residues lying along the outer face of MscS interact with the lipid tail groups of the bilayer in the closed state and are essential for effective tension sensation. Interestingly, these residues do not maintain their full lipid interactions throughout the channel's gating transition (Figure 6.6). In the closed state model of the channel and in our simulations, these residues face directly towards the surrounding lipid membrane. However, in the open state of the channel, as observed in the Wang et al. crystal structure of A106V MscS (Wang et al. 2008), these residues have turned such that they no longer face the membrane directly. The rotation of these residues during the transition from the closed state to the open state is likely driven by these residues finding new intra-protein hydrophobic contacts as tension on the bilayer pulls the membrane away from these residues breaking up their hydrophobic interactions with the lipid tail groups. Intriguingly, these residues also do not directly face the lipid in the Bass et al. MscS structure that has been interpreted as the desensitized state of the channel (Steinbacher et al. 2007; Bass et al. 2002). The fact that these residues have lost their direct lipid contact in this structure likely leads to its insensitivity to gating by tension. Moreover, these observations also show that future studies attempting to identify the tension sensor of a mechanosensitive channel should perform the analysis of protein-lipid interactions on the closed state of the channel.

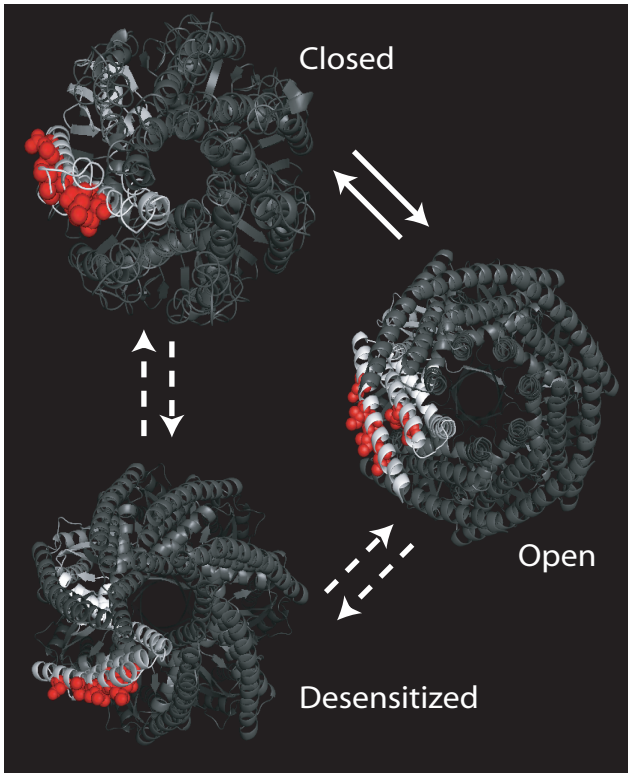


**Figure 6.6:** The positions of the tension sensing residues are shown in the closed (50 ns simulation), open (2VV5, (Wang et al. 2008)), and desensitized (2OAU, (Bass et al. 2002; Steinbacher et al. 2007)) states of MscS.

### *6.4 Conclusions*

Here, we have identified the critical residues that compose the region of MscS involved with directly sensing membrane tension through lipid interactions. This tension sensor is composed of lipid-facing hydrophobic residues within the first and second transmembrane domains of MscS. In the closed state of the channel these residues interact with the lipid tail groups. Upon transition from the closed state to the open state of the channel, these residues turn inward to form intra-protein hydrophobic interactions. Finally, when MscS undergoes desensitization, the pore of the channel becomes occluded while these residues remain in intra-protein hydrophobic interaction.

### *6.5 References*


Akitake B, Anishkin A, Sukharev S (2005) The "dashpot" mechanism of stretch-dependent gating in MscS. J Gen Physiol 125 (2):143-154. doi:jgp.200409198 [pii]

10.1085/jgp.200409198

Anishkin A, Akitake B, Sukharev S (2008a) Characterization of the resting MscS: modeling and analysis of the closed bacterial mechanosensitive channel of small conductance. Biophys J 94 (4):1252-1266. doi:S0006-3495(08)70643-X [pii]

10.1529/biophysj.107.110171

Anishkin A, Kamaraju K, Sukharev S (2008b) Mechanosensitive channel MscS in the open state: modeling of the transition, explicit simulations, and experimental measurements of conductance. J Gen Physiol 132 (1):67-83. doi:10.1085/jgp.200810000

jgp.200810000 [pii]

Anishkin A, Sukharev S (2004) Water dynamics and dewetting transitions in the small mechanosensitive channel MscS. Biophys J 86 (5):2883-2895. doi:S0006-3495(04)74340-4 [pii]

10.1016/S0006-3495(04)74340-4

Bass RB, Strop P, Barclay M, Rees DC (2002) Crystal structure of Escherichia coli MscS, a voltage-modulated and mechanosensitive channel. Science 298 (5598):1582-1587. doi:10.1126/science.1077945

298/5598/1582 [pii]

Battle AR, Petrov E, Pal P, Martinac B (2009) Rapid and improved reconstitution of bacterial mechanosensitive ion channel proteins MscS and MscL into liposomes using a modified sucrose method. FEBS Lett 583 (2):407-412. doi:S0014-5793(08)01024-7 [pii]

10.1016/j.febslet.2008.12.033

Belyy V, Anishkin A, Kamaraju K, Liu N, Sukharev S The tension-transmitting 'clutch' in the mechanosensitive channel MscS. Nat Struct Mol Biol 17 (4):451-458. doi:nsmb.1775 [pii]

10.1038/nsmb.1775

Belyy V, Kamaraju K, Akitake B, Anishkin A, Sukharev S Adaptive behavior of bacterial mechanosensitive channels is coupled to membrane mechanics. J Gen Physiol 135 (6):641-652. doi:jgp.200910371 [pii]

10.1085/jgp.200910371

Berger O, Edholm O, Jahnig F (1997) Molecular dynamics simulations of a fluid bilayer of dipalmitoylphosphatidylcholine at full hydration, constant pressure, and constant temperature. Biophys J 72 (5):2002-2013. doi:S0006-3495(97)78845-3 [pii]

10.1016/S0006-3495(97)78845-3

Booth IR, Edwards MD, Black S, Schumann U, Bartlett W, Rasmussen T, Rasmussen A, Miller S (2007) Physiological analysis of bacterial mechanosensitive channels. Methods Enzymol 428:47-61. doi:S0076-6879(07)28003-6 [pii]

10.1016/S0076-6879(07)28003-6

Caldwell DB, Malcolm HR, Elmore DE, Maurer JA Identification and experimental verification of a novel family of bacterial cyclic nucleotide-gated (bCNG) ion channels. Biochim Biophys Acta 1798 (9):1750-1756. doi:S0005-2736(10)00185-9 [pii]

10.1016/j.bbamem.2010.06.001

Darden T, York D, Pedersen L (1993) Particle mesh Ewald: An N□log(N) method for Ewald sums in large systems. Journal Chemical Physics 98 (12):10089-10092

DeLano WL (2002) The PyMOL Molecular Graphics System.

Elmore DE, Dougherty DA (2001) Molecular dynamics simulations of wild-type and mutant forms of the Mycobacterium tuberculosis MscL channel. Biophys J 81 (3):1345-1359. doi:S0006-3495(01)75791-8 [pii]

10.1016/S0006-3495(01)75791-8

Elmore DE, Dougherty DA (2003) Investigating lipid composition effects on the mechanosensitive channel of large conductance (MscL) using molecular dynamics simulations. Biophys J 85 (3):1512-1524. doi:S0006-3495(03)74584-6 [pii]

10.1016/S0006-3495(03)74584-6

Hess B, Bekker H, Berendsen HJC, Fraaiji JGEM (1997) LINCS: A linear constraint solver for molecular simulations. Journal of Computational Chemistry 18 (12):1463-1472

Hurst AC, Petrov E, Kloda A, Nguyen T, Hool L, Martinac B (2008) MscS, the bacterial mechanosensitive channel of small conductance. Int J Biochem Cell Biol 40 (4):581-585. doi:S1357-2725(07)00093-3 [pii]

10.1016/j.biocel.2007.03.013

Kandt C, Ash WL, Tieleman DP (2007) Setting up and running molecular dynamics simulations of membrane proteins. Methods 41 (4):475-488. doi:S1046-2023(06)00187-3 [pii]

10.1016/j.ymeth.2006.08.006

Kloda A, Petrov E, Meyer GR, Nguyen T, Hurst AC, Hool L, Martinac B (2008) Mechanosensitive channel of large conductance. Int J Biochem Cell Biol 40 (2):164-169. doi:S1357-2725(07)00048-9 [pii]

10.1016/j.biocel.2007.02.003

Koprowski P, Grajkowski W, Isacoff EY, Kubalski A Genetic screen for potassium leaky small mechanosensitive channels (MscS) in Escherichia coli: recognition of cytoplasmic beta domain as a new gating element. J Biol Chem 286 (1):877-888. doi:M110.176131 [pii]

10.1074/jbc.M110.176131

Levina N, Totemeyer S, Stokes NR, Louis P, Jones MA, Booth IR (1999) Protection of Escherichia coli cells against extreme turgor by activation of MscS and MscL mechanosensitive channels: identification of genes required for MscS activity. EMBO J 18 (7):1730-1737. doi:10.1093/emboj/18.7.1730

Li C, Edwards MD, Jeong H, Roth J, Booth IR (2007) Identification of mutations that alter the gating of the Escherichia coli mechanosensitive channel protein, MscK. Mol Microbiol 64 (2):560-574. doi:MMI5672 [pii]

10.1111/j.1365-2958.2007.05672.x

Lindahl E, Hess B, van der Spoel D (2001) GROMACS 3.0: a package for molecular simulation and trajectory analysis. Journal of Molecular Modeling 7 (8):306-317

Machiyama H, Tatsumi H, Sokabe M (2009) Structural changes in the cytoplasmic domain of the mechanosensitive channel MscS during opening. Biophys J 97 (4):1048-1057. doi:S0006-3495(09)01025-X [pii]

10.1016/j.bpj.2009.05.021

Madhusudhan MS, Marti-Renom MA, Eswar N, John B, Pieper U, Karchin R, Shen M-Y, Sali A (2005) Comparative protein structure modeling. In: Walker JM (ed) The Proteomics Protocols Handbook. Humana Press, Totowa, NJ,

Martinac B (2005) Structural plasticity in MS channels. Nat Struct Mol Biol 12 (2):104-105. doi:nsmb0205-104 [pii]

10.1038/nsmb0205-104

Maurer JA, Dougherty DA (2001) A high-throughput screen for MscL channel activity and mutational phenotyping. Biochim Biophys Acta 1514 (2):165-169. doi:S000527360100390X [pii]

Maurer JA, Dougherty DA (2003) Generation and evaluation of a large mutational library from the Escherichia coli mechanosensitive channel of large conductance, MscL: implications for channel gating and evolutionary design. J Biol Chem 278 (23):21076-21082. doi:10.1074/jbc.M302892200

M302892200 [pii]

Miyamoto S, Kollman PA (1992) Settle: An analytical version of the SHAKE and RATTLE algorithm for rigid water models. Journal of Computational Chemistry 13 (8):952-962

Moe P, Blount P (2005) Assessment of potential stimuli for mechano-dependent gating of MscL: effects of pressure, tension, and lipid headgroups. Biochemistry 44 (36):12239-12244. doi:10.1021/bi0509649

Nomura T, Sokabe M, Yoshimura K (2006) Lipid-protein interaction of the MscS mechanosensitive channel examined by scanning mutagenesis. Biophys J 91 (8):2874-2881. doi:S0006-3495(06)72001-X [pii]

10.1529/biophysj.106.084541

Nomura T, Sokabe M, Yoshimura K (2008) Interaction between the cytoplasmic and transmembrane domains of the mechanosensitive channel MscS. Biophys J 94 (5):1638-1645. doi:S0006-3495(08)70602-7 [pii]

10.1529/biophysj.107.114785

Ou X, Blount P, Hoffman RJ, Kung C (1998) One face of a transmembrane helix is crucial in mechanosensitive channel gating. Proc Natl Acad Sci U S A 95 (19):11471-11475

Rand RP, Parsegian VA (1989) Hydration Forces between phospholipid bilayers. Biochim Biophys Acta 988:351-376

Rasmussen T, Edwards MD, Black SS, Rasmussen A, Miller S, Booth IR Tryptophan in the pore of the mechanosensitive channel MscS: assessment of pore conformations by fluorescence spectroscopy. J Biol Chem 285 (8):5377-5384. doi:M109.071472 [pii]

10.1074/jbc.M109.071472

Sali A, Blundell TL (1993) Comparative protein modelling by satisfaction of spatial restraints. J Mol Biol 234 (3):779-815. doi:S0022-2836(83)71626-8 [pii]

10.1006/jmbi.1993.1626

Schumann U, Edwards MD, Rasmussen T, Bartlett W, van West P, Booth IR YbdG in Escherichia coli is a threshold-setting mechanosensitive channel with MscM activity. Proc Natl Acad Sci U S A 107 (28):12664-12669. doi:1001405107 [pii]

10.1073/pnas.1001405107

Steinbacher S, Bass R, Strop P, Rees DC (2007) Structures of the prokaryotic mechanosensitive channels MscL and MscS. Mechanosensitive Ion Channels, Part A 58:1-24. doi:Doi 10.1016/S1063-5823(06)58001-9

Sukharev SI, Blount P, Martinac B, Blattner FR, Kung C (1994) A large-conductance mechanosensitive channel in E. coli encoded by mscL alone. Nature 368 (6468):265-268. doi:10.1038/368265a0

Sukharev SI, Martinac B, Arshavsky VY, Kung C (1993) Two types of mechanosensitive channels in the Escherichia coli cell envelope: solubilization and functional reconstitution. Biophys J 65 (1):177-183. doi:S0006-3495(93)81044-0 [pii]

10.1016/S0006-3495(93)81044-0

Vasquez V, Cortes DM, Furukawa H, Perozo E (2007) An optimized purification and reconstitution method for the MscS channel: strategies for spectroscopical analysis. Biochemistry 46 (23):6766-6773. doi:10.1021/bi700322k

Vasquez V, Sotomayor M, Cordero-Morales J, Schulten K, Perozo E (2008a) A structural mechanism for MscS gating in lipid bilayers. Science 321 (5893):1210-1214. doi:321/5893/1210 [pii]

10.1126/science.1159674

Vasquez V, Sotomayor M, Cortes DM, Roux B, Schulten K, Perozo E (2008b) Three-dimensional architecture of membrane-embedded MscS in the closed conformation. J Mol Biol 378 (1):55-70. doi:S0022-2836(07)01457-X [pii]
10.1016/j.jmb.2007.10.086

Wang W, Black SS, Edwards MD, Miller S, Morrison EL, Bartlett W, Dong C, Naismith JH, Booth IR (2008) The structure of an open form of an E. coli mechanosensitive channel at 3.45 A resolution. Science 321 (5893):1179-1183. doi:321/5893/1179 [pii]
10.1126/science.1159262

Wild J, Altman E, Yura T, Gross CA (1992) DnaK and DnaJ heat shock proteins participate in protein export in Escherichia coli. Genes Dev 6 (7):1165-1172

Yoshimura K, Batiza A, Schroeder M, Blount P, Kung C (1999) Hydrophilicity of a single residue within MscL correlates with increased channel mechanosensitivity. Biophys J 77 (4):1960-1972. doi:S0006-3495(99)77037-2 [pii]
10.1016/S0006-3495(99)77037-2

Yoshimura K, Sokabe M Mechanosensitivity of ion channels based on protein-lipid interactions. J R Soc Interface 7 Suppl 3:S307-320. doi:rsif.2010.0095.focus [pii]
10.1098/rsif.2010.0095.focus

# Chapter Seven

# The Mechanosensitive Channel of Small Conductance (MscS) Functions as a Jack-In-The-Box.

---

### *7.1 Introduction*

The mechanosensitive channel of small conductance (MscS) from *Escherichia coli* (*E. coli*) gates in direct response to membrane tension (Anishkin et al. 2008; Malcolm et al. ; Miller et al. 2003; Sukharev 2002; Vasquez et al. 2008a; Levina et al. 1999). Upon osmotic downshock, MscS is activated by tension in the membrane and opens to relieve the osmolyte imbalance created from the hypoosmotic shock (Edwards et al. 2008; Koprowski and Kubalski 2003). The response of MscS to mechanical tension has been characterized by a variety of techniques and molecular interactions that alter channel gating have been identified through mutagenesis (Malcolm et al. ; Nomura et al. 2008; Wang et al. 2008; Edwards et al. 2005).

*E. coli* MscS is an ideal system for studying tension transduction in mechanosensitive ion channels, since molecular level structures of MscS exist for the open, closed, and desensitized state of this channel (Anishkin et al. 2008; Malcolm et al. ; Wang et al. 2008; Vasquez et al. 2008b; Steinbacher et al. 2007; Bass et al. 2002). X-ray crystal structures of MscS have been solved for MscS in the desensitized and open states (Wang et al. 2008; Bass et al. 2002; Steinbacher et al. 2007). While there is not a closed state crystal structure of MscS, there are several closed state models that have been developed based on experimentally obtained constraints (Vasquez et al. 2008b; Anishkin et al. 2008; Malcolm et al.). These structures make it possible to interpret functional data and mutagenic analysis in a structural and molecular context.

Mutagenic analysis of MscS has provided a powerful tool for understanding channel function in the context of a wealth of structural data. This has lead to the identification of molecular interactions that play critical roles in gating transitions (Edwards et al. 2005; Koprowski et al. 2011; Belyy et al. ; Nomura et al. 2006; Vasquez et al. 2008a; Malcolm et al. ; Nomura et al. 2008). For example, the triad of residues, D62, R128, and R131, are predicted to work, in concert, in the transition from the closed state of the channel to the open state with the salt-bridge between D62 and R128 stabilizing the closed state and the salt-bridge between D62 and R132 stabilizing the open state (Nomura et al. 2008). Mutational analysis has also been used to understand the movement of the transmembrane domains away from the central gating axis during the transition from the closed state to the open state. In this case, interactions between I37 and L86, and A51and F68 are thought to stabilize this transition (Nomura et al. 2006). Furthermore, mutations

at the interface of third transmembrane domain and the ß-domain have been shown to inhibit wildtype MscS function (Koprowski et al. 2011). Hydrophobic substitutions at V65 and N167 promote the desensitization of MscS under tension; additionally these mutations lead to a leaky inactivated state.

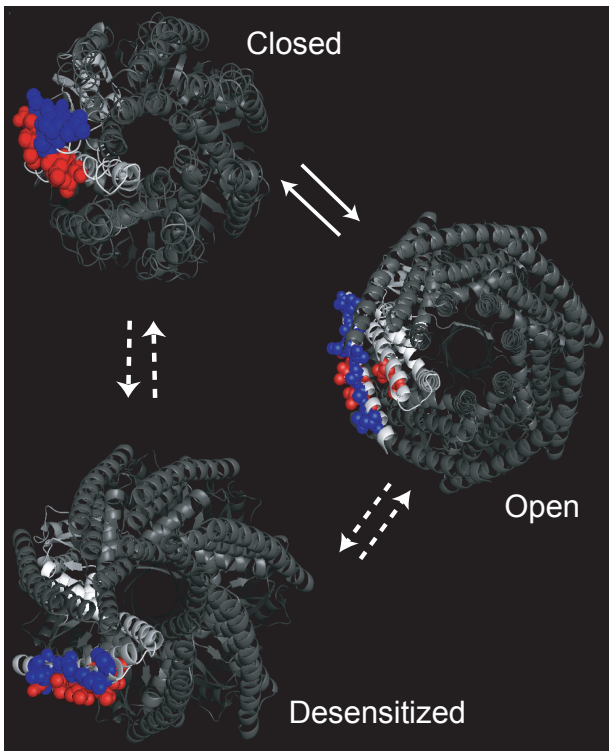


**Figure 7.1**: Lipid interacting amino acids in MscS. The positions of the previously identified closed state lipid interacting residues (red, L35, I39, L42, I43, N50, I78, L82) and the newly identified open state lipid interacting residues (blue, V29, V32, A36, V40, I43, I44, M47, A51, N53, L55, S58) on the closed (Malcolm et al.), open (2VV5, (Wang et al. 2008)), and desensitized (2OAU, (Bass et al. 2002; Steinbacher et al. 2007)) structures of MscS.

In the closed state of MscS, seven residues have been identified as critical for tension sensation (Malcolm et al.). These residues are postulated to form hydrophobic interactions with the lipid tail groups, thus stabilizing the closed state of the channel. The seven residues are clustered near the periplasmic face of the channel in the first and

second transmembrane domains. Mutations of these amino acids to alanine resulted in partial loss of function (LOF) phenotypes due to the reduction of hydrophobic interactions with the lipid bilayer. Moreover, while these residues interact with the lipid bilayer in the closed state of the channel, they are occluded from the lipid tails in both the open and desensitized states of the channel (Figure 7.1).

Since lipid interactions clearly play a critical role in the closed state of the channel, one might expect similar interactions with different residues to be important for open state stability. In this model of gating, a thermodynamic interplay between lipid-protein interactions in the open and closed states of MscS would at least partially account for channel function and the relative energetics of the open and closed states. An alternative model for channel gating is that lipid interactions are only important for closed state stability and do not impact the open state of the channel. In this model, the closed state of MscS would be stabilized by intrinsic bilayer tension, thus having important lipid interactions, and upon application of tension, relief of these interactions would give rise to channel opening. In other words, MscS would function as a spring-loaded channel that is compressed by intrinsic bilayer tension, like a Jack-In-The-Box. Application of extrinsic tension would then result in relief of the intrinsic lipid bilayer tension, causing the channel to spring open. To differentiate between these two gating models, we have identified the potential lipid interacting residues in the open state of the channel and made mutations that would alter any important hydrophobic interactions.

## *7.2 Methods*

### *7.2.1 Strains and Plasmids*

The *E. coli* strain, MJF465 (*MscS, MscL, MscK* null), was used for osmotic downshock assays and expression experiments (Levina et al. 1999; Wild et al. 1992). Mutational cloning was conducting using the Top10F` *E. coli* strain (Invitrogen, Carlsbad, CA). All mutants were created in the pB10b vector with a C-terminal six-His tag (Wild et al. 1992; Sukharev et al. 1994; Ou et al. 1998) and a LacUV5 promoter.

### *7.2.2 Site-Directed Mutagenesis*

Residues predicted to be involved in protein-lipid interactions were mutated to alanine or leucine using Megaprimer mutagenesis (Yoshimura et al. 1999). All mutations in MscS were made in the pB10b vector. For Megaprimer mutagenesis, forward and reverse primers located in the vector were used as the exterior primers and primers for mutagenesis were designed using Stratagene's QuikChange Primer design tool. Primer sequences are given in Table 7.1. Mutations were verified by enzymatic digestion and sequences confirmed using automated sequencing (Big Dye v3.1, Applied Biosystems, Carlsbad, CA).

| | Forward | Reverse |
|---|---|---|
| V29A | GCTGCTAAGTTATGCAGCAA ACATCGTGGCGGCACTCGCG GTC | GACCGCGAGTGCCGCCACG ATGTTTGCTGCATAACTTAG CAGC |

| | | |
|---|---|---|
| V29L | TGCTGCTAAGTTATGCATTA AACATCGTGGCGGCACTCGC GGTC | GACCGCGAGTGCCGCCACG ATGTTTAATGCATAACTTAG CAGCA |
| V32A | ATGCAGTAAACATCGCGGC GGCACTCGCGG | CCGCGAGTGCCGCCGCGATG TTTACTGCAT |
| V32L | AAGTTATGCAGTAAACATCT TGGCGGCACTCGCGG | CCGCGAGTGCCGCCAAGAT GTTTACTGCATAACTT |
| A36L | GTAAACATCGTGGCGGCACT CCTAATCATCATCGTTGGTT TGATT | AATCAAACCAACGATGATG ATTAGGAGTGCCGCCACGAT GTTTAC |
| V40A | ACTCGCGGTCATCATCGCTG GTTTGATTATCGCGC | GCGCGATAATCAAACCAGC GATGATGACCGCGAGT |
| V40L | CACTCGCGGTCATCATCCTT GGTTTGATTATCGCG | CGCGATAATCAAACCAAGG ATGATGACCGCGAGTG |
| I43L | GGTCATCATCGTTGGTTTGC TTATCGCGCGGATGATTTC | GAAATCATCCGCGCGATAA GCAAACCAACGATGATGAC C |
| I44L | CGGTCATCATCGTTGGTTTG ATTCTCGCGCGGATGA | TCATCCGCGCGAGAATCAAA CCAACGATGATGACCG |
| M47A | GGTTTGATTATCGCGCGGGC GATATCCAACGCGGTGAA | TTCACCGCGTTGGATATCGC CCGCGCGATAATCAAACC |
| M47L | GTTTGATTATCGCGCGGTTG ATATCCAACGCGGTG | CACCGCGTTGGATATCAACC GCGCGATAATCAAAC |
| A51L | CGCGCGGATGATATCCAACC TAGTGAATCGCCTGATGATC T | AGATCATCAGGCGATTCACT AGGTTGGATATCATCCGCGC G |
| N53A | TGATATCCAACGCGGTGGCT CGCCTGATGATCTCCC | GGGAGATCATCAGGCGAGC CACCGCGTTGGATATCA |
| N53L | GATGATATCCAACGCGGTGC TACGCCTGATGATCTCCCGT A | TACGGGAGATCATCAGGCGT AGCACCGCGTTGGATATCAT C |
| L55A | CCAACGCGGTGAATCGCGC GATGATCTCCCGTAAAATA | TATTTTACGGGAGATCATCG CGCGATTCACCGCGTTGG |
| S58A | GTGAATCGCCTGATGATCGC CCGTAAAATAGATG | CATCTATTTTACGGGCGATC ATCAGGCGATTCAC |
| S58L | GCGGTGAATCGCCTGATGAT CTTACGTAAAATAGATGCC | GGCATCTATTTTACGTAAGA TCATCAGGCGATTCACCGC |
| Outer cloning primers | CAATTTCACACAGGAAACA GGC | TACACGGAGGCATCAGTGA CCAAA |

**Table 7.1**: PCR primers for point mutations to alanine or leucine to MscS in the pB10b vector.

*7.2.3 Loss of Function Analysis*

Downshock experiments were conducted as previously described (Booth et al. 2007; Caldwell et al. ; Malcolm et al.), with the following modifications. A single colony was used to inoculate an overnight culture in Luria-Bertani Broth (LB Broth, BD Biosciences, San Jose, CA) supplemented with ampicillin (100μg/mL), the overnight culture was subsequently used to inoculate (1:20) a culture in LB Broth with 250 mM NaCl and ampicillin. The resulting culture was grown to an $OD_{600}$ of approximately 0.5 and induced with 0.1 mM isopropyl-beta-D-thiogalactopyranoside (IPTG) for 30 min. Following 30 min of induction, the culture was diluted (1:40) into 1:1 LB Broth and deionized water or isotonically into LB Broth with 250 mM NaCl, and allowed to recover for 30 min in a shaking incubator. After hypoosmotic downshock or isotonic dilution, bacterial cultures were serially diluted and plated on LB plates supplemented with ampicillin (100μg/mL). Plates containing between 25 and 250 colonies were used to determine the colony forming units (CFU) per millimeter of media. Percent recovery was defined as the CFU of the downshocked culture divided by the CFU of the isotonic dilution. Six trials for each mutation were conducted.

*7.2.4 Steady State Analysis*

A single colony was used to inoculate an overnight culture in LB Broth supplemented with ampicillin (100μg/mL), the overnight culture was subsequently used to inoculate (1:25) a culture in LB Broth with ampicillin. The resulting culture was grown to an $OD_{600}$ of approximately 0.5 and induced with 0.1 mM IPTG for 8 hours. After induction, the $OD_{600}$ was measured. Four trials for each mutation were carried out.

*7.2.5 Gain of Function Analysis*

Gain of function analysis was carried out as previously described (Maurer et al. 2000), with the following modifications. A single colony was used to inoculate an overnight culture in LB Broth supplemented with ampicillin (100µg/mL), the overnight culture was subsequently used to inoculate (1:75) a culture in LB Broth with ampicillin. The resulting culture was grown to an $OD_{600}$ between 0.5 and 0.8 and diluted to an $OD_{600}$ of 0.2±0.02. This culture was serially diluted into prewarmed LB with ampicillin, 5µL of the $10^{-2}$, $10^{-3}$, $10^{-4}$, $10^{-5}$, $10^{-6}$, and $10^{-7}$ dilutions were plated onto LB agar plates supplemented with ampicillin and LB agar plates supplemented with ampicillin and IPTG to a final concentration of 1mM. The resulting plates were scored after 20 hours of growth by giving a score of one for each concentration containing growth (maximum score of 6). Four trials for each mutation were carried out.

*7.2.6 Bacterial Expression Analysis*

To verify bacterial expression of the MscS mutants, cultures were grown as described above for the loss of function analysis and pelleted for 15 min at 16,000 x g after 30 min of induction. The supernatant was removed and the pellets resuspended in a buffer containing 50 mM Tris, 75 mM NaCl, 0.1% Fos-Choline-14 (Affymetrix, Cleveland, OH), and protease complete inhibitor (Roche, Basel, Switzerland) at 10µL of buffer per 10 mg of bacteria. Samples were detergent-solubilized using a probe sonicator for three cycles of 15 s on and 45 s off. After lysis and solubilization, insoluble material was removed by pelleting for 30 min at 16,000 x g. The supernatant was combined with

sodium dodecyl sulfate polyacrylamide-gel electrophoresis (SDS-PAGE) loading dye, and the samples were boiled for 5 min. Samples were then run on a 12.5% poly-acrylamide gel using a TRIS-glycine running buffer. Equivalent volumes of the supernatant were loaded to allow for comparisons of protein expression levels. Proteins were transferred to a 0.2 μm nitrocellulose membrane using a semidry transfer system and Cashini's Buffer (0.1 M Tris, 0.02% SDS, 0.2 M glycine, 5% methanol). The protein expression of the C-terminally 6-His-tagged MscS mutants was probed using a primary mouse-anti-His monoclonal IgG (Covance, Emeryville, CA) and a secondary HRP-conjugated goat anti-mouse antibody (Jackson ImunoResearch Laboratories, West Grove, PA).

## *7.3 Results and Discussion*

### *7.3.1 Identification of Lipid Interactions*

To determine the residues that interact with the lipids in the open state of MscS, the open state crystal structure of MscS (2VV5)(Wang et al. 2008) was embedded into a palmitoyl oleoyl phosphatidylethanolamine (POPE) lipid bilayer as previously described (Figure 7.2)(Malcolm et al.). Residues predicted to have significant lipid interactions with the lipid bilayer were identified by assessing the ability of an individual side chain to interact with the lipid tail groups. Based on this analysis, the amino acids predicted to interact with the bilayer are V29, V32, A36, V40, I43, I44, M47, A51, N53, L55, and S58 (Figure 7.1).

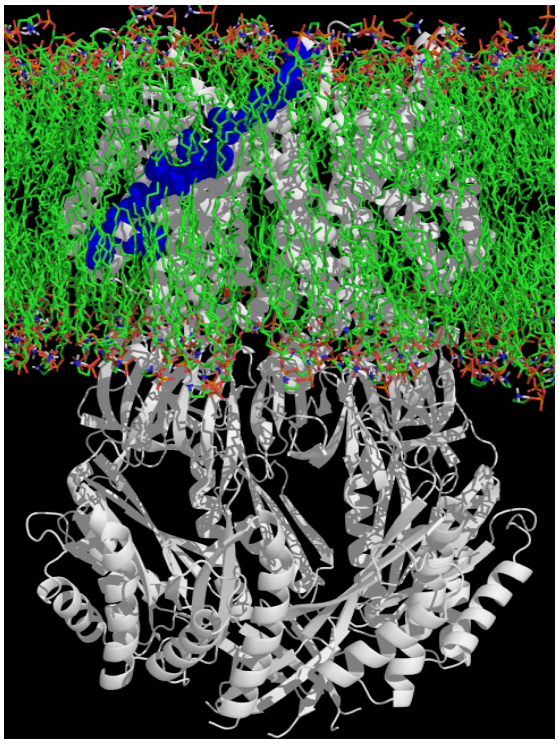

**Figure 7.2**: Open state lipid interactions. The open state crystal structure of MscS is shown embedded into a POPE membrane with the predicted lipid interacting residues (V29, V32, A36, V40, I43, I44, M47, A51, N53, L55, and S58) highlighted in blue (Wang et al. 2008).

These residues span the entire outer face of the first transmembrane domain from the periplasm to the cytoplasm. This distribution of interactions sharply contrasts with the lipid interactions in the closed state of the channel, where the lipid-interacting residues were found clustered toward the periplasmic face of the channel in both the first and second transmembrane domains (Malcolm et al.). In the open state of the channel, all of the residues in the second transmembrane domain are involved in protein-protein interactions and are excluded from the lipid bilayer.

While the majority of the residues identified as interacting with the lipid bilayer in the closed state of the channel were large hydrophobic amino acids (leucine or isoleucine), the putative lipid interacting residues in the open state are mainly a mixture of large hydrophobic residues (leucine, isoleucine, and methionine) and small hydrophobic amino acids (valine and alanine). This mixture of small and large hydrophobic amino acids fits a gating model in which the thermodynamics of the open and closed states of MscS are balanced by interactions with the lipid bilayer. As required by such a model, the protein-lipid interactions would be stronger in the closed state than in the open state. This is a result of the lipid interactions in the closed state of the channel only involving large hydrophobic amino acids, while the lipid interactions in the open state of the channel involve a mixture of large and small hydrophobic amino acids. While the closed state would be lower in energy than the open state, the presence of some large hydrophobic lipid-interacting amino acids in the open state would provide the needed stability for the open state of the channel.

### *7.3.2 Analysis of Lipid Interactions*

To determine the role of the putative open state lipid interacting residues on channel function, each residue was mutated to leucine and alanine (unless the residues were leucine or alanine in the wildtype channel). Based on previous mutagenic analysis, we anticipate that if lipid interactions are important for stabilizing the open state of the channel, then we should observe altered phenotypes for these mutations. Since one proposed gating mechanism involves a careful balance of hydrophobic lipid interactions, it is expected that increasing the hydrophobicity of the lipid exposed helix in the open

state would stabilize the open state of the channel and decreasing the hydrophobicity of the lipid exposed helix in the open state would destabilize the open state of the channel. Therefore, if lipid interactions are important in the open state, mutation of a small hydrophobic residue to leucine would result in open state stabilization and a gain of function phenotype. Conversely, mutation of a large hydrophobic residue to alanine would result in open state destabilization and a loss of function phenotype. However, if lipid interactions are not important in the open state of the channel and instead channel gating is driven by a reduction in intrinsic bilayer tension, then mutation of putative open state lipid interacting residues should give channels that are phenotypically wildtype.

To determine the effect of the mutations on the gating ability of MscS, the mutants were analyzed using *in vivo* functional assays. Osmotic downshock experiments were used to determine the ability of the MscS mutants to gate in response to changes in mechanical tension in the membrane. Bacterial growth assays were used to determine the viability of the MscS mutants and thus identify GOF phenotypes.

Osmotic downshock analysis of the mutant channels was used to assay for loss of function phenotypes. For each mutation, six trials were conducted and the percent recovery values were compared using a Student's T-test (Figure 7.3A). Most mutations were statistically similar to wildtype MscS with only I43A displaying a partial LOF phenotype. This is not surprising as I43 also interacts with the lipid bilayer in the closed state of the channel and has previously been shown to display a partial loss of function phenotype (Malcolm et al.). Mutants were defined as having a partial LOF phenotype if

they were statistically different from wildtype MscS at >95%, as determined using a Student's T test. Additionally, all MscS mutants expressed at levels comparable to wildtype MscS, indicating that these channels are expressed to the membrane in similar levels (Figure 7.3B).

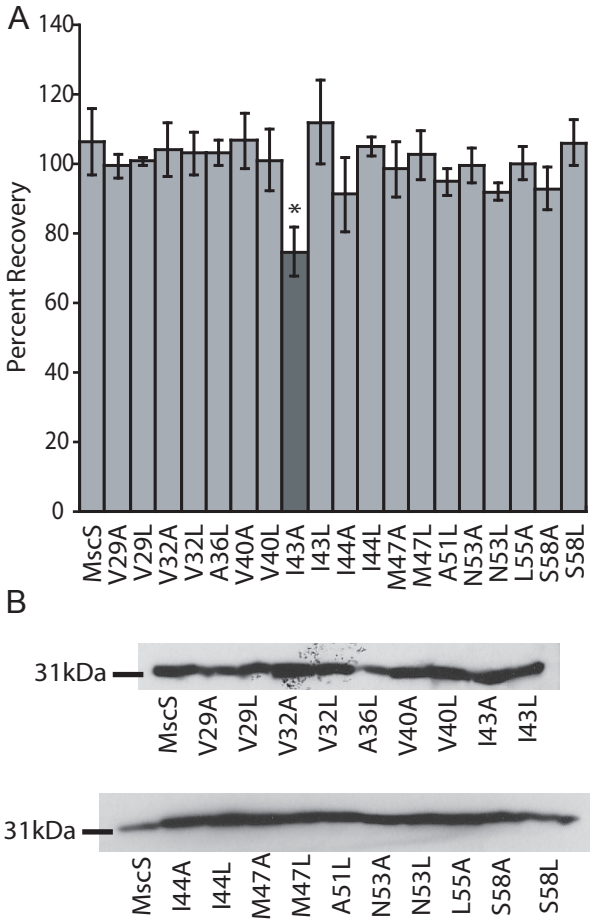


**Figure 7.3**: Loss of function analysis of MscS mutations. A) Results from osmotic downshock analysis of wildtype MscS and mutations of lipid interacting residues to alanine or leucine. Error bars represent the standard error of the mean for 6 independent trials. The dark gray bar indicates the construct that is statistically different from wild-type MscS as determined using a Student's T-test (* = $p < 0.05$). B) Western blot analysis of protein expression levels for wildtype MscS and mutants under expression conditions identical to those used for the osmotic downshock assay.

To assay MscS mutations for GOF phenotypes, two different growth based assays were applied to each mutation; steady state optical density analysis (Malcolm et al. ; Iscla et al. 2008; Levin and Blount 2004) and a plate based gain of function assay (Maurer et al. 2000). All MscS mutants were not statistically different from wildtype MscS in the steady state optical density measurements (Figure 7.4). To further confirm that these mutations were wildtype, a plate based gain of function assay was conducted comparing bacteria grown on normal LB plates with bacteria grown on plates supplemented with IPTG. Serial dilutions of bacterial cultures were plated onto the different growth media and plates were scored by counting the number of dilutions that showed bacterial growth. The ratio of the induced and uninduced scores was determined for wildtype MscS and each mutant (Figure 7.4). All of the mutations were found to be indistinguishable from wildtype MscS using a Student's T-test.

Taken together, the results of the LOF analysis and the GOF analysis indicate that all of the putative open state lipid interacting mutations are wildtype. This suggests that open state lipid interactions are not critical for channel gating and rules out a gating mechanism than involves a thermodynamic balance of lipid interactions. Instead, gating in MscS must be driven by relief of intrinsic lipid bilayer tension, which does not require significant lipid interactions in the open state of the channel.

| | LB+Ap $10^{-2}$ $10^{-3}$ $10^{-4}$ $10^{-5}$ $10^{-6}$ $10^{-7}$ | Un-induced Score | LB+IPTG+Ap $10^{-2}$ $10^{-3}$ $10^{-4}$ $10^{-5}$ $10^{-6}$ $10^{-7}$ | Induced Score | Ratio | Steady State at $OD_{600}$ |
|---|---|---|---|---|---|---|
| MscS |  | 4.0±0.8 |  | 3.5±0.6 | 0.9±0.2 | 1.74±0.02 |
| V29A |  | 4.0±0.0 |  | 4.5±1.0 | 1.1±0.3 | 1.69±0.05 |
| V29L |  | 4.25±0.5 |  | 4.0±0.0 | 0.9±0.1 | 1.69±0.02 |
| V32A |  | 4.25±0.5 |  | 3.75±1.0 | 0.9±0.3 | 1.67±0.02 |
| V32L |  | 4.25±0.5 |  | 4.0±0.0 | 0.9±0.1 | 1.69±0.01 |
| A36L |  | 4.0±0.0 |  | 3.75±1.0 | 0.9±0.2 | 1.71±0.03 |
| V40A |  | 3.75±1.0 |  | 4.0±0.8 | 1.1±0.4 | 1.67±0.02 |
| V40L |  | 4.25±0.5 |  | 3.75±0.5 | 0.9±0.2 | 1.66±0.01 |
| I43A |  | 4.25±0.5 |  | 3.75±1.0 | 0.9±0.3 | 1.65±0.03 |
| I43L |  | 3.75±1.0 |  | 4.0±0.0 | 1.1±0.3 | 1.69±0.02 |
| I44A |  | 3.75±0.5 |  | 4.25±0.5 | 1.1±0.2 | 1.66±0.05 |
| I44L |  | 4.5±0.6 |  | 3.5±0.6 | 0.8±0.2 | 1.69±0.05 |
| M47A |  | 3.5±0.6 |  | 4.25±0.5 | 1.2±0.3 | 1.68±0.01 |
| M47L |  | 4.25±0.5 |  | 3.75±0.5 | 0.9±0.2 | 1.65±0.02 |
| A51L |  | 3.5±0.6 |  | 3.75±0.5 | 1.1±0.2 | 1.63±0.03 |
| N53A |  | 3.75±0.5 |  | 4.5±0.6 | 1.2±0.2 | 1.63±0.04 |
| N53L |  | 4.25±0.5 |  | 4.0±0.0 | 0.9±0.1 | 1.66±0.03 |
| L55A |  | 4.25±0.5 |  | 4.25±0.5 | 1.1±02 | 1.66±0.02 |
| S58A |  | 4.0±0.0 |  | 4.25±0.5 | 1.1±0.1 | 1.66±0.04 |
| S58L |  | 4.0±0.8 |  | 3.75±0.5 | 0.9±0.2 | 1.65±0.07 |

**Figure 7.4**: Gain of function analysis of MscS mutations. Representative bacteria growth on LB medium with and without IPTG is shown for all mutations. Plates were scored by counting the number of dilutions with bacterial growth. The ratio of induced to uninduced was determined by dividing the induced score by the uninduced score. The steady state optical density was measured at 600 nm. In all cases, error represents the standard deviation for four independent trials.

### *7.3.3 The Jack-In-The-Box Model of MscS Gating*

Intrinsic tension from the lipid bilayer stabilizes the closed state of MscS by pushing in on the channel. As a result, under normal conditions the closed state of MscS lies energetically below the open state of the channel. Upon application of extrinsic tension to the membrane, the intrinsic lipid bilayer tension is relieved resulting in reversal of the

energetics of the open and closed states (Figure 7.5A). The relief of intrinsic tension upon application of extrinsic tension is a result of the force vectors, relative to the channel, being in opposite direction for intrinsic and extrinsic tension. This leads to a Jack-In-The-Box type gating mechanism for MscS, where the intrinsic lipid bilayer tension serves as the box that compresses the channel. Upon relief of this strain, the channel springs open allowing ions to pass (Figure 7.5B).

This is supported by the observed structural differences in the open state and closed states of MscS. In the closed state of the channel, the transmembrane helices are tightly packed into a small footprint. However, upon transition to the open state, the helices expand and become further apart. Figure 7.5B shows the changes in helical packing that occur upon gating with the relative positions of the transmembrane helices derived from the open state crystal structure and our closed state model (Malcolm et al. ; Wang et al. 2008). The expanded structure observed in the open state crystal structure would only be stable in the absence of significant intrinsic lipid tension, since intrinsic lipid tension would result in compression of the observed structure. Moreover, transient stability of the open state structure is required for channel gating, which supports the hypothesis that extrinsic tension cancels intrinsic bilayer tension allowing the structure to expand and gate.

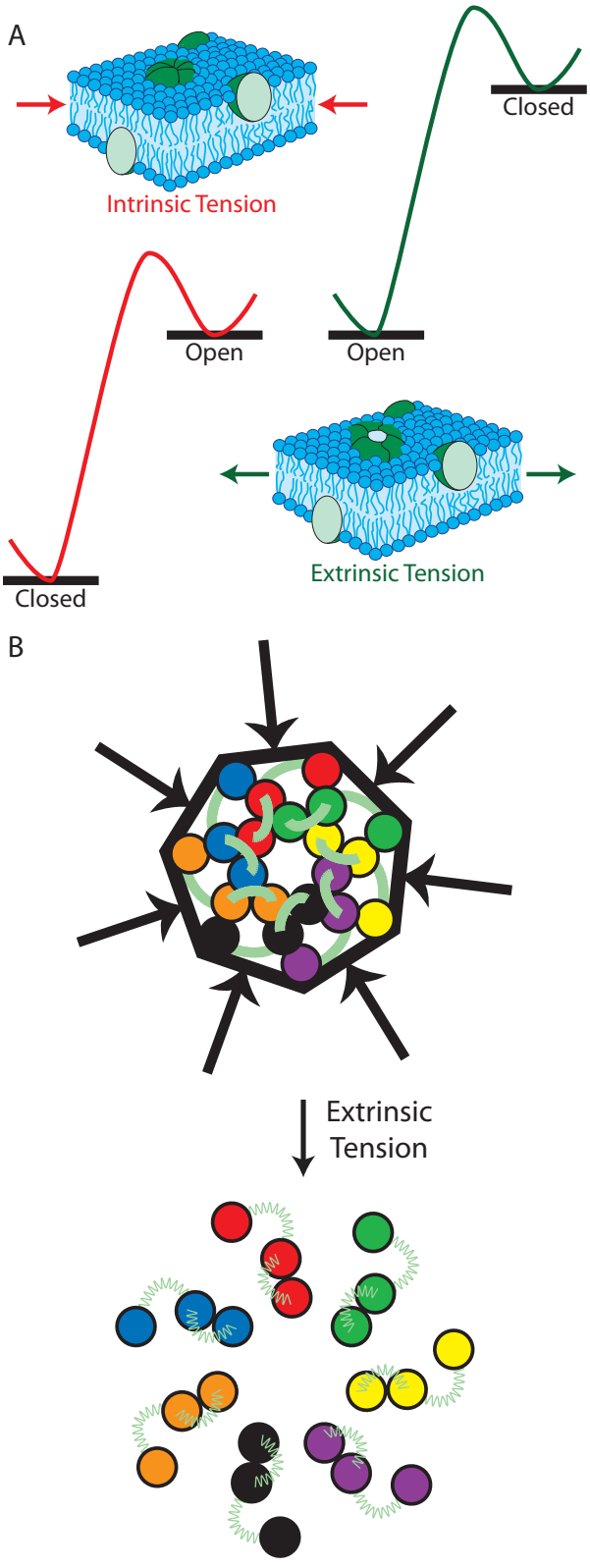


**Figure 7.5**: The Jack-In-A-Box model of MscS gating. A) Differences in the thermodynamic gating profile for MscS in the presence of intrinsic and extrinsic tension. B) Schematic representation of the Jack-In-A-Box model of MscS gating with helix positions based on the experimentally derived closed and open state structures of MscS (Malcolm et al. ; Wang et al. 2008).

Additional support for the Jack-In-The-Box gating mechanism comes from structural studies of MscS. While crystal structures have been obtained for both the open and desensitized states of the channel, a closed state crystal structure has so far been elusive. This may be because removal of MscS from the lipid bilayer into detergent micelles relieves the intrinsic lipid pressure resulting in stabilization of either the open state or desensitized state of the channel. The crystal structure of wildtype MscS was obtained in the desensitized state of the channel suggesting that the channel entered into a desensitized state upon detergent extraction. This is not surprising, since detergent micelles have lower levels of intrinsic tension compared to lipid bilayers. Moreover, the A106V mutation used to obtain the open state crystal structure is LOF not GOF (Wang et al. 2008), which seems counterintuitive. However, it is possible that the mutation reduced the probability of the channel to enter the desensitized state upon insertion of the channel into detergent micelles. If this is the case, the "Jack-In-The-Box" gating model would predict that this mutation should give rise to an open state structure, which is the observed structure for this mutant.

### *7.4 Conclusions*

Our analysis indicates that open-state lipid interactions are not critical for MscS channel gating. Mutations of amino acid residues identified as having putative lipid interactions, based on the open state crystal structure, to residues that would enhance or reduce these interactions gave phenotypically wildtype channels. This has lead us to propose a "Jack-In-The-Box" model of gating for MscS, in which intrinsic lipid bilayer tension holds the channel in the closed state. Upon relief of the intrinsic bilayer tension by application of

opposing extrinsic tension, MscS springs into the open state.

### *7.5 References*

Anishkin A, Akitake B, Sukharev S (2008) Characterization of the resting MscS: modeling and analysis of the closed bacterial mechanosensitive channel of small conductance. Biophys J 94 (4):1252-1266. doi:S0006-3495(08)70643-X [pii]
10.1529/biophysj.107.110171

Bass RB, Strop P, Barclay M, Rees DC (2002) Crystal structure of Escherichia coli MscS, a voltage-modulated and mechanosensitive channel. Science 298 (5598):1582-1587. doi:10.1126/science.1077945
298/5598/1582 [pii]

Belyy V, Anishkin A, Kamaraju K, Liu N, Sukharev S The tension-transmitting 'clutch' in the mechanosensitive channel MscS. Nat Struct Mol Biol 17 (4):451-458. doi:nsmb.1775 [pii]
10.1038/nsmb.1775

Booth IR, Edwards MD, Black S, Schumann U, Bartlett W, Rasmussen T, Rasmussen A, Miller S (2007) Physiological analysis of bacterial mechanosensitive channels. Methods Enzymol 428:47-61. doi:S0076-6879(07)28003-6 [pii]
10.1016/S0076-6879(07)28003-6

Caldwell DB, Malcolm HR, Elmore DE, Maurer JA Identification and experimental verification of a novel family of bacterial cyclic nucleotide-gated (bCNG) ion channels. Biochim Biophys Acta 1798 (9):1750-1756. doi:S0005-2736(10)00185-9 [pii]

10.1016/j.bbamem.2010.06.001

Edwards MD, Bartlett W, Booth IR (2008) Pore mutations of the Escherichia coli MscS channel affect desensitization but not ionic preference. Biophys J 94 (8):3003-3013. doi:S0006-3495(08)70458-2 [pii]

10.1529/biophysj.107.123448

Edwards MD, Li Y, Kim S, Miller S, Bartlett W, Black S, Dennison S, Iscla I, Blount P, Bowie JU, Booth IR (2005) Pivotal role of the glycine-rich TM3 helix in gating the MscS mechanosensitive channel. Nat Struct Mol Biol 12 (2):113-119. doi:nsmb895 [pii]

10.1038/nsmb895

Iscla I, Wray R, Blount P (2008) On the structure of the N-terminal domain of the MscL channel: helical bundle or membrane interface. Biophys J 95 (5):2283-2291. doi:10.1529/biophysj.107.127423

Koprowski P, Grajkowski W, Isacoff EY, Kubalski A (2011) Genetic screen for potassium leaky small mechanosensitive channels (MscS) in Escherichia coli: recognition of cytoplasmic beta domain as a new gating element. J Biol Chem 286 (1):877-888. doi:10.1074/jbc.M110.176131

Koprowski P, Kubalski A (2003) C termini of the Escherichia coli mechanosensitive ion channel (MscS) move apart upon the channel opening. J Biol Chem 278 (13):11237-11245. doi:10.1074/jbc.M212073200

M212073200 [pii]

Levin G, Blount P (2004) Cysteine scanning of MscL transmembrane domains reveals residues critical for mechanosensitive channel gating. Biophys J 86 (5):2862-2870. doi:10.1016/S0006-3495(04)74338-6

Levina N, Totemeyer S, Stokes NR, Louis P, Jones MA, Booth IR (1999) Protection of Escherichia coli cells against extreme turgor by activation of MscS and MscL mechanosensitive channels: identification of genes required for MscS activity. EMBO J 18 (7):1730-1737. doi:10.1093/emboj/18.7.1730

Malcolm HR, Heo YY, Elmore DE, Maurer JA Defining the role of the tension sensor in the mechanosensitive channel of small conductance. Biophys J 101 (2):345-352. doi:S0006-3495(11)00660-6 [pii]

10.1016/j.bpj.2011.05.058

Maurer JA, Elmore DE, Lester HA, Dougherty DA (2000) Comparing and contrasting Escherichia coli and Mycobacterium tuberculosis mechanosensitive channels (MscL). New gain of function mutations in the loop region. J Biol Chem 275 (29):22238-22244. doi:10.1074/jbc.M003056200

M003056200 [pii]

Miller S, Bartlett W, Chandrasekaran S, Simpson S, Edwards M, Booth IR (2003) Domain organization of the MscS mechanosensitive channel of Escherichia coli. EMBO J 22 (1):36-46. doi:10.1093/emboj/cdg011

Nomura T, Sokabe M, Yoshimura K (2006) Lipid-protein interaction of the MscS mechanosensitive channel examined by scanning mutagenesis. Biophys J 91 (8):2874-2881. doi:S0006-3495(06)72001-X [pii]

10.1529/biophysj.106.084541

Nomura T, Sokabe M, Yoshimura K (2008) Interaction between the cytoplasmic and transmembrane domains of the mechanosensitive channel MscS. Biophys J 94 (5):1638-1645. doi:S0006-3495(08)70602-7 [pii]

10.1529/biophysj.107.114785

Ou X, Blount P, Hoffman RJ, Kung C (1998) One face of a transmembrane helix is crucial in mechanosensitive channel gating. Proc Natl Acad Sci U S A 95 (19):11471-11475

Steinbacher S, Bass R, Strop P, Rees DC (2007) Structures of the prokaryotic mechanosensitive channels MscL and MscS. Mechanosensitive Ion Channels, Part A 58:1-24. doi:Doi 10.1016/S1063-5823(06)58001-9

Sukharev S (2002) Purification of the small mechanosensitive channel of Escherichia coli (MscS): the subunit structure, conduction, and gating characteristics in liposomes. Biophys J 83 (1):290-298. doi:S0006-3495(02)75169-2 [pii]

10.1016/S0006-3495(02)75169-2

Sukharev SI, Blount P, Martinac B, Blattner FR, Kung C (1994) A large-conductance mechanosensitive channel in E. coli encoded by mscL alone. Nature 368 (6468):265-268. doi:10.1038/368265a0

Vasquez V, Sotomayor M, Cordero-Morales J, Schulten K, Perozo E (2008a) A structural mechanism for MscS gating in lipid bilayers. Science 321 (5893):1210-1214. doi:321/5893/1210 [pii]

10.1126/science.1159674

Vasquez V, Sotomayor M, Cortes DM, Roux B, Schulten K, Perozo E (2008b) Three-dimensional architecture of membrane-embedded MscS in the closed conformation. J Mol Biol 378 (1):55-70. doi:S0022-2836(07)01457-X [pii]
10.1016/j.jmb.2007.10.086

Wang W, Black SS, Edwards MD, Miller S, Morrison EL, Bartlett W, Dong C, Naismith JH, Booth IR (2008) The structure of an open form of an E. coli mechanosensitive channel at 3.45 A resolution. Science 321 (5893):1179-1183. doi:321/5893/1179 [pii]
10.1126/science.1159262

Wild J, Altman E, Yura T, Gross CA (1992) DnaK and DnaJ heat shock proteins participate in protein export in Escherichia coli. Genes Dev 6 (7):1165-1172

Yoshimura K, Batiza A, Schroeder M, Blount P, Kung C (1999) Hydrophilicity of a single residue within MscL correlates with increased channel mechanosensitivity. Biophys J 77 (4):1960-1972. doi:S0006-3495(99)77037-2 [pii]
10.1016/S0006-3495(99)77037-2

# Chapter Eight

# Conclusions and Future Directions

---

### *8.1 bCNG Family Conclusions*

#### *8.1.1 bCNG Channel Family*

The bacterial cyclic nucleotide gated (bCNG) channel family is a member of the greater mechanosensitive channel of small conductance (MscS) superfamily (Caldwell et al. 2010). Sequence analysis shows that bCNG channels are composed of three domains: a channel domain highly homologous to MscS, an non-conserved linker domain, and a cyclic nucleotide binding domain homologous to known cyclic adenosine monophosphate (cAMP) binding domains. Three members of the bCNG channel family have been shown to gate in response to cAMP alone in planar lipid bilayer experiments. These channels represent the first ligand gated ion channels to be identified in bacteria. Additionally, Te-bCNGb shows increased channel gating upon increase cAMP concentration. The increased channel gating in response to increased cAMP concentration is indicative of ligand gated channels.

### *8.1.2 bCNG Mechanosensation*

The bCNG channel family is highly homologous to MscS in all regions that have been used to identify mechanosensitive channels: these regions are the pore lining helix and the upper vestibule domain (Malcolm et al. 2012). The high homology between bCNG channels and MscS suggests that all bCNG channels should be able to gate in response the mechanical tension in a manner similar to MscS. However, twelve bCNG channels were shown to be unable to gate in response to mechanical tension in osmotic downshock assays. Limited mechanosensation was observed upon the removal of the cAMP binding domain. This suggests that bCNG channels have evolved away from MscS with the appendage of the C-terminal cAMP binding domain, blocking the rearrangement required for channel gating.

### *8.1.3 Ss-bCNGa: a Unique Mechanosensitive bCNG Channel*

The channel domain of Ss-bCNGa is highly homologous to the entire channel domain of MscS and Ss-bCNGa has significant identity to MscS in the regions thought to be important for mechanosensation. We have demonstrated that Ss-bCNGa gates in response to mechanical tension and shows increased recovery over time. The observed increase in recovery during osmotic downshock experiments is accompanied by an increase in protein concentration. Ss-bCNGa rescues at a level greater than truncated bCNG channels, but still rescues at a level lower than MscS. Analysis of the amino acids using the Grantham index (Grantham 1974) in the first and second transmembrane domains shows that Ss-bCNGa and MscS are highly similar. To determine the difference in the

ability of MscS and Ss-bCNGa to gate in response to mechanical tension, a molecular dynamics simulation was used to identify the lipid interactions in Ss-bCNGa. Twelve residues were predicted to interact with the lipid tails and there was little conservation between these residues and the residues that we had previously identified as important for channel function in the closed state of MscS. The difference in these residues most likely contributes to the different responses of MscS and Ss-bCNGa to mechanical tension.

### *8.1.4 bCNG Heteromultimers*

Eleven bacterial genomes encode for two unique bCNG homologues, suggesting that heteromultimeric bCNG channels could be possible *in vivo*. To determine if bCNG channels are able to form heteromultimers *in vitro*, two bCNG channels were heterologously co-expressed in *E. coli*. Upon expression, two bCNG channels, from the same bacterial strain, form heteromultimers. To determine if heteromultimers are possible *in vivo*, RT-PCR was utilized to verify that mRNA from both bCNG channels was present at the same time. Ss-bCNGa and Ss-bCNGb are both present at the same time at similar levels when compared to RpoB, the ß-subunit of RNA polymerase. In *Acaryochloris marina* MBIC11017, the mRNA for Am-bCNGa and Am-bCNGb is found at equivalent levels. Additionally, the mRNA for bCNG homologues in *Rhizobium leguminosarum bv. viciae* 3841, *Cyanothece sp. ATCC* 51142, and *Burkholderia xenovorans* LB400 were present at similar levels. These results indicate that bacterial heteromultimeric channels are possible *in vivo*.

### *8.2 bCNG Future Directions*

#### *8.2.1 Electrophysiological Studies of bCNG Channels*

The bCNG channel family is composed of channels with two different sensory domains, a mechanosensitive domain and a ligand binding domain. To adequately study these two features in concert, patch clamp electrophysiology could be utilized (Hurst et al. 2008; Corry and Martinac 2008). Using patch clamp, the effect that cAMP has on tension sensation could be determined, as well as the converse: the effect of tension on ligand binding. Specifically, Ss-bCNGa would be an interesting target for patch clamp electrophysiology. In osmotic downshock experiments, Ss-bCNGa shows limited mechanosensation that increases over time in accordance with increased protein expression (Chapter 4). This ability to sense tension could be explored in patch clamp where the tension can be tightly regulated. Additionally, this regulation of tension would allow for the determination of the $P_{50}$ of Ss-bCNGa, the minimum pressure when fifty percent of the channels open. In patch clamp, tension below the gating threshold could be applied in the presence of varying cAMP concentrations to see if the two stimuli work cooperatively.

#### *8.2.2 In vivo Analysis of bCNG Comultimers*

We have shown that the genes for bCNG homologues are expressed at the same time *in vivo* indicating that heteromultimers are likely. In mammalian channels the homomultimers often function quite differently than the heteromultimer (Wu and Lukas 2011), it would be interesting to see if this trend held up in the bCNG channel family. Ss-bCNGa and Ss-bCNGb show different phenotypes when subjected to osmotic

downshock. Ss-bCNGa shows limited rescue of bacterial cells, while only baseline survival is observed in Ss-bCNGb. If the two channels were heterologously expressed and the resulting cells were subjected to osmotic downshock, these cells could have a greater survival rate.

These experiments would need to be conducted in the MJF465 cell line, null MscS, MscL, and MscK (Levina et al. 1999; Wild et al. 1992). To conduct heterologous osmotic downshock experiments, at least one gene of each pair would need to be subcloned into a vector with a different antibiotic cassette. Most likely the easiest method to accomplish this would be to switch the antibiotic cassette of the pB10b vector for another antibiotic cassette that is not being utilized in the cell strain, such as streptomycin or tetracyclin. This would allow for a two vector system analogous to the system used for the heterologous expression of bCNG channels. In addition to osmotic downshock experiments, these comultimers could be studied in gain of function plate assays to determine their ability to grow when the comultimers are expressed. Additionally, the different phenotypes of bCNG homomultimers and heteromultimers could be explored in both patch clamp and planar lipid bilayer electrophysiology. It would be interesting to ascertain changes in the $IC_{50}$ and $P_{50}$ for bCNG heteromultimers.

### *8.2.3 Studying bCNG Heteromultimers with MscS*

It would also be interesting to study the ability of bCNG channels from genomes with only one bCNG homologue to form heteromultimers with Ec-MscS. This would allow for a study of heteromultimers of differing numbers of transmembrane domains. These

channels would provide an interesting target for osmotic downshock assays, gain of function assays, and patch clamp experiments. With the differing numbers of transmembrane domains it would not be surprising if these heteromultimers created severe loss of function phenotypes. These channels could be pseudo-locked into a closed conformation, especially if the bCNG channel had greater than 3 transmembrane domains as the lipids could be occluded from the residues essential for tension sensation. Additionally, some genomes encode for a single bCNG homologue and a MscS homologue. If a unique phenotype was observed with Ec-MscS, it would not be surprising if the bCNG and MscS from a single bacterium formed a functional channel.

### *8.2.4 Determining the in vivo copy number*

To determine if bCNG channels form heteromultimers *in vivo*, the exact protein copy number of the two channels needs to be calculated. The mRNA levels are similar when compared to an internal standard of RpoB (Chapter 5). To quantify the number of copies of a particular bCNG channel, monoclonal antibodies for each bCNG channel could be ratioed to one another. This would require a region in each channel to be unique; with the high homology that bCNG channels share this could be problematic. A full-membrane prep of the native bacteria would be run on an SDS-PAGE and the amount of channel protein could be determined based on the antibody ratios.

### *8.2.5 Determining the number of ligand binding sites*

A bCNG channel is thought to function as both homoheptamers and heteroheptamers, one of the questions still needing an answer is how many binding sites are active in the

protein complex, all seven or a select few. To determine the number of binding sites, equilibrium binding assays would be utilized (Nimigean and Pagel 2007). Using [$^3$H]cAMP, the number of molecules bound to the channel could be determined and that number is relative the number of binding sites in a single channel. To determine the number of binding sites, intact channel protein would be immobilized onto Ni-affinity beads using a N-terminal His-tag. [$^3$H]cAMP is added to the bound protein and allowed to equilibrate for an hour. Bound radioactive ligand would be competed off with increasing concentrations of cAMP. The displaced radioactive ligand in the supernatant would be measured with a scintillation counter. To determine the number of binding sites, the free hot ligand is plotted as a function of the cold cAMP concentration. This plot can be used to calculate the Hill coefficient giving the number of binding sites (Hill and Flack 1910; Weiss 1997).

### *8.3 MscS Lipid Interactions in the Open and Closed States Conclusion*

*E. coli* MscS gates in response to mechanical tension in the cell membrane (Edwards et al. 2004; Malcolm et al. 2011). To further understand the essential interactions in MscS during gating in response to mechanical tension, a molecular dynamic simulation was utilized to identify the lipid interactions in the closed state. Any residue that was predicted to interact with the lipids was mutated to alanine to reduce but not eliminate the hydrophobic interactions. These mutants were subjected to osmotic downshock experiments to determine if they created a phenotypic difference.

Seven residues, L35, I39, L43, I43, N50, I78, and L82, were identified to have a partial loss of function phenotype upon mutation to alanine. These residues are clustered near the periplasmic face of MscS in the first and second transmembrane domains. This cluster of residues is clearly important for tension sensation. Analysis of these residues in the different states of MscS showed that they are exposed to the lipids in the closed state and that these residues are occluded from the lipids in both the open state and the desensitized (or inactivated) state of the channel. This movement of the tension sensor implied that new lipid contacts are created in the open state of MscS to stabilize the open state of the channel.

To determine the lipid contacts made in the open state of MscS, the open state crystal structure was embedded in a palmitoyloleoyl-phospha-tidylethanolamine (POPE) membrane and the ability of each residue to interact with the lipids was assessed. Eleven residues were predicted to interact with the lipid tails in the open state of MscS, V29, V32, A36, V40, I43, I44, M47, A51, N53, L55, and S58. These residues were mutated to alanine, to destabilize the open state of the channel creating a loss of function phenotype, or leucine, to stabilize the open state of the channel creating a gain of function phenotype, and analyzed using an osmotic downshock assay and gain of function assays. The eleven residues predicted to interact with the lipids in the open state of MscS, show no phenotypical changes upon mutation to alanine or leucine in both assays. The lack of phenotypic changes indicates that there are no alterations in the stability of the open state of MscS and that the open state of the channel is the thermodynamic minimum in the absence of lipid tension. This has lead us to propose a “Jack-In-The-Box” model of

gating for MscS, in which intrinsic lipid bilayer tension holds the channel in the closed state. Upon relief of the intrinsic bilayer tension by application of opposing extrinsic tension, MscS springs into the open state.

The tension sensor, comprised of seven hydrophobic amino acids, in the closed state of Ec-MscS does not correlate well with the proposed Jack-In-The-Box gating model, where the open state is not stabilized by lipid interactions. This model suggests that the tension sensor does not sense the tension in the membranes, but these residues are involved in intra-protein contacts and that disturbing these contacts leads to loss of function phenotypes. The mutation of the large hydrophobic residues to small hydrophobic residues would prevent the knobs and holes from forming tight contacts in the open state leading to the observed loss of function phenotypes (Wang et al. 2008).

Additionally, the Jack-In-The-Box gating model does not correlate with the knowledge that vestibule rearrangement drives gating in response to mechanical tension in bCNG channels. A possibility is that vestibule rearrangement and the movement of the transmembrane domains occurs simultaneously upon relief of the intrinsic tension. Additionally, it is possible that the relief of tension in the bilayer drives the movement in the vestibule that is essential for channel gating in bCNG channels.

### *8.4 MscS Future Directions*

#### *8.4.1 Exploring the Lipid Interactions of MscS*

To further study the lipid interactions of MscS, point mutations in the loops between the transmembrane domains could be utilized. These regions of the channel most likely interact with the lipid headgroups and alterations within these regions could lead to unique phenotypes (Maurer et al. 2000; Maurer and Dougherty 2003). Previous research has indicated that MscS and cardiolipin are co-localized in the cellular membrane, suggesting that the lipid environment is important for channel function (Romantsov et al. 2010). The loop between TM1 and TM2 is composed of small hydrophobic residues and charged residues. Our previous study of the lipid interactions in the closed state identified residues in the first loop region as having significant lipid interactions (Figure 8.1). However, in the second loop between TM2 and TM3 there are no predicted lipid interactions.

In the TM1-TM2 loop region large positive and negative deviations from baseline are observed, due to long distance charge interactions between the arginine residues, R46, R54, and R74, and the lipid head groups. However, the loops are predicted to interact with the head groups so the large deviations are most likely the interesting residues to study. These interactions could be assessed by mutating these charged residues to small hydrophobic residues and using osmotic downshock and gain of function assays to study their function. Since there are fewer loop residues than in the transmembrane residues, several unique mutations could be made for each residue to determine its function. The

identification of additional lipid interactions would lead to a greater understanding of how MscS responds to the tension in the membrane.

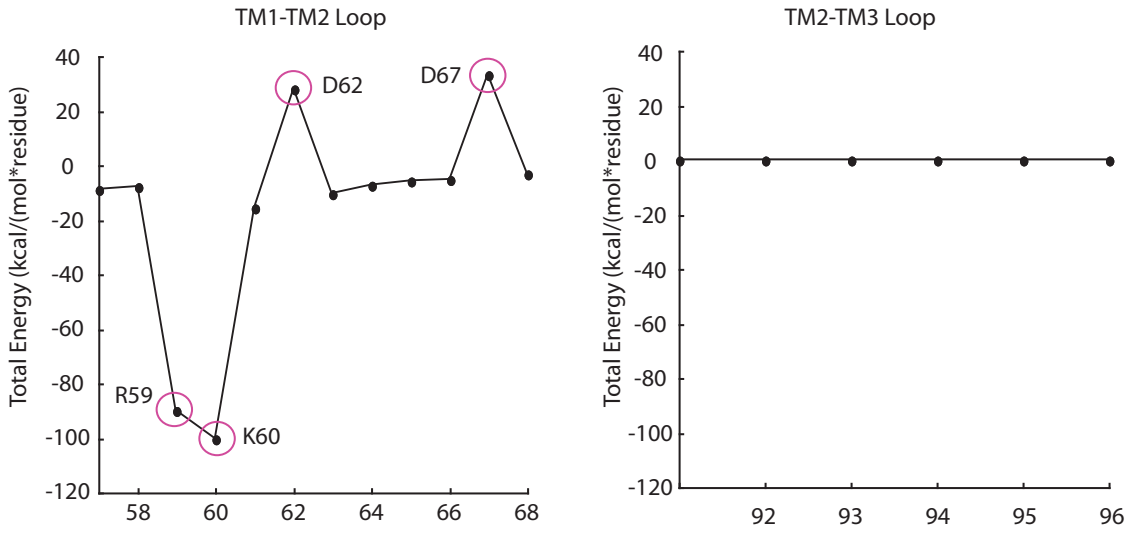


**Figure 8.1:** Protein-lipid interactions energies over the final 10 ns of the MD simulation for the two loops, TM1-TM2 and TM2-TM3

### *8.4.2 Can MscS Become a Ligand Gated Channel?*

In the MscS superfamily, there are large variations in the number of transmembrane domains as well as the N-terminal and C-terminal regions of the channels (Borngen et al. 2010; Malcolm et al. 2012; Caldwell et al. 2010). If bCNG channels differ from MscS by the addition of a C-terminal cAMP binding domain, can the function of MscS be altered to be a ligand gated channel? A functional cAMP binding domain, from Te-bCNGb, could be inserted into the MscS gene in frame at the C-terminus of MscS in a plasmid. One potential problem is the linker domain, since within the bCNG channel family there

is not much conservation in this region. Many different linkers could be explored to determine if the length of the linker domain is essential for gating in response to cAMP. The ability of MscS to function as a ligand gated channel would be assessed using patch clamp electrophysiology. Patch clamp would allow for the ability of MscS to gate in response to cAMP to be determined in the presence of tension. Additionally, by using patch clamp to study MscS's ability to gate in response to cAMP, changes in the threshold gating tension of MscS could also be determined. It is likely that the length and composition of the linker would need to be optimized since, if the linker domain was too short or too long the binding of cAMP would not be able to be translated to the channel for channel gating.

### *8.5 References*

Borngen K, Battle AR, Moker N, Morbach S, Marin K, Martinac B, Kramer R (2010) The properties and contribution of the Corynebacterium glutamicum MscS variant to fine-tuning of osmotic adaptation. Biochimica et biophysica acta 1798 (11):2141-2149. doi:10.1016/j.bbamem.2010.06.022

Caldwell DB, Malcolm HR, Elmore DE, Maurer JA (2010) Identification and experimental verification of a novel family of bacterial cyclic nucleotide-gated (bCNG) ion channels. Biochimica et biophysica acta 1798 (9):1750-1756. doi:10.1016/j.bbamem.2010.06.001

Corry B, Martinac B (2008) Bacterial mechanosensitive channels: experiment and theory. Biochimica et biophysica acta 1778 (9):1859-1870. doi:10.1016/j.bbamem.2007.06.022

Edwards MD, Booth IR, Miller S (2004) Gating the bacterial mechanosensitive channels: MscS a new paradigm? Current opinion in microbiology 7 (2):163-167. doi:10.1016/j.mib.2004.02.006

Grantham R (1974) Amino acid difference formula to help explain protein evolution. Science 185 (4154):862-864

Hill L, Flack M (1910) The influence of oxygen inhalations on muscular work. The Journal of physiology 40 (5):347-372

Hurst AC, Petrov E, Kloda A, Nguyen T, Hool L, Martinac B (2008) MscS, the bacterial mechanosensitive channel of small conductance. The international journal of biochemistry & cell biology 40 (4):581-585. doi:10.1016/j.biocel.2007.03.013

Levina N, Totemeyer S, Stokes NR, Louis P, Jones MA, Booth IR (1999) Protection of Escherichia coli cells against extreme turgor by activation of MscS and MscL mechanosensitive channels: identification of genes required for MscS activity. The EMBO journal 18 (7):1730-1737. doi:10.1093/emboj/18.7.1730

Malcolm HR, Elmore DE, Maurer JA (2012) Mechanosensitive behavior of bacterial cyclic nucleotide gated (bCNG) ion channels: Insights into the mechanism of channel gating in the mechanosensitive channel of small conductance superfamily. Biochemical and biophysical research communications 417 (3):972-976. doi:10.1016/j.bbrc.2011.12.049

Malcolm HR, Heo YY, Elmore DE, Maurer JA (2011) Defining the role of the tension sensor in the mechanosensitive channel of small conductance. Biophysical journal 101 (2):345-352. doi:10.1016/j.bpj.2011.05.058

Maurer JA, Dougherty DA (2003) Generation and evaluation of a large mutational library from the Escherichia coli mechanosensitive channel of large conductance, MscL: implications for channel gating and evolutionary design. The Journal of biological chemistry 278 (23):21076-21082. doi:10.1074/jbc.M302892200

Maurer JA, Elmore DE, Lester HA, Dougherty DA (2000) Comparing and contrasting Escherichia coli and Mycobacterium tuberculosis mechanosensitive channels (MscL). New gain of function mutations in the loop region. The Journal of biological chemistry 275 (29):22238-22244. doi:10.1074/jbc.M003056200

Nimigean CM, Pagel MD (2007) Ligand binding and activation in a prokaryotic cyclic nucleotide-modulated channel. Journal of molecular biology 371 (5):1325-1337. doi:10.1016/j.jmb.2007.06.030

Romantsov T, Battle AR, Hendel JL, Martinac B, Wood JM (2010) Protein Localization in Escherichia coli Cells: Comparison of the Cytoplasmic Membrane Proteins ProP, LacY, ProW, AqpZ, MscS, and MscL. Journal of bacteriology 192 (4):912-924. doi:Doi 10.1128/Jb.00967-09

Wang W, Black SS, Edwards MD, Miller S, Morrison EL, Bartlett W, Dong C, Naismith JH, Booth IR (2008) The structure of an open form of an E. coli mechanosensitive channel at 3.45 A resolution. Science 321 (5893):1179-1183. doi:10.1126/science.1159262

Weiss JN (1997) The Hill equation revisited: uses and misuses. FASEB journal : official publication of the Federation of American Societies for Experimental Biology 11 (11):835-841

Wild J, Altman E, Yura T, Gross CA (1992) DnaK and DnaJ heat shock proteins participate in protein export in Escherichia coli. Genes & development 6 (7):1165-1172

Wu J, Lukas RJ (2011) Naturally-expressed nicotinic acetylcholine receptor subtypes. Biochemical pharmacology 82 (8):800-807. doi:10.1016/j.bcp.2011.07.067